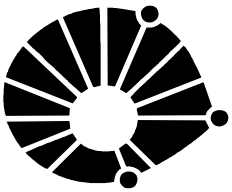

UNICAMP

UNIVERSIDADE ESTADUAL DE CAMPINAS

FACULDADE DE ENGENHARIA DE ALIMENTOS

M. SC. LUIS ALBERTO FOLLEGATTI ROMERO

EQUILÍBRIO LÍQUIDO–LÍQUIDO NA PRODUÇÃO DE BIODIESEL ETÍLICO

TESE DE DOUTORADO APRESENTADA À FACULDADE DE ENGENHARIA DE ALIMENTOS UNICAMP PARA OBTENÇÃO DO TÍTULO DE DOUTOR EM ENGENHARIA DE ALIMENTOS.

ANTONIO JOSÉ DE ALMEIDA MEIRELLES
ORIENTADOR

MARCELO LANZA
CO-ORIENTADOR

Este exemplar corresponde à versão final da tese: Equilíbrio Líquido–Líquido na Produção de Biodiesel Etílico, defendida por Luis Alberto Follegatti Romero, aprovada pela comissão julgadora em 21/10/2011 e orientado pelo Prof. Dr. Antonio José de Almeida Meirelles.

_____
Assinatura do Orientador

CAMPINAS, 2011

FICHA CATALOGRÁFICA ELABORADA POR
CLAUDIA AP. ROMANO DE SOUZA – CRB8/5816 – BIBLIOTECA DA FACULDADE DE ENGENHARIA DE ALIMENTOS – UNICAMP

Follegatti Romero, Luis Alberto, 1981–
F721e Equilíbrio líquido–líquido na produção de biodiesel etílico / Luis Alberto Follegatti Romero. –– Campinas, SP:
[s.n], 2011.

Orientador: Antonio José de Almeida Meirelles.
Tese (doutorado) – Universidade Estadual de Campinas. Faculdade de Engenharia de Alimentos.

1. Equilíbrio líquido–líquido. 2. Ésteres de ácidos graxos. 3. Etanólise. 4. NTRL. 5. Equação de estado. I. Meirelles, Antonio José de Almeida. II. Universidade Estadual de Campinas Faculdade de Engenharia de Alimentos. III. Título.

Informações para Biblioteca Digital

Título em inglês: Liquid–liquid equilibrium for the production of ethylic biodiesel
Palavras–chave em inglês (Keywords):
Liquid–liquid equilibrium
Fatty acid esters
Ethanolysis
NTRL
Equation of state
Área de concentração:Engenharia de Alimentos
Titulação: Doutor em Engenharia de Alimentos
Banca examinadora:
Antonio José de Almeida Meirelles [Orientador]
Pedro de Alcântara Pessôa Filho
Maria Regina Wolf Maciel
Christianne Elisabete da Costa Rodrigues
Martín Aznar
Data da defesa: 21/10/2011
Programa de Pós Graduação: Engenharia de Alimentos

COMISSÃO EXAMINADORA

_____

Prof. Dr. Antonio José de Almeida Meirelles – Orientador
DEA/FEA/UNICAMP

_____

Prof. Dr. Martín Aznar – Membro Titular
DPQ/FEQ/UNICAMP

_____

Prof. Dra. Christianne Elisabete da Costa Rodrigues – Membro Titular
ZEA/FZEA/USP

_____

Prof. Dra. Maria Regina Wolf Maciel – Membro Titular
DPQ/FEQ/UNICAMP

_____

Prof. Dr. Pedro de Alcântara Pessôa Filho – Membro Titular
DEQ/EP/USP

Prof. Dra. Maria Alvina Krähenbühl – Membro Suplente
DPQ/FEQ/UNICAMP

Prof. Dr. Eduardo Augusto Caldas Batista – Membro Suplente
DEA/FEA/UNICAMP

Prof. Dra. Jane Sélia dos Reis Coimbra – Membro Suplente
DTA/FEA/UFV

Dedíco este trabalho:

À minha mãe, Betty, ao meu paí, Carlos e às minhas írmãs, Mílagros, Dalíla, Marína e Carla.

AGRADECIMENTOS

- Ao meu orientador, Prof. Dr. Antonio José de Almeida Meirelles, pelos conhecimentos transmitidos, paciência, estímulo, confiança e amizade. Expresso aqui os meus sinceros agradecimentos.

- Ao Prof. Dr. João Araujo Pereira Coutinho, pela oportunidade de realizar estágio de curta duração no laboratório PATh da Faculdade de Química da Universidade de Aveiro (Portugal), pelas sugestões, disponibilidade e conhecimentos transmitidos.

- Ao Prof. Dr. Eduardo Augusto Caldas Batista, pelas correções e sugestões nos artigos que compõem esta Tese de Doutorado, pela disponibilidade e conhecimentos transmitidos.

- Ao Prof. Dr. Marcelo Lanza, pelo apoio e suporte na aplicação do modelo NRTL.

- À Dra. Mariana Oliveira, pelo apoio no laboratório PATh (U.A., Portugal), pelo suporte na aplicação da equação de estado CPA na modelagem dos dados experimentais deste trabalho.

- Quero agradecer aos meus colaboradores, ao Dr. César da Silva e ao Doutorando Fabio Rodolfo Batista, pelo suporte técnico e analítico durante a execução da parte experimental desta Tese de Doutorado.

- Quero também agradecer ao grupo ExTrAE, aos mais antigos e aos mais recentes, pelo convívio, apoio e por tornarem os dias de trabalho mais agradáveis e divertidos. Obrigado a todos.

- Um agradecimento especial aos meus pais, Betty e Carlos e às minhas irmãs, Milagros, Dalila, Marina e Carla pelo apoio emocional e encorajamento.

- Ao Programa de Estudante–Convênio de Pós–Graduação da CAPES (PEC–PG) pela concessão da bolsa de estudos.

ÍNDICE GERAL

ÍNDICE DE TABELAS

ÍNDICE DE FIGURAS

RESUMO GERAL

Os ésteres etílicos de ácidos graxos (biodiesel) podem ser produzidos através da reação da transesterificação ou etanólise. Os reagentes (óleo vegetal e etanol), normalmente com o álcool adicionado em excesso para garantir uma maior conversão em ésteres etílicos de ácidos graxos (FAEEs), formam um mistura heterogênea com miscibilidade parcial, sendo necessário nesta etapa realizar agitação no interior do reator para melhorar a difusão de componentes entre as fases formadas. Durante a reação, a mistura inicial é transformada em outras duas fases, uma rica em ésteres etílicos e outra rica em glicerina, com o etanol em excesso distribuindo–se entre as duas fases. Finalmente, os ésteres resultantes devem ser separados da glicerina, do álcool em excesso e do catalisador, via decantação ou centrifugação, seguido de um processo de lavagem com água (purificação) para eliminar os sabões, componentes graxos, restos de catalisador, álcool e glicerina. Algumas das dificuldades da produção industrial de biodiesel etílico estão associadas ao desconhecimento das composições das fases durante o processo reacional e a problemas adicionais na separação de fases em função da maior presença de etanol em ambas as fases resultantes da reação. Por esta razão, torna–se necessário o estudo do equilíbrio líquido–líquido das misturas envolvidas nas diferentes etapas do processo de produção deste biocombustível. O presente trabalho teve como objetivo a determinação de dados de equilíbrio líquido–líquido para uma série de sistemas pseudo–binários e multicomponentes envolvendo óleos vegetais, FAEEs, etanol, glicerol e água e a modelagem do equilíbrio de fases destes sistemas empregando a equação de estado CPA EoS (Cubic–Plus–Association Equation of State) e o modelo NRTL. Em uma primeira etapa, foi estudada a solubilidade dos reagentes: óleos vegetais + etanol em uma faixa de temperatura de 298,15 a 333,15 K. Estes dados foram correlacionados satisfatoriamente usando o modelo NRTL. Nesta modelagem, o óleo vegetal foi tratado como um pseudocomponente. A validade desta hipótese foi demonstrada em um trabalho subseqüente sobre a partição dos triacilgliceróis nas fases de equilíbrio (oleosa e alcoólica) em misturas compostas de óleos vegetais + etanol para a produção de biodiesel. Na segunda etapa desta tese foram investigados sistemas ternários relacionados com o período intermediário do processo reacional de produção de biodiesel: FAEEs + etanol + glicerol a 323,15 e 353,15 K. Estes dados foram

correlacionados corretamente com a CPA EoS, aproveitando–se a transferência dos parâmetros usados num trabalho anterior na predição do equilíbrio líquido–vapor de sistemas binários compostos por ésteres etílicos ou ésteres metílicos de ácidos graxos em uma faixa de pressão de 5332,9–13332,23 Pa. Sistemas relacionados com a etapa de lavagem do biodiesel também foram investigados: FAEEs + etanol + água a temperaturas entre 298,15 e 333,15 K. Os resultados mostraram que a lavagem com água é uma maneira muito eficaz de recuperação de etanol da fase rica em ésteres gerados. Estes dados de equilíbrio também foram correlacionados com a CPA EoS e os desvios médios apresentaram valores menores que 3,0 %.

ABSTRACT

Fatty acid ethyl esters (biodiesel) are produced through the transesterification reaction or ethanolysis. Reagents (vegetable oil and ethanol), usually with alcohol in excess to ensure a higher conversion into fatty acid ethyl esters (FAEEs), form a heterogeneous mixture with partial miscibility; in this step it is necessary to carry out agitation inside the reactor to improve component diffusion between the phases formed. During the course of the reaction, the initial mixture is transformed into two phases: an ethyl esters–rich phase and the other a glycerin–rich phase, with excess ethanol distributed in both phases. Finally, the esters must be separated from the glycerin, excess alcohol and catalyst, via decanting or centrifuging, followed by a washing process with water (purification) to remove the soaps, fatty compounds, residual catalyst, glycerin and alcohol. Some of the difficulties of industrial production of ethyl biodiesel are associated to the limited information about the phase compositions during the reaction process and additional problems during phase separations due to the high presence of ethanol in the two phases resulting of the reaction. For this reason, it becomes necessary studying the liquid–liquid phase equilibrium of the mixtures involved in different steps of the production of this biofuel. The objective of this work was to determine the liquid−liquid equilibria data for several pseudo–binary and multicomponent systems containing vegetable oils, FAEEs, ethanol, glycerol and water and the phase equilibrium modeling using the CPA EoS (Cubic–Plus–Association Equation of State) and NRTL model. In a first stage, the solubility of reagents (vegetable oil + ethanol) was studied in the temperature range from 298.15 to 333.15 K. These data were satisfactorily correlated using the NRTL model. In this model, the vegetable oil was treated as a pseudocomponent. The validity of this hypothesis was demonstrated in a subsequent work about the partition data of triacylglycerols between the two immiscible liquid equilibrium phases (oil and alcoholic) in vegetable oil + ethanol mixtures for biodiesel production. In the second stage of this thesis were investigated ternary systems related with the reaction process intermediate step of biodiesel production: FAEEs + ethanol + glycerol at 323.15 and 353.15 K. These data were correlated correctly with the CPA EoS, taking advantage of the transferability of the CPA parameters used in a previous work for predicting the vapor–liquid equilibrium of binary systems composed of fatty acid ethyl or

methyl esters in the pressure range 5332.9 – 13332.23 Pa. Ternary systems related with the biodiesel washing process were also investigated: FAEEs + ethanol + water within the temperature range of 298.15 and 333.15 K. These results indicate that washing with water is a very effective way of extracting ethanol from the ester phase generated. These equilibrium data were also correlated with the CPA EoS and the mean deviation values were lower than 3.0 %.

INTRODUÇÃO GERAL

A combustão de combustíveis fósseis, como o diesel e a gasolina, constitui uma das principais causas da emissão de gás carbônico (CO_2), considerado o principal componente causador do efeito estufa. Esse fato levou vários países a buscarem fontes alternativas para os combustíveis automotivos, que pudessem amenizar o problema e reduzir o aquecimento global. Combustíveis produzidos a partir da biomassa atendem a esse propósito, pois o CO_2 emitido pela combustão é absorvido durante o crescimento das plantas (TILMAN et al., 2006; REIJNDERS e HUIJBREGTS, 2008).

O Brasil possui um grande potencial de obtenção de combustível originário da biomassa, como é o caso do etanol carburante a partir da cana–de–açúcar, para substituição parcial ou total da gasolina em veículos leves (LOOTTY et al., 2009). Além disso, outro biocombustível biodegradável, ambientalmente benigno, com baixa toxidade vem chamando atenção nos últimos anos devido à sua sustentabilidade, o biodiesel.

O biodiesel é quimicamente definido como ésteres monoalquílicos de ácidos graxos derivados de óleos vegetais, gorduras animais ou matérias graxas de descarte. Dentro das matérias–primas para a produção de biodiesel destacam–se as oleaginosas e os álcoois de cadeia curta. Dentre as oleaginosas para a produção de biodiesel destacam–se, soja, mamona, palma, girassol, algodão, entre outras. O óleo de soja é uma matéria–prima ideal para a produção de biodiesel devido principalmente à disponibilidade com volume suficiente no Brasil. A palma tem ganhado ênfase pelo alto rendimento de produção (BARNWAL et al., 2005; POUSA et al., 2007). O álcool utilizado como matéria–prima para produzir biodiesel pode ser de origem vegetal ou mineral e, dentre os diversos alcoóis destacam–se o álcool metílico (metanol) e o álcool etílico (etanol). O metanol, proveniente

de fontes fósseis é o álcool mais utilizado no mundo atualmente, devido ao baixo custo e à alta produção quando comparado com o etanol. Isso ocorre porque na maioria dos países a disponibilidade de etanol derivado de biomassa é bastante reduzida. Entretanto, o Brasil é auto–suficiente em etanol devido à grande área disponível para a produção de cana–de–açúcar e à disponibilidade de tecnologia os quais permitem a produção economicamente viável deste álcool por processos fermentativos. Anualmente, produz cerca de 20 bilhões de litros de etanol a partir da cana e tem uma capacidade ociosa de mais de cinco bilhões de litros por ano (IBGE, 2011).

As vantagens brasileiras em se utilizar etanol na produção do biodiesel são muitas. O etanol é um combustível de baixa toxidade e totalmente biodegradável. O fato das matérias primas utilizadas para a sua produção serem completamente oriundas de fontes agrícolas renováveis torna o biodiesel produzido com álcool etílico um produto verdadeiramente renovável (DEMIRBAS, 2009).

O processo químico empregado mundialmente para a produção de biodiesel é o da transesterificação ou alcoólise. A transesterificação pode ocorrer principalmente por meio de duas rotas, a metílica e a etílica, na qual um óleo vegetal (triacilglicerols) reage com um álcool (metanol ou etanol) na presença de um catalisador (usualmente alcalino) para formar, majoritariamente, ésteres monoalquílicos (metílicos ou etílicos) e glicerol (GERPEN, 2005; MARCHETTI et al., 2007; SAIFUDDIN e CHUA, 2004; MEHER et al., 2006; DEMIRBAS, 2008).

No entanto, a transesterificação etílica é significativamente mais complexa que a metílica. O aumento do tamanho da cadeia do álcool acarreta uma maior sofisticação do processo e muitos dos parâmetros do processo não estão claramente definidos. Esta rota mostra um comportamento de fase complexo; um dos grandes problemas associados com a

reação de catálise (alcoólise) é a extremadamente baixa solubilidade do álcool com os triacilglicerols. No início da transesterificação, os triacilglicerols e o etanol não se misturam bem, devido a sua disparidade de tamanho e polaridade, formando um sistema líquido bifásico dentro do reator (FOLLEGATTI–ROMERO et al., 2010). Estas fases são: uma fase superior rica em álcool, em que o catalisador é dissolvido, e outra inferior que é a fase do óleo vegetal. A reação tem lugar principalmente na fase alcoólica. Portanto, a taxa de reação depende em grande parte da solubilidade do óleo no álcool (ZHOU e BOOCOCK, 2006), sendo afetada pela fração mássica dos componentes em mistura e pela temperatura do sistema.

Durante a reação, a mistura inicial é transformanda em outras duas fases, uma rica em ésteres etílicos (fase leve) e outra rica em glicerina (fase pesada) (ZHOU et al., 2006). Os ésteres resultantes devem ser separados da glicerina, do álcool em excesso e do catalisador via decantação ou centrifugação; seguidamente é necessário efetuar a purificação do biodiesel que consiste basicamente na lavagem e na secagem. No processo de lavagem com água são retiradas impurezas presentes no meio como: catalisador, excesso do álcool utilizado na reação, glicerina livre residual, sais de ácidos graxos, e tri–, di– e monoacilgliceróis (GONZALO et al., 2010), de forma a atender as especificações regulamentadas pela Agência Nacional do Petróleo, gás natural e biocombustíveis (ANP) através da resolução 42 (BRASIL, 2011).

Algumas das dificuldades da produção industrial de biodiesel etílico estão associadas ao desconhecimento das composições das fases durante o processo reacional, a problemas na separação de fases em função da maior presença de etanol nas fases resultantes da reação e às dificuldades adicionais relacionadas ao processo de lavagem do biodiesel. Por esta razão,

torna–se necessário o estudo do equilíbrio líquido–líquido das misturas envolvidas nas diferentes etapas do processo de produção deste bicombustível.

O presente trabalho teve como objetivo a determinação de dados de equilíbrio líquido–líquido (ELL) para uma série de sistemas pseudo–binários e multicomponentes envolvendo óleos vegetais, ésteres etílicos de ácidos graxos (FAEEs), etanol, glicerol e água que ocorrem nas etapas de produção do biodiesel etílico, necessários para determinar as melhores condições durante a reação dos reagentes (óleo vegetal + etanol), na separação dos produtos finais (FAEEs + etanol + glicerol) e na lavagem do biodiesel (FAEEs + etanol + água).

A capacidade de modelar o ELL destas misturas é a base fundamental para o projeto dos principais equipamentos de reação e de separação no processo de produção industrial, ou para simulação do desempenho das unidades existentes com a finalidade de atingir uma elevada produtividade a baixos custos de operação. Para sistemas complexos com fortes interações intermoleculares, com formação de ligação de hidrogênio e envolvendo reagentes e produtos do biodiesel etílico, os modelos clássicos de coeficientes de atividade (NRTL ou UNIQUAC) mostraram ser apropriados para descrever o ELL de alguns sistemas não ideais (LANZA et al., 2008; PRIAMO, 2008; NEGI et al., 2006; ZHANG et al., 2003); no entanto, estes modelos não conseguem correlacionar adequadamente o equilíbrio de fases de misturas polares numa ampla gama de composições e condições termodinâmicas (OLIVEIRA et al., 2011).

Nesse sentido, neste trabalho foi utilizada a equação de estado CPA EoS (Cubic–Plus–Association Equation of State) como uma feramenta flexível capaz de descrever e predizer equilíbrios líquido–vapor (OLIVEIRA et al., 2010), líquido–líquido (FOLLEGATTI–ROMERO et al., 2010) e em fluidos supercríticos (OLIVEIRA et al., 2010) em uma grande

faixa de temperatura e pressão, aproveitando inclusive a transferência dos seus parâmetros de interação. Desta maneira, a aplicação de um modelo que consiga descrever todos os equilíbrios formados nas etapas do processo de produção do biodiesel etílico pode ser de grande utilidade.

Os Capítulos que compõem esta tese de doutorado estão resumidos a seguir.

O Capítulo 1 apresenta uma breve revisão de literatura relacionada à importância do biodiesel, ao processo de produção e aos fundamentos termodinâmicos do ELL.

O Capítulo 2 apresenta o estudo da solubilidade mútua de sistemas pseudo–binários envolvendo óleos vegetais + etanol em uma faixa de temperatura de 298,15 a 333,15 K, bem como a correlação desses dados utilizando o modelo NRTL. Esta pesquisa foi desenvolvida para estudar o equilíbrio líquido–líquido de misturas que ocorrem durante a etapa inicial da reação de transesterificação.

No Capítulo 3 é apresentado o estudo do fenômeno de partição dos triacilgliceróis entre as fases oleosas e alcoólicas em misturas compostas por óleos vegetais + etanol a uma faixa de temperatura entre 298,15 e 333,15 K. Este trabalho foi desenvolvido para comprovar a hipótese de pseudo–componente, geralmente é usado para tratar os óleos vegetais em modelagens termodinâmicas.

O Capítulo 4 apresenta a aplicação da equação de estado CPA EoS para predizer o equilíbrio líquido–vapor de sistemas binários compostos por ésteres etílicos ou metílicos no faixa de pressão de 5332,9 a 13332,23 Pa. Esta pesquisa foi desenvolvida para testar o desempenho da equação de estado no equilíbrio líquido–vapor.

No Capítulo 5 são apresentados dados experimentais de equilíbrio líquido–líquido de ésteres etílicos (linoleato, oleato, palmitato e laurato de etila) + etanol + glicerol a 323,15 e 353,15 K. Estes dados foram correlacionados com a equação de estado CPA EoS. Este

trabalho foi realizado para o estudo de sistemas que se formam durante a reação de transesterificação.

No Capítulo 6 são apresentados os dados experimentais de equilíbrio líquido–líquido de ésteres etílicos puros (miristato e laurato de etila) + etanol + água a 298,15, 313,15 e 333,15 K. Estes dados foram correlacionados com a CPA EoS. Este trabalho foi realizado para o estudo de sistemas de interesse durante a etapa de lavagem com água do biodiesel etílico produzido a partir de óleos láuricos (coco, babaçu, palmiste e macaúba).

O Capítulo 7 apresenta dados experimentais de equilíbrio líquido–líquido de ésteres etílicos puros (linoleato e palmitato de etila) e misturas de ésteres etílicos (oleato de etila de grau técnico) + etanol + água a diferentes temperaturas e a correlação desses dados com a equação de estado CPA EoS. Esta pesquisa foi focada no estudo de sistemas envolvendo ésteres etílicos puros (insaturados e saturados) e em mistura, geralmente encontrados nos óleos de soja, girassol, canola e palma.

Finalmente, as conclusões gerais e sugestões para trabalhos futuros são apresentadas no Capítulo 8 desta tese de doutorado.

OBJETIVOS

O objetivo geral desta tese de doutorado foi a determinação do equilíbrio líquido–líquido (ELL) para uma série de sistemas pseudo–binários e multicomponentes que se formam durante as principais etapas de produção de biodiesel etílico, particularmente sistemas envolvendo óleos vegetais, FAEEs, etanol, glicerol e água e a correlação destes dados de equilíbrio de fases empregando a equação de estado CPA EoS ou o modelo NRTL. Considerando estes aspectos, o objetivo global do projeto foi alcançado mediante a execução dos seguintes objetivos específicos:

a) Determinação da solubilidade mútua da mistura: óleo vegetal (soja, girassol, arroz, algodão, oleina de palma e palma) + etanol em uma faixa de temperatura de 298,15 a 333,15 K.

b) Avaliar a hipótese de pseudo–componente geralmente usada para tratar óleos vegetais em modelagens termodinâmicas.

c) Avaliar a transferibilidade dos parâmetros da CPA EoS obtidas na correlação de dados de equilíbrio líquido–vapor de sistemas binários compostos por ésteres etílicos ou metílicos.

d) Determinação do ELL de sistemas compostos por produtos da transesterificação: FAEEs (linoleato, oleato, palmitato, laurato de etila) + etanol + glicerol.

e) Determinação do ELL de sistemas de interesse durante a etapa de lavagem com água do biodiesel: FAEEs de cadeia longa e curta (linoleato, oleato, palmitato, laurato e miristato de etila) + etanol + água.

CAPÍTULO 1

REVISÃO DE LITERATURA

1.1 Importâncias dos combustíveis alternativos

A poluição atmosférica, responsável pelas mudanças climáticas e pelo efeito estufa, vem a ser um dos grandes problemas ambientais da atualidade. Em um determinado território, a concentração de poluentes no ar atmosférico é o resultado das emissões de substâncias poluentes provenientes de fontes estacionárias (indústrias) e de fontes móveis (automóveis e outros meios de transporte), conjugado a fatores como o clima, a geografia, o uso do solo, a distribuição e a tipologia das fontes emissoras, as condições de emissão e de dispersão destes poluentes plantas (TILMAN et al., 2006, REIJNDERS e HUIJBREGTS, 2008).

A valorização energética sustentável de alguns recursos vegetais pode vir a reduzir, de forma direta e indireta, o impacto ambiental do efeito estufa. De forma direta, ao substituir os combustíveis fósseis por matéria orgânica vegetal, os gases emitidos durante a queima do combustível não são computados na avaliação de impacto efeito estufa. Considera–se que uma quantia equivalente à produzida durante a queima do combustível é reabsorvida, pelo processo de fotossíntese, durante o crescimento da espécie vegetal

empregada na fabricação do combustível (REIJNDERS e HUIJBREGTS, 2008). De forma indireta, desde que a biomassa seja produzida e utilizada de forma sustentável, pode ser reduzida a degradação do solo e das matas, bem como as emissões de gases do efeito estufa decorrentes destes processos.

No Brasil, o uso da energia renovável obtida através da conversão de biomassa vem ganhando destaque por possibilitar a redução da dependência de energia proveniente de combustíveis fósseis e a criação de novas oportunidades de emprego em comunidades rurais (dinamizando as economias regionais). Além disso, em termos sociais e ambientais, a utilização energética da biomassa promove o desenvolvimento e produção sustentável da agricultura familiar em comunidades isoladas, possibilita a redução das emissões atmosféricas (locais, regionais e globais) e atende aos anseios da sociedade em relação ao desenvolvimento sustentável (assegurando o suprimento de energia de fontes renováveis) (MACEDO et al., 2008; BRASIL, 2011).

Como principal desvantagem da adoção da biomassa em substituição às fontes fósseis pode ser citada a dificuldade das tecnologias das energias renováveis competirem com os mercados já consolidados dos combustíveis fósseis. De fato, esta dificuldade em competir, geralmente, devido ao custo elevado dos combustíveis alternativos, acontece no início da utilização comercial de novas fontes energéticas. No entanto, conforme o consumo destas novas fontes de energia cresce, seu custo tende a diminuir, como foi demonstrado pelo Programa Brasileiro de Álcool (PRÓ–ÁLCOOL) (BRASIL, 2011).

O Programa Brasileiro de Álcool pode ser citado como modelo de utilização adequada da biomassa como fonte energética. O PRÓ–ÁLCOOL apresentou resultados muito positivos em relação tanto aos aspectos econômicos quanto aos aspectos ambientais e

sociais, tornando–se o mais importante programa de energia de biomassa do mundo (BRASIL, 2011).

Os combustíveis obtidos a partir de óleos vegetais apresentam qualidades que os diferenciam como combustíveis sustentáveis, entre elas a ausência de enxofre na composição química, a limitada produção de substâncias danosas ao meio ambiente durante a fase industrial e, ainda, o fato de ser elaborado a partir de culturas vegetais que, durante o processo de fotossíntese, consomem dióxido de carbono (CO_2), principal gás causador do efeito estufa da atmosfera terrestre (TILMAN et al., 2006).

A utilização de biodiesel no transporte rodoviário e urbano pode oferecer grandes vantagens para o meio ambiente, tendo em vista que a sua emissão de poluentes é bem menor do que a do diesel de petróleo (LEE et al., 2004). De fato, o potencial do biodiesel em contribuir para a diminuição do aquecimento global tem sido avaliado por vários autores (EPA, 2002; MAKAREVICIENE E JANULIS, 2003), particularmente através da sua capacidade em reduzir o dióxido de carbono (CO_2) introduzido na atmosfera via combustão interna em motores do ciclo diesel.

De acordo com a literatura (PETERSON e HUSTRULID, 1998), as emissões de gases poluentes, tais como monóxido de carbono (CO), hidrocarbonetos (HC), compostos poliaromáticos (CPAs) de alto potencial carcinogênico, materiais particulados (MP), óxidos de enxofre (SOx) e CO_2, são bem menores para o biodiesel em comparação ao petrodiesel, demonstrando que o uso deste em substituição ao combustível fóssil traz grandes benefícios para o meio ambiente. A substituição total do diesel de petróleo por ésteres metílicos de óleo de soja diminui as emissões de CO_2, CO, HC, CPAs, SOx e MP nas proporções de 78–100, 48, 67, 80, 99 e 47 %, respectivamente (EPA, 2002; MURILLO et al., 2007).

1.2 Biodiesel

De um modo geral, o biodiesel é definido como o derivado mono–alquil éster de ácidos graxos de cadeia longa, proveniente de fontes renováveis como óleos vegetais ou gordura animal, cuja utilização está associada à substituição de combustíveis fósseis em motores de ignição por compressão (motores do ciclo Diesel) (ENCINAR, 2008).

O biodiesel é uma fonte de energia renovável, biodegradável, ambientalmente benigno, com baixa toxidade, livre de enxofre e compostos aromáticos. Por ser um combustível oxigenado, tem uma queima mais completa, reduzindo as emissões de diversos gases poluentes, tais como SO_2, monóxido de carbono, hidrocarbonetos e material particulado, minimizando, deste modo, a poluição do ar atmosférico e as conseqüentes implicações ambientais, como o efeito estufa, a contaminação do solo e a acidificação do ar. Quanto maior for a porcentagem de biodiesel utilizado na mistura de combustível, maior será a redução de poluentes emitidos. (ENCINAR et al., 2005; GERHARD et al., 1997).

O biodiesel também oferece vantagens sócio–econômicas interessantes, pois atua como elemento regulador do mercado de óleos vegetais, gera empregos, contribui para a fixação do homem no campo e não requer qualquer alteração tecnológica nos motores, podendo ser usado puro ou em misturas e, ainda, devido à sua alta lubricidade, pode até causar um aumento na vida útil dos motores (GELLER e GOODRUN, 2004). Por estas razões, o biodiesel apresenta–se como um candidato em potencial para a substituição total ou parcial dos combustíveis derivados do petróleo, além da vantagem de poder ser produzido com o emprego de uma tecnologia simples, fácil de ser transferida para o setor produtivo.

O biodiesel vem sendo utilizado principalmente na Europa, tanto na forma pura como na forma de misturas com o óleo diesel. A mistura B5 é muito utilizada em países como a

França, a Alemanha, a Áustria, a Espanha e em países da Europa central. Particularmente, na Alemanha, existe uma frota significativa de veículos leves, coletivos e de cargas utilizando biodiesel puro (B100). O biodiesel europeu é produzido, principalmente, a partir dos óleos de colza ou de girassol, associados ao álcool metílico (metanol). Os Estados Unidos também utilizam a mistura B5, sendo o biodiesel produzido a partir de óleo de soja combinado com metanol (BOZBAS, 2008).

1.3 Matérias–primas para produção do biodiesel

As principais matérias–primas para a produção de biodiesel são: óleos vegetais (a partir de oleaginosas) e álcool (metanol ou etanol). Dentre as principais fontes para extração de óleo vegetal que podem ser utilizadas estão: baga de mamona, semente de soja, polpa do dendê, amêndoa do coco de dendê, amêndoa do coco de babaçu, semente de girassol, amêndoa do coco da praia, caroço de algodão, grão de amendoim, semente de canola e semente de maracujá. Óleos vegetais e gorduras são basicamente compostos de triglicerídeos, ésteres de glicerol e ácidos graxos. Aproximadamente 99 % dos triacilgliceróis presentes nos óleos vegetais são compostos pelos ácidos graxos: esteárico, linolênico, palmítico, oléico e linoléico (FUKUDA et al., 2001; MA e HANNA, 1999).

O álcool utilizado na reação pode ser de origem vegetal ou mineral e, dentre os diversos alcoóis que podem ser utilizados na obtenção do biodiesel, o metanol e o etanol se destacam.

No entanto, é importante ressaltar que as propriedades químicas e físicas da matéria–prima empregada no processo estão diretamente associadas ao rendimento da

transesterificação, e, por conseguinte, à qualidade do produto final para fins combustíveis (LANG et al., 2001; BARNWAL e SHARMA, 2004).

1.3.1 Oleaginosas

O Brasil tem um grande potencial para produzir biodiesel, devido à sua localização geográfica, à sua vocação agrícola e, também, à grande diversidade em termos de oleaginosas (POUSA et al., 2007). Dentre as oleaginosas já investigadas para a produção de biodiesel, figuram a soja, o dendê, o girassol, a mamona, o pinhão manso, o milho, a canola e o babaçu, (TAT et al., 2007; PIMENTEL e PATZEK, 2005).

O Brasil é o segundo maior produtor mundial de soja, com produção de 68 milhões de toneladas ou 26,7 % da safra mundial, estimada em 254 milhões de toneladas. O dendezeiro está entre as palmáceas tropicais de maior rendimento em óleo existente, com produção entre 3500 e 6000 kg/ha (CONAB, 2011). As culturas que ocuparam as maiores áreas em 2009/2010 foram: soja, com 23,6 milhões de hectares, o milho com 7,3 milhões de hectares e o arroz com 2,86 milhões de hectares. O somatório das safras destes três produtos representa 90,8% da produção nacional estimada de grãos (IBGE, 2011). O levantamento feito pela CONAB para a safra 2010/2011 prevê uma área plantada com girassol de 66, 8 mil hectares. A região de maior produção é o centro–oeste, com destaque para os estados de Mato Grosso e Goiás (IBGE, 2011). No entanto, as grandes produções de biodiesel no Brasil deverão ser feitas inicialmente com óleo de soja, em função da maior capacidade produtiva atual dessa oleaginosa, já que produtores de pequeno e médio porte poderão recorrer a cultivos de amendoim e girassol.

Dado às características edafoclimáticas do sudeste da Bahia, o dendezeiro mostra–se como a cultura mais promissora para produção de óleo e sua conversão em biodiesel. O Brasil possui o maior potencial mundial para a produção do óleo de dendê, dado aos quase 75 milhões de hectares de terras aptas à dendeicultura. A Bahia participa com aproximadamente 900.000 há deste total, sendo o único estado do nordeste brasileiro com condições climáticas adequadas na faixa costeira para o plantio do dendezeiro. O dendezeiro é o vegetal que mais produz óleo por unidade de área cultivada. Um hectare de sua exploração comercial em moldes modernos produz de (3,500 a 8,000) Kg de óleo de palma ou azeite de dendê. Em contraponto, a soja produz cerca de (400 a 600) Kg de óleo por hectare. (MESQUITA, 2002).

1.3.2 Álcool Etílico x Álcool Metílico

O álcool utilizado como matéria–prima na reação de transesterificação pode ser de origem vegetal ou mineral e, dentre os diversos alcoóis que podem ser utilizados na produção do biodiesel destacam–se o álcool metílico (metanol) e o álcool etílico (etanol) (MENEGHETTI et al., 2006). O Biodiesel utilizado em alguns países da Europa e nos Estados Unidos é constituído de ésteres produzidos através da rota metílica. A preferência dessa rota em relação à etílica está associada a fatores econômicos e a facilidade de sua obtenção naqueles locais (BOZBAS, 2008).

O metanol é mais acessível financeiramente em relação ao etanol anidro e em sua grande parte é proveniente de fontes fósseis e, portanto, não renováveis, a partir do gás metano ou gás natural. Pode ser obtido, também, em pequenas quantidades, por destilação seca da madeira. Em relação ao etanol, apresenta vantagens no processo de produção do biodiesel,

tais como menor consumo de álcool, permite uma reação mais eficiente e a possibilidade de uma recuperação mais fácil da glicerina do produto final (JONES, 2010).

O Brasil não é auto–suficiente em metanol, mas sim em etanol devido à grande área disponível para a produção de cana–de–açúcar. A produção nacional de cana–de–açúcar no ciclo 2009/10 ultrapassou os 500 milhões de toneladas, dos quais quase 200 milhões/t de cana foram destinados para a produção de mais de 24 bilhões de litros de álcool (hidratado, anidro e neutro) (BRASIL, 2011). O Brasil é um grande produtor de etanol, além de ser altamente competitivo: possui a infra–estrutura de produção e distribuição, além do domínio das tecnologias desenvolvidas para a cadeia produtiva da cana de açúcar e do setor automotivo.

As vantagens brasileiras em se utilizar o etanol na produção do biodiesel são muitas. O etanol é um combustível de baixa toxidade e totalmente biodegradável. É considerado ambientalmente mais correto, por ser oriundo de biomassa, o que representa maior potencial de redução de emissão de gases do efeito estufa e desenvolvimento social. Além disso, seu preço, ao contrário do que ocorre com o metanol, não depende das variações do mercado oscilante do petróleo.

1.4 Produção do biodiesel

A reação de transesterificação (alcoólise) é considerada o processo químico mais viável, no momento, em todo o mundo para a produção do biodiesel. Consiste em reagir um lipídeo (conhecidos como triacilgliceróis ou triglicerídeos) com um mono–álcool de cadeia curta (metílico ou etílico), na presença de um catalisador (básico ou ácido), resultando na produção de uma mistura de ésteres alquílicos de ácidos graxos (denominado de biodiesel) e glicerol, conforme ilustra a Figura 1.1. Faz–se necessários na reação, três moles do álcool

para cada mol de triacilgliceróis, além de ser utilizado excesso de álcool, de modo a aumentar o rendimento em ésteres, e favorecer o deslocamento químico dos reagentes para os produtos, permitindo ainda, a separação do glicerol formado (GERPEN, 2005; MARCHETTI et al., 2007; SAIFUDDIN e CHUA, 2004; MEHER et al., 2006; DEMIRBAS, 2008).

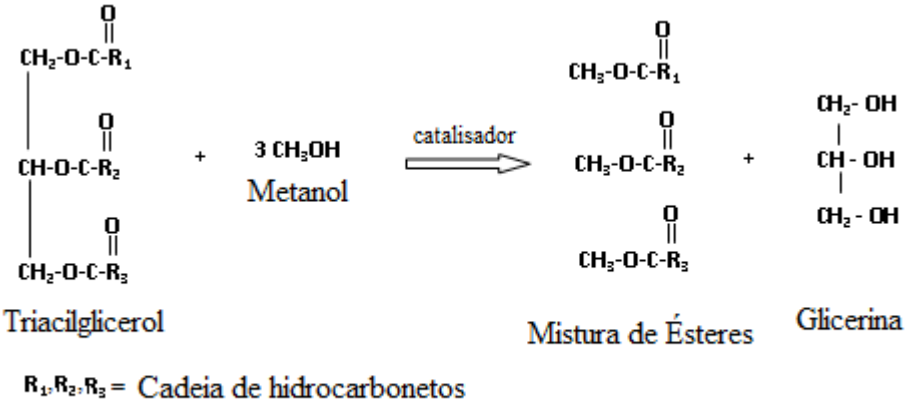

Figura 1. 1. Alcoólise de triglicerídeos (óleos vegetais) com metanol para a produção de ésteres monoalquílicos de ácidos graxos (biodiesel) (GERPEN, 2005).

A reação de transesterificação pode ser influenciada por alguns fatores como: a pureza dos reagentes, tipo do álcool, tipo e a quantidade de catalisador, razão molar óleo: álcool, agitação da mistura, temperatura e o tempo da reação (GERPEN, 2005). No entanto, a temperatura é a variável que mais influencia a velocidade da reação. A temperatura da reação de transesterificação está relacionada ao tipo de álcool utilizado, visto que, normalmente, a reação é conduzida a baixas temperaturas, tendo como limite superior a temperatura do ponto de ebulição do álcool utilizado à pressão atmosférica. No entanto,

altas temperaturas foram empregadas na transesterificação do óleo de soja usando carbonato de cálcio como catalisador em reator operando a 260 ºC, e com tempo de residência de 18 minutos, obtendo–se um 95 % de ésteres etílicos (SUPPES et al., 2001).

A transesterificação mostra um comportamento de fases complexo, um dos problemas associados com esta reação é a extremadamente baixa miscibilidade do álcool com os trigliacilglicerols. No início da transesterificação, os trigliacilglicerols e o álcool não se misturam bem, devido a sua disparidade de tamanho e polaridade, formando um sistema líquido bifásico (FOLLEGATTI–ROMERO et al., 2010). No caso da produção de biodiesel estas fases são: uma fase superior rica em alcohol, em que o catalisador é dissolvido, e outra inferior que é a fase do óleo vegetal (ZHOU et al., 2006; ZHOU e BOOCOCK, 2006). A reação tem lugar principalmente na fase alcoólica. Portanto, a taxa de reação depende em grande medida da solubilidade dos óleos nos alcoóis. Nesta etapa é necessário que os reagentes, óleo vegetal e álcool, sejam agitados para melhorar a difusão entre as fases (MEHER, 2006). A fim de conduzir a reação de transesterificação em um sistema monofásico, além de ser agitada, ZHOU et al. (2003) utilizaram o tetrahidrofurano (THF) como co–solvente. Estes autores concluíram que o THF mantém os reagentes completamente miscíveis e permite assim acelerar a reação. CHIU et al. (2005) observaram que o comportamento de fase e a respectiva distribuição do catalisador e do álcool entre as fases líquidas, podem impactar significativamente as taxas de reação e a formação do produto final.

Durante a reação o sistema inicial é transformando em outras duas fases, uma rica em éster (biodiesel) e outra rica em glicerol, que serão separadas ao final do processo (ZHOU e BOOCOCK, 2006; SAIFUDDIN e CHUA, 2004). Estes dois produtos possuem densidades

diferentes, de forma que a fase mais densa, a rica em glicerina, pode ser separada por gravidade da fase menos densa, a rica em ésteres por decantação. Como alternativa à decantação pode ser utilizada uma centrifugação, sendo esta uma operação mais rápida, porém mais dispendiosa. A glicerina arrasta consigo a maior parte do catalisador e do alcohol em excesso, além de sabões formados pela reação do catalisador básico com ácidos graxos livres presentes no óleo vegetal. A fase menos densa (fase de interesse) é constituída de uma mistura de ésteres, também impregnada de excessos reacionais de álcool e de impurezas (SIVAPRAKASAM e SARAVANAN, 2007).

Finalmente, os ésteres são submetidos a um processo de lavagem, onde são retiradas impurezas presentes no meio como o catalisador, o excesso do álcool utilizado na reação, a glicerina livre residual, sais de ácidos graxos; tri–, di– e monoacilgliceróis. (MARCHETTI et al., 2007; MEHER et al., 2006). Este biodiesel deverá ter suas características enquadradas nas especificações das normas técnicas estabelecidas para o biodiesel como combustível para uso em motores do ciclo diesel.

O excesso residual de álcool na fase leve (biodiesel) e pesada (glicerina), após os processos de lavagem do biodiesel, contém quantidades significativas de água, necessitando de uma recuperação, e ser novamente inserido no processo de produção. A recuperação do álcool é feita normalmente por destilação. No caso do metanol, a destilação é bastante simples e fácil de ser conduzida, uma vez que a volatilidade relativa dos constituintes dessa mistura é muito grande. Diferentemente à destilação complicada do etanol em razão da azeotropia, associada à volatilidade relativa não tão acentuada como é o caso da separação da mistura metanol – água (MEIRELLES et al., 1992).

1.5 Fundamentos Termodinâmicos

Neste subtítulo, é apresentada uma revisão completa dos fundamentos termodinâmicos relativos ao equilíbrio de fases líquido–líquido e, posteriormente, são mostrados alguns modelos termodinâmicos necessários para correlacionar e predizer dados experimentais de misturas pseudo–binárias, binárias, ternárias e multicomponentes, viabilizando assim, um projeto mais adequado e flexível de equipamentos empregados em processos de produção do biodiesel e também permitindo a definição de variáveis operacionais destes.

1.5.1Critérios de Equilíbrio de Fases

Os principais critérios utilizados para se considerar um sistema como estando em equilíbrio estão em termos dos quatro potencias termodinâmicos extensivos: energia interna (*U*), entalpia (*H*), energia livre de Helmholtz (*A*) e energia livre de Gibbs (*G*). Contudo, podemos obter critérios mais uteis em termos das quantidades intensivas: temperatura (*T*), pressão (*P*) e potencial químico do componente *i* (μ_i). Para que exista equilíbrio mecânico e térmico, a pressão e a temperatura dentro do sistema devem ser uniformes em todas as fases (SANDLER, 2006).

Da condição acima, surgem expressões de equilíbrio térmico, mecânico e químico, utilizados nos cálculos de equilíbrio:

$$T^I = T^{II} = \ldots = T^{\pi} \tag{1}$$

$$P^I = P^{II} = \ldots = P^{\pi} \tag{2}$$

$$\mu_i^I = \mu_i^{II} = \ldots = \mu_i^{\pi} \tag{3}$$

onde *i*, é o componente e os sobrescritos *I, II, ..., π,* representam as fases em equilíbrio.

O potencial químico é uma quantidade eminentemente abstrata, mas pode ser relacionado às quantidades fisicamente mensuráveis, tais como temperatura, pressão e composição através de funções auxiliares como o coeficiente de fugacidade que podem ser identificadas com a realidade física. Uma função auxiliar é a fugacidade, e o seu desenvolvimento começa com a relação:

$$\mu_i = \left(\frac{dG}{dn_i} \right)_{T,P,n_{j \neq j}} \tag{4}$$

$$d\mu_i = v_i dP - s_i dT \tag{5}$$

A temperatura constante tem–se:

$$\left(\frac{d\mu_i}{dP} \right)_T = v_i \tag{6}$$

e para um gás ideal:

$$\left(\frac{d\mu_i}{dP} \right)_T = \frac{RT}{P} \tag{7}$$

integrando a *T* constante:

$$\mu_i - \mu_i^o = RT \ln\left(\frac{P}{P^o} \right) \tag{8}$$

e definindo a fugacidade (*f*) como:

$$\frac{f_i}{y_i P} \to 1 \Leftrightarrow P \to 0 \tag{9}$$

Substituindo a Equação 9 na Equação 8:

$$\mu_i - \mu_i^o = RT \ln\left(\frac{f_i}{f_i^o}\right) \tag{10}$$

Escrevendo a Equação 10 para as fases *I* e *II* obtêm–se:

$$\mu_i^I - \mu_i^{oI} = RT \ln\left(\frac{f_i^I}{f_i^{oI}}\right) \tag{11}$$

$$\mu_i^{II} - \mu_i^{oII} = RT \ln\left(\frac{f_i^{II}}{f_i^{oII}}\right) \tag{12}$$

usando as Equações 11 e 12 na igualdade de potenciais (Equação 3), tem–se:

$$\mu_i^{oI} + RT \ln\left(\frac{f_i^I}{f_i^{oI}}\right) = \mu_i^{oII} + RT \ln\left(\frac{f_i^{II}}{f_i^{oII}}\right) \tag{13}$$

Supondo o mesmo estado padrão, tem–se:

$$\mu_i^{oI} = \mu_i^{oII} \tag{14}$$

$$f_i^{oI} = f_i^{oII} \tag{15}$$

o que leva à nova forma da equação fundamental para o equilíbrio de fases:

$$f_i^I = f_i^{II} = \ldots = f_i^{\pi} \tag{16}$$

1.5.2 Relações Termodinâmicas no Equilíbrio Líquido–Líquido

De uma forma geral, o equilíbrio de fases líquido–líquido (ELL) é representado pela condição de isofugacidade, quer dizer, as fugacidades de cada um dos componentes na mistura devem ser iguais ao longo de todas as fases; esta condição é representada pela Equação 17. Para o ELL em um sistema de n espécies a *T* e *P* uniformes, denotam–se as fases líquidas através de sobrescrito *I* e *II*, e escreve–se o critério de equilíbrio como:

$$f_i^I = f_i^{II} \tag{17}$$

No caso de se empregar a abordagem simétrica "*phi–phi*" ou ($\phi - \phi$) para representar as fugacidades de duas fases líquidas, a condição de isofugacidade no ELL é expressa por:

$$f_i^I = \phi_i^I x_i^I P \tag{18}$$

$$f_i^{II} = \phi_i^{II} x_i^{II} P \tag{19}$$

e, com essas substituições, o critério de equilíbrio (Equação 17) pode ser escrito:

$$\phi_i^I x_i^I = \phi_i^{II} x_i^{II} \tag{20}$$

Do ponto de vista termodinâmico, este método apresenta como vantagens a representação uniforme das propriedades termodinâmicas da solução, sem usar estados hipotéticos de referência, a inclusão de dependências com temperatura e pressão, e a possibilidade de calcular também propriedades calorimétricas e volumétricas. O método pode ser usado numa larga faixa de pressões e temperaturas, incluindo condições críticas e supercríticas (PRAUSNITZ et al., 1999).

Nesta abordagem, a capacidade da equação de estado de predizer propriedades de componentes puros, tais como pressão de vapor, entalpia de vaporização ou volume do líquido saturado, é um aspecto fundamental.

Os coeficientes de fugacidade para ambas as fases líquidas são calculados das seguintes relações termodinamicamente exatas:

$$\ln \phi_i^I = \frac{1}{RT} \int_{V^I}^{\infty} \left[\left(\frac{\partial P}{\partial n_i} \right)_{T,V,n_{i \neq j}} - \frac{RT}{V} \right] dV - n \left(\frac{PV^I}{RT} \right) \tag{21}$$

$$\ln \phi_i^{II} = \frac{1}{RT} \int_{V^{II}}^{\infty} \left[\left(\frac{\partial P}{\partial n_i} \right)_{T,V,n_{i \neq j}} - \frac{RT}{V} \right] dV - n \left(\frac{PV^{II}}{RT} \right) \tag{22}$$

Para desenvolver as equações precisa–se de uma equação de estado explicita em *P*, a qual determina a forma analítica de $\left(\frac{\partial P}{\partial n_i} \right)_{T,V,n_{i \neq j}}$.

Por exemplo, para a equação de Soave–Redlich–Kwong:

$$\ln \phi = (Z-1) - \ln(Z-B) - \frac{A}{B} \ln \left(\frac{Z+B}{Z} \right) \tag{23}$$

e para a equação de Peng–Robinson:

$$\ln\phi = (Z-1) - \ln\left(\frac{PV - bP}{RT}\right) + \frac{a}{2\sqrt{2}b}\ln\left[\frac{V + (1-\sqrt{2})b}{V + (1+\sqrt{2})b}\right] \tag{24}$$

Outra alternativa, e a mais usual de se tratar o equilíbrio líquido–líquido se baseia na abordagem $\gamma - \gamma$ que utiliza modelos de energia livre de Gibbs em excesso ($\overline{G}_i^E$); tais como as equações NRTL e UNIQUAC. A energia livre de Gibbs parcial molar está relacionada com a fugacidade por:

$$d\overline{G_i} = RTd\ln\hat{f}_i \tag{25}$$

O coeficiente de atividade γ_i aparece quando se integra a Equação 25 para uma solução real, de um estado puro até um estado em solução a T e P constante:

$$\overline{G} - G_{i\ puro} = RT\ln\frac{\hat{f}_i}{f_{i\ puro}} \tag{26}$$

Adicionando e subtraindo o termo $RT\ln x_i$ no lado direito da Equação 26:

$$\overline{G} - G_{i\ puro} = RT\ln\frac{\hat{f}_i}{x_i f_{i\ puro}} + RT\ln x_i \tag{27}$$

onde a razão $\frac{\hat{f}_i}{x_i f_{i\ puro}}$ é a definição do coeficiente de atividade do componente i na solução (γ_i), que mede o afastamento da solução do comportamento ideal e está relacionada com a maneira pela qual as moléculas se arranjam na solução e com a formação ou quebra de ligações entre as moléculas no processo de mistura a partir dos componentes puros (SANDLER, 2006).

Para uma solução ideal, a Equação 26 pode ser escrito como:

$$\overline{G_i}^{id} - G_{i\ puro} = RT \ln x_i \tag{28}$$

Se subtraímos as Equações 30 da 27 para eliminar o termo RT ln x_i, temos:

$$\overline{G} - \overline{G_i}^{id} = RT \ln \gamma_i \tag{29}$$

$$\overline{G_i}^{E} = RT \ln \gamma_i \tag{30}$$

Com a introdução do coeficiente de atividade a Equação 17 torna–se:

$$\left(\gamma_i^{\ s} x_i f_i^{o}\right)^{I} = \left(\gamma_i^{\ s} x_i f_i^{o}\right)^{II} \tag{31}$$

ou

$$\left(\gamma_i x_i\right)^{I} = \left(\gamma_i x_i\right)^{II} \tag{32}$$

onde x_i é a fração molar do componente i, f_i^o é á fugacidade do componente i no estado de referencia, γ_i^s é o coeficiente de atividade do componente i, encontrado a partir de expressões para a energia livre de Gibbs em excesso (G^E):

$$RT \ln \gamma_i^{\ s} = \left(\frac{\partial G^E}{\partial n_i}\right)_{T,P,n_j} \tag{33}$$

A Equação 32, juntamente com as restrições $\sum x_i^I = 1$ e $\sum x_i^{II} = 1$ constituem o sistema básico de equações para o calculo de equilíbrio liquido–liquido; nesta Equação os coeficientes de atividade do componente i para ambas as fases I e II, são calculados da mesma função a partir da energia livre de Gibbs molar em excesso.

$$\frac{\overline{G}^E}{RT} = \sum_i x_i \ln \gamma_i \tag{34}$$

A única diferença é a fração molar do component *i* em cada uma das fases. Assim, em um sistema liquido–liquido contendo *n* componentes:

$$\gamma_i^I = \gamma_i\left(x_1^I, x_2^I, ..x_{n-1}^I, T, P\right) \tag{35}$$

$$\gamma_i^{II} = \gamma_i\left(x_1^{II}, x_2^{II}, ..x_{n-1}^{II}, T, P\right) \tag{36}$$

De acordo com as Equações 35 e 36 pode–se escrever *n* equações de equilíbrio com *2n* variáveis intensivas (*T, P* e as *n–1* frações molares independentes em cada fase).

Para obter os coeficientes de atividade é necessária a construção de expressões nas quais se obtém G^E como função da composição, temperatura e pressão, onde a variável mais importante é a composição. Para misturas líquidas a baixas pressões, o efeito desta última variável é desprezível. O efeito da temperatura não é desprezível, mas freqüentemente não é muito elevado quando se considera uma faixa de temperatura moderada (TREYBAL, 1982).

No caso da abordagem "*phi–phi*" ($\phi - \phi$), a Equação 32 é substituída pela Equação 20 e os coeficientes de fugacidade foram calculados no presente trabalho empregando a equação de estado CPA EoS.

1.5.4 Modelos Termodinâmicos

A descrição exata do equilíbrio líquido–líquido equilíbrio (LLE) e dados de solubilidade de sistemas multicomponente é a chave para a projeção e simulação de um processo de

produção. As duas abordagens mais populares usadas para o cálculo de equilíbrio de fases de sistemas multicomponente são os modelos de energia de Gibbs em excesso (G^E), tais como as equações NRTL e UNIQUAC, e as equações de estado (EoS).

Os modelos de G^E são capazes de lidar com sistemas altamente não ideais a pressões baixas. No entanto, estes modelos não possuem a capacidade de lidar com gases e componentes em estado supercrítico, altas pressões e inconsistências na região crítica (OLIVEIRA et al., 2010).

As equações de estado são capazes de lidar com uma mistura de um ou mais componentes em estado supercrítico ou próximo do ponto crítico de uma forma consistente. A vantagem das equações de estado é sua grande escala de aplicabilidade na temperatura e na pressão, desde gases leves até líquidos densos e podem ser usadas para modelar equilíbrios líquido–vapor (ELV), líquido–líquido e em fluidos supercríticos (OLIVEIRA et al., 2011).

1.5.4.1 Equações de Estado

As equações de estado cumprem um importante papel na engenharia no estudo do equilíbrio de fases líquido–líquido. Inicialmente, estas foram usadas para componentes puros. As equações de estado cúbicas, como a SRK e PR são, atualmente, as duas equações de estado mais largamente difundidas e usadas na indústria, devido ao fato de aliarem uma estrutura matemática relativamente simples a uma boa capacidade preditiva para misturas constituídas por substâncias de caráter apolar (SOAVE, 1972; PENG e ROBINSON, 1976) ou fracamente polar (HURON et al., 1978; ASSELINEAU et al., 1979; GRABOSKI e DAUBERT, 1978). Esta última característica fez com que estas duas equações tenham se

tornado as preferidas para a modelagem de processos na indústria de petróleo e gás, principalmente na descrição da fase orgânica (i.e., não–aquosa) das misturas. No entanto, estes modelos não conseguem correlacionar adequadamente o ELV de misturas polares numa ampla gama de composições (FRENCH e MALONE, 2005).

Contudo, já foram propostas novas regras de mistura e/ou modelos que consideram explicitamente a associação entre moléculas, e que conseguem representar de forma satisfatória o equilíbrio de fases em misturas não–polares e polares. A equação de estado cúbica CPA (Cubic–Plus–Association Equation of State) é um desses modelos. Este modelo tem um incentivo adicional que é a sua capacidade de representar o ELL e ELV usando o mesmo conjunto de parâmetros (FRENCH e MALONE, 2005).

1.5.4.1.1 A CPA EoS

A equação CPA EoS (Cubic–Plus–Association Equation State) foi originalmente proposta por Kontogeorgis e colaboradores em 1996 (KONTOGEORGIS et al., 1996), tendo sido o seu desenvolvimento motivado pela necessidade de se modelar sistemas com fluidos que apresentem alto grau de associação, principalmente através de ligações de hidrogênio. Esta equação de estado é adequada para sistemas não ideais contendo compostos fortemente polares, tais como água, álcool, glicóis e aminas em grandes faixas de pressão e temperatura. Esta equação já foi aplicada satisfatoriamente a sistemas aquosos com alcanos (FOLAS et al., 2006) e sistemas envolvendo biodiesel e água (OLIVEIRA et al., 2007). VOUTSAS et al. (1999) aplicaram esta equação para misturas de etanol, alcanos e água a fim de predizer o ELL e ELV desse tipo de misturas.

Sua estrutura combina um termo não–associativo (contribuição física) constituído a partir da equação SRK, com um termo de associação que considera as ligações de hidrogênio intermoleculares e os efeitos de solvatação, originalmente propostos por Wertheim, também usados em outras equações de estado, tais como as diferentes versões da SAFT (Statistical Associating Fluid Theory) (MULLER e GUBBINS, 2001).

Usando um termo cúbico geral (SRK: $\delta_1 = 1$, $\delta_2 = 0$; $\delta_1 = 1+\sqrt{2}$, $\delta_2 = 1-\sqrt{2}$) as contribuições cúbicas e associativas da energia de Helmholtz são:

$$A^{cúbica} = \frac{an}{b(\delta_2 - \delta_1)} \ln\left(\frac{1+b\rho\delta_1}{1+b\rho\delta_2}\right) - nRT\ln(1-b\rho) \tag{37}$$

$$A^{assoc.} = RT\sum_i n_i \sum_{A_i}\left[\ln(X_{Ai}) - \frac{X_{Ai}}{2} + \frac{1}{2}\right] \tag{38}$$

a CPA EoS pode ser expressa em termos da pressão *P*, como:

$$P = P^{cúbica} + P^{assoc.} = \frac{RT}{V_m - b} - \frac{a(T)}{V_m(V_m+b)} - \frac{1RT}{2V_m}\left(1+\rho\frac{\partial \ln g}{\partial \rho}\right)\sum_i x_i \sum_{Ai}(1-X_{Ai}) \tag{39}$$

ou pode ser expressa em termos do fator de compressibilidade como:

$$Z = Z^{phys.} + Z^{assoc.} = \frac{1}{1-b\rho} - \frac{a\rho}{RT(1+b\rho)} - \frac{1}{2}\left(1+\rho\frac{\partial \ln g}{\partial \rho}\right)\sum_i x_i \sum_{Ai}(1-X_{Ai}) \tag{40}$$

onde a é o parâmetro de energia, b é o parâmetro de co–volume, ρ é a densidade molar, g é a função simplificada de distribuição radial, X_{Ai} é a fração molar do componente puro i não ligado no ponto A e x_i é a fração molar do componente i.

O parâmetro de energia do componente puro a, é obtido a partir da dependência de temperatura da equação SRK:

$$a(T) = a_0 \left[1 + c_1\left(1 - \sqrt{T_r}\right)\right]^2 \tag{41}$$

onde a_0 e c_1 são estimados (simultaneamente com b) usando–se dados experimentais de pressão de vapor e densidade do componente puro i.

Quando a CPA EoS é utilizada em misturas, os parâmetros de energia e do co–volume do termo físico são calculados utilizando a regra convencional de van der Waals para um líquido em mistura:

$$a = \sum_i \sum_j x_i x_j a_{ij} \qquad a_{ij} = \sqrt{a_i a_j}\left(1 - k_{ij}\right) \tag{42}$$

e

$$b = \sum_i x_i b_i \tag{43}$$

X^{Ai} está relacionada com a força de associação Δ^{AiBj} entre pontos pertencentes a duas moléculas diferentes e é calculado pela resolução do seguinte conjunto de equações:

$$X_{Ai} = \frac{1}{1+\rho\sum_j x_j \sum_{B_j} X_{Bj}\Delta^{A_iB_j}} \tag{44}$$

onde

$$\Delta^{A_iB_j} = g(\rho)\left[\exp\left(\frac{\varepsilon^{A_iB_j}}{RT}\right)-1\right]b_{ij}\beta^{A_iB_j} \tag{45}$$

Onde ε^{AiBj} e β^{AiBj} são a energia de associação e o volume de associação, respectivamente.

A função simplificada de distribuição radial $g(\rho)$ é dada por:

$$g(\rho) = \frac{1}{1-1.9\eta} \qquad \text{onde,} \qquad \eta = \frac{1}{4}b\rho \tag{46}$$

Para determinar os parâmetros de composto puro é necessário atribuir esquemas de associação, ou seja, a quantidade e tipo de sítios de associação presentes nas moléculas. Normalmente usa–se a nomenclatura proposta por Huang e Radosz (1990), conforme mostrado na Tabela 1.1. Nesta tabela, as letras **A, B, C** e **D** que aparecem junto às estruturas moleculares indicam diferentes sítios de associação numa mesma molécula. Os sítios doadores de elétrons são representados por pares de elétrons não ligados, enquanto que os sítios receptores são representados por átomos de hidrogênio ligados ao oxigênio. A observação desta figura mostra que uma mesma classe de composto pode ser modelada de uma ou mais maneiras diferentes, dependendo da conveniência.

Nesta clasificação, considera–se que uma molécula pode ser não–associada (interagindo com as demais somente por forças de dispersão) ou pode apresentar um ou mais sítios de associação.

Por exemplo, os álcoois podem ser modelados pelo esquema **2B** (em que dois pares de elétrons são considerados como um único sítio doador) ou pelo esquema **3B** (considerando os dois pares de elétrons como dois sítios doadores independentes) (KONTOGEORGIS et al., 2006).

Considerações análogas podem ser feitas para compostos não–associativos, ou seja aqueles que são modelados sem sítios de associação, supondo–se que interajam com os demais componentes da mistura apenas através de forças de dispersão. Neste caso, pode–se dizer que na equação de estado CPA para cada composto não associado requer três parâmetros para ser modelado (a_0, c_1 e b) juntamente com sua temperatura crítica.

Por tal motivo, os ésteres etílicos ou metílicos (não–associativos) somente precisam de três parâmetros do componente puro no termo cúbico (a_0, c_1 e b), enquanto para componentes associativos, tais como água, glicerol e etanol, necessitam–se de dois parâmetros adicionais no termo de associação (ε e β). Estes cinco parâmetros são regredidos simultaneamente a partir de dados de pressão de vapor e densidade líquida. A função objetivo para minimizar é a seguinte:

$$OF = \sum_{i}^{NP}\left(\frac{P_i^{\text{exptl}} - P_i^{\text{calcd}}}{P_i^{\text{exptl}}}\right)^2 + \sum_{i}^{NP}\left(\frac{\rho_i^{\text{exptl}} - \rho_i^{\text{calcd}}}{\rho_i^{\text{exptl}}}\right)^2 \tag{47}$$

Tabela 1. 1. Principais Esquemas de Associação Segundo a Terminologia de Huang e Radosz (KONTOGEORGIS et al, 2006).

Classe	Fórmula	Tipo de associação
ácidos carboxílicos	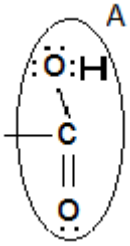	**1A**
álcoois	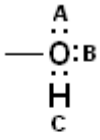 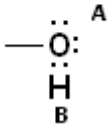	**3B** **2B**
glicóis	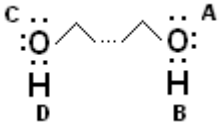	**4C**
água	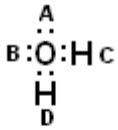 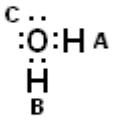 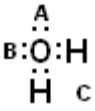	**4C** **3B** **3B**

Para uma mistura binária composta unicamente por componentes não–associativos, o parâmetro de interação binária, k_{ij} (Eq. 42), é o único parâmetro ajustável.

Em misturas, usam–se os parâmetros genéricos ε^{AiBj} e β^{AiBj} para representar, respectivamente, a energia de interação e o volume de associação entre o sítio *A* da molécula *i* com o sítio *B* da molécula *j*. Estes parâmetros associativos normalmente são calculados a partir dos parâmetros dos puros através do uso de regras de combinação. Diferentes regras de combinação têm sido propostas por vários autores, incluindo ε^{AiBj} e β^{AiBj} e também para a intensidade (ou força) de associação Δ^{AiBj} :

$$\varepsilon^{A_iB_j} = \frac{\varepsilon^{A_iB_i} + \varepsilon^{A_jB_j}}{2}, \qquad \beta^{A_iB_j} = \frac{\beta^{A_iB_i} + \beta^{A_jB_j}}{2} \qquad \text{(CR–1)} \qquad (48)$$

$$\varepsilon^{A_iB_j} = \frac{\varepsilon^{A_iB_i} + \varepsilon^{A_jB_j}}{2}, \qquad \beta^{A_iB_j} = \sqrt{\beta^{A_iB_i}\beta^{A_jB_j}} \qquad \text{(CR–2)} \qquad (49)$$

$$\varepsilon^{A_iB_j} = \sqrt{\varepsilon^{A_iB_i}\varepsilon^{A_jB_j}}, \qquad \beta^{A_iB_j} = \sqrt{\beta^{A_iB_i}\beta^{A_jB_j}} \qquad \text{(CR–3)} \qquad (50)$$

No entanto, quando a equação CPA é empregada para misturas contendo dois componentes auto–associados, é necessário usar a regra de combinação CR–4 (Combining Rule–4) ou também conhecida como ECR (Elliott Combining Rule). Esta regra é definida pela expressão que segue:

$$\Delta^{A_iB_j} = \sqrt{\Delta^{A_iB_i}\Delta^{A_jB_j}} \qquad (51)$$

1.5.4.2 Modelos Termodinâmicos para o Coeficiente de Atividade

Muitas expressões semi–empíricas têm sido propostas na literatura para relacionar a energia livre de Gibbs em excesso à composição da mistura e temperatura. Os principais modelos para coeficiente de atividade baseian–se na seguinte concepção: no interior de uma solução líquida, composições locais diferentes da composição global da mistura são responsáveis pelas orientações moleculares de curto alcance e não aleatórias que resultam de diferenças no tamanho molecular e das forças intermoleculares (SMITH et al., 2000). Este conceito foi primeiramente introduzido por Wilson em 1964 com a equação de Wilson e, baseadas nesta, surgiram às equações NRTL (Non–Random–Two–Liquid) de Renon e Prausnitz (1968) e UNIQUAC (Universal Quasi–Chemical) de Abrams e Prauznitz (1975). Estas equações representam as propriedades de misturas fortemente não ideais melhor que as equações clássicas, apresentam dependência de seus parâmetros com a temperatura e são facilmente estendidas para misturas multicomponentes usando parâmetros de interação binária.

1.5.4.2.1 Modelo NRTL

A equação NRTL (Non–Random, Two–Liquid), desenvolvida por RENON e PRAUSNITZ (1968), é também baseada no conceito de composição local, que estabelece que a composição do sistema nas vizinhanças de uma molécula dada não é igual à composição global, por causa das forças intermoleculares. Para sistemas ideais ou moderadamente ideais, o modelo NRTL não oferece muita vantagem sobre outros modelos, como van Laar ou Margules – três sufixos, mas para sistemas fortemente não ideais esta equação pode fornecer uma boa representação dos dados experimentais, embora sejam

necessários dados de boa qualidade para estimar os três parâmetros para cada sistema binário. O modelo NRTL também pode ser facilmente estendido para misturas multicomponentes e dispõe de três parâmetros ajustáveis para cada par de componentes presentes no sistema, ao invés de dois parâmetros, como o modelo UNIQUAC (STRAGEVITCH e d'ÁVILA, 1997).

Cabe ressaltar que estes modelos foram formulados em fração molar, mas em virtude da grande diferença das massas moleculares dos compostos envolvidos no presente estudo, como sistemas graxos e alcoóis de cadeia curta, com a finalidade de permitir um ajuste mais preciso do modelo aos dados experimentais, é aconselhável empregar como unidade de composição a fração mássica.

No modelo NRTL, o coeficiente de atividade com a composição expressa em fração mássica, para um sistema multicomponente, assume a seguinte forma:

$$\gamma_i^w = \left(\frac{\sum_{j=1}^{k} \frac{\tau_{ji} G_{ji} w_j}{\overline{M}_j}}{\sum_{j=1}^{k} \frac{G_{ji} w_j}{\overline{M}_j}} + \sum_{j=1}^{k} \left[\frac{w_j G_{ij}}{\overline{M}_j \sum_{k=1}^{k} \frac{G_{kj} w_k}{\overline{M}_k}} \left(\tau_{ij} - \frac{\sum_{k=1}^{k} \frac{\tau_{kj} G_{kj} w_k}{\overline{M}_k}}{\sum_{k=1}^{k} \frac{G_{kj} w_k}{\overline{M}_k}} \right) \right] \right) \Bigg/ \overline{M}_i \sum_{j=1}^{k} \frac{w_j}{\overline{M}_j} \tag{52}$$

$$\tau_{ij} = \frac{\left(g_{ij} - g_{jj}\right)}{RT} \tag{53}$$

$$\frac{\left(g_{ij} - g_{jj}\right)}{R} = A_{0,ij} + A_{1,ij} T \tag{54}$$

$$\mathrm{G}_{ij} = exp\left(-\alpha_{ij} \tau_{ij}\right) \tag{55}$$

$$\alpha_{ij} = \alpha_{ji} \tag{56}$$

onde γ_i^w é o coeficiente de atividade do composto *i*; w_i é a fração mássica do componente *i*; $\overline{M}_i$ é a massa molecular do componente *i*; $(g_{ij} - g_{jj})$e τ_{ij} $(\neq \tau_{ji})$ representam as interações energéticas moleculares entre os componentes *i* e *j*; α_{ij} $(=\alpha_{ji})$ é o parâmetro de não–randomicidade da mistura; T é a temperatura absoluta; e $A_{0,ij}$, $A_{0,ji}$, $A_{1,ij}$ e $A_{1,ji}$ são os parâmetros de interação energética entre os componentes *i* e *j* ajustáveis aos dados experimentais via programa computacional. O parâmetro α_{ij} está relacionado com a não–randomicidade (ou não–aleatoriedade) da mistura, quer dizer, que os componentes da mistura não se distribuem aleatoriamente (ou seja, uniformemente), mas seguem um padrão ditado pela composição local. Quando α_{ij} é zero, a mistura é completamente aleatória (SANDLER, 2006).

2. REFERÊNCIAS BIBLIOGRÁFICAS

- ABRAMS, D. S. e PRAUSNITZ, J. M. Statistical thermodynamics of liquid mixtures: a new expression for the excess Gibbs energy of partly or completely miscible systems. AIChE , 21, 116–128, 1975.
- ASSELINEAU, L.; BOGDANIC, G.; VIDAL, J. A versatile algorithm for calculating vapour—liquid equilibria. Fluid Phase Equilibr. 3, 273–290, 1979.
- BARNWAL, B. K. e SHARMA, M. P. Prospects of biodiesel production from vegetable oils in India. Renew Sust. Energ. Rev., 9, 363–378, 2005.
- BOZBAS, K. Biodiesel as an alternative motor fuel: Production and policies in the European Union. Renew Sust. Energ. Rev., 12, 542–552, 2008.
- BRASIL. Agência Nacional do Petróleo – ANP. Anuário Estatístico Brasileiro do Petróleo e do Gás Natural 2002. Disponível em: <http://www.anp.gov.br>. Acesso em: 20 jun. 2011.

- CHIU, C–W.; GOFF, M. J. e SUPPES, G. J. Distribution of methanol and catalysts between biodiesel and glycerin phases. AIChE J. 51, 1274–1278, 2005.
- CONAB – Companhia Nacional de Abastecimento Instituto Brasileiro de Geografia e Estatística. Disponível em: <http://www.conab.gov.br>. Acesso em: 20 maio de 2011.
- DEMIRBAS, A. Comparison of transesterification methods for production of biodiesel from vegetable oils and fats. Energ. Convers. Manage, 49, 125–130, 2008.
- DEMIRBAS, A. Progress and recent trends in biodiesel fuels. Energ. Convers. Manage, 50, 14–34, 2009.
- EPA – United States Environmental Protection Agency. A comprehensive analysis of biodiesel impacts on exhaust emissions. EPA 420–P–02001. Final report, October, 2002.
- FOLAS, G. K.; GABRIELSEN, J.; MICHELSEN, M. L.; STENBY, E. H.; KONTOGEORGIS, G. M. Application of the Cubic–Plus–Association (CPA) Equation of State to Cross–Associating systems. Ind. Eng. Chem. Res. 2005, 44, 382.
- FOLLEGATTI–ROMERO, L. A.; LANZA, M.; DA SILVA, C. A. S.; BATISTA, E. A. C AND MEIRELLES, A. J. A. Mutual solubility of pseudobinary systems containing vegetable oils and anhydrous ethanol at (298.15 to 333.15) K. J. Chem. Eng. Data, 55, 2750–2756, 2010.
- FOLLEGATTI–ROMERO, L. A.; BATISTA, F. R. M.; LANZA, M.; DA SILVA, C. A. S.; BATISTA, E. A. C AND MEIRELLES, A. J. A L.A. Liquid−liquid equilibrium for ternary systems containing ethyl esters, anhydrous ethanol and water at 298.15, 313.15, and 333.15 K. Ind. Eng. Chem. Res. 49, 12613–12619, 2010.
- FUKUDA, H.; KONDO, A.; NODA, H. Biodiesel fuel production by transesterification of oils. J. Biosci. Bioeng., 92, 405–416, 2001.
- FRENCH, R. e MALONE, P. Phase equilibria of ethanol fuel blends. Fluid Phase Equilibr., 228–229, 27–40, 2005.
- GONZALO, A.; GARCÍA, M.; SÁNCHEZ, J. L.; ARAUZO, J.; PEÑA, J. A. Water cleaning of biodiesel. Effect of catalyst concentration, water amount, and washing temperature on biodiesel obtained from rapeseed oil and used oil. Ind. Eng. Chem. Res., 49, 4436–4443, 2010.

- GELLER, D. P.; GOODRUM, J. W. Effects of specific fatty acid methyl esters on diesel fuel lubricity. Fuel, 83, 2351–236, 2004.
- GERHARD, K.; DUM, R. O.; BAGBY, M. O. Biodiesel: the use of vegetable oils and their derivatives as alternative diesel fuels. ACS Symp. Ser, 666, 172–208, 1997.
- GERPEN, J. V. Biodiesel processing and production. Fuel Process. Technol, 86 1097–1107, 2005.
- GRABOSKI, M. S. e DAUBERT, T.E. A Modified soave equation of state for phase equilibrium calculations. 1. Hydrocarbon systems. Ind. Eng. Chem. Proc. Dd., 17, 443–448, 1978.
- KONTOGEORGIS, G.M.; MICHELSEN, M. L.; FOLAS, G.K.; DERAWI, S.; SOLMS, N.V.; STENBY, E.H. Ten Years with the CPA (Cubic–Plus–Association) Equation of State. Part 1. Pure Compounds and Self–Associating Systems. Ind. Eng. Chem. Res., 45, 4855–4868, 2006.
- KONTOGEORGIS, G.M.; VOUTSAS, E. C.; YAKOUMIS, I. V. e TASSIOS, D. P. An equation of state for associating fluids. Ind. Eng. Chem. Res., 35, 4310–4318, 1996.
- HUANG, S.H. e RADOSZ, M. Equation of State for Small, Large, Polydisperse, and Associating Molecules. Ind. Eng. Chem. Res., 29, 2284−2294, 1990.
- HURON, M.–J. e VIDAL, J. New mixing rules in simple equations of state for representing vapour–liquid equilibria of strongly non–ideal mixtures. Fluid Phase Equilibr., 3, 255–271, 1979.
- IBGE – Instituto Brasileiro de Geografia e Estatística. Disponível em: <http://www.ibge.gov.br/home/estatistica/indicadores/agropecuaria/lspa/lspa_200809comentarios.pdf>. Acesso em: 21 jun. 2011.
- JONES, J. C. On the Use of ethanol in the processing of biodiesel fuels (Letter to the editor). Fuel, 89, 1183, 2010.
- LANG, X.; DALAI, A. K.; BAKHSHI, N. N.; REANEY, M. J.; HERTZET, P. B. Preparation and characterization of bio–diesels from various bio–oils. Bioresource Technol., 80, 53–62, 2001.
- LANZA, M.; NETO, W. B.; BATISTA, B.; POPPI, R. J.; MEIRELLES, A. J. A. Liquid–liquid equilibrium data for reactional systems of ethanolysis at 298.3 K. J. Chem. Eng. Data, 53, 5–15, 2008.

- LEE, S. W.; HERAGE, T.; YOUNG, B. Emission reduction potential from the combustion of soy methyl ester fuel blended with petroleum distillate fuel. Fuel, 83, 1607–1613, 2004.
- LIU, X.; HE, H.; WANG, Y.; ZHU, S.; PIAO, X. Transesterification of soybean oil to biodiesel using cao as a solid base catalyst. Fuel, 87, 216–221, 2008.
- LOOTTY, M.; PINTO, H.; EBELING, F. Automotive fuel consumption in Brazil: Applying static and dynamic systems of demand equations. Energ. Policy, 37, 5326–5333, 2009.
- MACEDO, I. C.; SEABRA, J. E. A.; SILVA, J. E. A. R. Green house gases emissions in the production and use of ethanol from sugarcane in Brazil: The 2005/2006 averages and a prediction for 2020. Biomass and Bioenergy, 32, 582–595, 2008.
- MAKAREVICIENE, V.; JANULIS, P. Environmental effect of rapeseed oil ethyl ester. Renew Energ, 28, 2395–2403, 2003.
- MARCHETTI, J. M.; MIGUEL, V. U.; ERRAZU, A.F. Possible methods for biodiesel production. Renew Sust. Energ. Rev., 11, 1300–1311, 2007.
- MEHER, L. C.; SAGAR, D. V.; NAIK, S. N. Technical aspects of biodiesel production by transesterification—a review. Renew Sust. Energ. Rev., 10, 248–268, 2006.
- MEIRELLES, A.; WEISS, S.; HERFURTH, H. Ethanol dehydration by extractive distillation. J. Chem. Technol. Biot., 53, 181–188, 1992.
- MENEGHETTI, S. M. P.; MENEGHETTI, M. R.; WOLF, C. R.; SILVA, E. C.; LIMA, G. E. S.; SILVA, L. L.; SERRA, T. M.; CAUDURO, F.; OLIVEIRA, L. G. Biodiesel from castor oil: A comparison of ethanolysis versus methanolysis. Energ. Fuels, 20, 2262–2265, 2006.
- MESQUITA, A. S.: Do azeite de dendê de ogum ao palm oil commodity: uma oportunidade que a Bahia não pode perder. Bahia Agricola, Salvador, 5, 22–27, 2002.
- MÜLLER, E. A. GUBBINS, K. E. Molecular–based equations of state for associating fluids: a review of saft and related approaches. Ind. Eng. Chem. Res., 40, 2193–2211, 2001.
- MURILLO, S.; MÍGUEZ, J. L.; PORTEIRO, J.; GRANADA, E.; MORÁN, J. C. Performance and exhaust emissions in the use of biodiesel in outboard diesel engines. Fuel, 86, 1765–1771, 2007.

- NEGI, D. S.; SOBOTKA, F.; KIMMEL, T.; WOZNY, G.; SCHOMÄCKER, R. Liquid–liquid phase equilibrium in glycerol–methanol–methyl oleate and glycerol–monoolein–methyl oleate ternary systems. Ind. Eng. Chem. Res., 45, 3693–3696, 2006.
- SAIFUDDIN, N. e CHUA, K. H. Production of ethyl ester (biodiesel) from used frying oil: optimization of transesterification process using microwave irradiation. Malaysian Journal of Chemistry, 6, 77–82, 2004.
- SANDLER, S. I. Chemical and Engineering Thermodynamics. Four edition, Cingapura: John Willey and Sons, p. 622, 2006.
- SIVAPRAKASAM, S. e SARAVANAN, C. G. Optimization of the transesterification process for biodiesel production and use of biodiesel in a compression ignition engine. Energ Fuels, 21, 2998–3003, 2007.
- SOAVE, G., Equilibrium constants from a modified Redlich–Kwong equation of state. Chem Eng. Sci., 27, 1197–1203, 1972.
- STRAGEVITCH, L.; D'ÁVILA, S. G. Application of a generalized maximum likelihood method in the reduction of multicomponent liquid–liquid equilibrium Data. Braz. J. Chem. Eng. Data, 14, 41–52, 1997.
- TILMAN, D.; HILL, J.; LEHMAN, C. Carbon–negative biofuels from low–input high–diversity grassland biomass. Science, 8, 1598–1600, 2006.
- OLIVEIRA, M. B., FREIRE, M. G.; MARRUCHO, I. M.; KONTOGEORGIS, G. M.; QUEIMADA, A. J. e COUTINHO J. A. P. Modeling the liquid−liquid equilibria of water + fluorocarbons with the cubic–plus–association equation of state. Ind. Eng. Chem. Res., 46, 1415–1420, 2007.
- OLIVEIRA, M. B.; MIGUEL, S. I.; QUEIMADA, A. J.; COUTINHO, J. A. P. Phase equilibria of ester plus alcohol systems and their description with the Cubic–Plus–Association Equation of State. Ind. Eng. Chem. Res.; 49, 3452–3458, 2010.
- OLIVEIRA, M. B.; QUEIMADA, A. J.; COUTINHO J. A. P. Prediction of near and supercritical fatty acid ester plus alcohol systems with the CPA EoS. J. Supercrit Fluid; 52, 241–248, 2010.
- OLIVEIRA, M. B., RIBEIRO, V.; QUEIMADA, A. J.; COUTINHO, J. A. P. Modeling phase equilibria relevant to biodiesel production: A comparison of g(E)

Models, Cubic EoS, EoS–g(E) and Association EoS. Ind. Eng. Chem. Res., 50, 2348–2358, 2011.

- PENG, D.–Y. e ROBINSON, D. B. A New Two–Constant Equation of State. Ind. Eng. Chem. Fund., 15, 59–64, 1976.
- PETERSON, C. L.; HUSTRULID, T. Cabon cycle for rapeseed oil biodiesel fuels. Biomass Bioenerg., 14, 91–101, 1998.
- PIMENTEL, D.; PATZEK, T. W. Ethanol production using corn, switchgrass, and wood; biodiesel production using soybean and sunflower. Natural Resources Research 14, 65–76, 2005.
- POUSA, G. P. A. G.; SANTOS, A. L. F.; SUAREZ, P. A. Z. History and policy of biodiesel in Brazil. Energ. Policy, 35, 5393–5398, 2007.
- PRAUSNITZ, J. M., LICHTENTHALER, R. N.; AZEVEDO, E. G. Molecular Thermodynamics of Fluid Phase Equilibria. 3rd ed., Englewood Cliffs, N.J.: Prentice Hall, 1999.
- PRIAMO, W. Determinação de dados de equilíbrio líquido–líquido de sistemas óleo de farelo de arroz/ácido graxo/etanol/hexano. Tese de doutorado. DEA/FEA/UNICAMP, Campinas – SP, p.173. 2008.
- REIJNDERS, L.; HUIJBREGTS, M. A. J. Biogenic greenhouse gas emissions linked to the life cycles of biodiesel derived from European rapeseed and Brazilian soybeans. J. Clean Prod., 16, 1943–1948, 2008.
- REIJNDERS, L.; HUIJBREGTS, M. A. J. Palm oil and the emission of carbon–based greenhouse gases. J. Clean Prod., 16, 477–482, 2008.
- RENON, H.; PRAUSNITZ, J. M. Estimation of parameters for the nrtl equation for excess Gibbs energies of strongly nonideal liquid mixtures, Ind. Eng. Chem. Proc. Des. Dev., 8, 413–419, 1969.
- SMITH, J. M.; VAN NESS, H. C.; ABBOTT, M. M. Introdução à Termodinâmica da Engenharia Química. 5ª ed. Rio de Janeiro: LTC, 2000.
- SUPPES, G. J.; BOCKWINKEL, K.; LUCAS, S.; BOTTS, J. B.; MASON, M. H. E.; HEPPERT J.A. Calcium carbonate catalyzed alcoholysis of fats and oils. JAOCS, 78, 139–145, 2001.

- TAT, M. E.; WANG, P. S.; GERPEN, J. H. V.; CLEMENTE, T. E. Exhaust emissions from an engine fueled with biodiesel from high–oleic soybeans. JAOCS, 84, 865–869, 2007.
- TREYBAL, R. E. Mass–Transfer Operations, 3° ed., McGraw–Hill Book Company, 1982.
- VOUTSAS, E. C.; YAKOUMIS, I. V.; TASSIOS, D. P. Prediction of phase equilibria in water/alcohol/alkane systems. Fluid Phase Equilibr., 160, 151–163, 1999.
- ZHANG, Y.; DUBÉ, M. A.; MCLEAN, D. D.; KATES, M. Biodiesel production from waste cooking oil: 1. Process design and technological assessment. Bioresource Technol., 89, 1–16, 2003.
- ZHOU, W. e BOOCOCK, D. G. B. Phase distributions of alcohol, glycerol, and catalystin the transesterification of soybean oil. JAOCS, 83, 1047–1052, 2006.
- ZHOU, H.; LU, H. e LIANG, B. Solubility of multicomponent systems in the biodiesel production by transesterification of jatropha curcas l. oil with methanol. J. Chem. Eng. Data, 51, 1130–1135, 2006.

CAPÍTULO 2

Solubility of Pseudobinary Systems Containing Vegetable Oils and Anhydrous Ethanol at (298.15 to 333.15) K

Luis A. Follegatti–Romero, Marcelo Lanza, César A. S. da Silva, Eduardo A. C. Batista, and Antonio J. A. Meirelles*

ExTrAE, Laboratory of Extraction, Applied Thermodynamics and Equilibrium, Department of Food Engineering, Faculty of Food Engineering, P.O. Box 6121, University of Campinas–UNICAMP, 13083–862, Campinas, SP, Brazil

*Corresponding author. Fax: +55 19 3521 4027, E–mail: tomze@fea.unicamp.br

Artigo publicado no Journal of Chemical & Engineering Data, 55 (1), pp 440–447, 2010.

Abstract

The two–phase base–catalyzed transesterification of vegetable oils with short chain alcohols is common in the production of biodiesel. The reactants (vegetable oil and ethanol) are partially soluble and this phase behavior can significantly impact on the reaction process. In order to better understand this phase behavior, the liquid–liquid equilibrium data for pseudobinary systems containing vegetable oils (soybean oil, sunflower oil, rice bran oil, cottonseed oil, palm olein and palm oil) + anhydrous ethanol in the range from (298.15 to 333.15) K were determined experimentally. The mutual solubility increased as the temperature rose in all the systems examined. The equilibrium data were correlated with the NRTL model using temperature–dependent parameters which represented satisfactorily the experimental results.

Keywords: Liquid–liquid equilibrium, transesterification, pseudobinary systems, vegetable oils, NRTL.

2.1 Introduction

Biodiesel, as an alternative fuel, has many merits. It is biodegradable, produced from renewable energy sources (vegetable oils and animal fats), nontoxic and may decrease the emission levels of some pollutants gases. Depending on the climate and soil conditions, different countries are looking for different types of vegetable oils for the production of biodiesel as a promising substitute of petroleum based fuels. For example, soybean oil is of primary interest as a source of biodiesel in Brazil and in the United States, whilst many European countries are using rapeseed oil and Asian countries prefer to use palm oil. In fact, any vegetable oil, such as cottonseed, sunflower or rice bran oils could be used to produce biodiesel.[1,2]

The interest in using of ethanol as a reactant in transesterification of oils has significantly increased in recent years since it is derived from agricultural products, is renewable, and is biologically less objectionable to the environment. Although ethanolysis has technological limitations when compared to methanolysis, it is the better route chosen in the Brazilian case, since Brazil is one of the biggest ethanol producers.[2]

The most widely used method to produce biodiesel is that of transesterification, where the chemical reaction between the vegetable oils and the alcohol occurs in the presence of an alkaline catalyst to generate a fatty acid ester and glycerol; the latter being considered as a by–product.[3] Biodiesel reaction can be catalyzed by sodium or potassium hydroxides, acids, enzymes, ion exchange resins and oxides. In most cases the reaction is conducted at a temperature within the range of 303.15–343.15 K.[4–8] As normally practiced transesterification shows a complex phase behavior, starting with two phases due to the fact that the reactants (alcohol and vegetable oil) are partially miscible. Thus there is an upper

alcohol phase in which the catalyst is dissolved, and a lower vegetable oil phase, requiring vigorous stirring to promote mass transfer between the oil and the ethanol phases.[9]

Several studies have identified the important variables that influence the transesterification reaction, including: the reaction time and temperature, the molar alcohol to oil ratio, the type and amount of catalyst and the purity of the reactants.[10,11] However, the mutual solubility of the reactants at these temperature has not been extensively studied. The solubility of ethanol in the oil can greatly influence the reaction rate during the production of biodiesel. For this reason, the liquid–liquid equilibrium for the pseudobinary systems containing alcohol and different vegetable oils must be known in order to design and develop the reactive process. Some research groups have recently published experimental results on the phase behavior of reactants and products present in the biodiesel reaction.[12–15]

In this work, the values for the mutual solubility of different vegetable oils (soybean, sunflower, rice bran, cottonseed and palm) and palm olein (liquid fraction from palm oil) in anhydrous ethanol were measured. The following pseudobinary systems were investigated at temperatures between (298.15 and 333.15) (± 0.1) K: refined soybean oil + anhydrous ethanol, refined sunflower oil + anhydrous ethanol, refined rice bran oil + anhydrous ethanol, pretreated cottonseed oil (neutral) + anhydrous ethanol, and refined palm olein + anhydrous ethanol. The refined palm oil + anhydrous ethanol system was investigated in the temperature range from (318.15 to 333.15) (± 0.1) K, because the melting point of this oil is about 309.15 K and it is semi–solid at room temperature.[16] The experimental data were correlated with the NRTL[17] (*non–random, two–liquid)* model using temperature–dependent parameters.

2.2 Experimental Section

2.2.1 Materials.

The solvents used in this work were anhydrous ethanol and hexane, both from Merck (Germany) and with a mass purity of 99.9 %. Refined soybean and sunflower oils were purchased from Cargill (Mairinque/SP, Brazil), and refined rice bran oil from Irgovel S.A. (Pelotas/RS, Brazil). The pretreated cottonseed oil (neutral oil) was submitted to a prior treatment (deacidification) in the refinery (kindly supplied by Maeda, Itumbiara/GO, Brazil), being qualified as a semi processed oil. Refined palm oil and palm olein were kindly supplied by Agropalma (Belém/PA, Brazil). Due to its composition, the palm oil can be fractionated by crystallization into a liquid fraction (65 to 70) %, known as palm olein, and a solid fraction (30 to 35) %, known as palm stearin.[16]

The fatty acid compositions of the vegetable oils studied in this work are presented in Table 2.1. These compositions were determined by gas chromatography of the fatty acid methyl esters using the official AOCS method (1–62).[18] Prior to the chromatographic analysis the fatty acids of the samples were transformed into the respective fatty acid methyl ester using the method of Hartman and Lago.[19] The chromatographic analyses were carried out using a capillary gas chromatographic system under the same experimental conditions shown in Lanza et al.[20]

Table 2. 1. Fatty Acid Compositions of the Vegetable Oils.

fatty acids	symbol	C*x*:y[a]	*M*[b]	refined soybean	refined sunflower	refined rice bran	pretreated cottonseed	refined palm olein	refined palm
			g·mol^{-1}	100 *w*	100 *w*	100 *w*	100 *w*	100 *w*	100 *w*
octanoic	Cp	C8:0	144.22						0.08
decanoic	C	C10:0	172.27						0.09
dodecanoic	L	C12:0	200.32					0.27	1.15
tetradecanoic	M	C14:0	228.38	0.09	0.09	0.24	0.75	0.80	1.24
hexadecanoic	P	C16:0	256.43	11.54	6.40	19.42	22.79	35.11	40.68
cis–hexadec–9–enoic	Po	C16:1	254.42	0.08	0.13	0.21	0.93	0.17	0.15
heptadecanoic	Ma	C17:0	270.45		0.05			0.09	0.10
cis–heptadec–9–enoic	Mg	C17:1	268.48		0.04			0.03	
octadecanoic	S	C18:0	284.49	2.98	3.23	1.51	2.35	4.42	4.72
cis–octadec–9–enoic	O	C18:1	282.47	22.91	31.89	39.59	16.04	46.55	41.78
cis,cis–octadeca–9,12–dienoic	Li	C18:2	280.45	55.76	56.27	36.37	56.41	11.4	8.84
trans,trans–octadeca–9,12–dienoic[c]		C18:2t[c]		0.24	0.17	0.15		0.13	0.31
all–cis–octadeca–9,12,15–trienoic	Le	C18:3	278.44	5.27	0.33	1.48	0.16	0.32	0.18
all–trans–octadeca–9,12,15–trienoic[c]		C18:3t[c]		0.55		0.16			
icosanoic	A	C20:0	312.54	0.25	0.27	0.42	0.26	0.38	0.39
cis–icos–9–enoic	Ga	C20:1	310.52	0.10	0.23	0.35	0.12	0.17	0.15
docosanoic	Be	C22:0	340.59	0.23	0.65	0.10	0.19	0.07	0.07
tetracosanoic	Lg	C24:0	368.65		0.25			0.09	0.07
IV[d]				130.90	126.01	100.18	110.47	59.20	49.61

[a] C*x*:*y*, *x* = number of carbon and *y* = number of double bonds. [b] *M* = molar mass [c] Trans isomers. [d] Iodine value (IV) calculated from the fatty acid composition according to the method Cd 1c–85.[35]

From the fatty acid compositions were calculated the probable triacylglycerol compositions (Table 2.2) of the vegetable oils using the algorithm suggested by Antoniosi Filho et al.[21] In order to calculate the probable triacylglycerol compositions, the quantities of *trans* isomers (see Table 2.1) were computed with their respective *cis* isomers. In Table 2.2 the main triacylglycerol represents the component with the greatest composition in the isomer set with *x* carbons and *y* double bonds. For the fitting process of the thermodynamic model, the vegetable oil was treated as a single triacylglycerol with the average molar mass of the oil. For this reason, the average molar masses of the vegetable oils were calculated using the probable triacylglycerol compositions (Table 2.2). The values obtained for the

refined soybean, sunflower, rice bran and cottonseed oils, refined palm olein and refined palm oil, were (871.8, 877.0, 880.0, 861.0, 853.5 and 845.7) g·mol^{-1}, respectively.

Table 2. 2 Probable Triacylglycerol Compositions of the Vegetable Oils

main TAG[a]	group	*M*	refined soybean	refined sunflower	refined rice bran	pretreated cottonseed	refined palm olein	refined palm
		g·mol^{-1}	100 *w*	100 *w*	100 *w*	100 *w*	100 *w*	100 *w*
LOP	46:1[b]	777.25					0.52	2.30
PPP	48:0	807.32					1.96	4.71
MOP	48:0	805.31					1.44	2.05
MLiP	48:2	803.30				0.73	0.59	
LOO	48:2	803.29						2.22
PPS	50:0	835.37					0.64	1.50
POP	50:2	833.36	1.01	0.50	5.10	2.90	23.45	26.68
PLiP	50:3	831.34	2.08	0.97	4.97	10.44	6.82	6.77
PPoLi	50:3	829.33				1.42		
PLeP	50:3	829.33			0.56			
MLiO	50:4	829.34					0.57	
MLiLi	52:1	827.31				0.92		
POS	52:2	861.41	0.71		0.79	0.58	5.24	5.81
POO	52:3	859.40	3.91	3.27	10.41	3.98	25.82	23.24
POLi	52:4	857.38	10.30	8.88	18.15	14.39	12.42	9.75
PLiLi	52:5	855.36	11.44	8.59	9.36	25.66	1.94	1.28
PoLiLi	52:5	853.35				0.98		
PLiLe	54:1	853.35	2.52		0.85			
POA	54:1	889.46					0.69	0.78
SOO	54:3	887.45	1.31	1.91	1.07		3.04	2.68
PLiA	54:3	887.45				0.53		
SOLi	54:4	885.43	5.27			1.84		
OOO	54:5	885.43		7.88	7.09		8.16	6.03
OOLi	54:6	883.42	13.79	20.65	17.84	6.23	5.28	3.41
OLiLi	54:7	881.40	21.86	29.53	16.75	13.47	1.42	0.79
LiLiLi	54:8	879.38	18.11	17.82	6.36	15.93		
LiLiLe	56:2	877.37	5.84		0.70			
OLiA	58:3	913.49	1.85					

[a] Groups with a total triacylglycerol (TAG) composition lower than 0.5 % were ignored, [b] *x:y*, *x* = number of carbons (except carbons of glycerol), *y* = number of double bonds.

2.2.2 Apparatus and Procedures.

The liquid–liquid equilibrium data for the model systems containing vegetable oils + anhydrous ethanol were measured at (298.15 to 333.15) (± 0.1) K. The mutual solubility data were determined using equilibrium glass cells (50 mL) similar to those used by Silva

et al.[22] Known quantities of each component, weighed on an analytical balance with a precision of 0.0001 g (Precisa, model XT220A, Sweden), were added directly to the equilibrium glass cells and allowed to reach equilibrium following the same procedures described by Lanza et al.[20]. At the end of the experiment, samples were taken separately from the upper and bottom phases using syringes containing previously weighed masses of hexane, in order to instantly dilute the samples and avoid their separation into two liquid phases at ambient temperature.

The composition of both phases was determined in triplicate by gravimetric analysis. The anhydrous ethanol and hexane were removed by evaporation using an air–circulating oven at 353.15 K for 12 h, and subsequently in a vacuum oven (pressure = 4.67 kPa, temperature = 323.15 K) to complete the removal of both solvents. The samples were then weighed again to determine the mass of vegetable oil in the sample, since this was nonvolatile. The compositions of the two phases were easily calculated from the masses of vegetable oils and ethanol.

2.2.3 Thermodynamic Modeling.

The concept of local composition basically establishes that the composition of the system in the neighborhood of a given molecule is not the same as the "bulk" composition because of intermolecular forces.[23] The NRTL model is based on the local composition concept, and is applicable to partially miscible systems.[24,25]

Due to the large difference in molar mass between vegetable oils and ethanol, some prior investigations have opted for expressing the NRTL model in terms of mass fraction.[12] In this case the NRTL–model for pseudobinary mixtures is expressed as follows:

$$\gamma_i^w = \exp\left\{\left(\frac{w_7}{M_7}\right)^2\left[\tau_{7i}\left(\frac{G_{7i}}{\frac{w_i}{\overline{M}_i}+\frac{G_{7i}w_7}{M_7}}\right)^2+\frac{\tau_{i7}G_{i7}}{\left(\frac{w_7}{M_7}+\frac{G_{i7}w_i}{\overline{M}_i}\right)^2}\right]\right\}\Bigg/\overline{M}_i\left(\frac{w_i}{\overline{M}_i}+\frac{w_7}{M_7}\right) \quad (1)$$

$$\gamma_7^w = \exp\left\{\left(\frac{w_i}{\overline{M}_i}\right)^2\left[\tau_{i7}\left(\frac{G_{i7}}{\frac{w_7}{M_7}+\frac{G_{i7}w_i}{\overline{M}_i}}\right)^2+\frac{\tau_{7i}G_{7i}}{\left(\frac{w_i}{\overline{M}_i}+\frac{G_{7i}w_7}{M_7}\right)^2}\right]\right\}\Bigg/M_7\left(\frac{w_i}{\overline{M}_i}+\frac{w_7}{M_7}\right) \quad (2)$$

and

$$\tau_{i7} = \frac{(g_{i7}-g_{77})}{RT} \quad (3)$$

$$\tau_{7i} = \frac{(g_{7i}-g_{ii})}{RT} \quad (4)$$

$$\frac{(g_{i7}-g_{77})}{R} = A_{0,i7} + A_{1,i7}T \quad (5)$$

$$\frac{(g_{7i}-g_{ii})}{R} = A_{0,7i} + A_{1,7i}T \quad (6)$$

$$\mathrm{G}_{i7} = exp(-\alpha_{i7}\tau_{i7}) \quad (7)$$

$$\mathrm{G}_{7i} = exp(-\alpha_{7i}\tau_{7i}) \quad (8)$$

$$\alpha_{i7} = \alpha_{7i} \quad (9)$$

Where: γ_i^w is the activity coefficient of the vegetable oil (i = 1 to 6); i.e. refined soybean oil (*1*), refined sunflower oil (*2*), refined rice bran oil (3), pretreated cottonseed oil (*4*), refined palm olein (*5*), refined palm oil (*6*); γ_7^w is the activity coefficient of ethanol, both expressed on the mass fraction scale; $\overline{M}_i$, M_7 and w are the average molar mass of vegetable oil, molar mass of ethanol, and mass fraction of the components in the mixture, respectively. $(g_{i7} - g_{77})$ and τ_{i7} $(\neq \tau_{7i})$ represent the molecular energy interactions between components *i*–7, α_{i7} $(=\alpha_{7i})$ is the non–randomness parameter of the mixture, meaning that the components are distributed in a pattern dictated by the local composition, and *T* is the absolute temperature; $A_{0,i7}$, $A_{0,7i}$, $A_{1,i7}$ and $A_{1,7i}$ are the characteristic energy parameters of the interactions between molecules *i* and 7.

The values for the nonrandomness parameter α were not adjusted in the present work, but fixed according to the following criteria: the molecular weight of the edible oils are very similar, with a difference not larger than 4.0 %, but their iodine values show significant differences (see Table 2.1). Sunflower and soybean oils have very similar unsaturation degree, so that the α–value for the system sunflower oil + ethanol was fixed at the value adjusted by Lanza et al.[20] for the soybean oil + ethanol system. The same occurs for palm oil and palm olein and the α–value adjusted by Lanza et al.[20] for the first system was also selected for the olein + ethanol system. Cottonseed and rice bran oils form a third group with an iodine value close to the average of the values observed for soybean and palm oils. For this reason the α–value for the systems cottonseed oil+ ethanol and rice bran oil + ethanol was fixed at 0.3. Note that in all cases the α–values are within the range 0.2–0.47 suggested by Renon and Prausnitz.[26]

In the present work, the parameters published by Lanza et al.[20] were used to predict the LLE data for the refined palm oil + ethanol and refined soybean oil + ethanol systems (see Table 2.4). For the other pseudobinary systems, the experimental data were used to fit the temperature–dependent parameters of the NRTL model. This fitting was done by treating the vegetable oil + anhydrous ethanol system as a pseudobinary one, being the vegetable oil considered as a single triacylglycerol with the average molar mass of the oil. This approach assumes that the different triacylglycerols present in the vegetable oil behave in a very similar way in the liquid–liquid system under analysis. In this case, such compounds can be adequately replaced by a pseudocomponent having the corresponding average physical–chemical properties. This approach was already evaluated by Lanza et al.,[12] who proved its veracity. Estimation of the parameters was based on minimization of the objective function of compositions, eq 10, following the algorithm developed in FORTRAN language by Stragevitch and d'Avila.[27]

$$\mathrm{OF}_{i,7}(w) = \sum_{n}^{N} \left[\left(\frac{w_{i,n}^{\mathrm{AP,exptl}} - w_{i,n}^{\mathrm{AP,calcd}}}{\sigma_{w_{i,n}^{\mathrm{AP}}}} \right)^2 + \left(\frac{w_{i,n}^{\mathrm{OP,exptl}} - w_{i,n}^{\mathrm{OP,calcd}}}{\sigma_{w_{i,n}^{\mathrm{OP}}}} \right)^2 \right] \qquad (10)$$

Where $\mathrm{OF}_{i7}(w)$ is the objective function for each system, N is the total number of tie lines of the corresponding system, w is the mass fraction, i is the vegetable oil (for instance, $i = 1$ for soybean oil), the subscript n is tie line number, and the superscripts AP and OP stand for the alcohol and oil phases, respectively; exptl and calcd refer to experimental and calculated compositions and $\sigma_{w_{i,n}^{\mathrm{AP}}}$ and $\sigma_{w_{i,n}^{\mathrm{OP}}}$ are the standard deviations observed in the compositions of the two liquid phases.

The parameter estimation procedure is based on liquid–liquid flash calculations using the compositions at the midpoint of the experimental tie lines as the feed stream concentration.[27,28] For both phases the average deviation (Δw_{i7}) between the experimental and calculated compositions were calculated according to eq 11, where K is the total number of pseudocomponents in the fatty system (K=2).

$$\Delta w_{i7} = \sqrt{\frac{\left[\left(w_{i,n}^{\mathrm{AP,exptl}} - w_{i,n}^{\mathrm{AP,calcd}}\right)^2\right] + \left[\left(w_{i,n}^{\mathrm{OP,exptl}} - w_{i,n}^{\mathrm{OP,calcd}}\right)^2\right] + \left[\left(w_{7,n}^{\mathrm{AP,exptl}} - w_{7,n}^{\mathrm{AP,calcd}}\right)^2\right] + \left[\left(w_{7,n}^{\mathrm{OP,exptl}} - w_{7,n}^{\mathrm{OP,calcd}}\right)^2\right]}{2NK}} \quad (11)$$

2.3 Results and Discussion

Table 2.3 gives the experimental liquid–liquid equilibrium data for the studied pseudo-binary systems.

Figures 2.1 to 2.5 show the equilibrium diagrams for the systems containing vegetable oils (soybean, sunflower, rice bran, cottonseed oil and palm olein) + anhydrous ethanol at (298.15 to 333.15) (± 0.1) K. The equilibrium diagram for the system containing refined palm oil + ethanol was studied at (318.15 to 333.15) (± 0.1) K, and it is shown in Figure 6. As can be observed in these figures, the mutual solubility of vegetable oils and ethanol was enhanced by the increase in temperature.

Table 2. 3 Experimental Liquid–Liquid Equilibrium Data for the Pseudobinary Systems Containing Vegetable Oils (*i*) + Anhydrous Ethanol (*7*) at (298.15 to 333.15) (± 0.1) K

T/K	oil (*i*)[a]	overall composition		alcohol phase		oil phase	
		100 w_i	100 w_7	100 w_i	100 w_7	100 w_i	100 w_7
298.15	soybean (*1*)	49.95	50.05	6.88	93.12	83.70	16.30
303.15		49.95	50.05	7.72	92.28	82.06	17.94
308.15		49.94	50.06	8.79	91.21	80.96	19.04
313.15		50.00	50.00	9.97	90.03	78.71	21.29
318.15		49.96	50.04	11.57	88.43	74.90	25.10
323.15		49.95	50.05	14.61	85.39	72.45	27.55
328.15		49.95	50.05	16.99	83.01	68.61	31.39
333.15		49.95	50.05	22.98	77.02	63.81	36.19
298.15	sunflower (*2*)	49.92	50.08	6.21	93.79	83.95	16.05
303.15		49.95	50.05	7.47	92.53	82.21	17.79
308.15		49.96	50.04	8.72	91.28	80.94	19.06
313.15		49.95	50.05	9.25	90.75	79.07	20.93
318.15		49.95	50.05	10.95	89.05	77.56	22.44
323.15		49.95	50.05	12.32	87.68	74.25	25.75
328.15		49.95	50.05	15.81	84.19	69.19	30.81
333.15		49.95	50.05	19.60	80.40	64.02	35.98
298.15	rice bran (*3*)	50.00	50.00	7.04	92.96	85.39	14.61
303.15		49.95	50.05	9.01	90.99	83.54	16.46
308.15		49.95	50.05	10.32	89.68	81.49	18.51
313.15		49.95	50.05	12.21	87.79	78.04	21.96
318.15		49.95	50.05	13.42	86.58	75.99	24.01
323.15		49.94	50.06	15.49	84.51	71.81	28.19
328.15		49.95	50.05	18.91	81.09	66.56	33.44
333.15		50.05	49.95	23.99	76.01	60.66	39.34
298.15	cottonseed (*4*)	49.95	50.05	7.93	92.07	84.39	15.61
303.15		49.95	50.05	9.01	90.99	82.22	17.78
308.15		49.95	50.05	10.35	89.65	79.19	20.81
313.15		49.94	50.06	12.55	87.45	75.84	24.16
318.15		49.96	50.04	13.70	86.30	73.21	26.79
323.15		49.95	50.05	17.38	82.62	70.28	29.72
328.15		49.95	50.05	20.52	79.48	64.87	35.13
333.15		49.95	50.05	26.54	73.46	58.57	41.43
298.15	palm olein (*5*)	49.95	50.05	7.13	92.87	85.50	14.50
303.15		49.95	50.05	8.49	91.51	83.37	16.63
308.15		49.96	50.04	9.63	90.37	81.81	18.19
313.15		49.95	50.05	10.63	89.37	78.31	21.69
318.15		49.97	50.03	12.58	87.42	75.98	24.02
323.15		49.95	50.05	14.85	85.15	73.49	26.51
328.15		49.95	50.05	17.60	82.40	70.50	29.50
333.15		49.95	50.05	20.25	79.75	65.73	34.27
318.15	palm (*6*)	49.99	50.01	12.04	87.96	77.89	22.11
323.15		49.95	50.05	15.65	84.35	73.70	26.30
328.15		49.95	50.05	17.03	82.97	69.41	30.59
333.15		49.95	50.05	22.61	77.39	62.39	37.61

[a] *i* = reference number of the oil used.

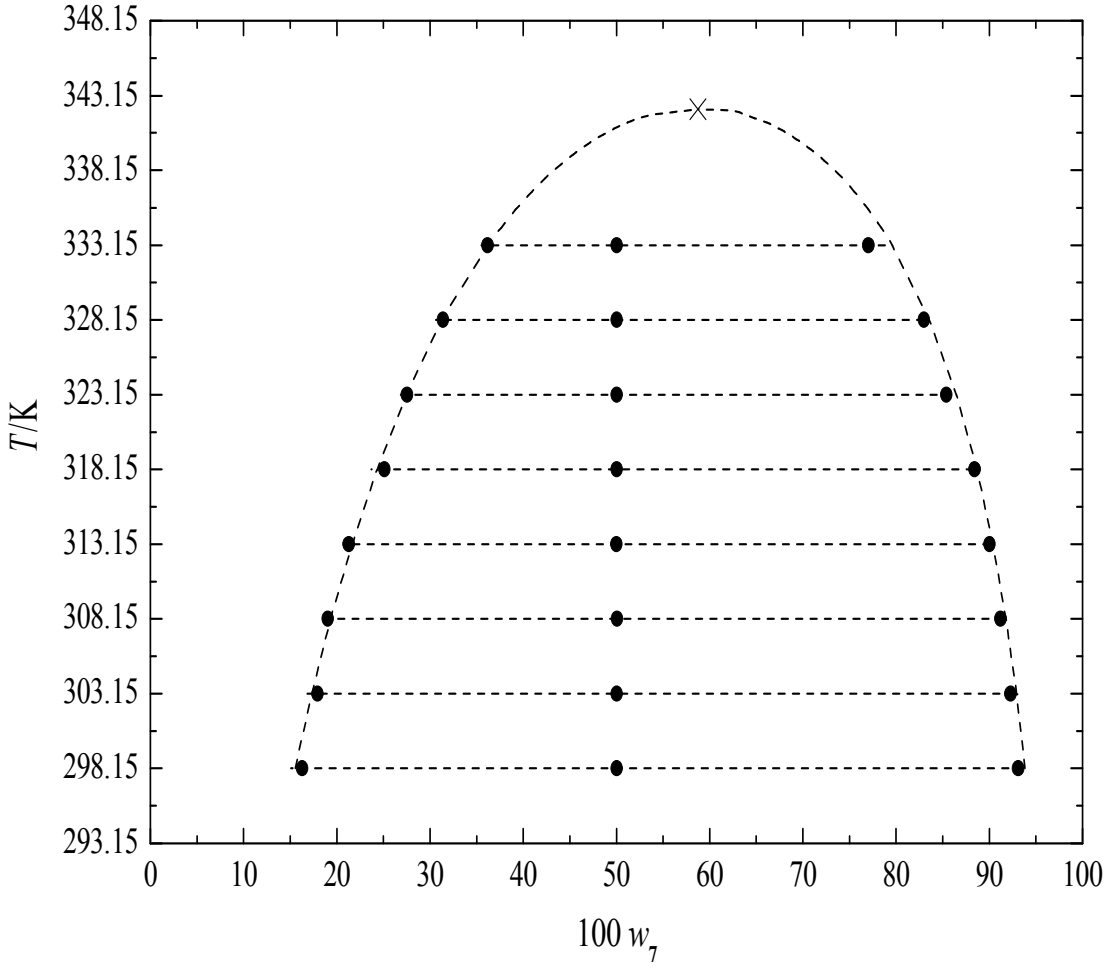

Figure 2. 1. Liquid–liquid equilibrium for the system containing soybean oil (*1*) + ethanol (*7*) at (298.15 to 333.15) (± 0.1) K: ●, experimental; ——, NRTL model; ×, extrapolated critical solution temperature.

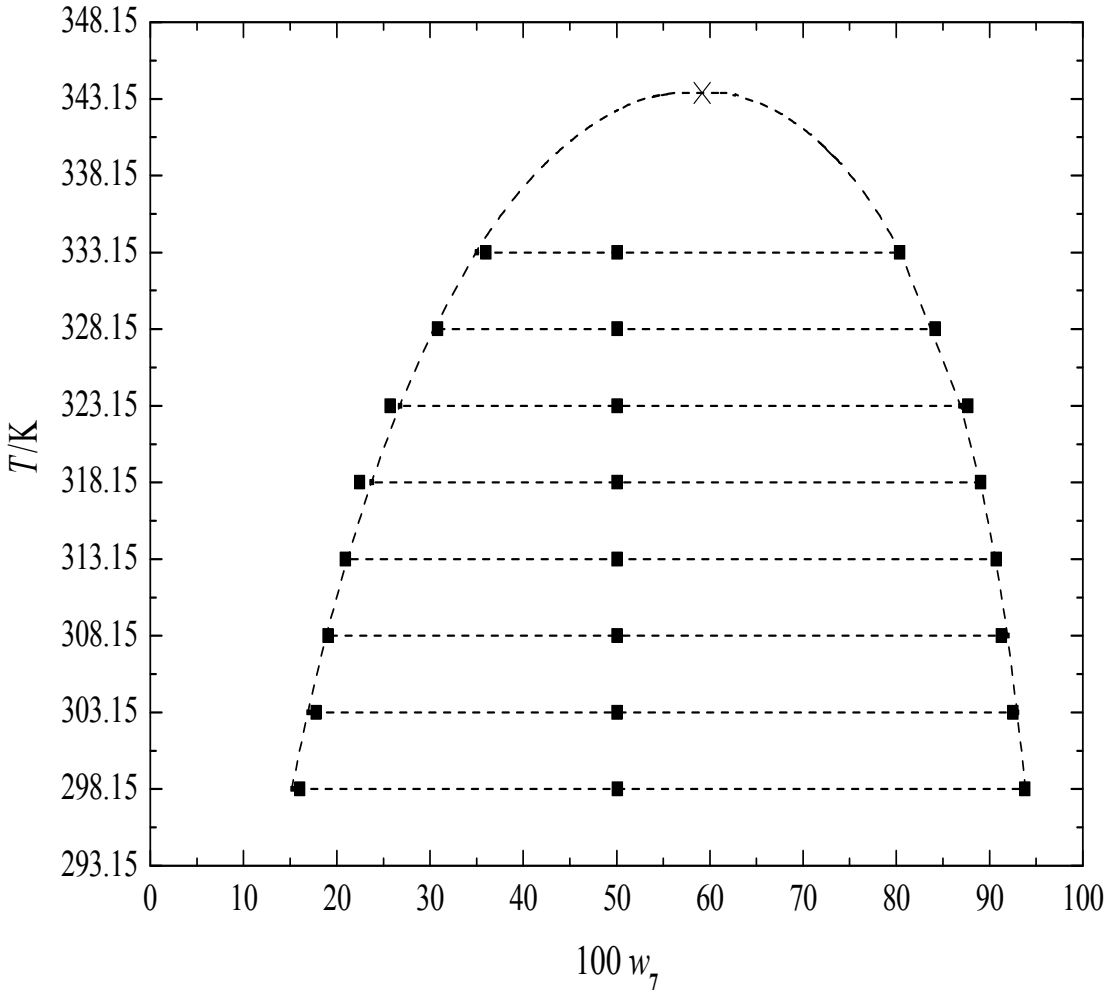

Figure 2. 2. Liquid–liquid equilibrium for the system containing sunflower oil (*2*) + ethanol (*7*) at (298.15 to 333.15) (± 0.1) K: ■, experimental; ——, NRTL model; ×, extrapolated critical solution temperature.

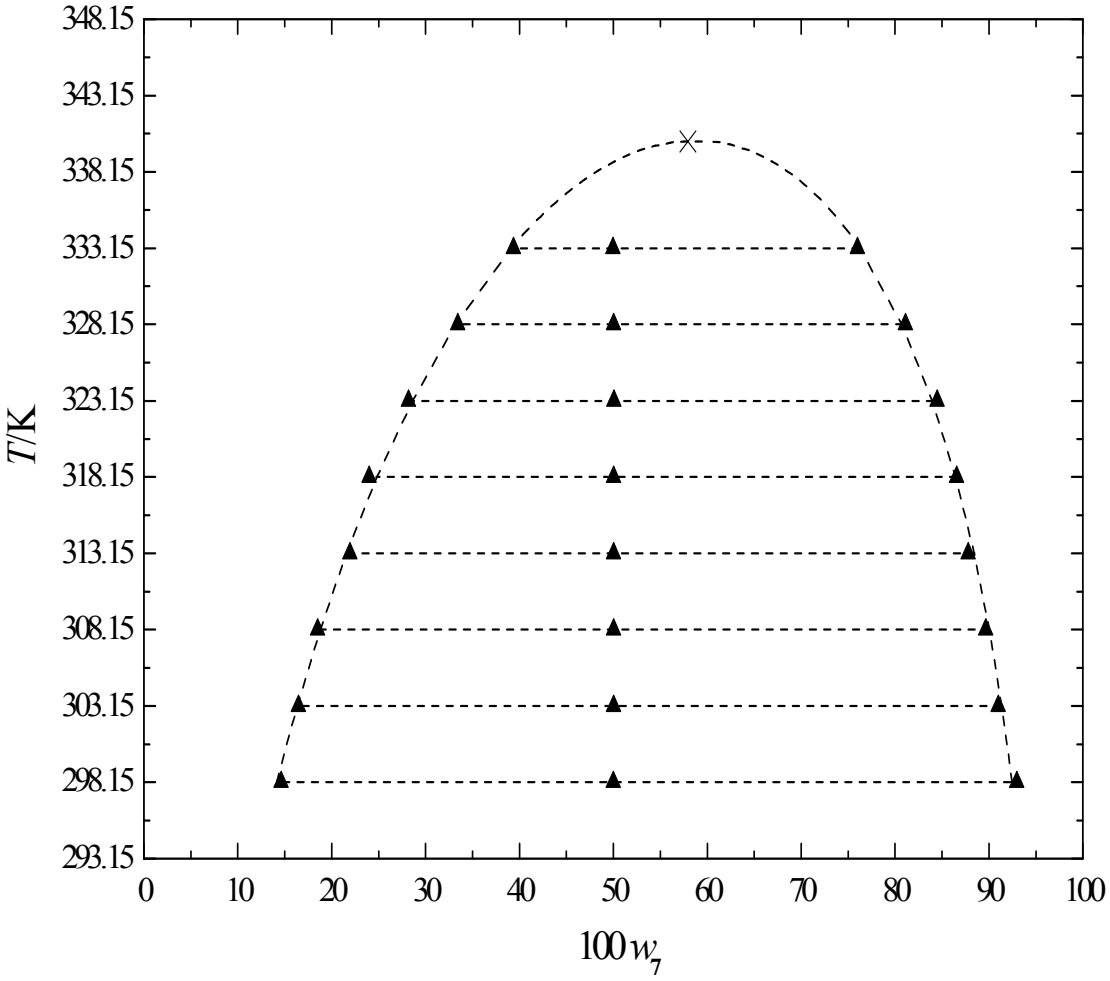

Figure 2. 3. Liquid–liquid equilibrium for the system containing rice bran oil (*3*) + ethanol (*7*) at (298.15 to 333.15) (± 0.1) K: ▲, experimental; ——, NRTL model; ×, extrapolated critical solution temperature.

.

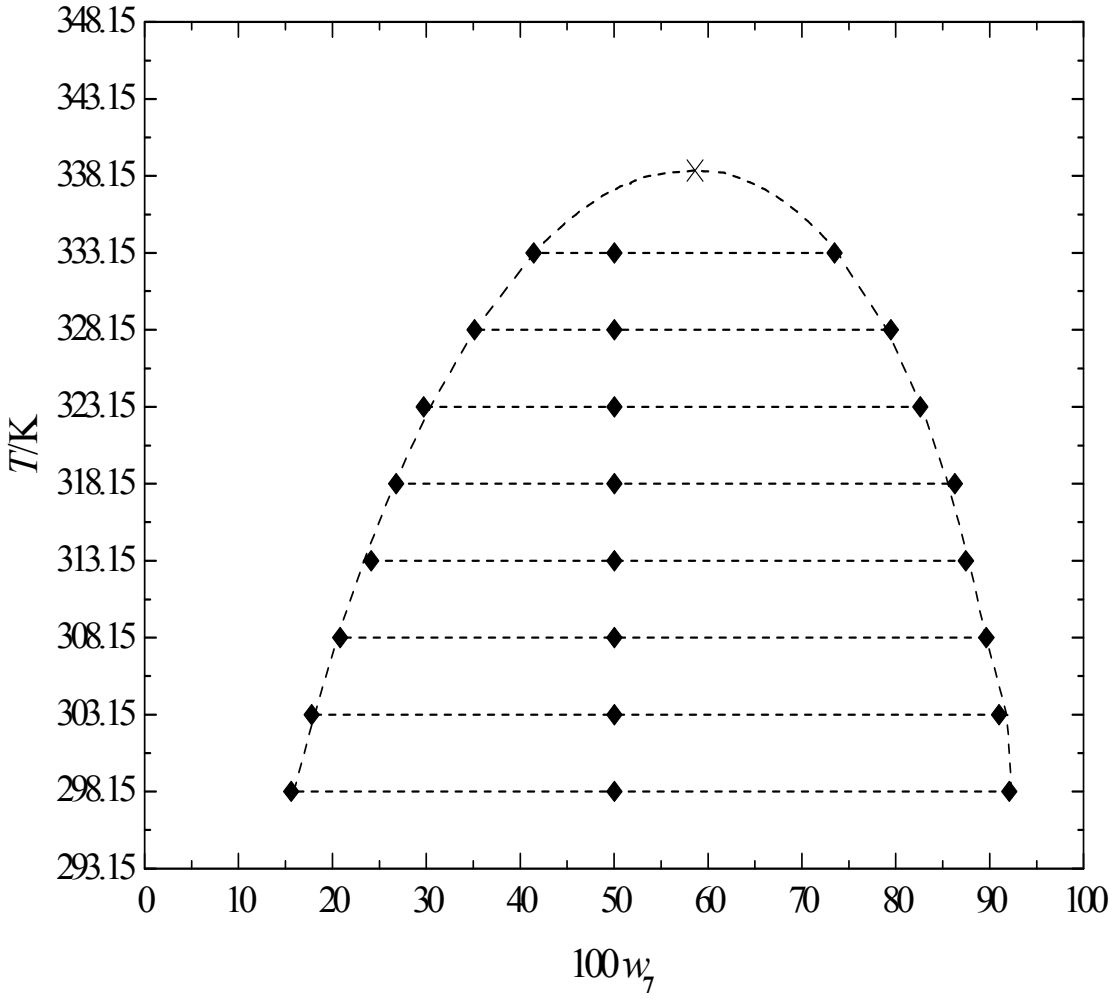

Figure 2. 4. Liquid–liquid equilibrium for the system containing cottonseed oil (*4*) + ethanol (*7*) at (298.15 to 333.15) (± 0.1) K: ♦, experimental; ——, NRTL model; ×, extrapolated critical solution temperature.

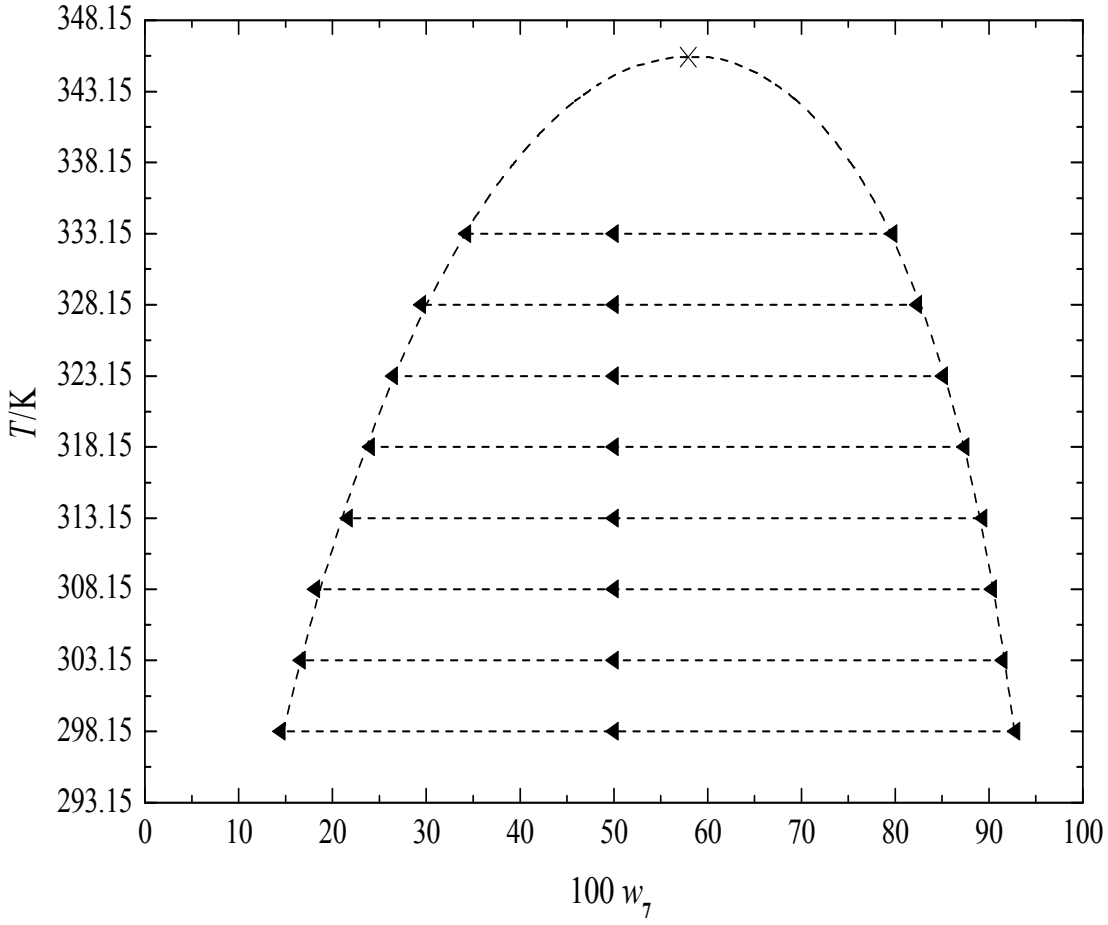

Figure 2. 5. Liquid–liquid equilibrium for the system containing palm olein (*5*) + ethanol (*7*) at (298.15 to 333.15) (± 0.1) K: ◄, experimental; ——, NRTL model; ×, extrapolated critical solution temperature.

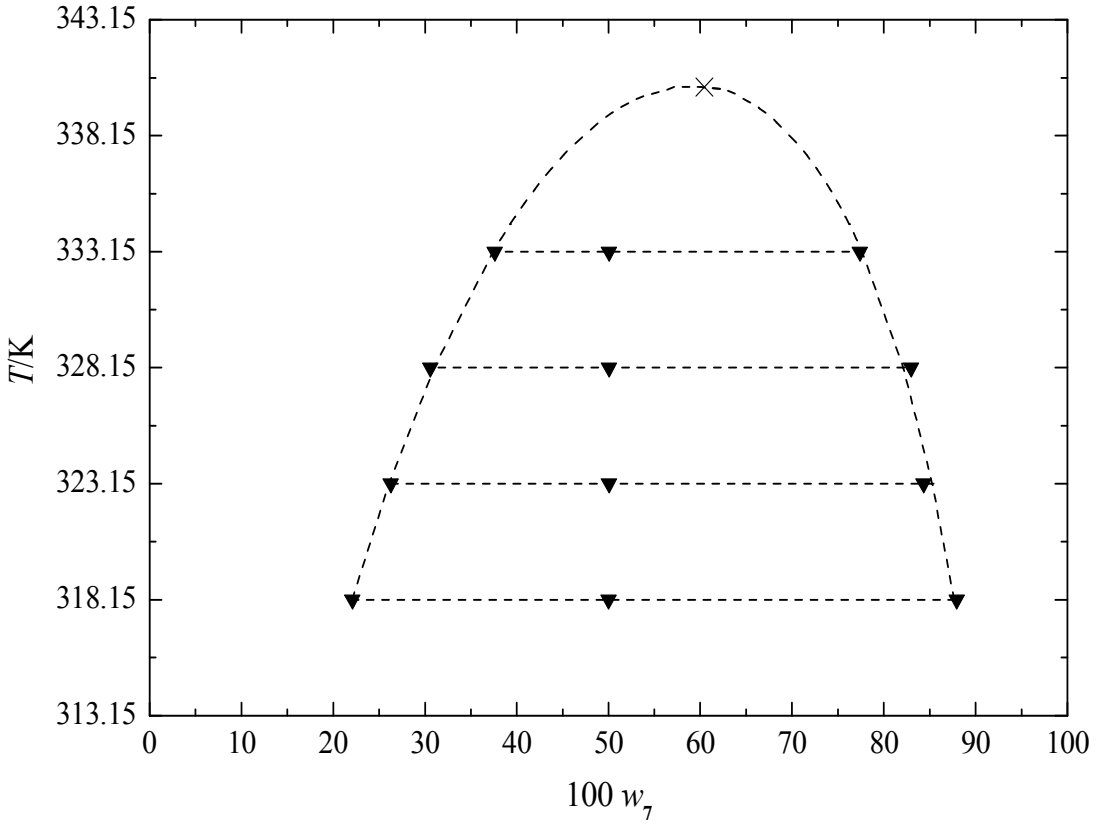

Figure 2. 6. Liquid–liquid equilibrium for the system containing palm oil (*6*) + ethanol (*7*) at (318.15 to 333.15) (± 0.1) K: ▼, experimental; ——, NRTL model; ×, extrapolated critical solution temperature.

.

The NRTL model was used to correlate the experimental data and the corresponding temperature–dependent parameters are shown in Table 2.4 The average deviations between the experimental and calculated compositions in both phases are given in Table 2.5. As can be seen, the thermodynamic model was able to accurately describe the phase compositions with deviations below 0.84 %.

Table 2. 4 Temperature–Dependent NRTL Parameters

pair	$A_{0,i7}$/K	$A_{0,7i}$/K	$A_{1,i7}$	$A_{1,7i}$	α_{i7}
soybean oil + ethanol[20]	2592.5	–12.56	–9.698	5.731	0.3761
sunflower oil + ethanol	2609.8	–66.07	–9.735	5.905	0.3761
rice bran oil + ethanol	3103.6	–1193.9	–11.913	10.295	0.3
cottonseed oil + ethanol	2736.7	–756.09	–10.812	8.921	0.3
palm olein + ethanol	2810.8	–1295.1	–11.689	11.826	0.2325
palm oil + ethanol[20]	4240.5	–2651.5	–16.070	15.961	0.2325

Table 2. 5 Average Deviations between Experimental and Calculated Phase Compositions of the Systems

systems	100 Δw
soybean oil + ethanol at (298.15 to 333.15) (± 0.1) K	0.84
sunflower oil + ethanol at (298.15 to 333.15) (± 0.1) K	0.51
rice bran oil + ethanol at (298.15 to 333.15 (± 0.1) K	0.39
cottonseed oil + ethanol at (298.15 to 333.15) (± 0.1) K	0.39
palm olein + ethanol at (298.15 to 333.15) (± 0.1) K	0.32
palm oil + ethanol at (318.15 to 333.15) (± 0.1) K	0.50

For each pseudobinary system (vegetable oil + ethanol), the critical solution temperature was determined using flash calculations with the same parameters presented in the Table 2.4. The procedure consisted in a gradual increase of the temperature and overall composition to determine new tie lines, until the critical solution temperature of each system is reached. The extrapolated critical solution temperatures are (342.25, 343.55, 340.08, 338.50, 345.55 and 340.25) K for the systems composed of soybean oil + anhydrous ethanol, sunflower oil + anhydrous ethanol, rice bran oil + anhydrous ethanol, cottonseed oil + anhydrous ethanol, palm olein + anhydrous ethanol, and palm oil + anhydrous ethanol, respectively. The critical temperatures and corresponding compositions can be seen in Figures 2.1 to 2.6, and represented by the symbol (×).

In the present work, all the measurements were performed in triplicate. The type A standard uncertainties[29] of the equilibrium data ranged from (0.03 to 0.57) % for the vegetable oils, and from (0.03 to 0.57) % for ethanol, the lowest figures being attained for the lowest compositions. These results were similar to the values reported in the literature for the uncertainties of the measurements for some systems containing vegetable oils, for example, for soybean oil from (0.06 to 0.55) %,[30] for cottonseed oil from (0.04 to 0.67) %,[31] and for rice bran oil from (0.01 to 0.28) %.[32]

Table 2.6 shows the deviations between the phase compositions determined in the present work and those reported by other authors in the literature for some pseudobinary systems containing vegetable oils + anhydrous ethanol. These results are considered consistent, considering factors such as: vegetable oils with different fatty acid compositions, the saturation degree of the vegetable oils (for example the iodine values calculated were 49.46 for palm oil,[33] and 127.46 for soybean oil,[30] and in the present work these values were 49.61 and 130.90, respectively), the methods of analysis, the ability of the analyst, etc.

Table 2. 6 Absolute Deviations Between Liquid–Liquid Equilibrium Data of this Work and Those Reported in the Literature for the Systems Containing Vegetable Oils + Ethanol

	alcohol phase	oil phase
systems	$100 \cdot \left\| w_i^{\text{this work}} - w_i^{\text{literature}} \right\|$	$100 \cdot \left\| w_i^{\text{this work}} - w_i^{\text{literature}} \right\|$
soybean oil + ethanol at 298.15 K[12]	0.76	0.69
soybean oil + ethanol at 313.15 K[20]	0.55	0.11
soybean oil + ethanol at 328.15 K[20]	1.11	2.05
soybean oil + ethanol at 323.15 K[30]	1.08	0.95
rice bran oil + ethanol at 298.15 K[32]	0.44	0.17
cottonseed oil + ethanol at 298.15 K[31]	1.23	0.80
palm oil + ethanol at 318.15 K[20]	0.67	0.48
palm oil + ethanol at 328.15 K[33]	0.40	2.89
palm oil + ethanol at 328.15 K[20]	0.38	0.49

One important variable in the transesterification process is the molar ratio of alcohol to vegetable oil. From a stoichimetric point of view a 3:1 molar ratio of alcohol to vegetable oil is needed. However, a large excess of alcohol is required to conduct the reversible reaction in the direction of product formation and, for maximum conversion to the ester, a molar ratio of 6:1 is normally used.[10] In this case ethanol must have, in the initial reaction mixture, a molar fraction of 0.8571, a value that is obtained at (317.75, 318.64, 316.12, 314.91, 319.69 or 321.45) K for soybean, sunflower, rice bran, cottonseed, palm olein or palm oils, respectively (Figure 2.7). These temperatures were checked by liquid–liquid flash calculations following the same procedure explained above. Moreover, it was observed that the solubility was influenced by the degree of unsaturation or iodine value (IV) of the studied vegetable oils (see Table 2.1). The results showed that the solubility of the unsaturated vegetable oils (soybean, sunflower, rice bran and cottonseed oils) in anhydrous ethanol was higher than that of the saturated oils under the same conditions, due to the fact that the solubility of fatty derivates in organic solvents increases with the reduction in the carbon chain length and the increase in the number of double bonds, increasing the polarity and hence the mutual solubility of the systems.[34]

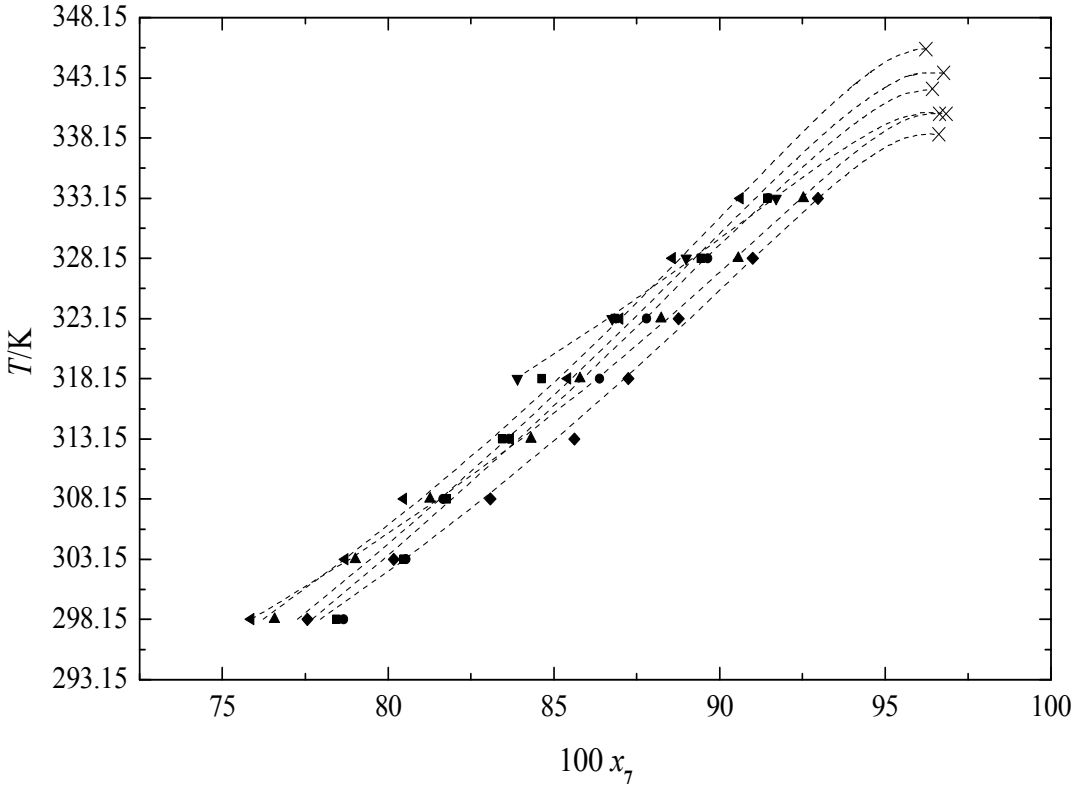

Figure 2. 7. Effect of temperature (*T*) on the ethanol molar fraction in the oil phase: ●, soybean oil; ■, sunflower oil; ▲, rice bran oil; ♦, cottonseed oil; ◄, palm olein; ▼, palm oil; ——, NRTL; ×, extrapolated critical solution temperatures.

2.4 Conclusions

Liquid–liquid equilibrium data for pseudobinary systems containing vegetable oils + ethanol were obtained in the temperature range from (298.15 to 333.15) (± 0.1) K. The solubility of vegetable oils in ethanol could be enhanced effectively by increasing the temperature. The experimental data were correlated successfully with the NRTL model,

and the average deviations between the experimental data and the calculated compositions presented values between (0.32 and 0.84) %.

Acknowledgments

The authors wish to acknowledge Agropalma (Belém/PA, Brazil) and Maeda (Itumbiara/GO, Brazil) for kindly supplying the refined palm oil and the pretreated cottonseed oil, respectively.

2.5 Literature Cited

(1) Barnwal, B. K.; Sharma, M. P. Prospects of Biodiesel Production from Vegetable Oils in India. *Renew. Sust. Energ. Rev.* **2005**, *9*, 363–378.
(2) Pousa, G. P. A. G.; Santos, A. L. F.; Suarez, P. A. Z. History and Policy of Biodiesel in Brazil. *Energy Policy* **2007**, *35*, 5393–5398.
(3) Fukuda, H.; Kondo, A.; Noda, H. Review: Biodiesel Fuel Production by Transesterification of Oils. *J. Biosci. Bioeng.* **2001**, *92*, 405–416.
(4) Kucek, K. T.; César–Oliveira, M. A. F.; Wilhelm, H. M.; Ramos, L. P. Ethanolysis of Refined Soybean Oil Assisted by Sodium and Potassium Hydroxides. *J. Am. Oil Chem. Soc*. **2007**, *84*, 385–392.
(5) Abreu, F. R.; Lima, D. G.; Hamú, E. H.; Wolf, C.; Suarez, P. A. Z. Utilization of Metal Complexes as Catalysts in the Transesterification of Brazilian Vegetable Oils with Different Alcohols. *J. Mol. Catal. A–Chem*. **2004**, *209*, 29–33.
(6) Oliveira, D.; Filho, I. N.; Di Luccio, M.; Faccio, C.; Dalla Rosa, C.; Bender, J. P.; Lipke, N.; Amroginski, C.; Dariva, C.; Oliveira, J. V. Kinetics of Enzyme–Catalyzed Alcoholysis of Soybean Oil in n–Hexane. *Appl. Biochem. Biotechnol*. **2005**, *21*, 231–242.
(7) Shibasaki–Kitakawa, N.; Honda, H.; Kuribayashi, H.; Toda, T.; Fukumura, T.; Yonemoto, T. Biodiesel Production Using Anionic Ion–Exchange Resin as Heterogeneous Catalyst. *Bioresour. Technol*. **2007**, *98*, 416–421.
(8) Liu, X.; He, H.; Wang, Y.; Zhu, S.; Piao, X. Transesterification of Soybean Oil to Biodiesel Using CaO as a Solid Base Catalyst. *Fuel*, **2008**, *87*, 216–221.
(9) Zhou, W.; Boocock, D. G. B. Phase Behavior of the Base–Catalyzed Transesterification of Soybean Oil. *J. Am. Oil Chem. Soc.* **2006**, *83*, 1041–1045.
(10) Meher, L. C.; Sagar, D. V.; Naik, S. N. Technical Aspects of Biodiesel Production by Transesterification – A review. *Renew. Sust. Energ. Rev.* **2006**, *10*, 248–268.

(11) Gerpen, J. V. Biodiesel Processing and Production. *Fuel Process. Technol.* **2005**, *86*, 1097–1107.
(12) Lanza, M.; Borges Neto, W.; Batista, E.; Poppi, R. J.; Meirelles, A. J. A. Liquid–Liquid Equilibrium Data for Reactional Systems of Ethanolysis at 298.3 K. *J. Chem. Eng. Data* **2008**, *53*, 5–15.
(13) Zhou, H.; Lu, H.; Liang, B. Solubility of Multicomponent Systems in the Biodiesel Production by Transesterification of *Jatropha curcas* L. Oil with Methanol. *J. Chem. Eng. Data* **2006**, *51*, 1130–1135.
(14) Tang. Z.; Du, Z.; Min, E.; Gao, L.; Jiang, T.; Han, B. Phase Equilibria of Methanol–Triolein System at Elevated Temperature and Pressure. *Fluid Phase Equilib.* **2006**, *239*, 8–11.
(15) Liu, X.; Piao, X.; Wang, Y.; Zhu, S. Liquid–Liquid Equilibrium for Systems of (Fatty Acid Ethyl Esters + Ethanol + Soybean Oil and Fatty Acid Ethyl Esters + Ethanol + Glycerol). *J. Chem. Eng. Data* **2008**, *53*, 359–362.
(16) Firestone, D. *Physical and Chemical Characteristics of Oils, Fats and Waxes*. AOCS Press, 1999.
(17) Renon, H.; Prausnitz, J. M. Local Composition in Thermodynamic Excess Functions for Liquid Mixtures, *AIChE J.* **1968**, *14*, 135–144.
(18) AOCS. *Official Methods and Recommended Practices of the American Oil Chemists' Society*, 3rd ed.; AOCS Press: Champaign, 1988; Vol. 1–2
(19) Hartman, L.; Lago, R. C. A. Rapid Preparation of Fatty Acid Methyl Esters from Lipids. *Lab Pract* **1973**, *22*, 475–476.
(20) Lanza, M.; Sanaiotti, G.; Batista, E.; Poppi, R. J.; Meirelles, A. J. A. Liquid–Liquid Equilibrium Data for Systems Containing Vegetable Oils, Anhydrous Ethanol, and Hexane at (313.15, 318.15, and 328.15) K. *J. Chem. Eng. Data* **2009**, *54*, 1850–1859.
(21) Antoniosi Filho, N. R.; Mendes, O. L.; Lanças, F. M. Computer Prediction of Triacylglycerol Composition of Vegetable Oils by HRGC. *Chromatographia* **1995**, *40*, 557–562.
(22) Silva, L. H. M.; Coimbra, J. S.; Meirelles, A. J. A. Equilibrium Phase Behavior of Poly(Ethylene Glycol) + Potassium Phosphate + Water Two Phase Systems at Various pH and Temperatures. *J. Chem. Eng. Data* **1997**, *42*, 398–401.
(23) Wilson, G. M. Vapor–Liquid Equilibrium. XI: A New Expression for the Excess Gibbs Energy of Mixing. *J. Am. Chem. Soc.* **1964**, *86*, 127–130.
(24) Aznar, M. Correlation of (Liquid + Liquid) Equilibrium of Systems Including Ionic Liquids. *Braz. J. Chem. Eng*. **2007**, *24*, 143–149.
(25) Sé, R. A. G.; Aznar, M. Thermodynamic Modelling of Phase Equilibrium for Water + Poly(Ethylene Glycol) + Salt Aqueous Two–Phase Systems. *Braz. J. Chem. Eng*. **2002**, *19*, 255–266.
(26) Renon, H.; Prausnitz, J. M. Estimation of Parameters for the NRTL Equation for Excess Gibbs Energies of Strongly Nonideal Liquid Mixtures, *Ind. Eng. Chem. Proc. Des. Dev.* **1969**, *8*, 413–419.
(27) Stragevitch, L.; d′Ávila, S. G. Application of a Generalized Maximum Likelihood Method in the Reduction of Multicomponent Liquid–Liquid Equilibrium Data. *Braz. J. Chem. Eng.* **1997**, *14*, 41–52.
(28) Null, H. R. *Phase Equilibrium in Process Design*. Wiley–Interscience, New York, 1970.

(29) Taylor, B. N.; Kuyatt, C. E. *Guidelines for the Evaluation and Expression of Uncertainty in NIST Measurement Results*; NIST Technical Note 1297, 1994.
(30) Rodrigues, C. E. C.; Peixoto, E. C. E.; Meirelles, A. J. A. Phase equilibrium for Systems Composed by Refined Soybean Oil + Commercial Linoleic Acid + Ethanol + Water, at 323.2 K. *Fluid Phase Equilib.* **2007**, *261* 122–128.
(31) Rodrigues, C. E. C.; Reipert, E. C. D.; Souza, A. F.; Pessôa Filho, P. A.; Meirelles, A. J. A. Equilibrium Data for Systems Composed by Cottonseed Oil + Commercial Linoleic Acid + Ethanol + Water + Tocopherols at 298.2 K. Fluid Phase Equilib. **2005**, *238*, 193–203.
(32) Rodrigues, C. E. C.; Antoniassi, R.; Meirelles, A. J. A. Equilibrium Data for the System Rice Bran Oil + Fatty Acids + Ethanol + Water at 298.2 K. *J. Chem. Eng. Data* **2003**, *48*, 367–373.
(33) Gonçalves, C. B.; Meirelles, A. J. A. Liquid–Liquid Equilibrium Data for the System Palm Oil + Fatty Acids + Ethanol + Water at 318.2 K. *Fluid Phase Equilib.* **2004**, *221*, 139–150.
(34) Swern, D. *Bailey's Industrial Oil and Fat Products*; Mattil, K. F., Norris, F. A., Stirton, A. J., Eds.; Wiley: New York, 1964.
(35) AOCS. *Official Methods and Recommended Practices of the American Oil Chemists' Society*, 5th ed.; AOCS Press: Champaign, IL, 1998.

The authors wish to acknowledge FAPESP (08/56258–8), CNPq (306250/2007–1 and 480992/2009–6), CAPES/PEC–PG, and CAPES/PNPD for their financial support.

CAPÍTULO 3

Triacylglycerols Distribution in Vegetable Oils + Ethanol Mixtures for Biodiesel Production

*Luis A. Follegatti–Romero, Eduardo A. C. Batista and Antonio J. A. Meirelles**

ExTrAE, Laboratory of Extraction, Applied Thermodynamics and Equilibrium, Department of Food Engineering, Faculty of Food Engineering, University of Campinas – UNICAMP, 13083–862, Campinas, SP, Brazil

* Corresponding author. Fax: +55 19 3521 4027, E–mail: tomze@fea.unicamp.br

Artigo submetido no Journal of Chemical & Engineering Data, 2011 (je–2011–00931c).

Abstract

Vegetable oils and other sources of triacylglycerols are commonly used as main raw material in the production of biodiesel. Triacylglycerol mixtures are partially soluble in ethanol during the initial step of the ethanolysis reaction, thus a two–phase pseudo–binary system is formed. Besides affecting the mutual solubility oil + ethanol, the presence of several triacylglycerols can alter the distribution of fatty compounds between both phases, with potential impact on the reactive process and on the reliability of the pseudo–component hypothesis. This commonly used hypothesis in the research associated with the biodiesel production assumes that the triacylglycerol source can be treated as a pseudo–component having physical–chemical properties equivalent to the average values observed in the edible oil. In the present work, partitioning data of triacylglycerols between the two immiscible liquid phases are reported in terms of their distribution coefficients for the systems soybean/sunflower/canola/palm olein/palm oil + ethanol within the temperature range of 298.15 and 333.15 K. It was demonstrated that most triacylglycerols have distribution coefficients within a relatively narrow range of values, validating in this way the pseudo–component hypothesis, at least for the selected systems within the investigated temperature range.

Keywords: Triacylglyerols, distribution coefficient, transesterification, biodiesel, vegetable oils.

Introduction

Recently, the world importance of biodiesel production significantly increased as a consequence of a range of environmental, economical and political problems related to the use of conventional petroleum based fuels. Ethylic biodiesel produced by ethanolysis of vegetable oils with ethanol has recently become more attractive on account of its environmental benefits and the fact that it is produced from renewable agricultural resources.[1] Among the many possible sources, ethylic biodiesel fuel derived from vegetable oils (soybean, sunflower, canola, palm and palm olein) has attracted attention as a promising substitute for conventional diesel fuels.[2]

Vegetable oils are composed mainly of triacylglycerols (TAG), components that consist of a single glycerol molecule esterified with three fatty acids.[3] These fatty acids can be saturated or unsaturated. For example, palm oil is a edible oil rich in saturated fatty acids, its triacylglycerols consisting of trisaturated (SSS) molecules, mainly PPP (tripalmitin), disaturated (SSU) ones, mainly POP (dipalmitin–olein), and monosaturated (UUS) ones, mainly POO (palmitin–diolein).[4] In the case of the polyunsaturated vegetable oils (soybean, sunflower and canola oils), the major unsaturated triacylglycerols (UUU) are of the type OLiLi (olein–dilinolein) and LiLiLi (trilinolein).[5]

Transesterification (ethanolysis) is used to convert triacylglycerols to fatty acid ethyl esters (FAEEs). The initial step of this reaction is influenced by the mutual solubility of the reactants, an information that is, in fact, of major importance to correctly design and operate transesterification units.[6] Follegatti–Romero et al.[7] reported liquid–liquid equilibrium data of pseudobinary systems composed of different vegetable oils + ethanol within the temperature range of 298.15 to 333.15 K and correlated the experimental data

with the NRTL model. In the modeling approach they assumed that each vegetable oil can be treated as a single pseudo–component, so that the same set of NRTL parameters would reflect the interaction between the different triacylglycerol molecules and ethanol. The same approach was adopted by a series of authors working with LLE–data of fatty systems, as for instance Lanza et al.[8] and Silva et al.[9] Although these studies have indicated a dependence of the solubility data in relation to the average molecular weights of the oils and their degrees of unsaturation, the chosen approach does not allow to directly considering the effects that the presence of different triacylglycerols has on these average properties. On the other hand, prior attempts to take into account, at least in part, the edible oil´s complexity for predicting LLE–data of fatty systems revealed the poor precision of the obtained results: in fact, the work of Batista et al.[10] indicated that a new set of LLE interaction parameters was required in order to improve the predictive capability of the UNIFAC method. In contrast to this result, group contribution approaches or predictive methods based on the multicomponent character of edible oils were successfully used in the case of vapor–liquid (VLE)[11,12] and solid–liquid (SLE) equilibria.[13]

The preceding discussion highlights the importance of measuring experimental data related to the partitioning of fatty compounds in systems of two liquid phases, as a first step to develop more reliable approaches to predict the corresponding LLE. By affecting the solubility of the components, the partition of triacylglycerols influences reaction and purification steps used in the oil–chemistry, for example, those used to produce biodiesel. Indeed, this information may be important for process design and optimization in the oil–chemistry.

In this work, triacylglycerol partitioning was investigated in systems containing vegetable oils (soybean/sunflower/canola/palm olein/palm oils) + ethanol within the temperature range from 298.15 to 333.15 K. The results were evaluated on the basis of the experimental partition coefficients and their distribution around the average values was used as an indication for the validity of the approach based on the pseudo–component concept.

Experimental Section

Materials.

The solvents used in this work were anhydrous ethanol and hexane, both from Merck (Germany) and with a purity of 99.9 %. Refined soybean, sunflower and canola oils were purchased from Cargill (Mairinque/SP, Brazil). Refined palm oil and palm olein were kindly supplied by Agropalma (Belém/PA, Brazil). These edible oils were characterized by gas chromatography for determining their fatty acid profile and by high performance size exclusion chromatography (HPSEC) for obtaining their lipid class profile, according to the procedures indicated below.

Apparatus and Procedures.

The fatty acid compositions were determined using the official AOCS method (1–62).[14] In order to carry out the chromatographic analysis, fatty acid methyl esters (FAME) from vegetable oils were prepared by the Hartman & Lago[15] method. The analysis was

performed using a CGC Agilent 6850 Series GC capillary gas chromatographic system under the same conditions published in a previous work of our research group.[8]

The lipid class composition of the vegetable oils was determined using a HPSEC system composed of a pump model 200 (Perkin–Elmer, Norwalk, CT, USA), a Rheodyne 7125 valve injector, a 20 μL loop and a refractive index detector 2414 (Waters Associates, Milford, MA, USA). The separation was performed on two 100 and 500 Å Jordi Gel DVB columns (5 μm, 300 mm × 7.8 mm), from Jordi Associates (Bellingham, MA, USA), connected in series, with HPLC–grade tetrahydrofuran from Sigma–Aldrich (Steinheim, Germany) as the mobile phase at a flow rate of 1mL/min. The column oven and RID detector were maintained at 313.15. The samples were diluted in tetrahydrofuran (10 mg of sample/1 mL THF) and 20 μL of the sample solutions were injected. For each sample a mean value was calculated from three runs. The relative percentage of each component was calculated by the HPSEC software dividing the peak area of each lipid class (triacylglycerols, dilacylglycerols or monoacylglycerols) by the sum of the peak areas of all components.

The mutual solubility data for the systems containing soybean/sunflower/canola/palm olein/palm oil + anhydrous ethanol were measured at 313.15 and 333.15 K. The experiments were performed using equilibrium glass cells (50 mL) similar to those used by Follegatti–Romero et al.[7] Known quantities of each component, weighed on an analytical balance with a precision of 0.0001 g (Precisa, model XT220A, Sweden), were added directly to the equilibrium glass cells. After resting undisturbed for 16 h at the same temperature, two separate transparent liquid phases were obtained.

Two samples were separately taken from each phase by using syringes containing previously weighed masses of hexane (0.04 g of sample diluted to 2 g with hexane). In this way every sample was cooled and simultaneously diluted in order to avoid an additional phase splitting inside the syringe. The first sample of each phase was used for determining ethanol and oil mass fractions by a gravimetric analysis described elsewhere.[7] After complete evaporation, the second sample was quantitatively analyzed via Gas Chromatography (GC) for determining the triglyceride profile of the oily part of each phase. This last analysis was performed on a Shimadzu (GC–17A) capillary gas chromatograph system with programmable pneumatics and a flame ionization detector (FID). An Rtx–65 TG capillary column (0.25 μm, 30 m × 0.25 mm i.d) from J&W Scientific (Rancho Cordoba, CA, USA) was used, and the carrier gas was helium from White Martins (Brazil), with a mass purity of 99.9 %. The following CG configurations were used: the detector and injector temperatures were 643 K and 625 K, respectively; the column oven was maintained at 313.15 K for 4 min, subsequently heated from 313.15 to 628.15 K at a rate of 10 $K \cdot min^{-1}$, and maintained at 628.15 K for 20 min; the absolute pressure of the column was approximately 200 kPa; the carrier gas flowed at a rate of 1.6 $mL \cdot min^{-1}$ and a linear velocity of 34 $cm \cdot s^{-1}$ and the sample injection volume was 1.0 μL.

For identification of triacylglycerols, a mixture of trilinolein, triolein, tristearin, tripalmitin, trimyristin, trilaurin, tricaprin, and tricaprylin were first analyzed in order to determine the best chromatographic conditions and the corresponding retention times. Then, individual peaks were identified by comparing the retention times with those of pure triacylglycerol standards and also with chromatographic peaks observed in samples of common vegetable oils with known triacylglycerol composition. Moreover, the oil

compositions reported in the literature were also used as reference for helping in identifying peaks related to the different triacylglycerols.[4-5, 7, 9, 16] The triacylglycerol compositions of the oily part of each phase were quantified by the normalized area of each triacylglycerol, i.e. by the individual peak area divided by the sum of all peak areas. The distribution coefficients were calculated according to equation (1) using the experimental complete compositions of both phases.

$$K_j = \frac{(w_j.w_i)^{\mathrm{AP}}}{(w_j.w_i)^{\mathrm{OP}}} \tag{1}$$

where K_j is the distribution coefficient of TAG j, w_j is the mass fraction of TAG j in the oily part of each phase, w_i is the mass fraction of the vegetable oil in each phase and the superscripts AP and OP stand for ethanol and oil phases, respectively.

The uncertainties of the triacylglycerol distribution coefficients were obtained by error propagation from the uncertainties of the ethanol and edible oil mass fractions determined by gravimetry and from the uncertainties observed in the gas chromatographic analysis, according to equation (2) below.[17]

$$(\Delta K_j)^2 = \left(\frac{\partial K}{\partial w_j^{AP}}\right)^2 (\Delta w_j^{AP})^2 + \left(\frac{\partial K}{\partial w_i^{AP}}\right)^2 (\Delta w_i^{AP})^2 + \left(\frac{\partial K}{\partial w_j^{OP}}\right)^2 (\Delta w_j^{OP})^2 + \left(\frac{\partial K}{\partial w_i^{OP}}\right)^2 (\Delta w_i^{OP})^2 \tag{2}$$

The distribution coefficients and the corresponding uncertainties for each edible oil as a whole were also evaluated, in this case taking into account the total amount of oily fraction present in each equilibrium phase.

Results and Discussion

The fatty acid compositions of the vegetable oils are presented in **Table 3.1**. Note that soybean, canola and sunflower oils are rich in oleic (O) and linoleic (Li) acids, but only the first two have significant amounts of linolenic (Le) acid. In contrast, palm oil and palm olein are rich in oleic and palmitic (P) acids. Nevertheless, the saturated fatty acids (L, M, P, S), including palmitic acid, have lower concentration in palm olein than in palm oil due to the fractionation by crystallization performed at the refinery (Agropalma, Belém/PA, Brazil).

Table 3.2 shows the lipid profile of the oils investigated. Soybean, sunflower and canola oils exhibit low levels of partial acylglycerols. In contrast, palm oil and palm olein contain 7.7 and 5.3 % of diacylglycerols, respectively.

Table 3. 1. Fatty Acid Compositions of Vegetable Oils

fatty acids	symbol	C*x*:y [a]	*M* [b]	soybean[7]	sunflower[7]	canola	palm olein[7]	palm[7]
			g·mol^{-1}	100 *w*	100 *w*	100 *w*	100 *w*	100 *w*
octanoic	Cp	C8:0	144.22					0.08
decanoic	C	C10:0	172.27					0.09
dodecanoic	L	C12:0	200.32				0.27	1.15
tetradecanoic	M	C14:0	228.38	0.09	0.09	0.07	0.8	1.24
hexadecanoic	P	C16:0	256.43	11.54	6.4	4.15	35.11	40.68
cis–hexadec–9–enoic	Po	C16:1	254.42	0.08	0.13	0.3	0.17	0.15
heptadecanoic	Ma	C17:0	270.45		0.05		0.09	0.1
cis–heptadec–9–enoic	Mg	C17:1	268.48		0.04		0.03	
octadecanoic	S	C18:0	284.49	2.98	3.23	2.59	4.42	4.72
cis–octadec–9–enoic	O	C18:1	282.47	22.91	31.89	61.59	46.55	41.78
cis,*cis*–octadeca–9,12–dienoic	Li	C18:2	280.45	55.76	56.27	21.13	11.4	8.84
trans,trans–octadeca–9,12–dienoic[c]		C18:2t[c]		0.24	0.17		0.13	0.31
all–*cis*–octadeca–9,12,15–trienoic	Le	C18:3	278.44	5.27	0.33	7.38	0.32	0.18
all–trans–octadeca–9,12,15–trienoic[c]		C18:3t[c]		0.55		0.69		
icosanoic	A	C20:0	312.54	0.25	0.27	0.68	0.38	0.39
cis–icos–9–enoic	Ga	C20:1	310.52	0.1	0.23	0.86	0.17	0.15
docosanoic	Be	C22:0	340.59	0.23	0.65	0.19	0.07	0.07
tetracosanoic	Lg	C24:0	368.65		0.25	0.25	0.09	0.07
cis–tetracos–15–enoic	Ne	C24:1	366.63			0.12		
octanoic	Cp	C8:0	144.22					0.08
Total saturated				14.61	9.72	6.81	40.6	47.96
Total monounsaturated				14.61	9.72	6.81	40.6	47.96
Total polyunsaturated				23.09	32.38	62.75	46.89	42.08
IV[d]				128.45	127.3	112.27	56.3	52.87

[a] C*x*:*y*, *x* = number of carbon and *y* = number of double bonds. [b] *M* = molar mass [c] Trans isomers. [d] Iodine value (IV) calculated from the fatty acid composition according to the method Cd 1c–85.[18]

Table 3. 2. Lipid Class Compositions of Vegetable Oils.

lipid class	soybean	sunflower	canola	palm olein	palm
	100 *w*	100 *w*	100 *w*	100 *w*	100 *w*
triacylglycerol	99.40	98.30	99.50	91.40	94.20
diacylglycerol				7.70	5.30
monoacylglycerol + FFA[a]	0.60	1.70	0.50	0.90	0.50

[a]FFA: Free fatty Acids

Liquid−liquid equilibria data at atmospheric pressure for the soybean/sunflower/canola/palm olein/palm oil + ethanol pseudobinary systems, within the temperature range of 298.15 and 333.15 K, are presented in **Table 3.3.** The absolute deviations between the phase compositions determined in the present work and those reported in the literature were within the range of (0.10 to 2.77) % by mass (see **Table 3.3**), which indicate the good quality of the experimental data for all the pseudobinary systems.

Table 3. 3. Experimental Liquid–Liquid Equilibrium Data for the Pseudobinary Systems Containing Vegetable Oils (*i*) + Anhydrous Ethanol (*7*) from 298.15 to 333.15 K.

oil (*i*)	*T*/K	Overal comp.		ethanol phase		oil phase		AD[a]		*K*	Δ_K
		100 w_i	100 w_7	100 w_i	100 w_7	100 w_i	100 w_7	AP	OP		
soybean (*1*)	318.15	49.96	50.04	11.87	88.13	74.60	25.40	0.15	0.11	0.159	0.004
	333.15	49.95	50.05	20.21	79.79	64.5	35.50	2.77	0.21	0.310	0.005
sunflower (*2*)	308.15	49.96	50.04	8.34	91.66	81.42	18.58	0.38	0.48	0.100	0.002
	318.15	49.96	50.04	11.05	88.95	77.90	22.10	0.10	0.34	0.140	0.003
	333.15	49.95	50.05	18.92	81.08	65.10	34.90	0.68	1.08	0.290	0.004
canola (*3*)	318.15	49.96	50.04	8.65	91.35	79.20	20.80	0.30	0.73	0.100	0.004
	333.15	49.95	50.05	16.56	83.44	66.43	33.57	0.62	1.23	0.240	0.003
palm olein (*4*)	298.15	49.95	50.05	7.43	92.57	86.08	13.92	0.30	0.58	0.080	0.002
	318.15	49.97	50.03	12.81	87.19	76.98	23.02	0.23	1.00	0.160	0.003
	333.15	49.95	50.05	21.02	78.98	64.8	35.2	0.77	0.93	0.320	0.003
palm (*5*)	318.15	49.99	50.01	12.73	87.27	77.67	22.33	0.69	0.22	0.164	0.003
	333.15	49.95	50.05	21.34	78.66	63.64	36.36	1.27	1.25	0.330	0.002

[a]Absolute Deviation in relation to literature data[6,10], calculated by: $\mathrm{AD} = 100 \cdot \left| w_i^{\text{this work}} - w_i^{\text{literature}} \right|$

The distribution coefficients (*K*) for all vegetable oils + ethanol systems were also shown in **Table 3** and illustrated in **Figure 1,** together with vegetable oils distribution coefficients from liquid–liquid equilibrium data published in the literature[7, 9]. Distribution coefficients of the unsaturated soybean and sunflower oils have very similar values, as observed in

Figure 3.1, probably due to their linoleic acid levels, around 56 % in both cases, with a little difference in their contents of oleic and linolenic acids. On the other hand, canola oil is richer in monounsaturated fatty acids (62.87 % by mass) and has distribution coefficients with smaller values, as can be observed by the lower curve shown in **Figure 3.1**. In addition, the distribution coefficients of the saturated oils (palm olein and palm oil) are slightly higher than the corresponding values of the unsaturated ones (soybean and sunflower oils), a behavior caused in part by the larger amounts of palmitic acid in the saturated oils. In fact, the lower carbon chain of this fatty acid increases the oil + ethanol mutual solubility and, consequently, the oil distribution coefficients. Furthermore, the higher values of partial acylglycerols in these saturated oils also enhance the oil + ethanol mutual solubility (see **Table 3.2**) and, in this way, affect the oils distribution coefficients.

Tables 4 to 8 show the triacylglycerol profiles for each vegetable oil and for the oily part present in the samples taken from the oil and ethanol immiscible phases.[13] The results for the triacylglycerols compositions for all vegetable oils (soybean, sunflower, canola, palm olein, palm oil) were according with TAG composition data reported in previous works.[7, 9]

The distribution coefficients (K) of each triacylglycerol, calculated according to Eq. 1, and the uncertainties, determined by error propagation (Δ_K) of the experimental measurements, were also given in **Tables 3.4 to 3.8**. The average values of these uncertainties varied within the range from 0.002 to 0.007, but relatively higher uncertainties were observed in case of TAGs with lower concentration, such as POS in Canola oil (Δ_K=0.010) or POA in palm oil (Δ_K=0.017). The low uncertainty values indicate the good quality of the experimental data and allow a reliable discussion based on the experimental results.

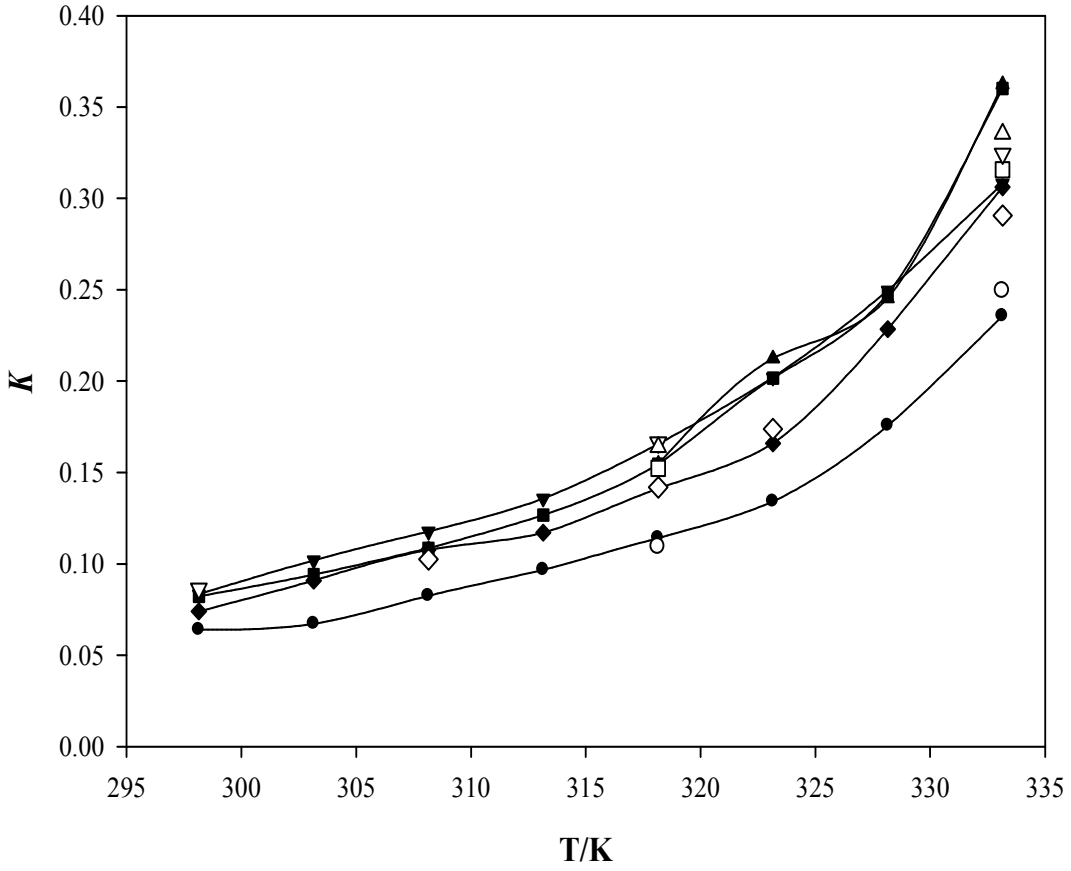

Figure 3. 1. Vegetable oil distribution coefficients (K) for the systems composed of: ■□, soybean/ ●○, canola/ ♦◊, sunflower/ ▼▽, palm olein/▲Δ, palm oil + ethanol pseudobinary systems from 298.15 to 333.15 K. Full symbols represent K calculated from data taken from data taken from literature[7,9] and the empty symbols represent *K* calculated from experimental data measured in the present work.

Table 3. 4. Triacylglycerols Molecular Species Profiles of Soybean Oil (SO)

main TAG[a]	group	SO[a]	SO[b]	318.15 K				333.15 K			
				w^{AP}	w^{OP}	K^e	Δ_K	w^{AP}	w^{OP}	K^e	Δ_K
PPP	48:0										
PPoP	48:1										
POP	50:1		1.41	1.61	1.50	0.171	0.005	3.8	3.52	0.338	0.005
PPoO	50:2										
PLiP	50:2	3.11	4.33	4.85	4.60	0.168	0.004	6.99	7.13	0.307	0.005
POS	52:1		0.63	0.77	0.82	0.149	0.005	1.8	1.98	0.285	0.005
POO	52:2	3.39	4.41	4.76	4.87	0.156	0.004	9.14	9.4	0.305	0.005
PSLi	52:2	3.28	2.35	2.25	2.32	0.154	0.004	3.17	3.31	0.300	0.005
POLi	52:3	6.89	14.18	14.63	14.51	0.160	0.004	16.8	16.9	0.311	0.005
PoOLi	52:4										
PLeO	52:4										
PLiLi	52:4	10.23	18.16	18.47	18.33	0.160	0.004	13.33	12.70	0.329	0.005
PLeLi	52:5		1.96	2.30	2.09	0.175	0.005	0.87	0.90	0.303	0.007
PoLiLi	52:5										
SOS	54:1										
SOO	54:2		0.82	0.87	0.88	0.157	0.005	1.99	2.05	0.304	0.005
OOO	54:3	3.28	3.07	2.88	3.25	0.141	0.004	5.81	5.89	0.309	0.005
SOLi	54:3	3.71	3.26	2.53	2.53	0.159	0.004	3.60	3.90	0.289	0.005
OOLi	54:4	6.30	9.98	9.36	9.47	0.157	0.004	9.97	10.45	0.299	0.005
OLiLi	54:5	15.28	17.64	16.84	16.02	0.167	0.004	10.84	10.89	0.312	0.005
OOLe	54:5										
SLiLi	54:4	4.22									
OLiLe	54:6	4.83									
LiLiLi	54:6	17.64	15.37	15.4	16.24	0.151	0.004	5.81	5.27	0.345	0.005
LiLiLe	54:7	7.90									
OLiGa	56:4										
N. U. F. C.[d]		9.94	1.83	1.88	1.97			5.48	5.11		
average						0.159	0.004			0.310	0.005
standard deviation						0.009				0.017	
CV (%)						5.701				5.535	

[a]Lida et al.[16]
[b]This work.
[c]Eq. 1.
[d]N. U. F. C.: Non–unidentified Fatty compounds

Table 3. 5. Triacylglycerols Molecular Species Profiles of Sunflower Oil (SO)

main TAG[a]	group	SO[b]	SO[c]	308.15 K				318.15 K				333.15 K			
				w^{AP}	w^{OP}	K^c	Δ_K	w^{AP}	w^{OP}	K^c	Δ_K	w^{AP}	w^{OP}	K^c	Δ_K
PPP	48:0														
PPS	50:0														
POP	50:1	0.50	0.32	1.97	2.31	0.087	0.0024	2.60	2.45	0.151	0.0032	0.33	0.33	0.291	0.0253
PPoO	50:2														
PLiP	52:2	0.97	0.61	3.86	2.71	0.146	0.0037	1.60	1.42	0.160	0.0042	0.91	0.79	0.335	0.0123
POS	52:1														
POO	52:2	3.27	3.33	9.60	8.74	0.113	0.0027	14.60	14.54	0.142	0.0026	5.74	5.55	0.301	0.0047
PSLi	52:2														
POLi	52:3	8.88	8.52	12.03	12.25	0.101	0.0024	10.80	10.46	0.146	0.0027	10.80	10.47	0.300	0.0046
PoOLi	52:4														
PLeO	52:4														
PLiLi	52:4	8.59	10.46	6.56	7.31	0.092	0.0022	3.80	2.98	0.181	0.0036	9.90	9.51	0.303	0.0046
PLeLi	52:5														
SOS	54:1														
SOO	54:2	1.91	1.19	2.75	3.11	0.091	0.0023	6.80	6.11	0.158	0.0030	1.67	2.31	0.210	0.0044
OOO	54:3	7.88	7.58	16.19	15.26	0.109	0.0026	27.90	27.16	0.146	0.0027	12.22	12.19	0.291	0.0044
SOLi	54:3		2.78	3.40	3.04	0.115	0.0029	4.00	3.26	0.174	0.0035	2.20	2.71	0.236	0.0045
OOLi	54:4	20.65	15.18	17.97	16.85	0.109	0.0026	13.02	13.34	0.138	0.0025	16.31	17.23	0.275	0.0041
OLiLi	54:5	29.53	26.76	15.91	15.48	0.105	0.0025	6.68	7.54	0.126	0.0023	21.97	22.09	0.289	0.0043
OOLe	54:5														
LiLiLi	54:6	17.82	18.61	4.91	5.06	0.099	0.0025	2.05	1.96	0.148	0.0034	10.90	10.25	0.309	0.0047
LiLiLe	54:7														
N. U. F. C.[d]			2.96	3.15	6.18			4.45	7.08			5.35	4.87		
average						0.106	0.003			0.152	0.003			0.285	0.007
standard deviation						0.0161				0.0157				0.0347	
CV (%)						15.161				10.352				12.153	

[a]Lida et al.[16]
[b]This work.
[c]Eq. 1.
[d]N. U. F. C.: Non–unidentified Fatty compounds

Table 3. 6. Triacylglycerols Molecular Species Profiles of Canola Oil (CO)

main TAG	group	CO[a]	CO[b]	318.15 K				333.15 K			
				w^{AP}	w^{OP}	K^c	Δ_K	w^{AP}	w^{OP}	K^c	Δ_K
PPS	50:0										
POP	50:1	0.53	0.46	6.39	5.89	0.118	0.0026	3.10	2.80	0.276	0.0043
PPoO	50:2										
POS	52:1	0.51	0.47	1.15	1.09	0.115	0.0038	0.86	0.79	0.271	0.0099
POO	52:2	6.42	8.91	18.55	17.81	0.114	0.0025	15.25	12.93	0.294	0.0037
POLi	52:3	4.45	6.63	2.61	3.26	0.087	0.0021	4.42	4.80	0.230	0.0032
PoOLi	52:4										
PLeO	52:4	2.39	3.19	0.71	0.76	0.102	0.0045	1.38	1.37	0.251	0.0060
PLiLi	52:4										
PLeLi	52:5	0.61	0.97	1.19	1.06	0.123	0.0041	1.04	0.98	0.265	0.0081
SOS	54:1										
SOO	54:2	3.30	3.61	6.60	6.07	0.119	0.0026	5.68	5.50	0.257	0.0034
OOO	54:3	27.02	32.48	48.40	44.98	0.118	0.0026	46.78	43.19	0.270	0.0033
SOLi	54:3										
OOLi	54:4	25.33	22.34	7.03	7.79	0.099	0.0022	9.65	14.36	0.168	0.0021
OLiLi	54:5										
OOLe	54:5	17.19	11.97	1.20	1.65	0.079	0.0024	2.38	4.11	0.144	0.0023
OLiLe	54:6	6.79	4.09	4.55	5.17	0.096	0.0022	4.45	3.59	0.309	0.0044
LiLiLi	54:6		1.24	1.03	1.33	0.085	0.0028	1.00	1.18	0.211	0.0061
LiLiLe	54:7										
OLeLe	55:7	2.06									
OOA	56:2	0.81									
OOGa	56:3	1.61									
N. U. F. C.d		0.98	3.64	0.59	3.14			4.01	4.40		
average						0.105	0.003			0.246	0.005
standard deviation						0.015				0.049	
CV (%)						14.492				20.122	

[a]Silva et al.[9]
[b]This work.
[c]Eq. 1.
[d]N. U. F. C.: Non–unidentified Fatty compounds

Table 3. 7. Triacylglycerols Molecular Species Profiles of Palm Olein (PO)

main TAG	group	PO[a]	PO[b]	298.15 K				318.15 K				333.15 K			
				w^{AP}	w^{OP}	K^c	Δ_K	w^{AP}	w^{OP}	K^c	Δ_K	w^{AP}	w^{OP}	K^c	Δ_K
LOP	46:1	0.52													
PPP	48:0	1.96	1.60	2.09	1.96	0.0921	0.0028	2.03	1.69	0.200	0.0044	2.07	1.87	0.359	0.0065
MOP	48:1	1.44													
PPS	50:0	0.64													
POP	50:1	23.45	28.28	30.17	31.28	0.0832	0.0022	30.22	29.49	0.171	0.0027	32.43	31.78	0.331	0.0037
PPoO	50:2														
PLiP	50:2	6.82	8.30	1.78	6.27	0.0244	0.0007	6.04	6.82	0.147	0.0024	4.62	6.21	0.241	0.0030
PPoLi	50:3														
POS	52:1	5.24	4.80	4.22	5.56	0.0656	0.0018	4.75	5.46	0.144	0.0024	4.73	5.45	0.282	0.0035
POO	52:2	25.82	27.30	20.33	28.90	0.0607	0.0016	28.54	29.95	0.159	0.0025	27.50	29.33	0.304	0.0034
PSLi	52:2														
POLi	52:3	12.42	9.16	2.52	6.60	0.0330	0.0009	6.04	7.38	0.136	0.0022	4.22	6.38	0.215	0.0027
PLiLi	52:4	1.94	1.63	0.38	0.80	0.0410	0.0026	0.78	0.82	0.159	0.0061	0.54	0.66	0.267	0.0131
PLeLi	52:5														
POA	54:1	0.69													
SOO	54:2	3.04	2.62	1.41	2.83	0.0429	0.0013	2.28	2.70	0.141	0.0027	2.43	2.93	0.269	0.0041
OOO	54:3	8.16	3.70	1.71	3.79	0.0390	0.0012	3.43	3.77	0.151	0.0027	3.25	3.87	0.272	0.0037
SOLi	54:3														
OOLi	54:4	5.28	1.50	1.39	1.18	0.1020	0.0036	0.89	0.91	0.164	0.0057	1.04	1.04	0.324	0.0095
OLiLi	54:5	1.42													
N. U. F. C.[d]			11.11	34.00	10.83				15.00	11.00			17.17		
average						0.058	0.002			0.157	0.003			0.286	0.005
standard deviation						0.026				0.0184				0.0436	
CV (%)						45.768				11.691				15.224	

[a]Follegatti–Romero et al.[7]
[b]This work.
[c]Eq. 1.
[d]N. U. F. C.: Non–unidentified Fatty compounds

Table 3. 8. Triacylglycerols Molecular Species Profiles of Palm Oil (PO)

main TAG	group	PO[a]	PO[b]	318.15 K				333.15 K			
				w^{AP}	w^{OP}	K^c	Δ_K	w^{AP}	w^{OP}	K^c	Δ_K
LOP	46:1	2.30									
PPP	48:0	4.71	6.64	6.44	8.38	0.126	0.0021	6.78	6.92	0.329	0.0021
MOP	48:1	2.05	1.62	1.70	1.74	0.160	0.0037	1.71	1.68	0.341	0.0059
MLiP	48:2										
LOO	48:2	2.22									
PPS	50:0	1.50	1.20	0.81	1.53	0.087	0.0028	0.70	0.84	0.279	0.0105
POP	50:2	26.68	31.75	31.50	33.30	0.155	0.0025	30.85	32.80	0.315	0.0016
PLiP	50:2	6.77	7.00	6.83	4.00	0.280	0.0047	6.23	5.71	0.366	0.0025
PPoLi	50:3										
MLiLi	50:4										
POS	52:1	5.81	5.70	4.15	5.40	0.126	0.0021	4.30	5.79	0.249	0.0019
POO	52:2	23.24	23.50	20.50	21.80	0.154	0.0024	20.60	22.81	0.303	0.0015
POLi	52:3	9.75	6.87	6.22	4.06	0.251	0.0042	5.64	5.49	0.344	0.0024
PLiLi	52:4	1.28	1.21	1.19	0.98	0.199	0.0061	0.95	0.85	0.375	0.0120
PoLiLi	52:5										
PLiLe	52:5										
POA	54:1	0.78	0.52	0.36	0.55	0.107	0.0073	0.45	0.52	0.290	0.0171
SOO	54:2	2.68	1.28	1.63	1.96	0.136	0.0031	1.70	1.86	0.306	0.0051
PLiA	54:2										
OOO	54:3	6.03	2.71	2.56	2.72	0.154	0.0029	2.66	2.73	0.327	0.0038
SOLi	54:3										
OOLi	54:4	3.41	0.90	0.97	0.60	0.265	0.0112	0.83	0.86	0.324	0.0110
OLiLi	54:5	0.79									
N. U. F. C.[d]			9.10	15.14	14.38			16.60	11.14		
average						0.169	0.004			0.319	0.006
standard deviation						0.061				0.034	
CV (%)						36.252				10.835	

[a]kallio et al. [4]
[b]This work.
[c]Eq. 1.
[d]N. U. F. C.: Non–unidentified Fatty compounds

In case of the soybean oil system at 318.15 K, the distribution coefficients of TAGs varied within the range of 0.141 to 0.171, with an average value of 0.159; for the temperature 333.15 K the corresponding *K*–values varied within the range of 0.285 to 0.345, with an average value of 0.310**.** The same occurred in the case of sunflower and canola oils: most

triacylglycerols have distribution coefficients within a relatively narrow range of values, although the dispersion of values is higher than the observed for soybean oil. In fact, the coefficients of variation (CV) of the *K*–values were lower than 6 % for the soybean oil system, 16 % for sunflower oil and 20 % for canola oil. The average values of the triacylglycerol distribution coefficients can be compared with the *K*–values obtained for edible oils a whole, according to the values reported in **Table 3.3.** Note that both *K*–values, i.e. the value for the whole oil and the average values for the TAGs contained in each edible oil, are very similar for the three unsaturated vegetable oils. Taking into account these results, it seems possible to conclude that the dispersion of the triacylglycerols *K*–values for each unsaturated oil system is not large, so that the triacylglycerols within each edible oil can be approximated by a unique pseudocomponent, despite their differences in terms of carbon chain size and, mainly, of the number of double bonds.

On the other hand, if one compares the behavior of the major triacylglycerols present in these three oils, relatively large differences can be detected. For instance, OOLi and POLi are among the five triacylglycerols with higher concentrations in all the three unsaturated oils and their distribution coefficients are, respectively, 0.157 and 0.160 for soybean oil at 318.15 K, 0.138 and 0.146 for sunflower oil and 0.099 and 0.087 for canola oil. It is clear that both triacylglycerols have *K*–values close to each other in the case of each edible oil, but significant differences when the same triacylglycerol is considered in all the three systems. OOO is the major triacylglycerol in canola oil and exhibits a distribution coefficient equal to 0.118 at 318.15 K, while the corresponding values are 0.146 and 0.141 for sunflower and soybean oils, respectively. OLiLi and LiLiLi are the major triacylglycerols in sunflower oil, with *K*–values of 0.289 and 0.309 at 333.15 K,

respectively. In case of soybean oil these components are the second and third ones with higher concentration and the corresponding *K*–values are 0.312 and 0.345, in both cases larger than the values observed for sunflower oil, probably due to the higher concentration of polyunsaturated compounds in soybean oil (see **Table 3.1**). Seven triacylglycerols (POP, POO, POLi, SOO, OOO, OOLi, and LiLiLi) are present in all three unsaturated oils, making possible to calculate the average K–values and the standard deviations for each triacylglycerol. The corresponding coefficients of variation are larger than 15% for 6 triacylglycerols at 318.15 K and for 4 triacylglycerols at 333.15 K, indicating that the dispersion of the *K*–values of a specific triacylglycerol contained in different oils is usually greater than the dispersion of the *K*–values of different triacylglycerols contained in the same oil system.

The distribution coefficients of the palm olein + ethanol system are reported in **Table 3.7**. At 318.15 K, the *K*–values varied within the range of 0.136 to 0.200, with an average value of 0.157 and coefficient of variation (CV) of 11.69 %; for the temperature of 333.15 K the *K*–values varied within the range of 0.215 to 0.359, with an average value of 0.286 and a CV of 15.22 %, in both cases a behavior similar to that observed for the unsaturated oils. On the other hand, at 298.15 K the *K*–values varied within a much broader range (0.0244 to 0.1020) causing a much higher coefficient of variation (45.77 %). A similar behavior was obtained for palm oil at 318.15 K (see **Table 3.8**), resulting in a CV–value of 36.25 %; nevertheless, the usual trend observed for the unsaturated oils occurred at 333.15 K (CV of 10.84 %). A possible explanation for the broader dispersion of *K*–values observed at lower temperatures is that these temperatures correspond to equilibrium conditions close to the crystallization temperatures of saturated triacylglycerols. Note that the temperature

decrease has a much larger impact on the distribution coefficients of saturated triacylglycerols than on the corresponding values for unsaturated ones. For instance, the *K*–values of PPP decrease from 0.200 to 0.092 and for OOLi from 0.164 to 0.102 when the temperature of the palm olein system is diminished from 318.15 to 298.15 K. In case of palm oil, a temperature decrease from 333.15 to 318.15 K diminishes the PPP *K*–values from 0.329 to 0.126 and the OOLi *K*–values from 0.324 to 0.265. The higher dispersion of *K*–values makes the pseudocomponent hypothesis less reliable, because these values indicate that the oil fractions contained in both equilibrium phases do not have the same internal composition, even if only in an approximate way. It should also be observed that the triacylglycerols distribution coefficients in the palm olein and palm oil systems can have been influenced by their contents of partial acylglycerols, since these components increase the mutual solubility ethanol + oil.

Figures 3.2 to 3.6 show the distribution coefficients of the major triacylglycerols contained in the refined oils used in the present work. As can be observed, the distribution coefficients for the soybean oil and its main triacylglycerols follow the same trend with the increase of the temperature (**Figure 3.2).** The *K*–values of the major soybean TAGs varied also in a narrow range around the oil distribution coefficients, as already indicated by the low values of coefficient of variation observed in this case (see **Table 3.4**). A similar behavior was observed for sunflower and canola oils, although with a higher dispersion of the major TAGs' *K*–values, especially in case of canola oil (**Figures 3.3** and **3.4).** The trends observed for the major TAGs of palm olein (**Figure 3. 5**) and palm oil (**Figure 3.6**) are also similar.

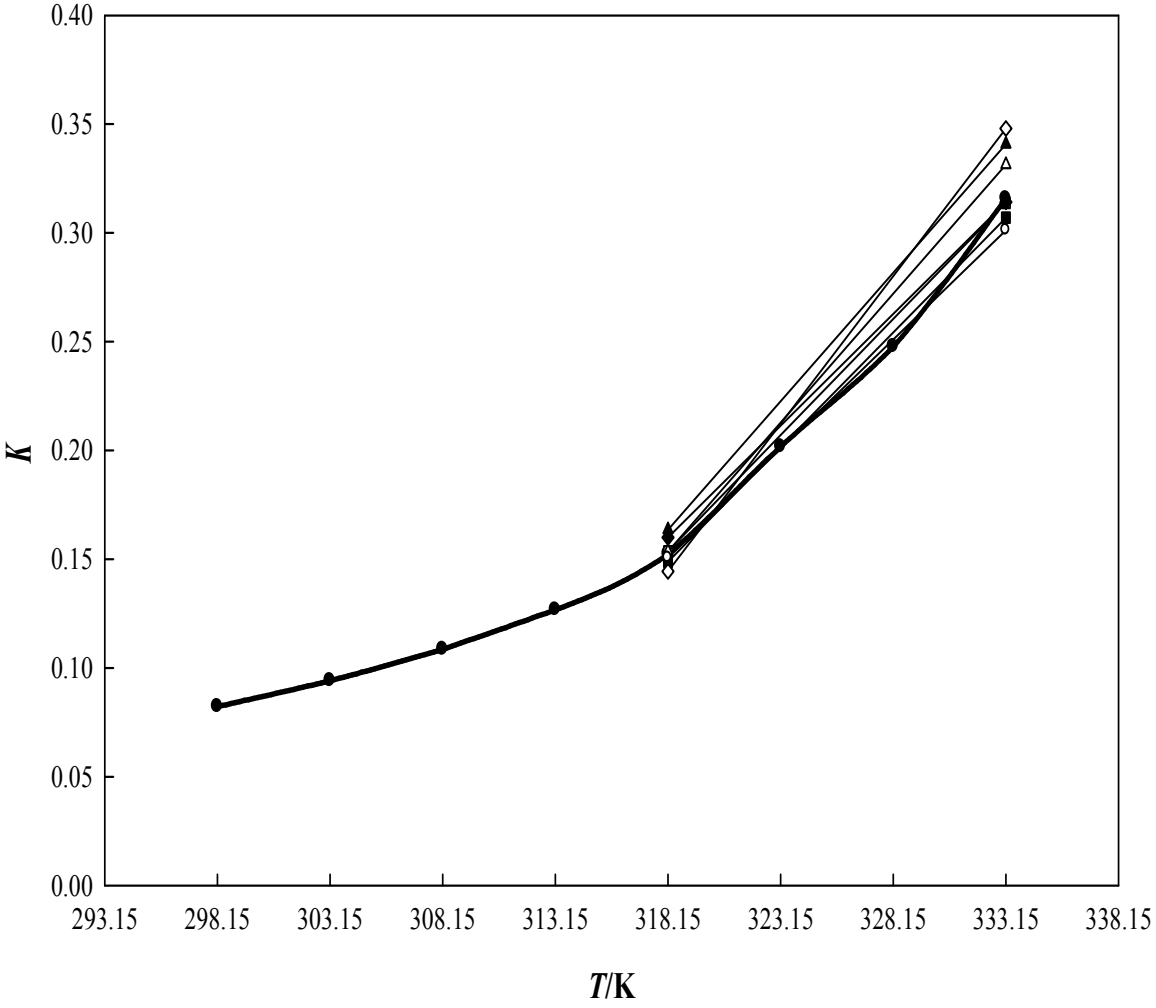

Figure 3. 2. Coefficient distribution for soybean oil (*1*) + ethanol (*7*): (–●–), soybean oil; (▲), POP; (■), POO; (□), POLi; (∆), PLiLi; (○), OOLi; (♦), OLiLi; (◊), LiLiLi

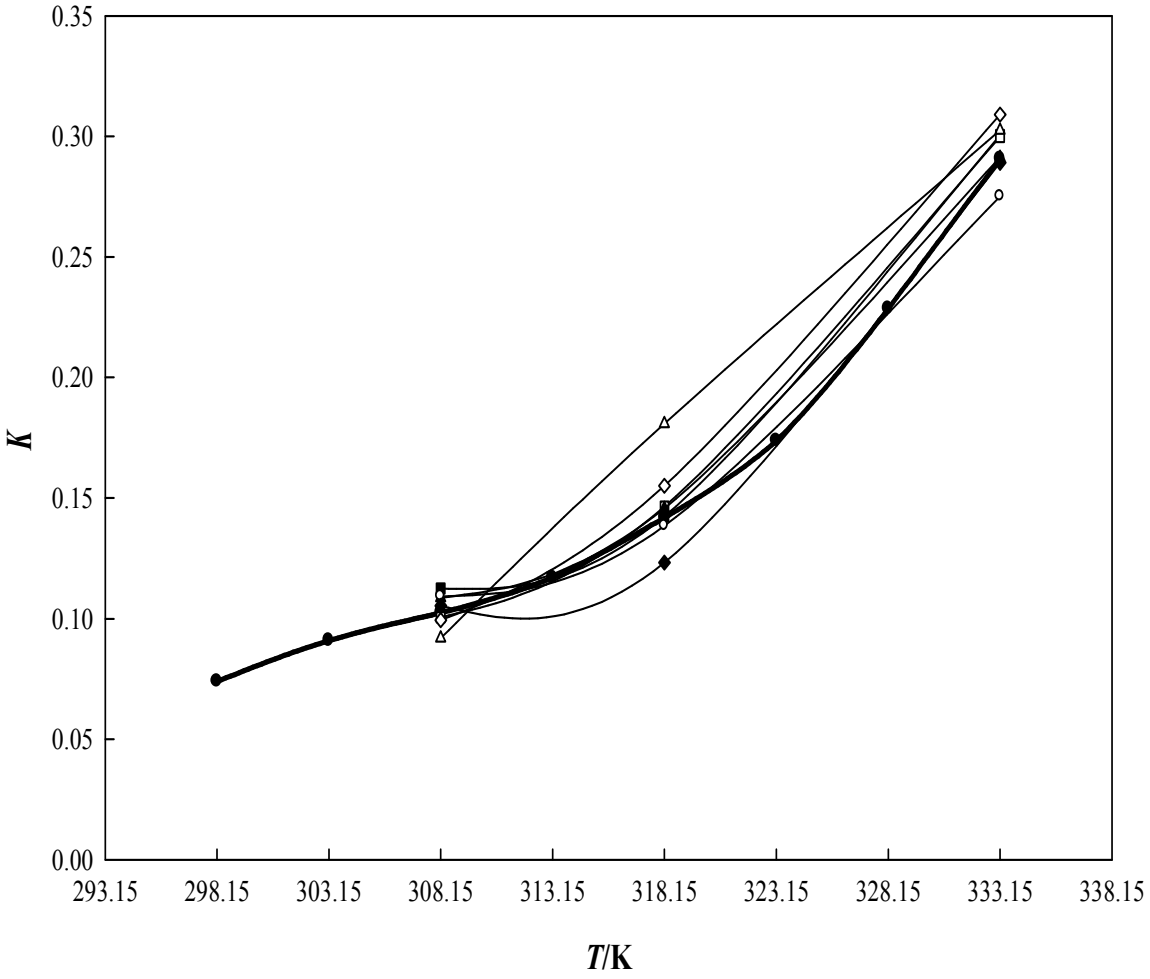

Figure 3. 3. Coefficient distribution for sunflower oil (*2*) + ethanol (*7*): (–●–), sunflower oil; (▲), OOO; (■), POO; (□), POLi; (Δ), PLiLi; (○), OOLi; (♦), OLiLi; (◊), LiLiLi.

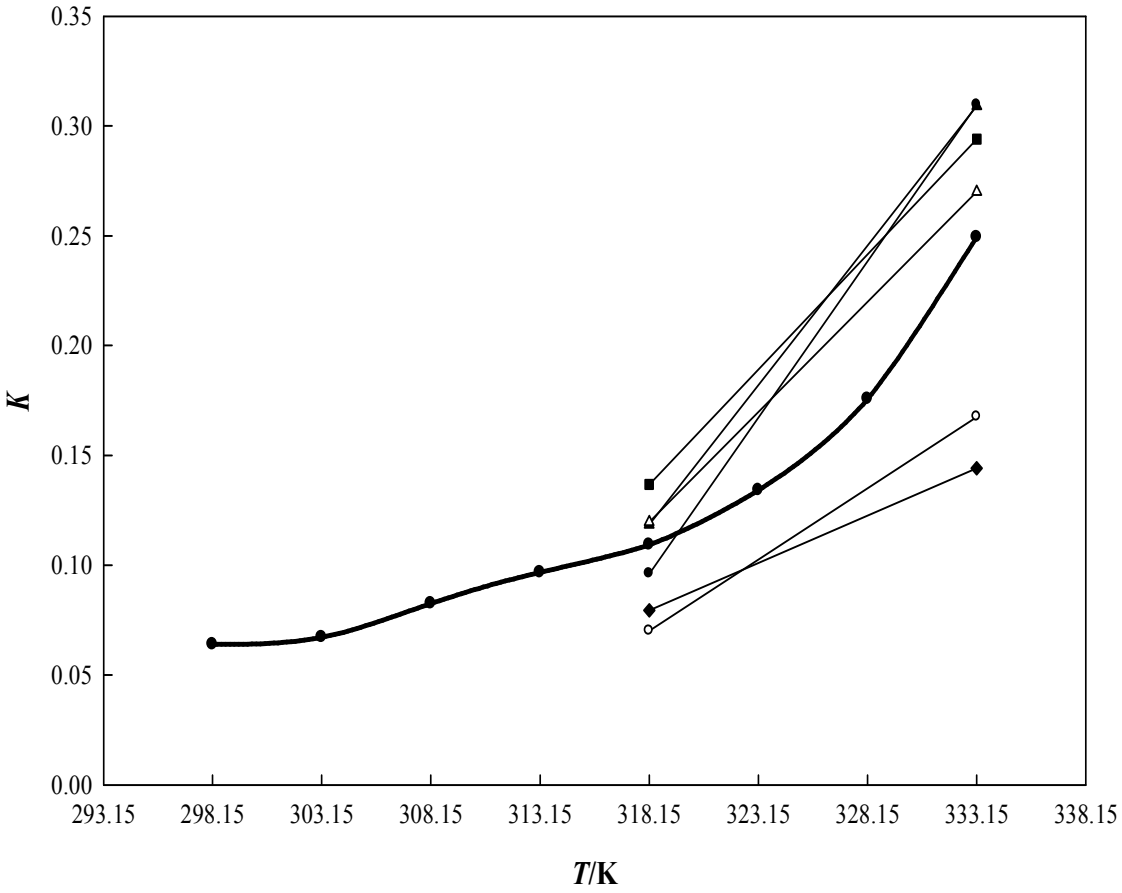

Figure 3. 4. Coefficient distribution for canola oil (*3*) + ethanol (*7*): (–●–), canola oil; (◊), PPP; (▲), POP; (□), PLiP; (■), POO; (○), POLi; (∆), OOO.

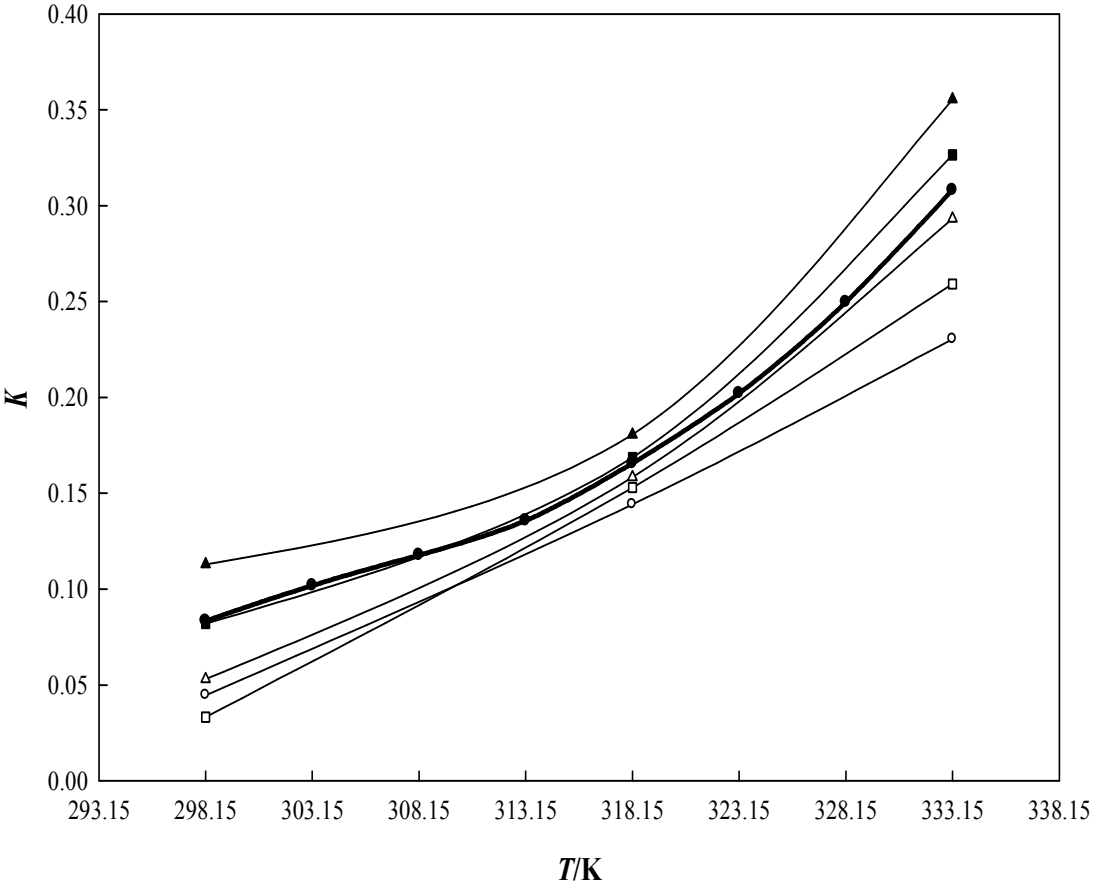

Figure 3. 5. Coefficient distribution for palm olein (*4*) + ethanol (*7*): (–●–), palm olein; (▲); POP; (■), POO; (□), PLiP; (○), POLi; (∆), OOO.

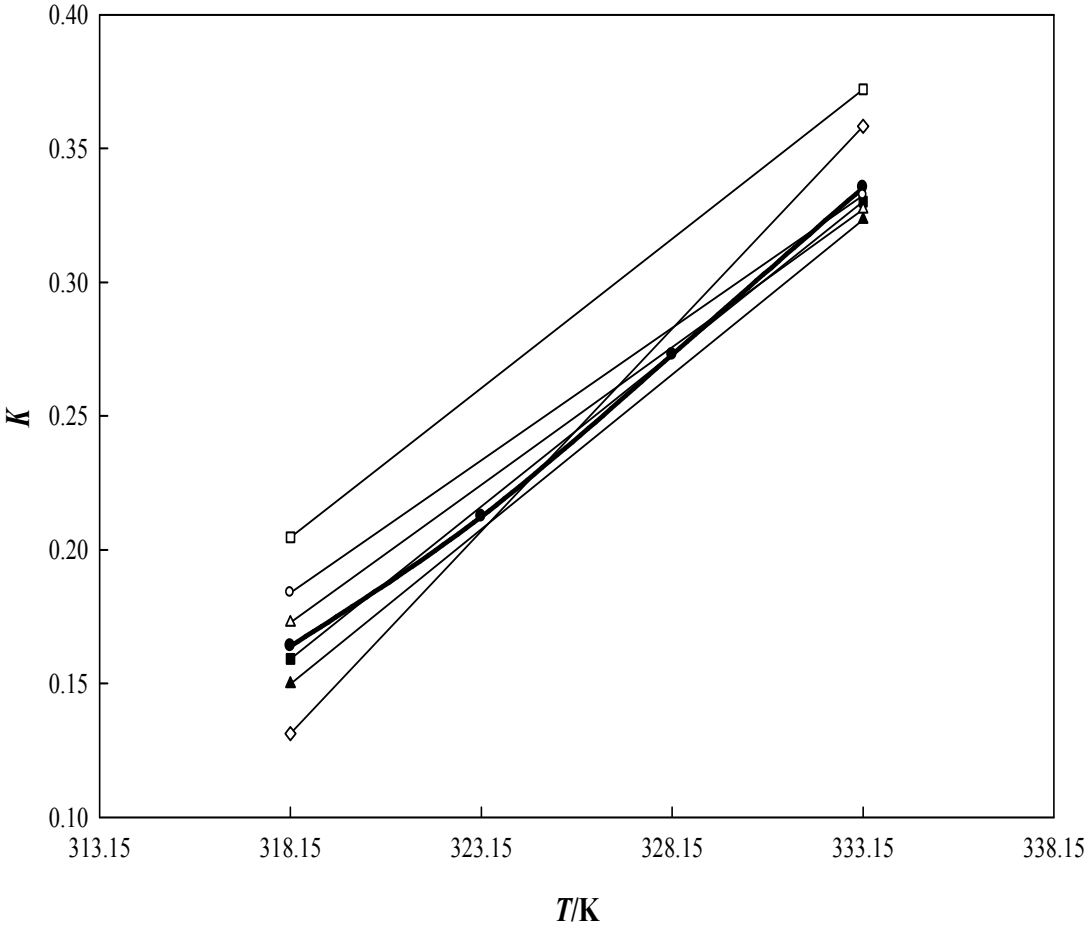

Figura 3. 6. Coefficient distribution for palm oil (*5*) + ethanol (*7*): (–●–), palm oil; (▲), POP; (■), POO; (□), PLiP; (○), POLi; (Δ), OOO.

Conclusions

The partition of triacylglycerols between oily and alcoholic phases was investigated for various oil + ethanol systems within the temperature range from 298.15 to 333.15 K. The triacylglycerols´ distribution coefficients varied within a relatively narrow range of values around the value observed for the corresponding oil considered a pseudocomponent. On the other hand, the dispersion of the distribution coefficients of triacylglycerols increased very

significantly when the temperature was near to the crystallization temperatures of some triacylglycerols, as was detected in the case of saturated edible oils. It was also observed that the dispersion of the distribution coefficients for a specific triacylglycerol contained in different oils is usually higher than the dispersion of the distribution coefficients of different triacylglycerols contained in the same oil. These results seem to justify simplifying assumptions for measuring and modeling equilibrium data for specific oil systems, such as the pseudocomponent hypothesis, but also reveal that the phenomenon of partition depends on the variable composition of the edible oils of interest. In this way, they also emphasize the importance of taking into account the multicomponent character of these systems for a better prediction of their liquid–liquid equilibrium data.

Literature Cited

1. Murugesan, A.; Umarani, C.; Chinnusamy, T. R.; Krishnan, M.; Subramanian, R.; Neduzchezhain, N., Production and analysis of bio–diesel from non–edible oils—A review. Renewable and Sustainable Energy Reviews 2009, 13 (4), 825–834.
2. Srivastava, A.; Prasad, R., Triglycerides–based diesel fuels. Renewable and Sustainable Energy Reviews 2000, 4 (2), 111–133.
3. Firestone, D., Physical and Chemical Characteristics of Oils, Fats and Waxes. 2nd Edition ed 2006, AOCS Press.
4. Kallio, H.; Yli–Jokipii, K.; Kurvinen, J.–P.; Sjövall, O.; Tahvonen, R., Regioisomerism of Triacylglycerols in Lard, Tallow, Yolk, Chicken Skin, Palm Oil, Palm Olein, Palm Stearin, and a Transesterified Blend of Palm Stearin and Coconut Oil Analyzed by Tandem Mass Spectrometry. Journal of Agricultural and Food Chemistry 2001, 49 (7), 3363–3369.
5. Reske, J.; Siebrecht, J.; Hazebroek, J., Triacylglycerol composition and structure in genetically modified sunflower and soybean oils. Journal of the American Oil Chemists' Society 1997, 74 (8), 989–998.
6. Zhou, H.; Lu, H.; Liang, B., Solubility of Multicomponent Systems in the Biodiesel Production by Transesterification of Jatropha curcas L. Oil with Methanol. Journal of Chemical & Engineering Data 2006, 51 (3), 1130–1135.
7. Follegatti–Romero, L. A.; Lanza, M.; da Silva, C. s. A. S.; Batista, E. A. C.; Meirelles, A. J. A., Mutual Solubility of Pseudobinary Systems Containing Vegetable Oils and Anhydrous Ethanol from (298.15 to 333.15) K. Journal of Chemical & Engineering Data 2010, 55 (8), 2750–2756.

8. Lanza, M.; Sanaiotti, G.; Batista, E. A. C.; Poppi, R. J.; Meirelles, A. J. A., Liquid−Liquid Equilibrium Data for Systems Containing Vegetable Oils, Anhydrous Ethanol, and Hexane at (313.15, 318.15, and 328.15) K. Journal of Chemical & Engineering Data 2009, 54 (6), 1850–1859.
9. da Silva, C. s. A. S.; Sanaiotti, G.; Lanza, M.; Follegatti–Romero, L. A.; Meirelles, A. J. A.; Batista, E. A. C., Mutual Solubility for Systems Composed of Vegetable Oil + Ethanol + Water at Different Temperatures. Journal of Chemical & Engineering Data 2009, 55 (1), 440–447.
10. Batista, E.; Monnerat, S.; Stragevitch, L.; Pina, C. G.; Gonçalves, C. B.; Meirelles, A. J. A., Prediction of Liquid−Liquid Equilibrium for Systems of Vegetable Oils, Fatty Acids, and Ethanol. Journal of Chemical & Engineering Data 1999, 44 (6), 1365–1369.
11. Ceriani, R.; Meirelles, A. J. A., Predicting vapor–liquid equilibria of fatty systems. Fluid Phase Equilibria 2004, 215 (2), 227–236.
12. Tang, Z.; Du, Z.; Min, E.; Gao, L.; Jiang, T.; Han, B., Phase equilibria of methanol–triolein system at elevated temperature and pressure. Fluid Phase Equilibria 2006, 239 (1), 8–11.
13. Costa, M. C.; Rolemberg, M. P.; Boros, L. A. D.; Krähenbühl, M. A.; de Oliveira, M. G.; Meirelles, A. J. A., Solid−Liquid Equilibrium of Binary Fatty Acid Mixtures. Journal of Chemical & Engineering Data 2006, 52 (1), 30–36.
14. AOCS, Official Methods and Recommended Practices of the American Oil Chemists' Society 3rd ed.; AOCS Press: Champaign, 1988; Vol. 1–2.
15. Hartman, L.; Lago, R. C. A., Rapid Preparation of Fatty Acid Methyl Esters from Lipids. Lab Pract. 1973, 22, 475–476.
16. Noor Lida, H.; Sundram, K.; Siew, W.; Aminah, A.; Mamot, S., TAG composition and solid fat content of palm oil, sunflower oil, and palm kernel olein belends before and after chemical interesterification. Journal of the American Oil Chemists' Society 2002, 79 (11), 1137–1144.
17. Tellinghuisen, J., Statistical Error Propagation. The Journal of Physical Chemistry A 2001, 105 (15), 3917–3921.
18. AOCS, Official Methods and Recommended Practices of the American Oil Chemists' Society. 5th ed.; AOCS Press: Champaign, 1998.

CAPÍTULO 4

Vapor–Liquid Equilibria Modeling of Fatty Acid Esters Systems with the Cubic–Plus–Association (CPA) Equation of State

Luis A. Follegatti–Romero[a], Mariana B. Oliveira[b,], Marcelo Lanza[d], Fabio R. M. Batista[a], Eduardo A. C. Batista[a], António J. Queimada[c], Antonio J. A. Meirelles[a] and João A. P. Coutinho[b]*

[a]ExTrAE, Laboratory of Extraction, Applied Thermodynamics and Equilibrium, Department of Food Engineering, Faculty of Food Engineering, University of Campinas – UNICAMP, 13083–862, Campinas, SP, Brazil

[b]CICECO, Chemistry Department, University of Aveiro, 3810–193, Aveiro, Portugal

[c]LSRE, Laboratory of Separation and Reaction Engineering, Faculdade de Engenharia, Universidade do Porto, 4200 – 465 Porto, Portugal

[d]EQA/CTC, Chemical and Food Engineering Department, Federal University of Santa Catarina–UFSC, 88040–900, Florianópolis, SC, Brazil

*Corresponding author. Tel.: +351 234 370 958. Fax: +351 234 370 084, e–mail: mbelo@ua.pt

Artigo submetido no FUEL, 2011 (JFUE–A–12–01604).

Abstract

Fatty acid esters have a wide range of applications in various chemical industries, such as pharmaceutical, food and biodiesel. Being able to predict the phase equilibria at reduced pressures of systems composed of fatty acid esters is of major relevance for these industries where partial distillation at reduced pressures is typically the process of choice to separate these compounds.

In the present work, the Cubic–Plus–Association Equation of State (CPA EoS) was applied to predict the reduced pressure vapor–liquid equilibria of binary systems composed of fatty acid ethyl or methyl esters in the pressure range 5332.9 – 13332.23 Pa. It is shown that this model provides very good predictions for these systems with global average deviations inferior to 0.5 % in bubble temperatures.

Keywords: Fatty Acid Esters, VLE, Reduced Pressures, CPA EoS

1. Introduction

Fatty acid esters are broadly available in nature and have been widely used as high–value fine chemicals in the food [1], cosmetic [2], pharmaceutical [3] and rubber [4] industries.

Recently, due to environmental and economical problems related to the use of conventional fuels fatty acid esters (biodiesel) are being considered as reliable alternatives to fossil fuels [5]. Biodiesel is manufactured from naturally occurring fats and oils trough the transesterification of the refined triglycerides with methanol or ethanol in the presence of a catalyst [5]. Depending on the alcohol used, the obtained product can be a mixture of fatty acid methyl esters (FAMEs) or fatty acid ethyl esters (FAEEs) [6].

Distillation under reduced pressure is gaining increasing importance in chemical industries, including the ones dealing with fatty acid ester systems, as it avoids the use of high temperatures thus reducing the energy consumption and high temperature degradation reactions [7]. It takes advantages of existing differences in the boiling point and molecular weight of these compounds under reduced pressure [8].

Knowledge about the vapor–liquid equilibria of fatty acid ester systems is of major importance to correctly design and operate distillation units. Since the efficiency of this process decreases with increasing fatty acid esters molecular weight, as pointed by Sahidi et al. [9], the accurate description of the equilibrium behavior of fatty acid ester mixtures at reduced pressures is of fundamental importance for the design, optimization and operation of vacuum distillation processes.

Few research groups have published experimental data on the vapor–liquid behavior for systems containing only fatty acid esters, and the majority uses the conventional activity coefficient models to model these data. Rose and Supina [10] conducted vapor–liquid

equilibria experiments for binary mixtures composed of fatty acid methyl esters with 6 to 18 carbon atoms in the range between 3999.7 and 13332.2 Pa and predicted the data with the Raoult's and Dalton's Law for ideal behavior. Lately, Silva et al. [11] presented vapor–liquid equilibria (VLE) data for the binaries between ethyl palmitate and ethyl stearate/oleate/linoleate at 5332.9 and 9332.6 Pa and correlated the data with the Wilson, the NRTL and the UNIQUAC models.

Previous works by Oliveira et al. [12, 13, 14] have shown the excellent predictive capability of the Cubic–Plus–Association equation of state (CPA EoS). This association equation of state was previously applied to predict the vapor–liquid equilibria of different systems involving fatty acid esters that are of relevance for the biodiesel production and purification processes, in a wide range of thermodynamic conditions. Very good results using the CPA EoS were obtained by Oliveira et al. [15, 16] for the vapor–liquid equilibria (VLE) of several alcohol + fatty acid esters at atmospheric pressure and at near and supercritical conditions. The same authors also applied this association equation of state to describe the VLE of several CO_2 + fatty acid ester systems in a broad range of temperatures and pressures [17].

In the present work, the CPA EoS is applied to predict the vapor–liquid equilibria at reduced pressures of several binary systems composed of fatty acid esters (FAMEs and FAEEs). The following binary systems were considered: ethyl palmitate + ethyl stearate/oleate/linoleate at 5332.9 Pa; ethyl palmitate + ethyl oleate at 9332.6 Pa and methyl palmitate/methyl laurate + methyl myristate at 3999.7, 5332.9, 6666.1 and at 13332.2 Pa.

2. Model

The Cubic–Plus–Association (CPA) equation of state [18, 19, 20] combines a physical contribution from a cubic equation of state, in this work the Soave–Redlich–Kwong (SRK), with an association term accounting for intermolecular hydrogen bonding and solvation effects [21, 22], originally proposed by Wertheim and used in other association equations of state such as SAFT [23].

It can be expressed in terms of the compressibility factor as:

$$Z = Z^{phys.} + Z^{assoc.} = \frac{1}{1-b\rho} - \frac{a\rho}{RT(1+b\rho)} - \frac{1}{2}\left(1+\rho\frac{\partial \ln g}{\partial \rho}\right)\sum_i x_i \sum_{A_i}\left(1-X_{Ai}\right) \tag{1}$$

where a is the energy parameter, b the co–volume parameter, ρ is the molar density, g a simplified hard–sphere radial distribution function, X_{Ai} the mole fraction of pure component i not bonded at site A, and x_i is the mole fraction of component i.

The pure component energy parameter, a, is obtained from a Soave–type temperature dependency:

$$a(T) = a_0\left[1+c_1\left(1-\sqrt{T_r}\right)\right]^2 \tag{2}$$

When CPA is extended to mixtures, the energy and co–volume parameters of the physical term are calculated employing the conventional van der Waals one–fluid mixing rules:

$$a = \sum_i \sum_j x_i x_j a_{ij} \qquad a_{ij} = \sqrt{a_i a_j}\left(1-k_{ij}\right) \tag{3}$$

and

$$b = \sum_i x_i b_i \tag{4}$$

X_{Ai} is related to the association strength Δ^{AiBj} between sites belonging to two different molecules and is calculated by solving the following set of equations:

$$X_{Ai} = \frac{1}{1 + \rho \sum_j x_j \sum_{B_j} X_{Bj} \Delta^{A_i B_j}} \tag{5}$$

where

$$\Delta^{A_i B_j} = g(\rho) \left[exp\left(\frac{\varepsilon^{A_i B_j}}{RT} \right) - 1 \right] b_{ij} \beta^{A_i B_j} \tag{6}$$

where ε^{AiBj} and β^{AiBj} are the association energy and the association volume, respectively. For a binary mixture composed solely of non–associating compounds, as it is the case of the systems here considered, the binary interaction parameter, k_{ij} (Eq. 3), is the only adjustable parameter.

The simplified radial distribution function, $g(\rho)$, is given by [24]:

$$g(\rho) = \frac{1}{1 - 1.9\eta} \qquad \text{where} \qquad \eta = \frac{1}{4} b \rho \tag{7}$$

For non–associating components, such as esters, CPA has only three pure component parameters in the cubic term (a_0, c_1 and b). These parameters are regressed simultaneously from vapor pressure and liquid density data. The objective function to be minimized is the following.

$$OF = \sum_i^{NP} \left(\frac{P_i^{\text{exptl}} - P_i^{\text{calcd}}}{P_i^{\text{exptl}}} \right)^2 + \sum_i^{NP} \left(\frac{\rho_i^{\text{exptl}} - \rho_i^{\text{calcd}}}{\rho_i^{\text{exptl}}} \right)^2 \tag{8}$$

Using pure compound parameters estimated from pure component data, instead of using critical properties as happens with the SRK EoS, allows an accurate description of liquid

densities and especially of vapor pressures that is essential for a good representation of the VLE:

3. Results and Discussion

The capability of the CPA EoS to predict the vapor–liquid equilibria of binary systems containing FAMEs or FAEEs was evaluated in this work. Experimental data were taken from Silva et al. [11] that presented vapor–liquid equilibria (VLE) data for the binary systems: ethyl palmitate + ethyl stearate/ethyl linoleate/ethyl oleate, all at 5332.9, and ethyl palmitate + ethyl oleate at 9332.6 Pa. The other vapor–liquid equilibria data for methyl esters systems were taken from Rose and Supina [10].

3.1. Correlation of the CPA pure compound parameters

The FAEEs and FAMEs studied in this work are all non–self–associating compounds and so only the three CPA pure compound parameters of the physical term (a_0, c_1 and b) are estimated for each fatty acid ester. These parameters were regressed from experimental saturated vapor pressure data [25] and liquid density data taken from Pratas et al. [26], correlations extrapolated to temperatures between 400 to 500 K. The pure compound parameters for the fatty acid esters studied, along with their critical temperatures, are reported in **Table 4.1**. Critical temperatures were computed with the group contribution method of Wilson and Jasperson [27] for methyl esters and with the Nikitin et al. method [27] in the case of ethyl esters, previously assessed to be the best for these families of esters [28]. An excellent description of vapor pressures and liquid densities for all the fatty acid

esters is achieved with the CPA EoS, with global average deviations of 0.74 % and of 0.37 %, respectively as shown in **Table 4.1**.

Table 4. 1. CPA Pure Compound Parameters Regressed in the Temperature Range 400 – 500 K and Critical Temperatures for the Fatty Acid Esters Studied

Compound	T_c (*K*)	a_0 (J·m^3·mol^{-2})	c_1	$b\times10^5$ (m^3·mol^{-1})	% AAD[a]	
					P	*ρ*
ethyl palmitate	766.41	9.82	2.13	33.80	0.37	0.17
ethyl stearate	786.12	8.85	3.15	37.80	0.93	0.08
ethyl oleate	771.07	14.36	1.34	37.64	2.49	0.61
ethyl linoleate	785.19	11.99	1.82	36.13	0.27	0.26
methyl laurate	710.41	6.76	1.53	23.10	0.67	0.79
methyl myristate	742.40	8.06	1.61	26.51	0.39	0.39
methyl palmitate	765.92	10.71	1.50	31.76	0.09	0.30
global AAD %					0.74	0.37

[a] $\text{AAD} = \%\text{AAD} = \frac{1}{N}\sum_{i=1}^{Np}\left|(\text{exptl}_i - \text{calcd}_i)/\text{exptl}_i\right| \times 100$

3.2. Correlation of the vapor–liquid equilibria

Having estimated the pure compound parameters, it is possible to describe the experimental vapor–liquid equilibria data of binary systems composed of fatty acid esters with the CPA EoS. The CPA EoS is here used in a purely predictive way with the binary interaction parameters, k_{ij}, set to zero. The first systems studied were ethyl palmitate + ethyl stearate/ethyl linoleate at 5332.9 and 9332.6 Pa, respectively. The CPA EoS is able to provide very good predictions for the vapor–liquid equilibria of these systems, as presented in **Figures 4.1** and **4.2**, respectively. Global average deviations inferior to 0.2 % and to 3.6 % were obtained for these systems, respectively for bubble temperatures and for vapor compositions, as reported in **Table 4.2**.

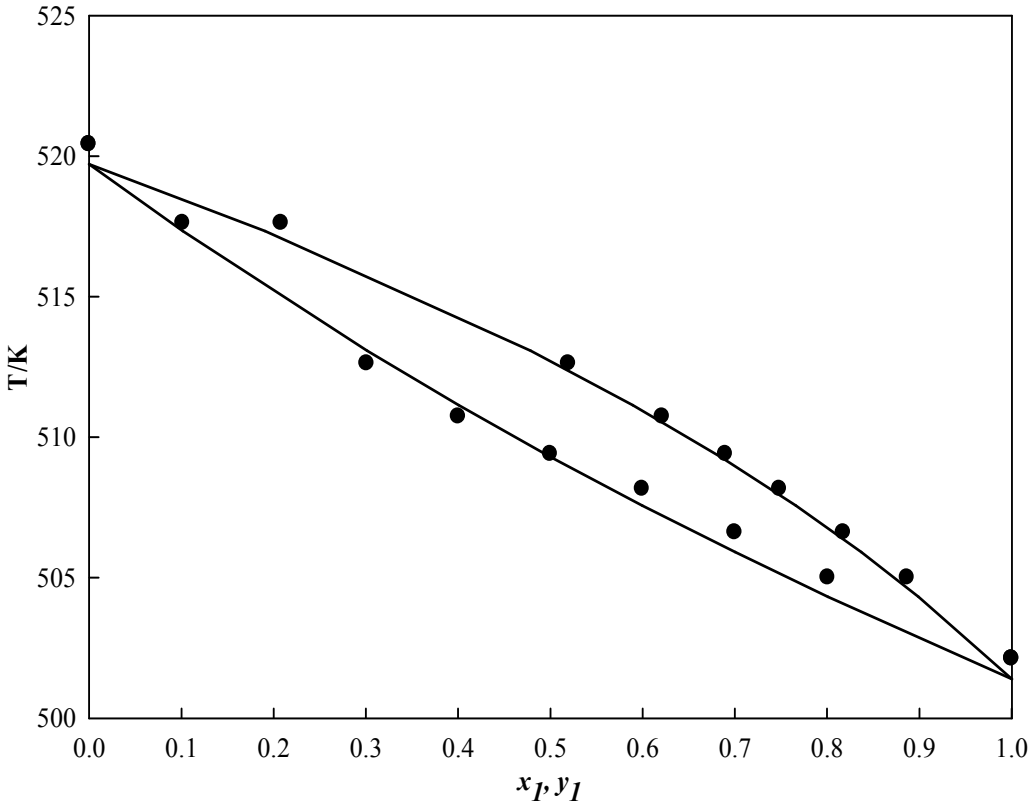

Figure 4. 1. Liquid–vapor equilibrium for the ethyl palmitate (*1*)+ ethyl stearate (*2*) system at 5332.9 Pa. Experimental [11] (●) and CPA results (—).

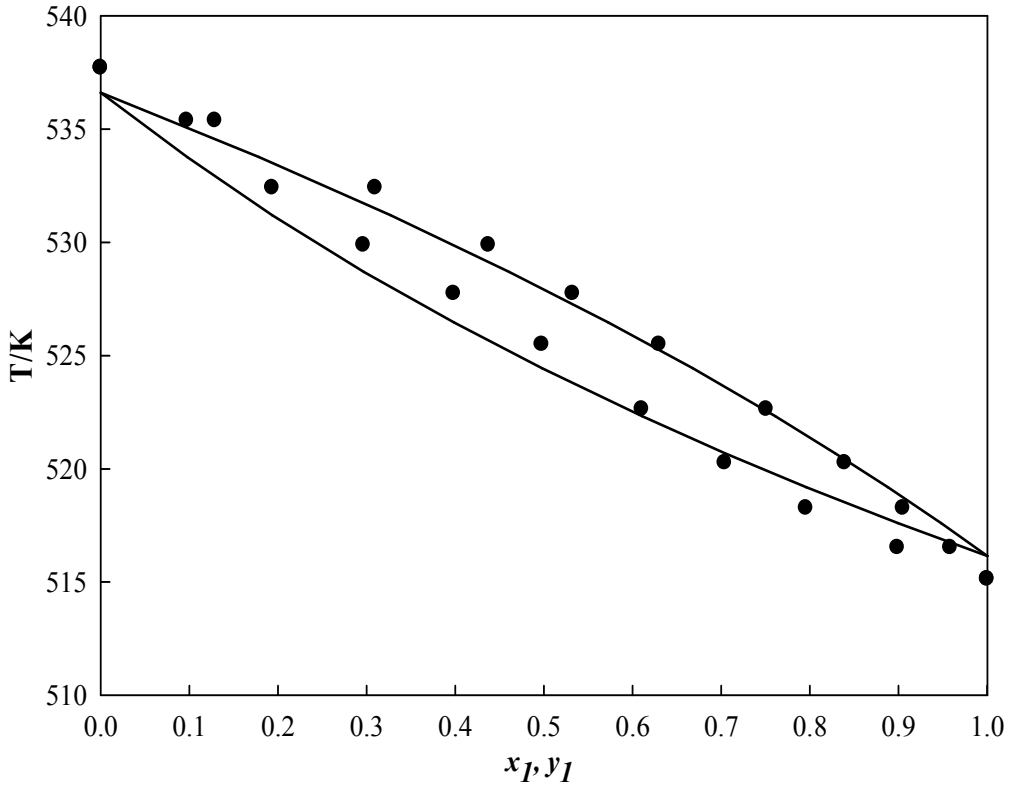

Figure 4. 2. Liquid–vapor equilibrium for the ethyl palmitate (*1*) + ethyl linoleate (*4*) system at 9332.6 Pa. Experimental [11] (●) and CPA results (—).

Table 4. 2. Modeling results for the binary fatty acid systems

system	Pressure (Pa)	% AAD T_b	% AAD y
ethyl palmitate (*1*) + ethyl stearate (*2*)	5332.9	0.10	3.55
ethyl palmitate (*1*) + ethyl linoleate (*3*)	9332.6	0.19	2.70
ethyl palmitate (*1*) + ethyl oleate (*4*)	5332.9	0.23	4.99
ethyl palmitate (*1*) + ethyl oleate (*4*)	9332.6	0.19	4.15
methyl laurate (*5*) + methyl myristate (*6*)	3999.7	0.59	1.27
methyl laurate (*5*) + methyl myristate (*6*)	5332.89	0.67	2.07
methyl laurate (*5*) + methyl myristate (*6*)	6666.1	0.79	3.40
methyl laurate (*5*) + methyl myristate (*6*)	13332.23	0.94	0.72
methyl myristate (*6*) + methyl palmitate (*7*)	3999.7	0.53	3.31
methyl myristate (*6*) + methyl palmitate (*7*)	5332.89	0.48	1.36
methyl myristate (*6*) + methyl palmitate (*7*)	6666.1	0.56	4.22
methyl myristate (*6*) + methyl palmitate (*7*)	13332.23	0.70	2.01
global AAD %		**0.50**	**2.81**

Figure 4.3 shows the vapor–liquid equilibria prediction for the ethyl palmitate + ethyl oleate system at 5332.9 and 9332.6 Pa. At the higher pressures, global average deviations of only 0.19 % and 4.15 were obtained for bubble temperatures and vapor compositions, respectively, as presented in **Table 4.2**. The larger deviations observed for this system at 5332.9 Pa are surely related to the uncertainty of the experimental data at this pressure, since a good prediction with the CPA EoS was observed at 9332.6 Pa.

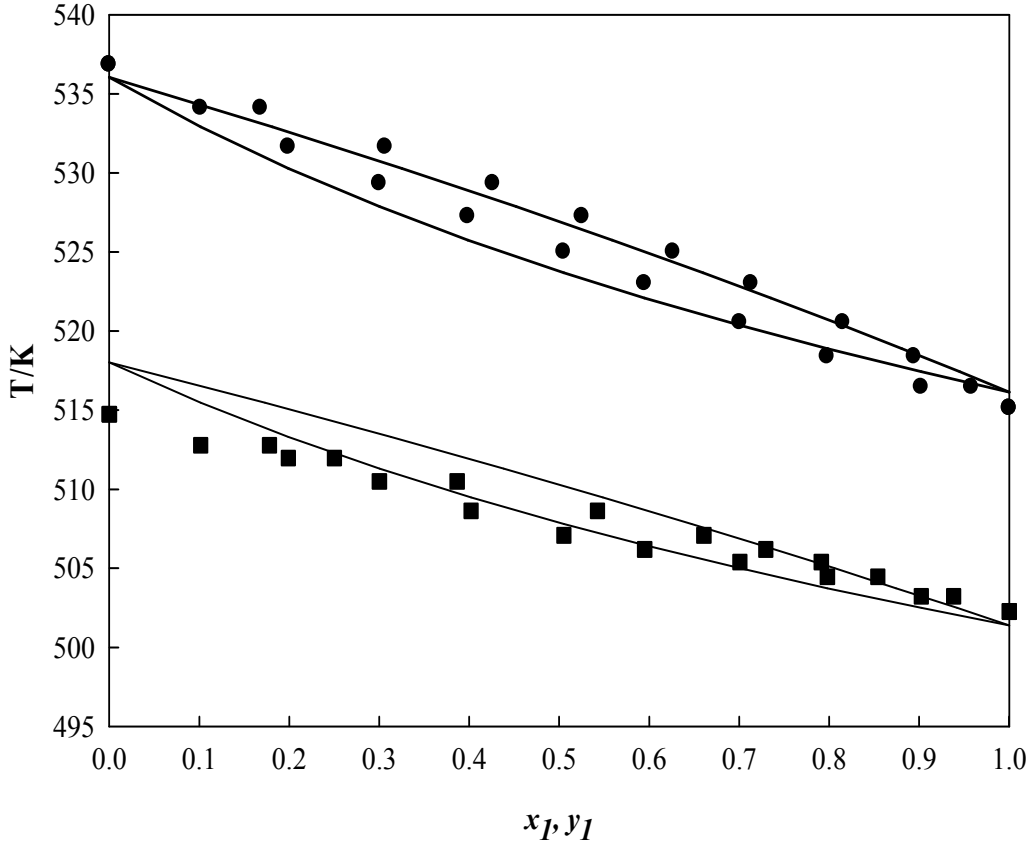

Figure 4. 3. Liquid–vapor equilibrium for the ethyl palmitate (*1*) + ethyl oleate (*3*) system. Experimental [11] at 5332.9 Pa (■) and at 9332.6 Pa (●) and CPA results (—).

The VLE of FAMEs systems found in literature were also predicted in this work with the CPA EoS. Data were available for the methyl laurate + methyl myristate and methyl myristate + methyl palmitate systems at 3999.7, 5332.9, 6666.1 and 13332.2 Pa. Good prediction results for the vapor–liquid equilibria were obtained for all systems at all the studied pressures, as the deviations reported in **Table 4.2** show. However, a degradation of the predictions with increasing pressure was observed, as shown in **Figures 4.4** and **4.5**, what can be justified by the increasing experimental data scattering at higher pressures. Considering all binary systems containing FAMEs, average absolute deviations inferior to 0.66 % were obtained for bubble temperatures and inferior to 2.30 % for vapor compositions.

The overall prediction of the VLE phase diagrams of the binary fatty acid ester systems here studied is very good, taking into account that the CPA EoS is here used as a completely predictive tool, showing the adequacy of this equation of state to predict the phase equilibria relevant for the purification processes involving fatty acid ester systems.

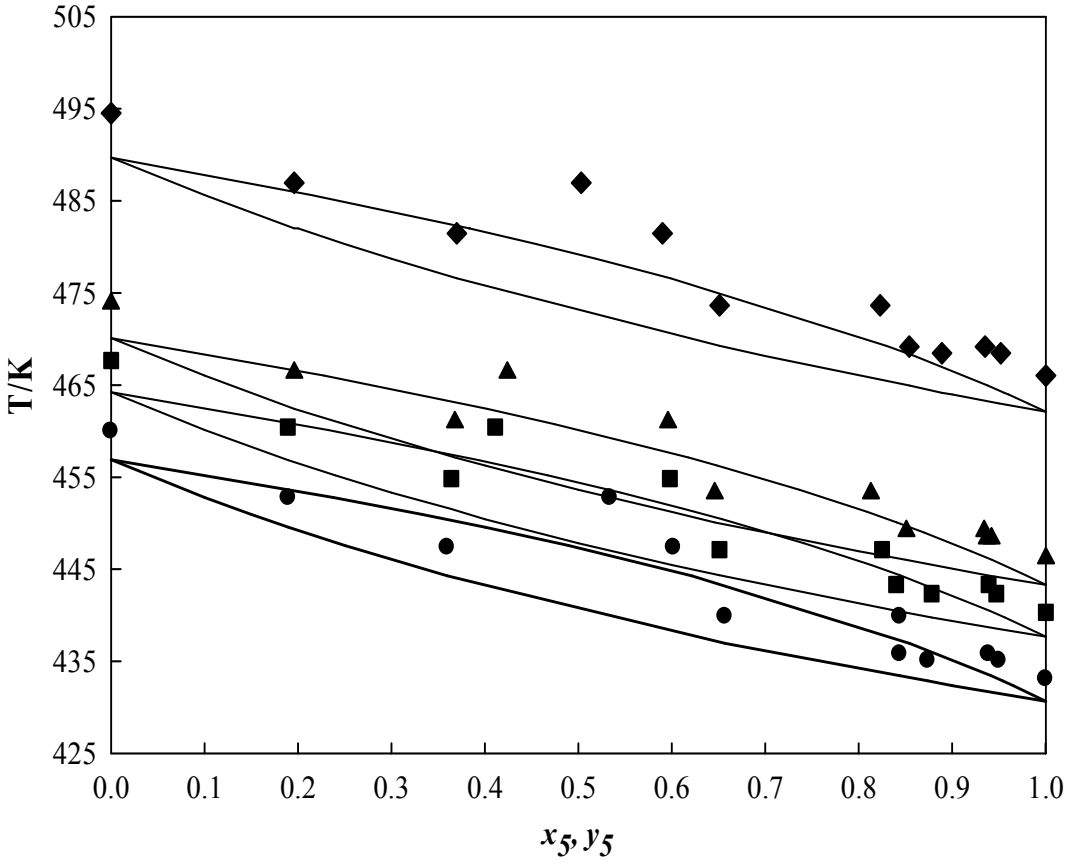

Figure 4. 4. Liquid–vapor equilibrium for the methyl laurate (*5*) + methyl myristate (*6*) system. Experimental [10] at 3999.7 Pa (●), at 5332.89 Pa (■), at 6666.1 Pa (▲) and at 13332.23 Pa (♦) and CPA results (—).

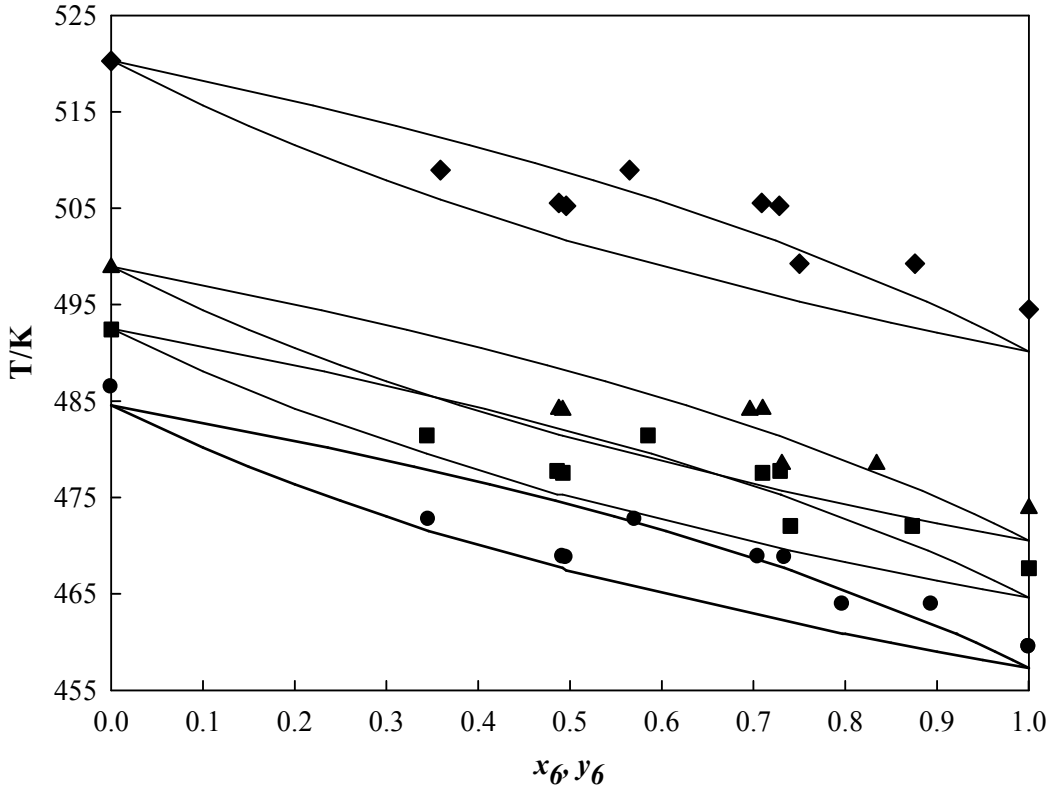

Figure 4. 5. Liquid–vapor equilibrium for the methyl myristate (*5*) + methyl palmitate (*6*) system. Experimental [10] at 3999.7 Pa (●), at 5332.89 Pa (■), at 6666.1 Pa (▲) and at 13332.23 Pa (♦) and CPA results (—).

4. Conclusions

In this work, the Cubic–Plus–Association (CPA) equation of state was successfully applied to predict the reduced pressure vapor–liquid equilibria data of binary systems composed of fatty acid esters. It was shown that it is possible to accurately predict, without using binary interaction parameters, the VLE of the studied systems at reduced pressure conditions with global average deviations inferior to 0.5 % for bubble temperatures and

below 3% for vapor phase compositions. The CPA equation of state is shown here to be a fundamental predictive tool for the design and operation of production facilities of fatty acid esters at the biodiesel, pharmaceutical and food industries.

Acknowledgments

The authors wish to acknowledge FAPESP (08/56258–8), CNPq (306250/2007–1 and 480992/2009–6), CAPES/PEC–PG, CAPES and CAPES/PNPD for their financial support and scholarship. Financial support was provided to LSRE by FEDER/POCI/2010.

Nomenclature

Abbreviations

AAD = global average deviation
CPA = Cubic–Plus–Association
EoS = equation of state
FAEE = fatty acid ethyl ester
FAME = fatty acid methyl ester
NRTL = non–random two liquid model
SAFT = statistical associating fluid theory
SRK = Soave–Redlich–Kwong
UNIQUAC = universal quasi–chemical activity coefficient model
VLE = vapor–liquid equilibria

List of Symbols

a = energy parameter in the physical term of the CPA EoS ($J.m^3.mol^{-2}$)

a_0 = parameter for calculating a ($J.m^3.mol^{-2}$)

A_i = site A in molecule *i*

b = co–volume parameter in the physical term of the CPA EoS ($m^3.mol^{-1}$)

g = radial distribution function

k_{ij} = binary interaction parameter

P = vapor pressure (*Pa*)

R = gas constant ($J.mol^{-1}.K^{-1}$)

T = temperature (*K*)

x = mole fraction

X_{Ai} = fraction of molecule *i* not bonded at site *A*

w = mass fraction

Z = compressibility factor

Greek Symbols

β= association volume in the association part of the CPA EoS

Δ^{AiBj} = association strength between site A in molecule *i* and site B in molecule *j* in the association part of the CPA EoS ($m^3.mol^{-1}$)

ε = association energy in the association part of the CPA EoS ($J.mol^{-1}$)

η = reduced fluid density

Subscripts

c = critical

i,j = pure component indexes

r = reduced

Superscripts

assoc. = association

phys. = physical

calcd = calculated

exptl = experimental

Literature Cited

[1] Kim J, Altreuter DH, Clark DS, Dordick JS. Rapid synthesis of fatty acid esters for use as potential food flavors. J Am Oil Chem Soc 1998; 75:1109–1113.
[2] Keng PS, Basri M, Zakaria MRS, Rahman MBA, Ariff AB, Rahman RNZA, Salleh AB. Newly synthesized palm esters for cosmetics industry. Ind Crop Prod 2009; 29:37–44.
[3] Perez–Feas C, Barciela–Alonso MC, Sedes–Diaz A, Bermejo–Barrera P. Phthalates determination in pharmaceutical formulae used in parenteral nutrition by LC–ES–MS: importance in public health. Anal Bioanal Chem 2010; 397:529–535.
[4] Vermeulen R, Jonsson BAG, Lindh CH, Kromhout H, Biological monitoring of carbon disulphide and phthalate exposure in the contemporary rubber industry, in: Int Arch Occ Env Hea, 2005, pp. 663–669.
[5] Ma FR, Hanna MA. Biodiesel production: a review. Bioresource Technology 1999; 70:1–15.
[6] Van Gerpen J. Biodiesel processing and production. Fuel Process Technol 2005; 86:1097–1107.
[7] Wanasundara UN, Wanasundara PKJPD, Shahidi F, Novel Separation Techniques for Isolation and Purification of Fatty Acids and Oil By–Products, John Wiley & Sons, Inc., 2005.
[8] Brown LB, Kolb DX. Application of Low Temperature Crystallization in the Separation of the Fatty Acids and their Compounds. Prog. Chem. Fats Lipids 3 1955; 57–94.
[9] Shahidi F, Wanasundara UN. Omega–3 fatty acid concentrates: Nutritional aspects and production technologies. Trends Food Sci Tech 1998; 9:230–240.
[10] Rose A, Supina WR. Vapor Pressure and Vapor–Liquid Equilibrium Data for Methyl Esters of the Common Saturated Normal Fatty Acids. Journal of Chemical & Engineering Data 1961; 6:173–179.
[11] Akisawa Silva LY, Matricarde Falleiro RM, Meirelles AJA, Krähenbühl MA. Vapor–liquid equilibrium of fatty acid ethyl esters determined using DSC. Thermochimica Acta 2011; 512:178–182.
[12] Oliveira MB, Pratas MJ, Marrucho IM, Queimada AJ, Coutinho JAP. Description of the Mutual Solubilities of Fatty Acids and Water With the CPA EoS. Aiche J 2009; 55:1604–1613.
[13] Oliveira MB, Queimada AJ, Coutinho JAP. Modeling of Biodiesel Multicomponent Systems with the Cubic–Plus–Association (CPA) Equation of State. Ind Eng Chem Res 2010; 49:1419–1427.
[14] Oliveira MB, Ribeiro V, Queimada AJ, Coutinho JAP. Modeling Phase Equilibria Relevant to Biodiesel Production: A Comparison of g(E) Models, Cubic EoS, EoS–g(E) and Association EoS. Ind Eng Chem Res 2011; 50:2348–2358.
[15] Oliveira MB, Miguel SI, Queimada AJ, Coutinho JAP. Phase Equilibria of Ester plus Alcohol Systems and Their Description with the Cubic–Plus–Association Equation of State. Ind Eng Chem Res 2010; 49:3452–3458.
[16] Oliveira MB, Queimada AJ, Coutinho JAP. Prediction of near and supercritical fatty acid ester plus alcohol systems with the CPA EoS. J Supercrit Fluid 2010; 52:241–248.

[17] Oliveira MB, Queimada AJ, Kontogeorgis GM, Coutinho JAP. Evaluation of the CO2 behavior in binary mixtures with alkanes, alcohols, acids and esters using the Cubic–Plus–Association Equation of State. J Supercrit Fluid 2011; 55:876–892.
[18] Kontogeorgis GM, Michelsen ML, Folas GK, Derawi S, von Solms N, Stenby EH. Ten years with the CPA (Cubic–Plus–Association) equation of state. Part 1. Pure compounds and self–associating systems. Ind Eng Chem Res 2006; 45:4855–4868.
[19] Kontogeorgis GM, Michelsen ML, Folas GK, Derawi S, von Solms N, Stenby EH. Ten years with the CPA (Cubic–Plus–Association) equation of state. Part 2. Cross–associating and multicomponent systems. Ind Eng Chem Res 2006; 45:4869–4878.
[20] Oliveira MB, Coutinho JAP, Queimada AJ. Mutual solubilities of hydrocarbons and water with the CPA EoS. Fluid Phase Equilibr 2007; 258:58–66.
[21] Michelsen ML, Hendriks EM. Physical properties from association models. Fluid Phase Equilibr 2001; 180:165–174.
[22] Wu JZ, Prausnitz JM. Phase equilibria for systems containing hydrocarbons, water, and salt: An extended Peng–Robinson equation of state. Ind Eng Chem Res 1998; 37:1634–1643.
[23] Muller EA, Gubbins KE. Molecular–based equations of state for associating fluids: A review of SAFT and related approaches. Ind Eng Chem Res 2001; 40:2193–2211.
[24] Kontogeorgis GM, Yakoumis IV, Meijer H, Hendriks E, Moorwood T. Multicomponent phase equilibrium calculations for water–methanol–alkane mixtures. Fluid Phase Equilibr 1999; 160:201–209.
[25] Silva LYA, Determinação experimental de dados de pressão de vapor e de equilíbrio líquido–vapor de componentes do biodiesel através da calorimetria exploratória diferencial, in: Department of Chemical Processes, University of Campinas, Campinas, 2010.
[26] Pratas MJ, Freitas S, Oliveira MB, Monteiro SC, Lima AS, Coutinho JAP. Densities and Viscosities of Fatty Acid Methyl and Ethyl Esters. J Chem Eng Data 2010; 55:3983–3990.
[27] Poling B, Prausnitz J, O'Connel J. The Properties of gases and liquids (5th edition). Mc–Graw Hill, 2001.
[28] Lopes JCA, Boros L, Krahenbuhl MA, Meirelles AJA, Daridon JL, Pauly J, Marrucho IM, Coutinho JAP. Prediction of cloud points of biodiesel. Energ Fuel 2008; 22:747–752.

The program used to perform the calculations with the CPA EoS is available at: http://path.web.ua.pt/biodiesel.asp

CAPÍTULO 5

Liquid–Liquid Equilibria for Ternary Systems Containing Ethyl Esters, Ethanol and Glycerol at 323.15 and 353.15 K

Luis A. Follegatti–Romero[a], *Mariana B. Oliveira*[b], *Fabio R. M. Batista*[a], *Eduardo A. C. Batista*[a], *João A. P. Coutinho*[b] *and Antonio J. A. Meirelles*[a,*]

[a]ExTrAE, Laboratory of Extraction, Applied Thermodynamics and Equilibria, Department of Food Engineering, Faculty of Food Engineering, University of Campinas – UNICAMP, 13083–862, Campinas, SP, Brazil

[b]CICECO, Chemistry Department, University of Aveiro, 3810–193, Aveiro, Portugal

*Corresponding author. Tel.: +55 19 3521 4037. Fax: +55 19 3521 4027. E–mail: tomze@fea.unicamp.br

Artigo aceito para publicação no FUEL, 20011 (JFUE–D–11–00602).

Abstract

The knowledge and the capacity to describe the phase equilibria of systems composed by transesterification products are very important for an adequate design and operation of biodiesel production and purification facilities. Despite their importance for the production of ethylic biodiesel, fatty acid ethyl ester + ethanol + glycerol systems have been, up to now, object of less attention than the corresponding systems formed during biodiesel production using methanol.

In this work, new experimental measurements were performed for the liquid–liquid equilibria of the systems ethyl linoleate/ethyl oleate/ethyl palmitate/ethyl laurate + ethanol + glycerol at 323.15 and 333.15 K. It is shown that the Cubic–Plus–Association equation of state (CPA EoS) can successfully predict the new experimental data with global average deviations inferior to 6 %.

Keywords: Ethylic biodiesel, LLE, fatty acid ethyl esters, ethanol, glycerol, CPA EoS

1. Introduction

Biodiesel is at the front line of the new energy solutions to the environmental, political and economical problems related to the use of petroleum based fuels [1]. It can be mixed in all proportions with regular diesel with no motor changes, it's easy to store and transport, has a more favorable combustion profile, it's biodegradable, non toxic and provides lower emissions profiles [2−3]. Biodiesel consists on a blend of fatty acid esters that are industrially produced through the transesterification of a vegetable oil or a fat with an alcohol, usually using a basic catalyst to increase the reaction speed and yield [2].

Methanol is the most commonly used alcohol considering its low price and chemical advantages in the process [3−4], although alternatively other alcohols may be used in the esterification route [5−6]. In fact, bearing in mind that methanol is mainly obtained from non−renewable sources such as natural gas or coal, methylic biodiesel production and use is not completely carbon neutral concerning environmental problems [7−8]. Biodiesel produced from ethanol is entirely based on renewable agricultural sources, has a superior dissolving capability, lower toxicity, higher heat content, higher cetane index and lower cloud and pour points [5, 9−10]. Considering these advantages, its use is a quite promising route in the case of biodiesel production in Brazil, where ethanol is produced in large quantities from sugar cane [11].

The transesterification reaction occurs in a multiphase reactor where the oil reacts with ethanol to produce fatty acid ethyl esters and glycerol [12]. The initial ethanol–vegetable oil two phase reactive mixture [13] changes into an ethanol–glycerol–fatty acid ethyl ester (biodiesel) partially miscible system. Due to the restricted solubilities between FAEEs and glycerol, the current of products leaving the reactor is a biphasic stream composed of the

glycerol rich phase and ethyl esters rich phase. The unreacted ethanol is distributed between these two phases [14].

Understanding and predicting the products distribution between the immiscible phases in a broad range of thermodynamics conditions is required to properly evaluate operating conditions of existing or new ethylic biodiesel production and purification processes. Operation costs can be reduced and biodiesel quality assured, subsequently increasing the industrial feasibility of the process and biodiesel acceptance among consumers. Liquid–liquid equilibria of ternary systems composed of fatty acid esters (usually fatty acid methyl esters), glycerol and alcohols have recently been the focus of several research works. Csernica et al. [15] experimentally determined the LLE data for a commercial biodiesel + glycerol + methanol system. Negi et al. [16] and Andreatta et al. [17] measured the LLE of the methyl oleate + glycerol + methanol system and compared the experimental data with predictions from different UNIQUAC models and the Association Group Contribution Equation of State (GCA EoS). Two versions of the UNIFAC model were also used by Tizvar et al. [18] to predict their experimental results for the LLE of the system methyl oleate + glycerol + methanol + hexane. And finally, França et al. [19] and Macedo et al. [20] measured the LLE of the castor oil methyl ester biodiesel + glycerol + methanol/ethanol systems at 298.15 and 333.15 K and compared the experimental data with predictions from the UNIQUAC and the NRTL models, respectively.

Fatty acid ethyl esters containing systems have been much less studied. Up to now, LLE data have only been presented for the soybean oil ethylic biodiesel + ethanol + glycerol [21] and for the canola oil based ethyl ester biodiesel + ethanol + glycerol [22] systems

An alternative to the usually applied activity coefficient models to predict systems with polar compounds with strong associative interactions found at the biodiesel production and purification processes is the use of association equations of state. Recently, Barreau et al. [23] used the Group Contribution Statistical Associating Fluid Theory (SAFT) to describe the measured LLE data for the methyl oleate + glycerol + methanol system.

A much simpler and reliable alternative was recently proposed by Coutinho and co−workers [24−30] using the Cubic–Plus–Association equation of state (CPA EoS). The CPA EoS was applied to describe the LLE of the above mentioned multicomponent systems showing a similar, if not even better, performance than the group contribution methods referred above, using no more than two, transferable and temperature independent binary interaction parameters[27].

The objective of this work was to increase the available liquid−liquid equilibria data for systems containing fatty acid ethyl esters, ethanol and glycerol of interest for the production of ethylic biodiesel, in particular the equilibria data for systems containing ethyl linoleate/ethyl oleate/ethyl palmitate/ethyl laurate + ethanol + glycerol at 323.15 and 353.15 K.

The excellent extrapolation and predictive performance of the CPA EoS was also used here to predict the measured LLE data, using binary interaction parameters previously established from binary phase equilibria data.

2. Experimental Section

2.1. Materials.

Ethyl palmitate and ethyl laurate used in this work were purchased from Tecnosyn (Cajamar/SP, Brazil), and their mass purities were 99.5, and 99.3 %, respectively. Ethyl oleate and ethyl linoleate used were purchased from Sigma Aldrich, with mass purities of 77.5 and 97 %, respectively. The purities of all fatty acid ethyl esters were determined by Gas Chromatography. In case of the technical grade ethyl oleate the main contaminant was ethyl linoleate. The solvents used were anhydrous ethanol from Merck, with a mass purity of 99.9 %, and THF from Tedia, with a mass purity of 99.8 %. The glycerol used was purchased from Merck, with mass purities of 99.5 %.

Ethyl esters, ethanol and glycerol quantification was carried out in a Shimadzu VP series HPLC equipped with two LC–10ADVP solvent delivery units for binary gradient elution, a model RID10A differential refractometer, an automatic injector with an injection volume of 20 μL, a model CTO−10ASVP column oven for precision temperature control even at sub−ambient temperatures, a single HPSEC Phenogel column (100 Å, 300 mm × 7.8 mm ID, 5 mm), a Phenogel column guard (30 mm × 4.6 mm), a model SCL–10AVP system controller and LC–Solution 2.1 software for remote management.

2.2. Apparatus and Procedures.

The liquid–liquid equilibria data for the systems containing ethyl linoleate/ethyl oleate/ethyl palmitate/ethyl laurate + ethanol + glycerol were determined at 323.15 and

353.15 ± 0.1 K. Tie lines were determined using glass test tubes with screw caps (32 and 10 mL). Known quantities of each component were weighed on an analytical balance with a precision of 0.0001 g (Precisa, model XT220A, Sweden) and added directly to the glass test tubes. The mixture of ethyl ester, ethanol and glycerol was maintained under intensive agitation for 10 min at constant temperature and pressure using a test tube shaker (Phoenix, model AP 56). The ternary mixture was then left at rest for 24 h in a thermostatic water bath at the desired temperature, until two separate, transparent liquid phases were clearly observed. At the end of the experiment, samples were taken separately from the upper and bottom phases using syringes and diluted immediately with tetrahydrofuran (THF) to guarantee an immediate dilution of the samples and avoid further separation into two liquid phases at ambient temperature. It was used the same procedure described in a previous work by Follegatti–Romero et al. [31]

Samples from the two phases were analyzed by liquid chromatography (HPLC). The quantitative determination was carried out using calibration curves (external calibration) obtained using standard solutions for each system component: ethyl esters, ethanol, and glycerol. These compounds were diluted with THF in the concentration range from 0.5–100 mg/mL. The experimental data for each tie–line were replicated at least three times and the values reported in the present work are the average ones. The mass fractions of ethyl esters, ethanol and glycerol were determined from the areas of the corresponding HPSEC chromatographic peaks, adjusted by the response factors obtained by previous calibration.

Distribution coefficients and the solvent selectivity were calculated according to equations 1 and 2, respectively, using the experimental compositions of both phases.

$$K_{d5} = \frac{w_5^{GP}}{w_5^{EP}} \qquad (1) \qquad\qquad S_{5/i} = \frac{K_{d5}}{K_{di}} \qquad (2)$$

where K_{d5} is the distribution coefficient for ethanol, w_5 is its mass fraction in the glycerol (GP) or ester (EP) phases, respectively, and $S_{5/i}$ stands for the solvent selectivity. Note that glycerol can be considered as a solvent able to extract ethanol from the ester phase and, in this way, the solvent selectivity reflects its effectiveness in recovering ethanol from the lipophilic phase (i=1 to 4 for ethyl esters).

2.3. Thermodynamic Modeling.

The Cubic–Plus–Association Equation of State (CPA–EoS) was used to predict the experimental data for the systems containing fatty acid ethyl ester + ethanol + glycerol at 323.15 and 333.15 K.

The CPA–EoS takes into account specific interactions between like (self–association) and unlike (cross–association) molecules [32−34]. It combines a physical contribution from a cubic equation of state, in this work the Soave–Redlich–Kwong (SRK) one, with an association term accounting for intermolecular hydrogen bonding and solvation effects, [35−36] originally proposed by Wertheim for fluids with highly directed attractive forces and used in other association equations of state such as SAFT [37].

It can be expressed in terms of the compressibility factor as:

$$Z = Z^{phys.} + Z^{assoc.} = \frac{1}{1-b\rho} - \frac{a\rho}{RT(1+b\rho)} - \frac{1}{2}\left(1+\rho\frac{\partial \ln g}{\partial \rho}\right)\sum_i x_i \sum_{A_i}\left(1-X_{A_i}\right) \qquad (3)$$

where a is the energy parameter, b the co–volume parameter, ρ is the molar density, g a simplified hard–sphere radial distribution function, X_{Ai} the mole fraction of pure component i not bonded at site A, and x_i is the mole fraction of component i.

The pure component energy parameter, a, is obtained from a Soave–type temperature dependency:

$$a(T) = a_0 \left[1 + c_1\left(1 - \sqrt{T_r}\right)\right]^2 \tag{4}$$

where a_0 and c_1 are regressed (simultaneously with b) from pure component vapor pressure and liquid density data.

When CPA is extended to mixtures, the energy and co–volume parameters of the physical term are calculated employing the conventional van der Waals one–fluid mixing rules:

$$a = \sum_i \sum_j x_i x_j a_{ij} \qquad\qquad a_{ij} = \sqrt{a_i a_j}\left(1 - k_{ij}\right) \tag{5}$$

and

$$b = \sum_i x_i b_i \tag{6}$$

X_{Ai} is related to the association strength Δ^{AiBj} between sites belonging to two different molecules and is calculated by solving the following set of equations:

$$X_{Ai} = \frac{1}{1 + \rho \sum_j x_j \sum_{B_j} X_{Bj} \Delta^{A_i B_j}} \tag{7}$$

where

$$\Delta^{A_i B_j} = g(\rho)\left[\exp\left(\frac{\varepsilon^{A_i B_j}}{RT}\right) - 1\right] b_{ij} \beta^{A_i B_j} \tag{8}$$

where ε^{AiBj} and β^{AiBj} are the association energy and the association volume, respectively.

The simplified radial distribution function, $g(\rho)$, is given by [38]:

$$g(\rho) = \frac{1}{1 - 1.9\eta} \qquad \text{where} \qquad \eta = \frac{1}{4} b\rho \tag{9}$$

For non–associating components, such as ethyl esters, CPA has three pure component parameters in the cubic term (a_0, c_1 and b), while for associating components, such as glycerol and ethanol, it has two additional parameters in the association term (ε and β). In both cases, the parameters were regressed simultaneously from the vapor pressure and liquid density data found in the literature. The objective function to be minimized is the following:

$$OF = \sum_{i}^{NP} \left(\frac{P_i^{\text{exptl}} - P_i^{\text{calcd}}}{P_i^{\text{exptl}}} \right)^2 + \sum_{i}^{NP} \left(\frac{\rho_i^{\text{exptl}} - \rho_i^{\text{calcd}}}{\rho_i^{\text{exptl}}} \right)^2 \tag{10}$$

For a binary mixture composed solely of non–associating compounds, the binary interaction parameter, k_{ij} (Eq. 5), is the only adjustable parameter.

When CPA is used for mixtures containing two self–associating compounds, combining rules for the association term are required [39−40], and in this work the Elliott Combining Rule (ECR) [40] was used:

$$\Delta^{A_i B_j} = \sqrt{\Delta^{A_i B_i} \Delta^{A_j B_j}} \tag{11}$$

Solvation can occur in some systems containing self–associating and non self–associating compounds, as in the case of the ester + glycerol or ester + ethanol mixtures investigated in this work. For this type of systems, the solvation phenomena is considered as a cross–association by the CPA EoS, where the cross–association energy (ε^{AiBj}) is considered to be half the value of the association energy for the self–associating component and the cross

association volume (β^{AiBj}) is left as an adjustable parameter, fitted to the equilibria data. This approach, proposed by Folas et al. [41], was successfully applied to model the phase equilibria of the ethyl laurate/ethyl myristate + ethanol + water system [31] and of multicomponent systems involving fatty acid esters, alcohols and glycerol [22, 27].

In these cases, the following objective function was minimized to estimate the parameters k_{ij} and β^{AiBj}:

$$OF = \sum_{i}^{NP} \left(\frac{x_i^{\text{calcd}} - x_i^{\text{exptl}}}{x_i^{\text{exptl}}} \right)^2 \tag{12}$$

where single phase or all phase data can be selected during the parameter optimization. The association term depends on the number and type of association sites. According to the nomenclature of Huang and Radosz [42] for alcohols, the two–site (2B) association scheme is applied, which proposes that hydrogen bonding occurs between the hydroxyl hydrogen and one of the lone pairs of electrons from the oxygen atom of another alcohol molecule. For the ester family, a single association site is considered that can cross–associate with self–associating molecules. For glycerol, a new association scheme previously proposed for glycerol, the 3 × 2B scheme, is applied [28].

The average deviations (AD) between the experimental compositions and those estimated by the CPA EoS were calculated according to Eq. (13).

$$\text{AD} = \sqrt{\frac{\sum_{n}^{N}\sum_{i}^{R}\left[\left(w_{i,n}^{\text{WP,exptl}} - w_{i,n}^{\text{WP,calcd}}\right)^2 + \left(w_{i,n}^{\text{EP,exptl}} - w_{i,n}^{\text{EP,calcd}}\right)^2\right]}{2NR}} \tag{13}$$

where AD is the average deviation for each system, N is the total number of tie lines of the corresponding system, R is the total number of components (R=3), w is the mass fraction in the glycerol (GP) or ester phases (EP), respectively, i is the component, the subscript n stands for the tie line number and the superscripts exptl and calcd refer to the experimental and calculated compositions.

3. Results and Discussion

Liquid−liquid equilibria data at atmospheric pressure for the ethyl linoleate/ethyl oleate/ethyl palmitate/ethyl laurate + ethanol + glycerol systems at 323.15 and 353.15 K are presented at **Table 5.1.** The accuracy and precision of the experimental data were evaluated through Type A uncertainty, calculated by the standard deviations of the analytical measurements [42]. The uncertainties of the equilibria compositions ranged from (0.05 to 0.88) % by mass for ethyl esters, (0.03 to 0.37) % for ethanol and (0.02 to 0.33) % for glycerol, with the lowest figures associated with the lowest mass fractions within the composition range investigated.

Based on the total system mass and on the phase and overall compositions, mass balances were checked according to the procedure suggested by Marcilla et al. [43] and recently applied to systems containing ethyl esters by Follegatti–Romero et al. [30]. According to this procedure, the mass of both liquid phases was calculated and checked against the total initial mass used in the experimental runs.

Table 5. 1. Experimental Liquid–Liquid Equilibria Data for the Ternary Systems Containing Ethyl Ester (*i*) + Anhydrous Ethanol (*5*) + Glycerol (*6*) at 323.15 and 353.15 ± 0.1 K

ethyl		overall composition			glycerol–rich phase			ester–rich phase			K_{d5} [a]	$S_{5/i}$ [b]
ester (*i*)	T/K	100 w_i	100 w_5	100 w_6	100 w_i	100 w_5	100 w_6	100 w_i	100 w_5	100 w_6		
linoleate (*1*)	323.15	27.483	45.309	27.208	9.936	54.765	35.299	72.285	24.316	3.399	2.25	16.385
		25.813	41.583	32.604	7.155	50.205	42.640	74.970	21.352	3.678	2.35	24.637
		32.158	33.227	34.615	3.564	44.020	52.416	82.498	15.243	2.259	2.89	66.848
		36.702	24.976	38.322	1.540	34.771	63.689	86.552	11.819	1.629	2.94	165.346
		20.501	20.502	58.997	1.123	23.494	75.383	90.790	7.786	1.424	3.02	243.950
		20.613	13.927	65.460	0.970	15.511	83.519	94.234	4.647	1.119	3.34	324.267
		22.360	0.000	77.640	0.900	0.000	99.100	99.200	0.000	0.800		
	353.15	18.650	47.149	34.201	12.597	50.377	37.026	66.197	27.077	6.726	1.86	9.777
		16.563	41.919	41.518	7.639	46.268	46.093	74.647	21.620	3.733	2.14	20.912
		15.600	37.952	46.448	4.663	41.977	53.360	78.431	18.562	3.007	2.26	38.037
		17.271	28.658	54.071	1.469	33.044	65.487	82.944	15.127	1.929	2.18	123.340
		20.322	21.198	58.480	1.228	23.469	75.303	89.617	8.711	1.672	2.69	196.616
		20.904	12.712	66.384	1.092	15.492	83.416	93.158	5.326	1.516	2.91	248.144
		26.471	0.000	73.529	0.970	0.000	99.030	99.101	0.000	0.899		
oleate (*2*)	323.15	23.895	52.256	23.849	16.171	56.170	27.659	61.097	31.992	6.911	1.76	6.634
		29.577	40.816	29.607	8.713	50.359	40.928	73.713	21.801	4.486	2.31	19.542
		31.981	35.881	32.138	5.489	46.320	48.191	77.313	19.210	3.477	2.41	33.963
		35.524	29.041	35.435	2.835	38.716	58.449	83.052	14.437	2.511	2.68	78.562
		41.474	17.048	41.478	0.576	25.640	73.784	89.422	8.406	2.172	3.05	473.533
		44.727	10.542	44.731	0.252	15.447	84.301	92.794	5.232	1.974	2.95	1087.166
		37.681	0.000	62.319	0.190	0.000	99.810	98.161	0.000	1.839		
	353.15	29.577	40.526	29.897	9.219	47.900	42.881	69.551	24.936	5.513	1.92	14.492
		34.124	31.384	34.492	3.762	42.254	53.984	79.830	17.532	2.638	2.41	51.143
		39.271	21.590	39.140	2.521	30.898	66.581	85.889	11.972	2.139	2.58	87.928
		41.531	17.990	40.479	1.886	24.325	73.789	88.400	9.630	1.970	2.53	118.396
		44.317	11.510	44.173	0.900	14.600	84.500	91.891	6.335	1.774	2.30	235.308
		28.996	0.000	71.004	0.320	0.000	99.680	98.027	0.000	1.973		
palmitate (*3*)	323.15	24.958	49.842	25.200	12.350	55.910	31.740	57.058	32.496	10.446	1.72	7.949
		28.544	42.076	29.380	5.852	51.753	42.395	73.558	21.545	4.897	2.40	30.194
		34.244	31.200	34.556	2.323	41.218	56.459	80.684	16.306	3.010	2.53	87.797
		39.341	21.007	39.652	1.384	28.931	69.685	88.353	10.635	1.012	2.72	173.665
		43.000	13.733	43.267	0.592	21.123	78.285	92.431	7.261	0.308	2.91	454.208
		45.690	8.616	45.694	0.299	12.961	86.740	94.761	5.013	0.226	2.59	819.406
		54.967	0.000	45.033	0.174	0.000	99.826	99.947	0.000	0.053		
	353.15	31.087	37.493	31.420	6.510	47.480	46.010	74.236	20.437	5.327	2.32	26.493
		34.325	32.040	33.635	4.707	42.686	52.607	77.302	18.281	4.417	2.33	38.347
		38.156	24.250	37.594	1.202	33.092	65.706	81.289	15.720	2.991	2.11	142.363
		40.452	18.784	40.764	0.794	24.802	74.404	85.124	12.753	2.123	1.94	208.500
		44.317	11.414	44.269	0.322	14.096	85.582	92.123	7.438	0.439	1.90	542.191
		66.466	0.000	33.534	0.190	0.000	99.810	99.919	0.000	0.081		
laurate (*4*)	323.15	29.750	40.540	29.710	7.345	46.431	46.224	58.317	33.686	7.997	1.38	10.944
		34.696	30.646	34.658	2.625	38.388	58.987	72.829	23.709	3.462	1.62	44.922
		39.341	21.557	39.102	1.282	28.699	70.019	83.601	14.846	1.553	1.93	126.061
		43.603	12.752	43.645	0.876	15.434	83.690	91.651	7.824	0.525	1.97	206.387
		64.251	0.000	35.749	0.280	0.000	99.720	99.972	0.000	0.028		
	353.15	32.014	36.841	31.145	10.984	42.193	46.823	58.393	31.852	9.755	1.32	7.042
		34.504	30.895	34.601	3.806	37.925	58.269	71.053	24.273	4.674	1.56	29.169
		38.131	23.819	38.050	1.278	29.904	68.818	77.561	19.873	2.566	1.50	91.323
		41.184	17.265	41.551	0.893	20.283	78.824	84.710	13.855	1.435	1.46	138.870
		44.780	10.027	45.193	0.525	11.786	87.689	91.601	7.640	0.759	1.54	269.162
		56.267	0.000	43.733	0.649	0.000	99.351	99.871	0.000	0.129		

[a] K_{d5} is the ethanol distribution coefficient according to Eq. (1).
[b] $S_{5/i}$ is the solvent selectivity according to Eq. (2).

Average results obtained for the mass balance deviations of each set of experimental data are shown in **Table 5.2**. In all cases, values were lower than 0.30 %, indicating the good quality of the measured data. The equilibrium data were tested using the Othmer–Tobias and Hand correlations [44, 45]. Regression coefficients higher than 0.965 were obtained for all the sets of data measured in the present work, confirming their consistency.

Ethanol distribution coefficients (**Table 5.1**) were calculated as the ratio of the ethanol mass fraction in the glycerol rich phase to the ethanol mass fraction in the ethyl ester rich phase (Eq. 1). Distribution coefficient values were superior to 1.3 showing, as expected, that the glycerol phase is richer in ethanol than the ethyl ester phase.

Table 5. 2. Deviations (δ) for the Global Mass Balance of the Phase Compositions

system	100 δ[a]
ethyl linoleate + ethanol + glycerol at 323.15 K	0.19
ethyl linoleate + ethanol + glycerol at 353.15 K	0.25
ethyl oleate + ethanol + glycerol at 323.15 K	0.12
ethyl oleate + ethanol + glycerol at 353.15 K	0.27
ethyl palmitate + ethanol + glycerol at 323.15 K	0.19
ethyl palmitate + ethanol + glycerol at 353.15 K	0.16
ethyl laurate + ethanol + + glycerol at 323.15 K	0.18
ethyl laurate + ethanol + glycerol at 353.15 K	0.16
average global deviation	0.19

[a] relative deviation of the overall mass balance, calculated by $\delta = \frac{1}{N}\sum_{n}^{N}\left|\left(m^{\mathrm{EP}} + m^{\mathrm{GP}} - m^{\mathrm{OS}}\right)/m^{\mathrm{OS}}\right|$, where m^{EP} is the calculated mass of the ester–rich phase, m^{GP} is the corresponding value of the glycerol–rich phase, m^{OS} is the total mass of the system, and *n* is the tie line number.

The distribution diagram for ethanol in the ethyl oleate + ethanol + glycerol system (this work) is presented in **Figure 5.1** along with the methanol distribution diagram in the methyl oleate + methanol + glycerol system [17]. Methanol distribution coefficients are higher, meaning that in ethanol containing systems the mutual solubility among

components (ethyl esters and glycerol) is higher than those in methanol systems. That can be explained taking into account that esters of long–chain fatty acids are non polar compounds and consequently ethanol (less polar) is more soluble in the fatty acid ester phase than methanol. This fact was already emphasized by Zhou et al. [46] (2006) in their study about the alcohol distribution between the glycerol and ester rich phases during the transesterification reaction with ethanol and methanol.

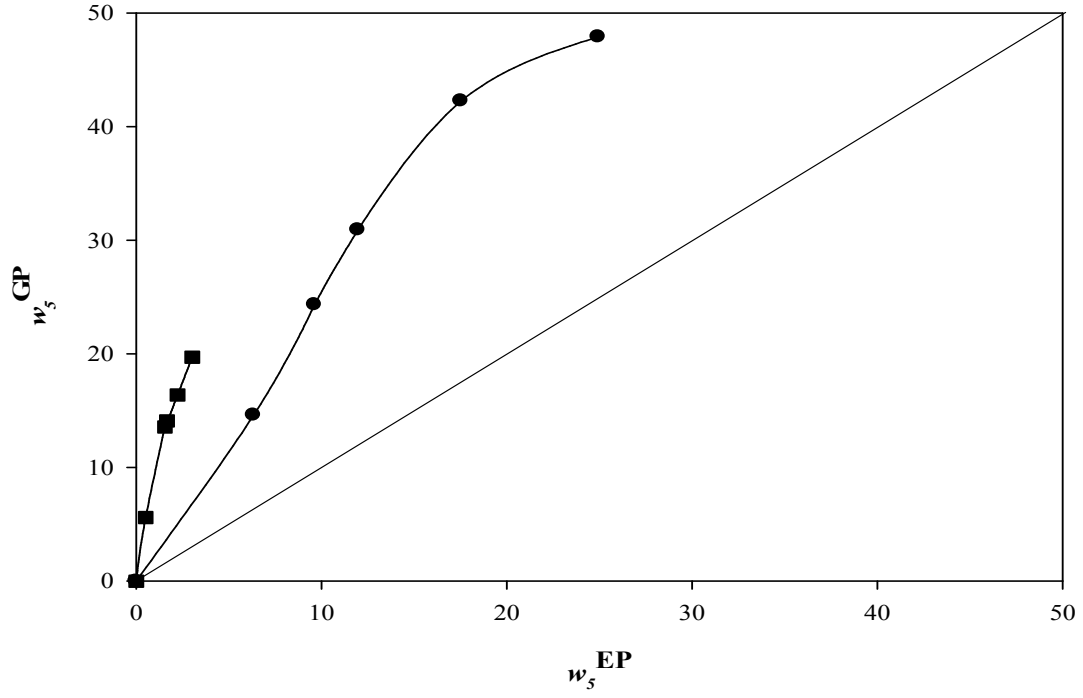

Figure 5. 1. Distribution diagram for ethyl oleate (*2*) + ethanol (*5*) + glycerol (*6*) (–●–, this work) and for methyl oleate + methanol + glycerol (–■–, Andreatta et al.[17]) at 353.15 K.

These authors observed that 42.0% of the alcohol was in the ester rich phase at the end of methanolysis but this percentage increased to 75.4% in case of ethanolysis. Glycerol selectivity was high and in most cases above 100. However, it decreases with increasing

ethanol mass fraction (see **Table 5.1**). This occurs because higher amounts of ethanol enhance the mutual solubility of the glycerol and ester rich phases.

The CPA EoS was used to predict the experimental liquid–liquid equilibria data. The CPA EoS was previously used with success for the description of the LLE of biodiesel multicomponent systems such as ethyl laurate/myristate + ethanol + water [30], methyl stearate/methyl myristate + ethanol + glycerol, methyl oleate/methyl myristate + methanol + glycerol [27] and canola oil ethylic biodiesel + ethanol + glycerol [22], using the same temperature independent binary interaction and cross–association parameters.

To apply the CPA EoS to model the phase equilibria of multicomponent systems, the CPA pure compound parameters (a_0, c_1 and b) are first estimated, usually, trough a simultaneous regression of vapor pressure and liquid density data. In this way, CPA EoS parameters for several esters families were proposed in a previous work [22] where it was also shown that the parameters a_0, c_1 and b follow a linear trend with the ester carbon number. Consequently, correlations to compute these parameters were proposed enabling to estimate them for new compounds when liquid density and vapour pressure data are not available. These correlations were already applied to compute fatty acid esters CPA pure compound parameters enabling to properly predict, for instance, the near and supercritical VLE of fatty acid ester + alcohol systems [25, 26].

With the recent appearance of experimental data for ethyl esters vapor pressures [47] and liquid densities [48] it was also possible to estimate esters CPA pure compound parameters by a simultaneous regression of these pure component data. Critical temperatures (T_c) for fatty acid ethyl esters were determined from the group contribution method of Nikitin et al. [49], that was previously assessed to be the best one to compute this property for ethyl

esters [50]. Thus, two set of CPA pure compound parameters for esters were considered in the present work, a first set based on the regression of vapor pressure and liquid density data and a second one estimated from literature correlations. Both sets were used in the LLE prediction. The parameters obtained with the two referred approaches are presented at **Table 5.3** as well as the liquid densities and vapor pressures deviations.

Table 5. 3. CPA Pure Compound Parameters, modeling Results and Critical Temperatures

compound	T_c (K)	a_0 (J·m^3·mol^{-2})	c_1	$b\times10^5$ (m^3·mol^{-1})	ε (J·mol^{-1})	β	100 AAD[c]	
							P	ρ
[a] ethyl linoleate	785.19	11.99	1.82	36.13	–	–	0.27	0.26
[a] ethyl oleate	771.07	14.36	1.34	37.64	–	–	6.00	0.61
[a] ethyl palmitate	766.41	9.82	2.12	33.80	–	–	0.37	0.17
[a] ethyl laurate	719.13	7.00	1.92	26.12	–	–	4.29	0.33
[b] ethyl linoleate	785.19	12.09	1.75	37.17	–	–	38.05	3.58
[b] ethyl oleate	771.07	12.09	1.75	37.17	–	–	44.06	0.28
[b] ethyl palmitate	766.41	10.80	1.65	33.37	–	–	39.00	0.55
[b] ethyl laurate	719.13	8.23	1.45	25.93	–	–	1.03	14.44
ethanol	514.70	0.68	0.94	4.75	21336	0.0190	0.35	0.51
glycerol	766.10	1.21	1.06	6.96	19622	0.009	0.77	1.49

[a]Parameters calculated from vapor pressure and density data.
[b]Parameters calculated using linear correlations with the ester carbon number.
[c]AAD is calculated by

$$\mathbf{AAD} = \frac{1}{N}\sum_{i=1}^{Np}\left|\left(\text{exptl}_i - \text{calcd}_i\right)/\text{exptl}_i\right|$$

The five CPA pure parameters for ethanol were previously established while performing a systematic study on the pure compound parameters for the n–alcohol family from methanol to n–eicosanol, using the 2B association scheme [51]. The CPA pure parameters for glycerol were previously established considering the 3×2B scheme, and used for modeling the phase equilibria of several glycerol + alcohol and glycerol + water systems [28].

The remaining parameters to be obtained are the binary interaction parameters, k_{ij}, and the cross– association volumes, β_{ij}. In the same way as performed when predicting the LLE of multicomponent systems composed of fatty acid methyl esters + methanol + glycerol

[27], and taking advantage of the transferability of the CPA parameters, binary interaction parameters for the binary subsystems were obtained from binary equilibria data. The possible subsystems comprise fatty acid ethyl ester + glycerol, glycerol + ethanol and fatty acid ethyl ester + ethanol mixtures. The binary interaction parameter, k_{ij}, between ethyl esters and ethanol were obtained from a linear correlation with the ethyl ester carbon number and the β_{ij} for this binary was fixed to 0.1. These correlations and the constant value were previously established by Oliveira et al. [26] when correlating isothermal vapor–liquid equilibria of ethanol + ester systems, with esters from 5 up to 19 carbons, at atmospheric pressure and at temperatures ranging from 339 to 440 K. For fatty acid ester + glycerol mixtures, the binary interaction parameter (k_{ij}) and the cross–association volume (β_{ij}) were fixed in 0.129 and 0.1, respectively, for all systems studied. These values were fitted from mutual solubility data of the methyl dodecanoate + glycerol system, at atmospheric pressure and at temperatures ranging from 370 to 438 K and already applied for modeling other biodiesel multicomponent systems [27]. In the case of the ethanol + glycerol binary, the k_{ij} parameter was taken from the work by Oliveira et al. [28] who used a 3 × 2B scheme for correlating the corresponding vapor–liquid equilibria data, at atmospheric pressure and at temperatures ranging from 363 to 453 K. All parameters mentioned above are given in **Table 5.4**. Note that all required binary interaction parameters and cross−association volumes were taken from the literature and no readjustment was performed in this case.

Table 5. 4. Binary Interaction and Cross–Association Parameters Used to Model Ternary Systems LLE

k_{ij} (unsaturated fatty acid ester + ethanol)	– 0.026
k_{ij} (ethyl palmitate + ethanol)	– 0.020
k_{ij} (ethyl laurate + ethanol)	– 0.083
k_{ij} (fatty acid ester + glycerol)	0.129
β_{ij} (fatty acid ester + ethanol)	0.100
β_{ij} (fatty acid ester + glycerol)	0.100
k_{ij} (ethanol + glycerol)	0.060

Having the CPA pure compounds parameters, the binary interaction parameters and the cross−association volumes, it was then possible to predict the measured multicomponent phase equilibria. A slightly better LLE prediction was obtained when using pure parameters estimated from the ester carbon number correlations proposed in the literature, as shown in **Figure 5.2**, where the predicted and experimental ethanol distribution coefficients are plotted. The average deviations between the experimental and calculated compositions in both phases are shown in **Table 5.5**. Deviations are within the range 2.71 – 12.48 % and a global average deviation of 5.88 % was obtained using pure parameters obtained from the ester carbon number correlations. In the case of pure parameters based on the regression of vapor pressure and liquid density data, the deviations were slightly higher.

Table 5. 5. Average Deviations (AD) between the Experimental and CPA Phase Compositions

system	100AD[a]
ethyl linoleate + ethanol + glycerol at 323.15 K	6.45
ethyl linoleate + ethanol + glycerol at 353.15 K	3.13
ethyl oleate + ethanol + glycerol at 323.15 K	7.89
ethyl oleate + ethanol + glycerol at 353.15 K	4.18
ethyl palmitate + ethanol + glycerol at 323.15 K	2.74
ethyl palmitate + ethanol + glycerol at 353.15 K	2.23
ethyl laurate + ethanol + + glycerol at 323.15 K	8.40
ethyl laurate + ethanol + glycerol at 353.15 K	9.97
average global deviation	5.62

[a]Eq. (13).

Figures 5.3 to 5.8 shows the experimental and predicted tie–lines for ethyl linoleate, oleate and palmitate ternary systems in the selected temperature range The predicted tie–lines given in these figures were calculated using the pure parameters determined from the ester carbon number correlations proposed in the literature. As can be observed in these figures, the deviations between experimental and calculated values are larger in the region close to the plait point. Similar average deviation between the experimental and calculated compositions by CPA EoS were recently reported by Follegatti–Romero et al. [28] for fatty systems containing ethyl esters, ethanol and water.

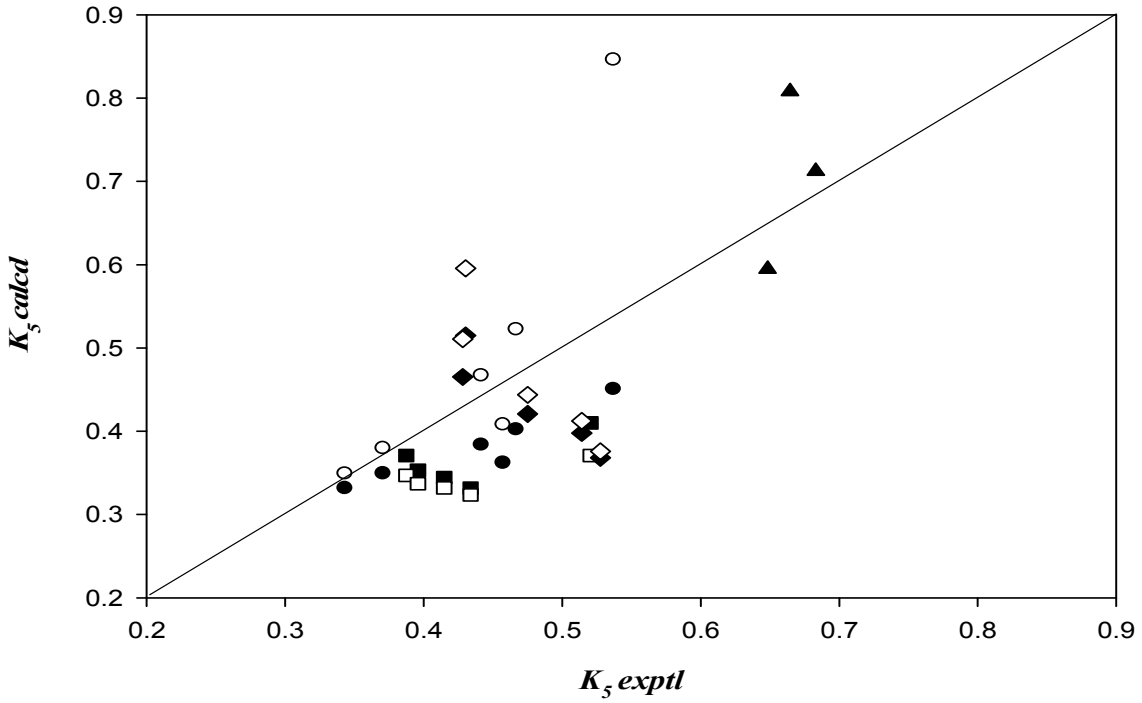

Figure 5. 2. Ethanol distribution coefficient from the CPA EoS versus the experimental ethanol distribution coefficient for the systems ethyl ester (*i*) + ethanol (*5*) + glycerol (*6*) at 323.15 K: ●○, ethyl linoleate; ■□, ethyl oleate; ♦◊, ethyl palmitate; ▲, ethyl laurate. Full symbols represent CPA EoS results using CPA pure parameters for esters computed from ester carbon number correlations and the empty symbols represent the CPA EoS results using pure parameters for esters calculated from density and vapor pressure data.

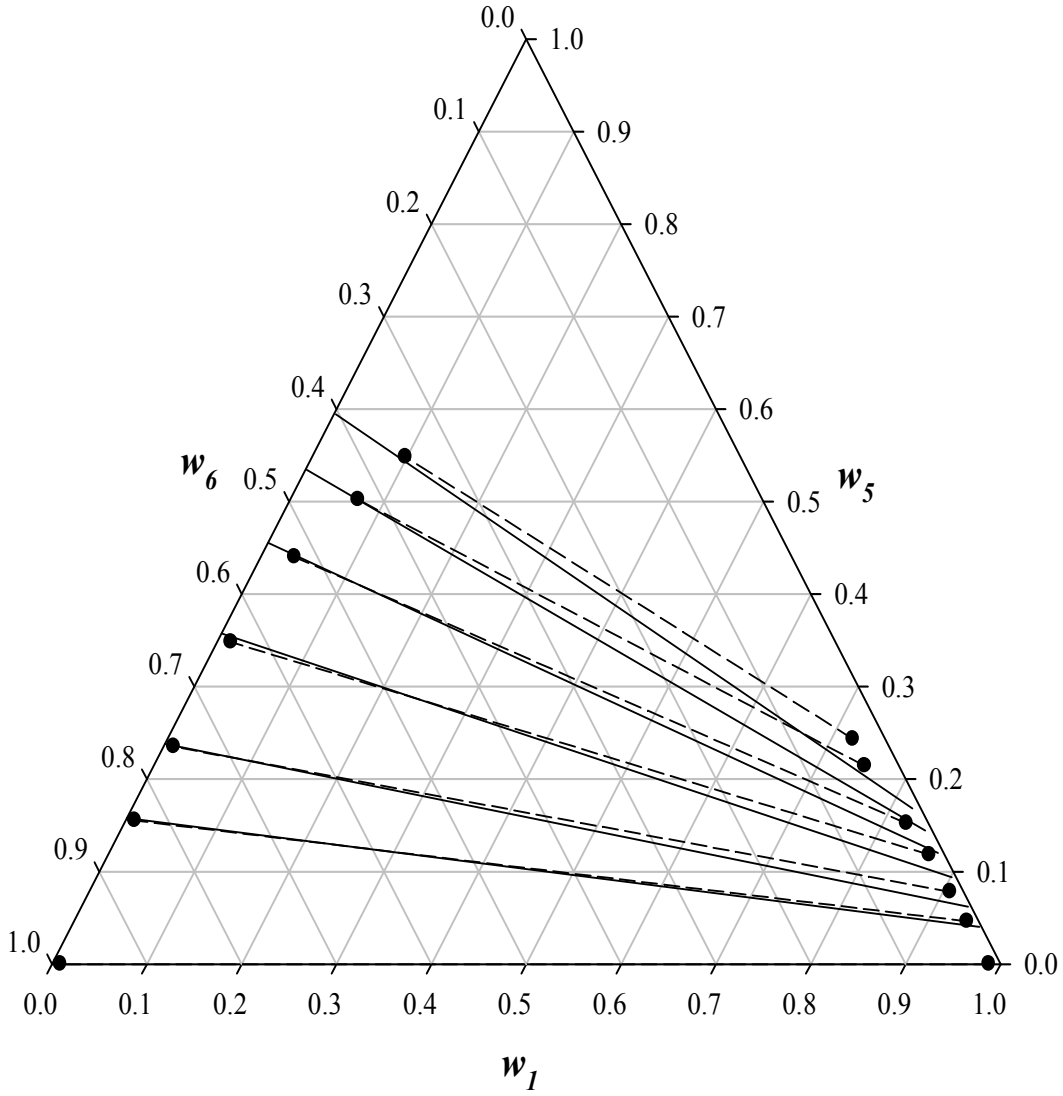

Figure 5. 3. Liquid–liquid equilibria for the system containing ethyl linoleate (*1*) + ethanol (*5*) + glycerol (*6*) at 323.15 K. Experimental (● and ——) and CPA EoS results using CPA pure compound parameters for esters computed from ester carbon number correlations (—).

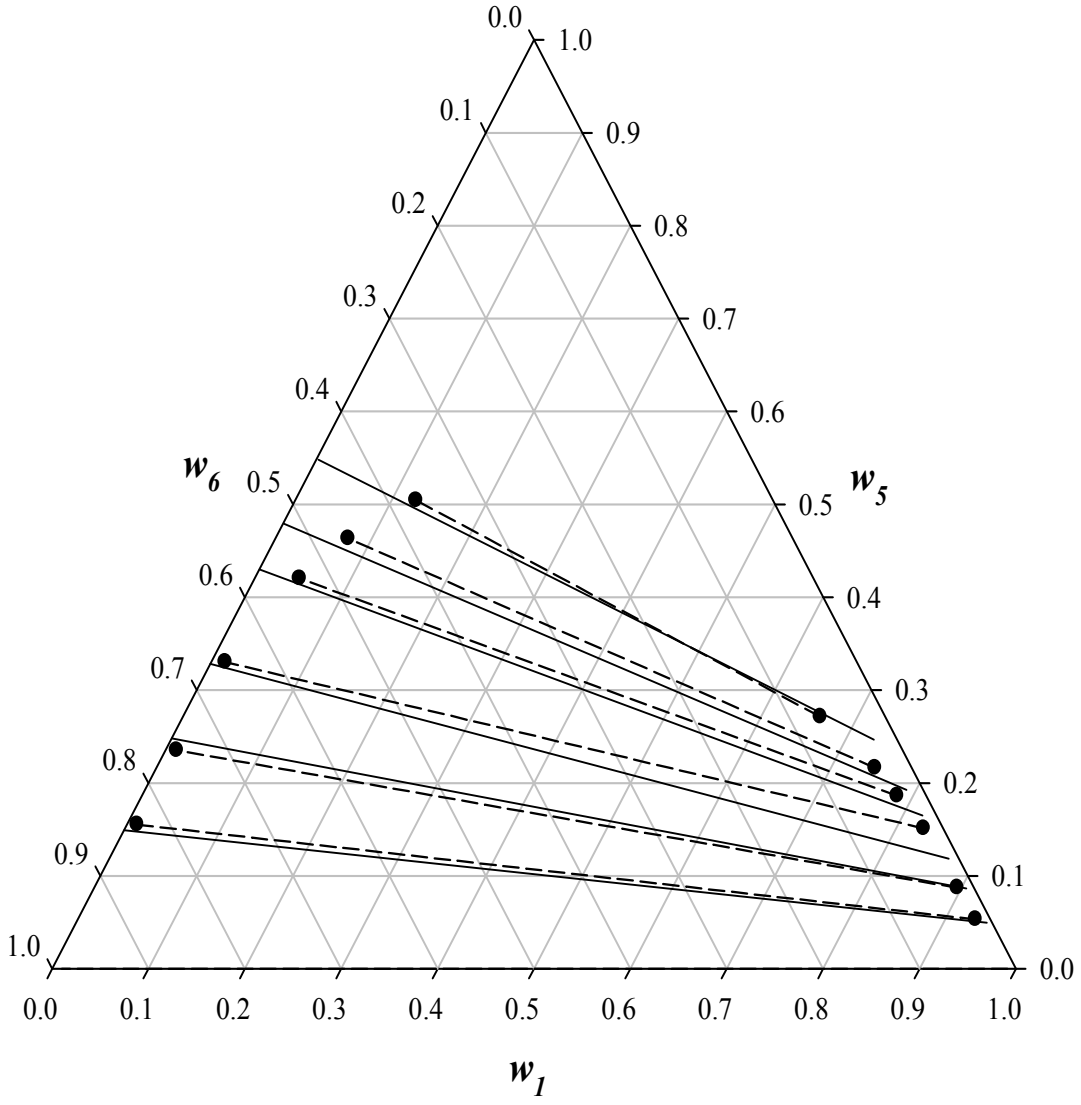

Figure 5. 4. Liquid–liquid equilibria for the system containing ethyl linoleate (*1*) + ethanol (*5*) + glycerol (*6*) at 323.15 K. Experimental (● and ——) and CPA EoS results using CPA pure compound parameters for esters computed from ester carbon number correlations (—).

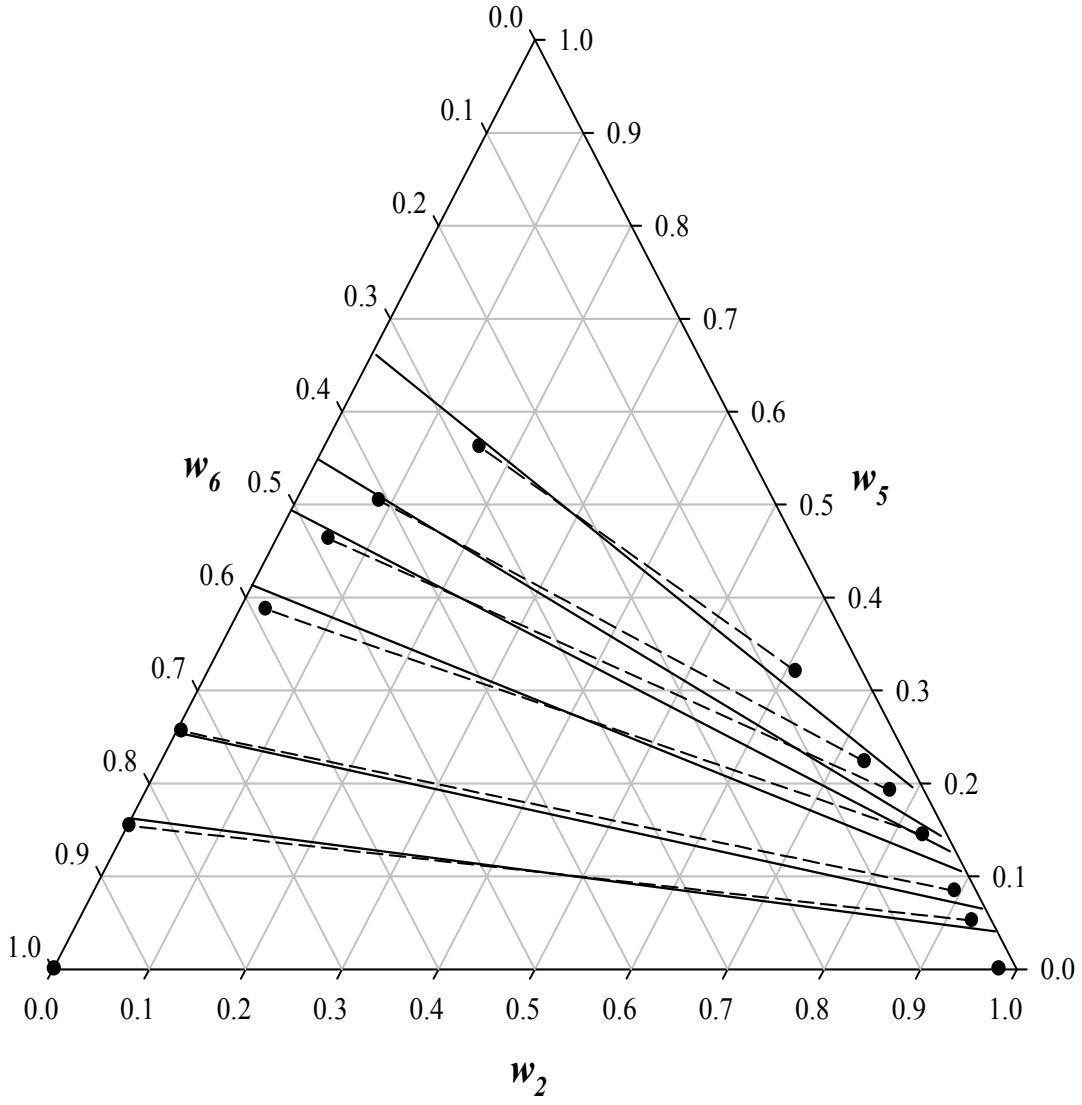

Figure 5. 5. Liquid–liquid equilibria for the system containing ethyl oleate (*2*) + ethanol (*5*) + glycerol (*6*) at 323.15 K. Experimental (● and ——) and CPA EoS results using CPA pure compound parameters for esters computed from ester carbon number correlations (—).

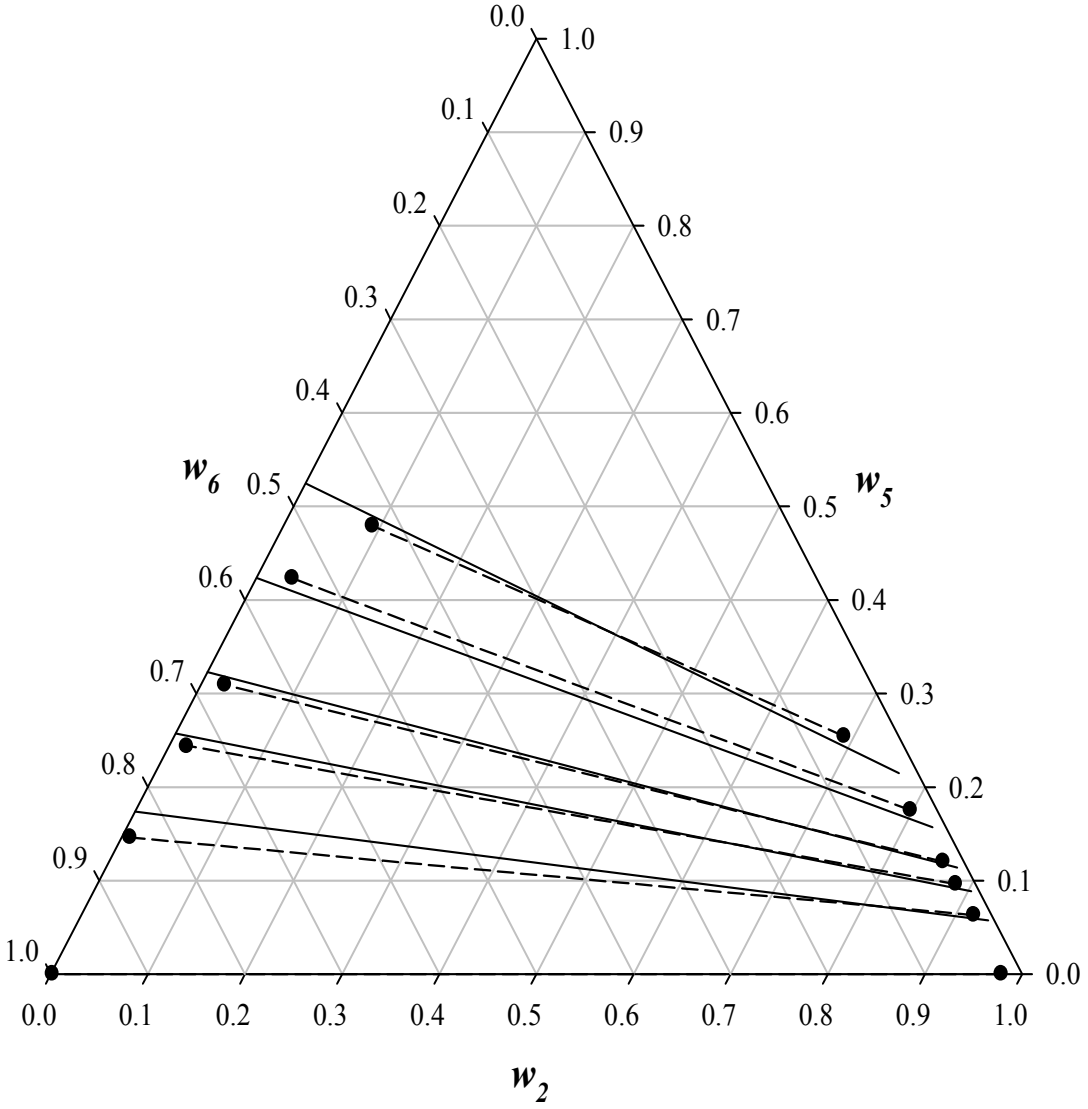

Figure 5. 6. Liquid–liquid equilibria for the system containing ethyl oleate (*2*) + ethanol (*5*) + glycerol (*6*) at 353.15 K. Experimental (● and ——) and CPA EoS results using CPA pure compound parameters for esters computed from ester carbon number correlations (—).

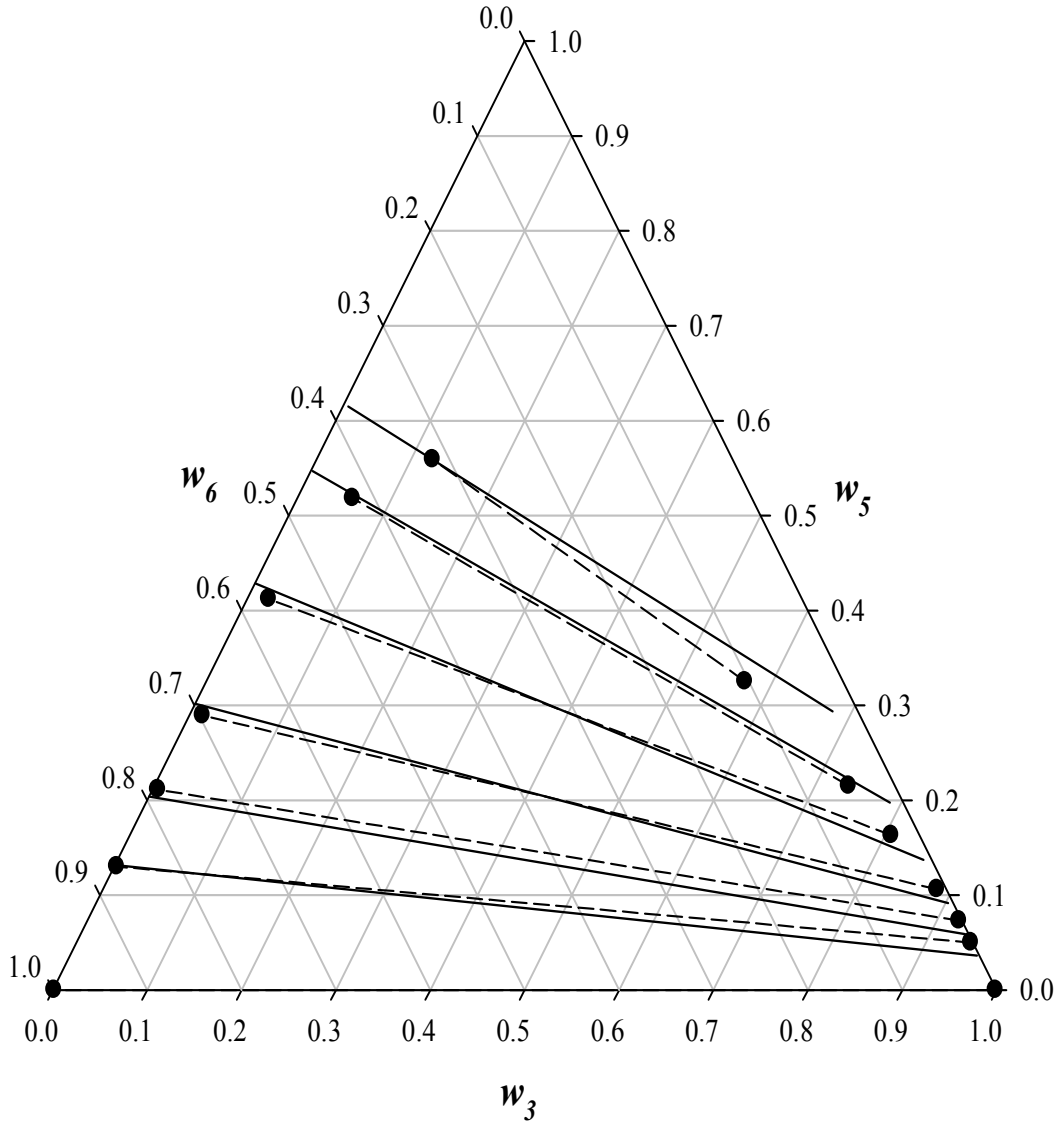

Figure 5. 7. Liquid–liquid equilibria for the system containing ethyl palmitate (*3*) + ethanol (*5*) + glycerol (*6*) at 323.15 K. Experimental (● and ——) and CPA EoS results using CPA pure compound parameters for esters computed from ester carbon number correlations (—).

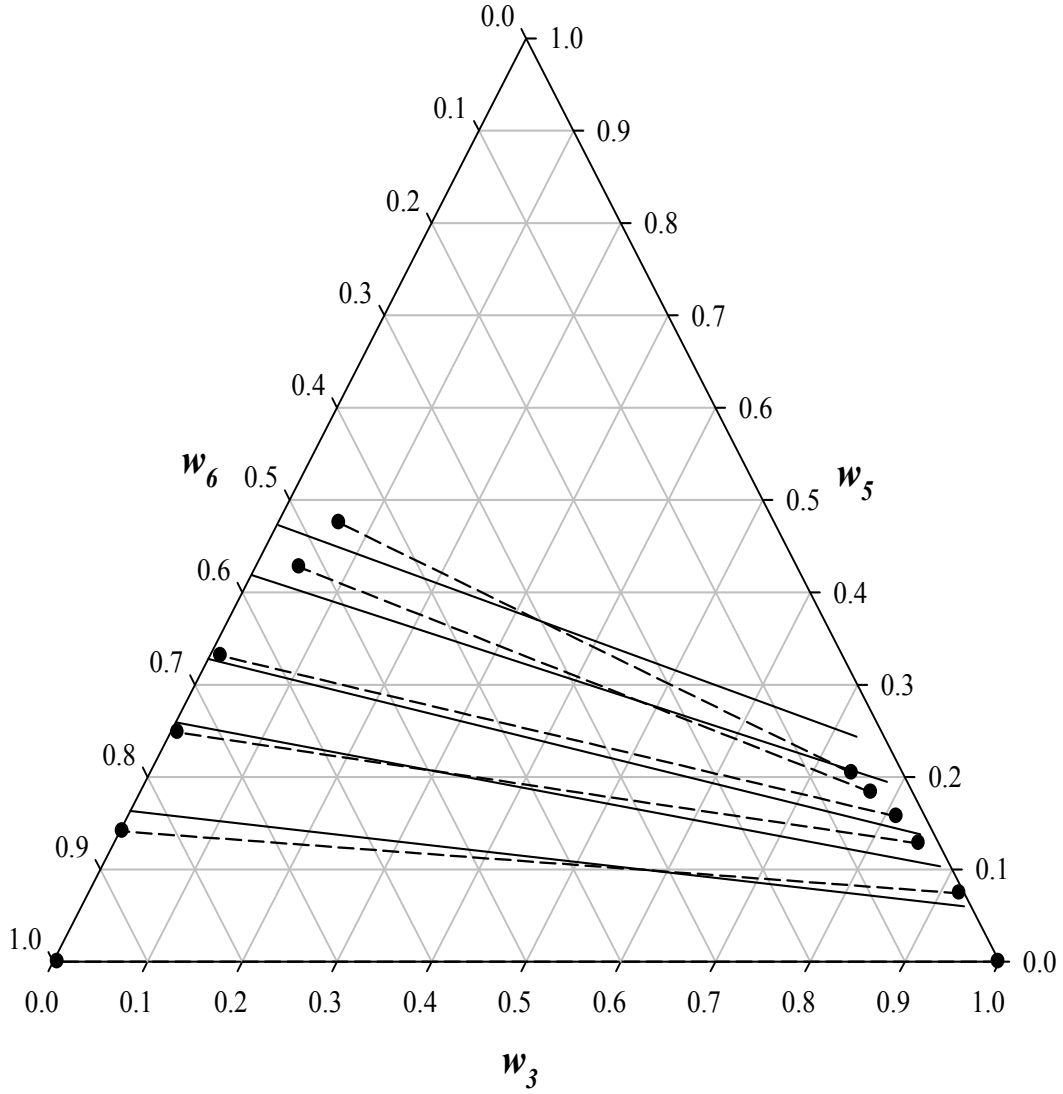

Figure 5. 8. Liquid–liquid equilibria for the system containing ethyl palmitate (*3*) + ethanol (*5*) + glycerol (*6*) at 353.15 K. Experimental (● and ——) and CPA EoS results using CPA pure compound parameters for esters computed from ester carbon number correlations (—).

Transesterification reaction is strongly influenced by molar ratio of alcohol to vegetable oil. In fact, this is a reversible reaction, requiring an excess of ethanol for enhancing the oil conversion. For this reason a 6:1 ethanol/oil molar ratio is generally considered the most appropriate. In the case of this molar ratio, the following approximate overall composition is usually obtained at the end of the ethanolysis reaction, if one assumes the complete oil conversion: 80 mass % of biodiesel, 12 mass % of excess ethanol and 8 mass % of glycerol. This composition indicates that the lower part of the phase splitting region in the phase equilibrium diagrams is the most important one for designing the separation process of ethylic biodiesel. This part is exactly the region particularly well described by the CPA equation of state.

Once again, and following previous works [24, 27, 30], the results here presented show the very good predictive capability of the CPA EoS and the transferability of its binary parameters obtained from binary phase equilibria data, to predict phase equilibria of multicomponent systems of relevance for biodiesel production processes.

4. Conclusions

New measurements for the liquid–liquid equilibria data were carried out in this work for the ethyl linoleate/ethyl oleate/ethyl palmitate/ethyl laurate + ethanol + glycerol systems at 323.15 and 353.15 K.

The experimental data were successfully predicted with the Cubic–Plus–Association equation of state (CPA EoS). Two approaches were used to estimate esters CPA pure compound parameters and the LLE results were taken into account for the selection of the most adequate set.

Global average deviations below 6 % were obtained, using temperature independent interaction parameters previously correlated from binary data.

Acknowledgments

We acknowledge FAPESP (Grant 08/56258–8), CNPq (Grants 304495/2010–7 and 480992/2009–6), and CAPES/PEC–PG, for their financial support and scholarship.

Nomenclature

K_d = distribution coefficient

S = solvent selectivity

a = energy parameter in the physical term

a_0, c_1 = parameters for calculating a

A_i = site A in molecule i

b = co–volume

g = simplified hard–sphere radial distribution function

k_{ij} = binary interaction parameter

P = vapor pressure

R = gas constant

T = temperature

x = mole fraction

w = mass fraction

X_{Ai} = fraction of molecule i not bonded at site A

Z = compressibility factor

Greek Symbols

β = association volume

ε = association energy

η = reduced fluid density

ρ = mole density

Δ = association strength

Subscripts

c = critical

i,j = pure component indexes

r = reduced

1= ethyl linoleate

2 = ethyl oleate

3 = ethyl palmitate

4= ethyl laurate

5 = ethanol

6 = glycerol

Superscripts

assoc. = association

phys. = physical

calcd = calculated

exptl = experimental

Literature Cited

[1] E.M. Shahid, Y. Jamal, A review of biodiesel as vehicular fuel, Renew Sust Energ Rev, 12 (2008) 2484–2494.
[2] F.R. Ma, M.A. Hanna, Biodiesel production: a review, Bioresource Technol, 70 (1999) 1–15.
[3] J. Van Gerpen, Biodiesel processing and production, Fuel Process Technol, 86 (2005) 1097–1107.
[4] A.V. Marjanovic, O.S. Stamenkovic, Z.B. Todorovic, M.L. Lazic, V.B. Veljkovic, Kinetics of the base–catalyzed sunflower oil ethanolysis, Fuel, 89 (2010) 665–671.
[5] T.A. Foglia, L.A. Nelson, R.O. Dunn, W.N. Marmer, Low–temperature properties of alkyl esters of tallow and grease, J Am Oil Chem Soc, 74 (1997) 951–955.
[6] B.R. Moser, Biodiesel production, properties, and feedstocks, In Vitro Cell Dev–Pl, 45 (2009) 229–266.

[7] J.C. Jones, On the use of ethanol in the processing of biodiesel fuels, Fuel, 89 (2010) 1183–1183.
[8] J.C. Jones, On the processing of biodiesel fuels, Fuel, 88 (2009) 583–583.
[9] L. Boros, M.L.S. Batista, R.V. Vaz, B.R. Figueiredo, V.F.S. Fernandes, M.C. Costa, M.A. Krahonbuhl, A.J.A. Meirelles, J.A.P. Coutinho, Crystallization Behavior of Mixtures of Fatty Acid Ethyl Esters with Ethyl Stearate, Energ Fuel, 23 (2009) 4625–4629.
[10] G. Knothe, R.O. Dunn, A Comprehensive Evaluation of the Melting Points of Fatty Acids and Esters Determined by Differential Scanning Calorimetry, J Am Oil Chem Soc, 86 (2009) 843–856.
[11] S.M.P. Meneghetti, M.R. Meneghetti, C.R. Wolf, E.C. Silva, G.E.S. Lima, L.D. Silva, T.M. Serra, F. Cauduro, L.G. de Oliveira, Biodiesel from castor oil: A comparison of ethanolysis versus methanolysis, Energ Fuel, 20 (2006) 2262–2265.
[12] M.J. Haas, A.J. McAloon, W.C. Yee, T.A. Foglia, A process model to estimate biodiesel production costs, Bioresource Technol, 97 (2006) 671–678.
[13] L.A. Follegatti–Romero, M. Lanza, C.A.S. da Silva, E.A.C. Batista, A.J.A. Meirelles, Mutual Solubility of Pseudobinary Systems Containing Vegetable Oils and Anhydrous Ethanol from (298.15 to 333.15) K, J Chem Eng Data, 55 (2010) 2750–2756.
[14] R. Di Felice, D. De Faveri, P. De Andreis, P. Ottonello, Component Distribution between Light and Heavy Phases in Biodiesel Processes, Ind Eng Chem Res, 47 (2008) 7862–7867.
[15] S.N. Csernica, J.T. Hsu, Reverse–Phase Ternary Phase Diagram, Tie Lines, and Plait Point for Commercial Biodiesel−Glycerol−Methanol, Ind Eng Chem Res, 50 (2010) 1012–1016.
[16] D.S. Negi, F. Sobotka, T. Kimmel, G. Wozny, R. Schomäcker, Liquid−Liquid Phase Equilibrium in Glycerol−Methanol−Methyl Oleate and Glycerol−Monoolein−Methyl Oleate Ternary Systems, Ind Eng Chem Res, 45 (2006) 3693–3696.
[17] A.E. Andreatta, L.M. Casás, P. Hegel, S.B. Bottini, E.A. Brignole, Phase Equilibria in Ternary Mixtures of Methyl Oleate, Glycerol, and Methanol, Ind Eng Chem Res, 47 (2008) 5157–5164.
[18] R. Tizvar, D.D. McLean, M. Kates, M.A. Dube, Liquid–liquid equilibria of the methyl oleate–glycerol–hexane–methanol system, Ind Eng Chem Res, 47 (2008) 443–450.
[19] B.B. Franca, F.M. Pinto, F.L.P. Pessoa, A.M.C. Uller, Liquid–Liquid Equilibria for Castor Oil Biodiesel plus Glycerol plus Alcohol, J Chem Eng Data, 54 (2009) 2359–2364.
[20] A.B. Machado, Y.C. Ardila, L.H. de Oliveira, M.n. Aznar, M.R. Wolf Maciel, Liquid−Liquid Equilibrium Study in Ternary Castor Oil Biodiesel + Ethanol + Glycerol and Quaternary Castor Oil Biodiesel + Ethanol + Glycerol + NaOH Systems at (298.2 and 333.2) K, Journal of Chemical & Engineering Data, (2011) null–null.
[21] X.J. Liu, X.L. Piao, Y.J. Wang, S.L. Zhu, Liquid–liquid equilibrium for systems of (fatty acid ethyl esters plus ethanol plus soybean oil and fatty acid ethyl esters plus ethanol plus glycerol), J Chem Eng Data, 53 (2008) 359–362.
[22] M.B. Oliveira, S. Barbedo, J.I. Soletti, S.H.V. Carvalho, A.J. Queimada, J.A.P. Coutinho, Liquid–liquid equilibria for the canola oil biodiesel + ethanol + glycerol system, Fuel, 90 (2011) 2738–2745.
[23] A. Barreau, I. Brunella, J.C. de Hemptinne, V. Coupard, X. Canet, F. Rivollet, Measurements of Liquid−Liquid Equilibria for a Methanol + Glycerol + Methyl Oleate System and Prediction Using Group Contribution Statistical Associating Fluid Theory, Ind Eng Chem Res, 49 (2010) 5800–5807.

[24] M.B. Oliveira, V. Ribeiro, A.J. Queimada, J.A.P. Coutinho, Modeling Phase Equilibria Relevant to Biodiesel Production: A Comparison of g(E) Models, Cubic EoS, EoS–g(E) and Association EoS, Ind Eng Chem Res, 50 (2011) 2348–2358.
[25] M.B. Oliveira, A.J. Queimada, J.A.P. Coutinho, Prediction of near and supercritical fatty acid ester plus alcohol systems with the CPA EoS, J Supercrit Fluid, 52 (2010) 241–248.
[26] M.B. Oliveira, S.I. Miguel, A.J. Queimada, J.A.P. Coutinho, Phase Equilibria of Ester plus Alcohol Systems and Their Description with the Cubic–Plus–Association Equation of State, Ind Eng Chem Res, 49 (2010) 3452–3458.
[27] M.B. Oliveira, A.J. Queimada, J.A.P. Coutinho, Modeling of Biodiesel Multicomponent Systems with the Cubic–Plus–Association (CPA) Equation of State, Ind Eng Chem Res, 49 (2010) 1419–1427.
[28] M.B. Oliveira, A.R.R. Teles, A.J. Queimada, J.A.P. Coutinho, Phase equilibria of glycerol containing systems and their description with the Cubic–Plus–Association (CPA) Equation of State, Fluid Phase Equilibr, 280 (2009) 22–29.
[29] M.B. Oliveira, M.J. Pratas, I.M. Marrucho, A.J. Queimada, J.A.P. Coutinho, Description of the Mutual Solubilities of Fatty Acids and Water With the CPA EoS, Aiche J, 55 (2009) 1604–1613.
[30] M.B. Oliveira, F.R. Varanda, I.M. Marrucho, A.J. Queimada, J.A.P. Coutinho, Prediction of water solubility in biodiesel with the CPA equation of state, Ind Eng Chem Res, 47 (2008) 4278–4285.
[31] L.A. Follegatti–Romero, M. Lanza, F.R.M. Batista, E.A.C. Batista, M.B. Oliveira, J.o.A.P. Coutinho, A.J.A. Meirelles, Liquid−Liquid Equilibrium for Ternary Systems Containing Ethyl Esters, Anhydrous Ethanol and Water at 298.15, 313.15, and 333.15 K, Ind Eng Chem Res, 49 (2010) 12613–12619.
[32] M.B. Oliveira, J.A.P. Coutinho, A.J. Queimada, Mutual solubilities of hydrocarbons and water with the CPA EoS, Fluid Phase Equilibr, 258 (2007) 58–66.
[33] G.M. Kontogeorgis, M.L. Michelsen, G.K. Folas, S. Derawi, N. von Solms, E.H. Stenby, Ten years with the CPA (Cubic–Plus–Association) equation of state. Part 1. Pure compounds and self–associating systems, Ind Eng Chem Res, 45 (2006) 4855–4868.
[34] G.M. Kontogeorgis, M.L. Michelsen, G.K. Folas, S. Derawi, N. von Solms, E.H. Stenby, Ten years with the CPA (Cubic–Plus–Association) equation of state. Part 2. Cross–associating and multicomponent systems, Ind Eng Chem Res, 45 (2006) 4869–4878.
[35] M.L. Michelsen, E.M. Hendriks, Physical properties from association models, Fluid Phase Equilibr, 180 (2001) 165–174.
[36] J.Z. Wu, J.M. Prausnitz, Phase equilibria for systems containing hydrocarbons, water, and salt: An extended Peng–Robinson equation of state, Ind Eng Chem Res, 37 (1998) 1634–1643.
[37] E.A. Muller, K.E. Gubbins, Molecular–based equations of state for associating fluids: A review of SAFT and related approaches, Ind Eng Chem Res, 40 (2001) 2193–2211.
[38] G.M. Kontogeorgis, I.V. Yakoumis, H. Meijer, E. Hendriks, T. Moorwood, Multicomponent phase equilibrium calculations for water–methanol–alkane mixtures, Fluid Phase Equilibr, 160 (1999) 201–209.
[39] E.C. Voutsas, I.V. Yakoumis, D.P. Tassios, Prediction of phase equilibria in water/alcohol/alkane systems, Fluid Phase Equilibr, 160 (1999) 151–163.

[40] G.K. Folas, J. Gabrielsen, M.L. Michelsen, E.H. Stenby, G.M. Kontogeorgis, Application of the cubic–plus–association (CPA) equation of state to cross–associating systems, Ind Eng Chem Res, 44 (2005) 3823–3833.
[41] G.K. Folas, G.M. Kontogeorgis, M.L. Michelsen, E.H. Stenby, Application of the cubic–plus–association (CPA) equation of state to complex mixtures with aromatic hydrocarbons, Ind Eng Chem Res, 45 (2006) 1527–1538.
[42] S.H. Huang, M. Radosz, Equation of State for Small, Large, Polydisperse, and Associating Molecules, Ind Eng Chem Res, 29 (1990) 2284–2294.
[43] B.N. Taylor, C.E. Kuyatt, Guidelines for the Evaluation and Expression of Uncertainty in NIST Measurement Results Technical Note 1297 for NIST. 1994, Gaithersburg: MD.
[44] A. Marcilla, F. Ruiz, A.N. García, Liquid–liquid–solid equilibria of the quaternary system water–ethanol–acetone–sodium chloride at 25 °C, Fluid Phase Equilibr, 112 (1995) 273–289.
[45] D.F. Othmer, P.E. Tobias, Liquid –Liquid Extraction Data –Toluene and Acetaldehyde Systems, Industrial & Engineering Chemistry, 34 (1942) 690–692.
[46] V. Brandani, A. Chianese, M. Rossi, Ternary liquid–liquid equilibrium data for the water–ethanol–benzene system, Journal of Chemical & Engineering Data, 30 (1985) 27–29.
[47] W.Y. Zhou, D.G.B. Boocock, Phase distributions of alcohol, glycerol, and catalyst in the transesterification of soybean oil, J Am Oil Chem Soc, 83 (2006) 1047–1052.
[48] L.Y.A. Silva, R.M.M. Falleiro, A.J.A. Meirelles, M.A. Krähenbühl, Determination of the vapor pressure of ethyl esters by Differential Scanning Calorimetry, The Journal of Chemical Thermodynamics, 43 (2011) 943–947.
[49] M.J. Pratas, S. Freitas, M.B. Oliveira, S.C. Monteiro, A.S. Lima, J.A.P. Coutinho, Densities and Viscosities of Fatty Acid Methyl and Ethyl Esters, J Chem Eng Data, 55 (2010) 3983–3990.
[50] B. Poling, J. Prausnitz, J. O'Connel, The Properties of gases and liquids (5th edition), Mc–Graw Hill,, (2001).
[51] J.C.A. Lopes, L. Boros, M.A. Krahenbuhl, A.J.A. Meirelles, J.L. Daridon, J. Pauly, I.M. Marrucho, J.A.P. Coutinho, Prediction of cloud points of biodiesel, Energ Fuel, 22 (2008) 747–752.
[52] M.B. Oliveira, I.M. Marrucho, J.A.P. Coutinho, A.J. Queimada, Surface tension of chain molecules through a combination of the gradient theory with the CPA EoS, Fluid Phase Equilibr, 267 (2008) 83–91.

CAPÍTULO 6

Liquid–Liquid Equilibrium for Ternary Systems Containing Ethyl Esters, Anhydrous Ethanol and Water at (298.15, 313.15 and 333.15) K

*Luis A. Follegatti–Romero,[1] Marcelo Lanza,[1] Fabio R. M. Batista,[1] Eduardo A. C. Batista,[1] Mariana B. Oliveira,[2] João A. P. Coutinho,[2] and Antonio J. A. Meirelles[1]**

[1]ExTrAE, Laboratory of Extraction, Applied Thermodynamics and Equilibrium, Department of Food Engineering, Faculty of Food Engineering, University of Campinas – UNICAMP, 13083–862, Campinas, SP, Brazil

[2] CICECO, Chemistry Department, University of Aveiro, 3810–193, Aveiro, Portugal

* Corresponding author. Fax: +55 19 3521 4027, E–mail: tomze@fea.unicamp.br

Artigo publicado no Ind. Eng. Chem. Res, 49, 12613–12619, 2010.

Abstract

The most common method used for purifying biodiesel is washing with water. During the biodiesel washing process, two phases are formed, a water–rich phase and an ester–rich one. For this reason, knowledge of the corresponding phase equilibrium is an important step in optimizing the final purification of biodiesel. The objective of this work was to investigate the liquid–liquid equilibrium related to some esters of interest in the production of ethylic biodiesel, in particular the equilibrium data for systems containing ethyl laurate/ethyl myristate + ethanol + water at (298.15, 313.15 and 333.15) K. The data obtained were correlated with the cubic–plus–association equation of state (CPA EoS). It was shown that this model was able to provide a very good description of the phase diagrams of the systems studied.

Keywords: Liquid–liquid equilibrium, biodiesel, ethyl esters, transesterification, ternary systems, CPA EoS.

Introduction

Ethylic biodiesel, composed of fatty acid ethyl esters (FAEE) and produced by transesterification of vegetable oils with bioethanol, is a biofuel entirely based on renewable agricultural sources. In contrast to methylic biodiesel, produced using methanol typically obtained from natural gas or coal, ethylic biodiesel tends to be carbon neutral with respect to the environmental issue.[1] Ethylic biodiesel also shows the following advantages in comparison to its methylic counterpart: it exhibits lower pour and cloud points and better storage properties.[2] On the other hand, the production of biodiesel by ethanolysis appears to consume more energy, and recovery of the ethyl esters from the reaction product is more difficult.[2] Several vegetable oils have been successfully used as renewable sources for biodiesel production, including those rich in lauric and myristic acids, such as palm kernel (South–East Asia, Nigeria, Colombia and Ecuador) and babassu oils (Brazil).[3–5]

Three main steps are usually necessary to convert vegetable oils into FAEE. The first step is a pre–treatment of the vegetable oil, carried out with the main purpose of removing free fatty acids that could interfere with the appropriate reaction path. The second is the reactive step, also denominated the transesterification reaction, and the third is a sequence of purification procedures aimed at obtaining a final product that conforms to the legislation standards. During the transesterification step palm kernel and babassu oils are mainly transformed into ethyl laurate and ethyl myristate, since lauric and myristic acids represent more than 60 % of the total amount of fatty acids.[6]

The transesterification reaction can generate very pure ethylic esters, but a purification step is usually required in order to separate the esters obtained from the glycerol, the excess of alcoholic reagent, the residual acylglycerols that did not react, and from any

contaminants introduced into the process together with the reagents, such as other minor fatty compounds. The purity grade of biodiesel has an important influence on its fuel properties, so it must be almost free of water, alcohol, glycerol, catalyst and acylglycerols. The washing of biodiesel is used to remove the residues of ethanol, glycerol, catalyst and soaps.[7,8] Karaosmanoğlu et al.[9] tested different alternatives for purifying biodiesel and selected washing with hot distilled water at 323.15 K as the best refining option, capable of producing a biofuel with purity of around 99 %.

Despite the importance of this purification step, experimental equilibrium data on the two phases formed during biodiesel washing are scarce, especially in the case of ethylic biodiesel. Some research groups have recently published experimental results on the phase behavior of the reactants and products present in the biodiesel reaction.[10–13]

In this work, liquid–liquid equilibrium data for the following ternary systems of interest in the production of ethylic biodiesel were investigated: ethyl laurate + ethanol + water, and ethyl myristate +ethanol + water at (298.15, 313.15 and 333.15) (± 0.1) K. The CPA EoS was used to correlate the measured phase diagrams. This model has already been successfully applied to mixtures similar to those investigated in the present work, such as water–alcohol[14] and methyl oleate–glycerol–methanol[15] mixtures.

Experimental Section

Materials.

The ethyl laurate and ethyl myristate used in this work were purchased from Tecnosyn (Cajamar/SP, Brazil), and their mass purities were 99.3 and 99.5 %, respectively. The

solvents used were anhydrous ethanol from Merck (Germany), with a mass purity of 99.9 %, and acetonitrile from Vetec (Brazil), with a mass purity of 99.8 %.

Quantification of the ethyl esters and ethanol was carried out in a Shimadzu (GC–17A) capillary gas chromatograph system with programmable pneumatics and a flame ionization detector (FID). A DB–WAX capillary column (0.25 μm, 30 m × 0.25 mm i.d) from J&W Scientific (Rancho Cordoba, CA, USA) was used, and the carrier gas was helium from White Martins (Brazil), with a mass purity of 99.9 %. The water content of both phases was determined by Karl Fischer titration using a model 701 Metrohm apparatus (Switzerland) equipped with a 5 mL burette. The Karl Fischer reagent used in the titration was from Merck (Germany).

Apparatus and Procedures

The liquid–liquid equilibrium data for the systems containing laurate/ethyl myristate + ethanol + water were determined at (298.15, 313.15 and 333.15) (± 0.1) K. The binodal curves for both ternary systems at each temperature were determined by the cloud–point method following the same procedures described by Lanza et al.[16] The tie lines were determined using glass test tubes with screw caps (32 mL). Known quantities of each component were weighed on an analytical balance with a precision of 0.0001 g (Precisa, model XT220A, Sweden), and added directly to the glass test tubes. The mixture of ethyl ester, ethanol, and water was maintained under intensive agitation for 10 min at constant temperature and pressure using a test tube shaker (Phoenix, model AP 56). The ternary mixture was then left at rest for 24 h in a thermostatic water bath at the desired temperature,

until two separate, transparent liquid phases were clearly observed. At the end of the experiment, samples were taken separately from the upper and bottom phases using syringes containing previously weighed masses of acetonitrile, so as to guarantee an immediate dilution of the samples and avoid further separation into two liquid phases at ambient temperature.

The samples from the two phases were analyzed by gas chromatography (GC). The detector and injector temperatures were 553 K and 523 K, respectively. The column oven was maintained at 313.15 K for 8 min and subsequently submitted to the following heating program: from 313.15 to 473.15 K at a rate of 20 $K \cdot min^{-1}$, maintained at 473.15 K for 8 min; from 473.15 to 483.15 K at a rate of 10 $K \cdot min^{-1}$, and finally maintained at 483.15 K for 2 min. The absolute pressure of the column was approximately 114 kPa; the carrier gas flowed at a rate of 1.6 $mL \cdot min^{-1}$; the linear velocity was 34 $cm \cdot s^{-1}$ and the sample injection volume was 1.0 μL.

The quantitative determination was carried out using calibration curves (external calibration) obtained using standard solutions for each system component: ethyl laurate, ethyl myristate and ethanol. These compounds were diluted with acetonitrile in the concentration range from 0.5–100 mg/mL. The experimental data for each tie–line were replicated at least three times and the values reported in the present work are the average ones. The mass fractions of ethyl esters and ethanol were determined from the areas of the corresponding GC chromatographic peaks, adjusted by the response factors obtained by previous calibration. The water mass fractions were also determined at least three times using the Karl Fisher titration and the values reported are the average ones.

The distribution coefficients and the solvent selectivity were calculated according to eq 1 and 2, respectively, using the experimental compositions of both phases.

$$K_{d3} = \frac{w_3^{WP}}{w_3^{EP}} \qquad (1) \qquad S_{3/i} = \frac{K_{d3}}{K_{di}} \qquad (2)$$

where k_{d3} is the distribution coefficient for ethanol, w_3 is its mass fraction in the water (WP) or ester (EP) phases, respectively, and $S_{3/i}$ stands for the solvent selectivity. The solvent selectivity reflects its effectiveness in separating ethanol from the ester phase (i=1 for ethyl laurate or i=2 for ethyl myristate).

Thermodynamic Modeling.

The modeling of polar and highly non ideal systems in wide ranges of temperature and pressure requires the use of association equations of state that explicitly take into account specific interactions between like (self–association) and unlike (cross–association) molecules. One of these equations is the Cubic–Plus–Association (CPA) equation of state, proposed by Kontogeorgis and co–workers,[17–19] that combines a physical contribution from a cubic equation of state, in this work the Soave–Redlich–Kwong (SRK) one, with an association term accounting for intermolecular hydrogen bonding and solvation effects,[20–22] originally proposed by Wertheim and used in other association equations of state such as SAFT.[23]

It can be expressed in terms of the compressibility factor as:

$$Z = Z^{phys.} + Z^{assoc.} = \frac{1}{1-b\rho} - \frac{a\rho}{RT(1+b\rho)} - \frac{1}{2}\left(1+\rho\frac{\partial \ln g}{\partial \rho}\right)\sum_i x_i \sum_{A_i}(1-X_{Ai}) \qquad (3)$$

where a is the energy parameter, b the co–volume parameter, ρ is the molar density, g a simplified hard–sphere radial distribution function, X_{Ai} the mole fraction of pure component i not bonded at site A, and x_i is the mole fraction of component i.

The pure component energy parameter, a, is obtained from a Soave–type temperature dependency:

$$a(T) = a_0 \left[1 + c_1\left(1 - \sqrt{T_r}\right)\right]^2 \tag{4}$$

where a_0 and c_1 are regressed (simultaneously with b) from pure component vapor pressure and liquid density data.

When CPA is extended to mixtures, the energy and co–volume parameters of the physical term are calculated employing the conventional van der Waals one–fluid mixing rules:

$$a = \sum_i \sum_j x_i x_j a_{ij} \qquad a_{ij} = \sqrt{a_i a_j}\left(1 - k_{ij}\right) \tag{5}$$

and

$$b = \sum_i x_i b_i \tag{6}$$

X_{Ai} is related to the association strength Δ^{AiBj} between sites belonging to two different molecules and is calculated by solving the following set of equations:

$$X_{Ai} = \frac{1}{1 + \rho \sum_j x_j \sum_{B_j} X_{Bj} \Delta^{A_i B_j}} \tag{7}$$

where

$$\Delta^{A_i B_j} = g(\rho)\left[\exp\left(\frac{\varepsilon^{A_i B_j}}{RT}\right) - 1\right] b_{ij} \beta^{A_i B_j} \tag{8}$$

where ε^{AiBj} and β^{AiBj} are the association energy and the association volume, respectively.

The simplified radial distribution function, $g(\rho)$ is given by[24]:

$$g(\rho) = \frac{1}{1 - 1.9\eta} \qquad \text{where} \qquad \eta = \frac{1}{4} b\rho \tag{9}$$

For non–associating components, such as esters, CPA has three pure component parameters in the cubic term (a_0, c_1 and b) while for associating components, such as water and alcohols, it has two additional parameters in the association term (ε and β). In both cases, the parameters are regressed simultaneously from the vapor pressure and liquid density data. The objective function to be minimized is the following:

$$OF = \sum_{i}^{NP} \left(\frac{P_i^{\text{exptl}} - P_i^{\text{calcd}}}{P_i^{\text{exptl}}} \right)^2 + \sum_{i}^{NP} \left(\frac{\rho_i^{\text{exptl}} - \rho_i^{\text{calcd}}}{\rho_i^{\text{exptl}}} \right)^2 \tag{10}$$

For a binary mixture composed solely of non–associating compounds, the binary interaction parameter, k_{ij} (Eq. 5), is the only adjustable parameter.

When CPA is used for mixtures containing two self–associating compounds, combining rules for the association term are required,[24,25] and in this work, the Elliott Combining Rule (ECR)[25] was used:

$$\Delta^{A_i B_j} = \sqrt{\Delta^{A_i B_i} \Delta^{A_j B_j}} \tag{11}$$

The Elliot combining rule provided very good results in modeling the phase equilibrium of several systems of interest for the production of biodiesel, such as, for example, the LLE of water + fatty acid systems[26] and the VLE of glycerol + alcohol systems.[27]

Solvation can occur in some systems containing self–associating and non self–associating compounds, as in the case of the ester + water or ethanol mixtures investigated in this work. For this type of system, the solvation phenomena is considered as a cross–association by the CPA EoS, where the cross–association energy (ε^{AiBj}) is considered to be half the value of the association energy for the self–associating component, and the cross association volume (β^{AiBj}) is left as an adjustable parameter, fitted to the equilibrium data. This approach, proposed by Folas et al.,[28] was successfully applied to model the phase equilibrium of several water + aromatic[29] and water + fatty acid ester[30] systems and to correlate the water solubility in biodiesels.[30] In these cases, the following objective function was minimized to estimate the parameters k_{ij} and β^{AiBj}:

$$OF = \sum_{i}^{NP} \left(\frac{x_i^{\text{calcd}} - x_i^{\text{exptl}}}{x_i^{\text{exptl}}} \right)^2 \tag{12}$$

where single phase or all phase data can be selected during optimization of the parameter. The association term depends on the number and type of association sites. According to the nomenclature of Huang and Radosz,[31] for alcohols, the two–site (2B) association scheme is applied, which proposes that hydrogen bonding occurs between the hydroxyl hydrogen and one of the lone pairs of electrons from the oxygen atom of another alcohol molecule. For the ester family, a single association site is considered that can cross–associate with self–associating molecules. For water, a four–site (4C) association scheme is adopted, considering that hydrogen bonding occurs between the two hydrogen atoms and the two lone pairs of electrons of the oxygen of the water molecule.

The average deviations (AD) between the experimental compositions and those estimated by the CPA EoS were calculated according to eq 13.

$$\mathrm{AD} = \sqrt{\frac{\sum_{n}^{N}\sum_{i}^{R}\left[\left(w_{i,n}^{\mathrm{WP},\mathrm{exptl}} - w_{i,n}^{\mathrm{WP},\mathrm{calcd}}\right)^2 + \left(w_{i,n}^{\mathrm{EP},\mathrm{exptl}} - w_{i,n}^{\mathrm{EP},\mathrm{calcd}}\right)^2\right]}{2NR}} \tag{13}$$

where AD is the average deviation for each system, N is the total number of tie lines of the corresponding system, R is the total number of components (R=3), w is the mass fraction, i is the component, the subscript n stands for the tie line number and the superscripts exptl and calcd refer to the experimental and calculated compositions.

Results and Discussion

Table 6.1 shows the experimental equilibrium data given in percentage by mass. The type A standard uncertainties[32] of the equilibrium compositions ranged from (0.0005 to 0.0882) % by mass for ethyl esters, (0.0029 to 0.8378) % for ethanol and (0.0888 to 0.8343) % for water, with the lowest figures associated with the lowest mass fractions within the composition range investigated. On the basis of the total system mass and of the phase and overall compositions, the mass balances were checked according to the procedure suggested by Marcilla et al.[33] and recently applied to fatty systems by Silva et al.[34] According to this procedure, the masses of both liquid phases were calculated and checked against the total initial mass used in the experimental runs

Table 6. 1. Experimental Liquid–Liquid Equilibrium Data for the Ternary Systems Containing Ethyl Ester (*i*) + Anhydrous Ethanol (*3*) + Water (*4*) at (298.15, 313.15, and 333.15) (± 0.1) K

ethyl ester (*i*)	T/K	overall composition			water–rich phase			ester–rich phase			K_{d3} [a]	$S_{3/1}$ [b]
		100 w_i	100 w_3	100 w_4	100 w_i	100 w_3	100 w_4	100 w_i	100 w_3	100 w_4		
Laurate (*1*)	298.15	19.981	59.919	20.100	12.950	64.407	22.643	71.266	24.313	4.421	2.649	14.5
		24.695	50.560	24.745	3.411	63.025	33.564	82.086	15.829	2.085	3.982	95.8
		31.364	37.269	31.367	0.497	51.614	47.889	90.119	8.765	1.116	5.889	1067.7
		37.794	25.661	36.546	0.059	39.817	60.124	93.233	5.955	0.812	6.686	10565.8
		39.141	21.817	39.043	0.032	34.090	65.878	95.323	4.137	0.540	8.240	24546.4
		44.751	11.441	43.808	0.004	17.496	82.500	97.159	2.499	0.342	7.001	170057.4
		51.216	0.000	48.784	0.003	0.000	99.997	99.790	0.000	0.210		
	313.15	24.705	50.55	24.743	5.468	61.753	32.780	77.534	19.107	3.359	3.232	45.8
		31.358	37.29	31.355	0.825	52.240	46.935	87.564	10.492	1.945	4.979	528.4
		37.784	25.68	36.535	0.219	41.658	58.123	92.344	6.106	1.550	6.822	2876.7
		39.138	21.82	39.044	0.183	34.424	65.393	94.354	4.453	1.193	7.731	3985.8
		44.758	11.43	43.817	0.079	18.246	81.676	96.050	2.919	1.031	6.251	7599.8
		52.133	0.00	47.867	0.043	0.000	99.957	99.161	0.000	0.839		
	333.15	24.720	50.543	24.737	6.500	63.116	30.384	71.599	22.671	5.730	2.784	30.6
		31.346	37.307	31.347	0.985	52.541	46.474	85.282	12.201	2.517	4.306	372.8
		35.889	28.348	35.763	0.496	42.304	57.200	88.990	9.000	2.010	4.700	843.3
		39.110	21.869	39.021	0.205	35.236	64.559	91.867	6.449	1.683	5.464	2448.5
		44.748	11.434	43.819	0.090	20.011	79.899	94.647	3.765	1.588	5.315	5589.4
		49.022	0.000	50.978	0.050	0.000	99.950	98.980	0.000	1.020		
Myristate (*2*)	298.15	18.798	62.257	18.945	6.010	72.466	21.524	73.536	23.343	3.121	3.104	37.9
		23.183	53.477	23.340	2.431	65.162	32.407	83.759	14.392	1.849	4.528	156.0
		30.112	39.431	30.457	0.370	54.139	45.491	90.462	8.616	0.922	6.284	1536.2
		35.077	29.810	35.113	0.129	42.971	56.900	92.960	6.279	0.761	6.844	4931.6
		39.229	21.532	39.239	0.103	33.467	66.430	94.499	4.934	0.567	6.783	6223.1
		44.564	10.341	45.095	0.092	17.008	82.900	98.520	1.020	0.460	16.675	17856.2
		48.741	0.000	51.259	0.070	0.000	99.930	99.740	0.000	0.260		
	313.15	23.155	53.492	23.353	2.945	66.051	31.004	80.607	16.365	3.027	4.036	110.4
		31.319	38.748	29.933	0.829	54.352	44.819	88.819	9.265	1.917	5.866	628.5
		35.081	29.808	35.111	0.200	43.554	56.246	91.986	6.994	1.020	6.227	2864.1
		39.116	21.665	39.219	0.115	33.643	66.242	94.024	5.210	0.766	6.457	5279.5
		55.341	8.337	36.322	0.100	17.489	82.411	98.390	1.110	0.500	15.756	15502.1
		48.718	0.000	51.282	0.075	0.000	99.925	99.720	0.000	0.280		
	333.15	23.192	53.483	23.325	7.258	62.135	30.607	58.636	34.468	6.895	1.803	14.5
		30.109	39.435	30.456	1.299	54.447	44.253	73.114	21.500	5.386	2.532	142.5
		35.114	29.862	35.024	0.242	43.767	55.991	84.579	12.480	2.941	3.507	1225.6
		39.491	21.014	39.495	0.128	33.666	66.206	92.140	5.810	2.050	5.794	4171.1
		44.559	10.353	45.088	0.012	17.706	82.282	95.129	2.890	1.981	6.127	48568.4
		48.741	0.000	51.259	0.080	0.000	99.920	99.110	0.000	0.890		

[a] K_{d3} is the ethanol distribution coefficient according to eq 1.
[b] $S_{3/1}$ is the solvent selectivity according to eq 2.

The average results obtained for the mass balance deviations of each set of experimental data are shown in Table 6.2. In all cases, the values were lower than 0.50 %, which indicates the good quality of the experimental data.

Table 6. 2. Deviations for the Global Mass Balance of the Phase Compositions

system	100 δ [a]
ethyl laurate + ethanol + water at 298.15 K	0.20
ethyl laurate + ethanol + water at 313.15 K	0.16
ethyl laurate + ethanol + water at 333.15 K	0.43
ethyl myristate + ethanol + water at 298.15 K	0.35
ethyl myristate + ethanol + water at 313.15 K	0.11
ethyl myristate + ethanol + water at 333.15 K	0.27

[a] relative deviation of the overall mass balance, calculated by $\delta = \frac{1}{N}\sum_{n}^{N}\left|\left(m^{\mathrm{EP}} + m^{\mathrm{WP}} - m^{\mathrm{OS}}\right)/m^{\mathrm{OS}}\right|$, where m^{EP} is the calculated mass of the ester–rich phase, m^{WP} is the corresponding value of the water–rich phase, m^{OS} is the total mass of the system, and *n* is the tie line number.

Figure 6.1 shows the binodal curves for the ethyl laurate and ethyl myristate systems (The experimental data used are presented in the Supporting Information, Table 6.3).

The size of the phase splitting region only decreased slightly with the increase in temperature. The same behavior was observed for both systems, but in the case of ethyl myristate the size of the phase splitting region was larger. The distribution diagram for ethanol in the ethyl myristate system is shown in Figure 6.2.

Table 6. 3. Experimental Data for Binodal Curves of Ethyl Ester (*i*) + Ethanol (*3*) + Water (*4*) at Several Temperatures

ethyl ester (*i*)	298.15 K			313.15 K			333.15 K		
	100 w_i	100 w_3	100 w_4	100 w_i	100 w_3	100 w_4	100 w_i	100 w_3	100 w_4
laurate (*1*)	0.99790	0.00000	0.00210	0.99790	0.00000	0.00210	0.99790	0.00000	0.00210
	0.71820	0.24310	0.03870	0.72470	0.23490	0.04040	0.75780	0.20210	0.04010
	0.50260	0.40820	0.08920	0.60450	0.32520	0.07030	0.63010	0.29850	0.07140
	0.43290	0.45840	0.10870	0.44970	0.43540	0.11490	0.46810	0.41030	0.12160
	0.25140	0.58360	0.16510	0.34760	0.50370	0.14870	0.34800	0.49300	0.15900
	0.18630	0.62370	0.19000	0.26060	0.55980	0.17960	0.26300	0.54000	0.19700
	0.14800	0.64210	0.20990	0.18850	0.60160	0.20990	0.16730	0.58470	0.24810
	0.11100	0.65500	0.23400	0.14870	0.62130	0.22990	0.11650	0.59870	0.28470
	0.08000	0.66000	0.26000	0.11310	0.63210	0.25470	0.06400	0.60000	0.33600
	0.05160	0.65600	0.29240	0.07540	0.63640	0.28820	0.04460	0.58880	0.36660
	0.02900	0.63000	0.34100	0.04020	0.62260	0.33720	0.02490	0.56000	0.41510
	0.01430	0.59430	0.39140	0.01600	0.56900	0.41500	0.00985	0.52540	0.46470
	0.00059	0.39820	0.60120	0.00219	0.41660	0.58120	0.00496	0.42300	0.57200
	0.00032	0.34090	0.65880	0.00183	0.34420	0.65390	0.00205	0.35240	0.64560
	0.00004	0.17500	0.82500	0.00079	0.18250	0.81680	0.00090	0.20010	0.79900
	0.00003	0.00000	0.99997	0.00043	0.00000	0.99960	0.00050	0.00000	0.99950
myristate (*2*)	0.99790	0.00000	0.00210	0.99790	0.00000	0.00210	0.99790	0.00000	0.00210
	0.70250	0.26100	0.03650	0.71350	0.24790	0.03860	0.74100	0.21930	0.03970
	0.55010	0.38430	0.06560	0.58080	0.35340	0.06570	0.60040	0.32650	0.07300
	0.39200	0.50850	0.09950	0.31880	0.54790	0.13330	0.45470	0.43110	0.11420
	0.28800	0.59120	0.12080	0.23550	0.60770	0.15680	0.24940	0.57750	0.17310
	0.21410	0.64140	0.14450	0.17530	0.64510	0.17960	0.19320	0.61250	0.19430
	0.12510	0.69360	0.18120	0.13310	0.66800	0.19880	0.14830	0.63170	0.22000
	0.07660	0.71100	0.21230	0.09570	0.68390	0.22040	0.10100	0.64200	0.25700
	0.04140	0.70740	0.25120	0.06320	0.68490	0.25190	0.06000	0.64000	0.30000
	0.02050	0.69530	0.28420	0.03090	0.66830	0.30080	0.02900	0.61400	0.35700
	0.01000	0.66000	0.33000	0.02210	0.63600	0.34190	0.01900	0.58200	0.39900
	0.00370	0.54140	0.45490	0.00829	0.54350	0.44820	0.01300	0.54450	0.44250
	0.00129	0.42970	0.56900	0.00200	0.43550	0.56250	0.00242	0.43770	0.55990
	0.00103	0.33470	0.66430	0.00115	0.33640	0.66240	0.00128	0.33670	0.66210
	0.00092	0.17010	0.82900	0.00100	0.17490	0.82410	0.00012	0.17710	0.82280
	0.00070	0.00000	0.99930	0.00075	0.00000	0.99930	0.00080	0.00000	0.99920

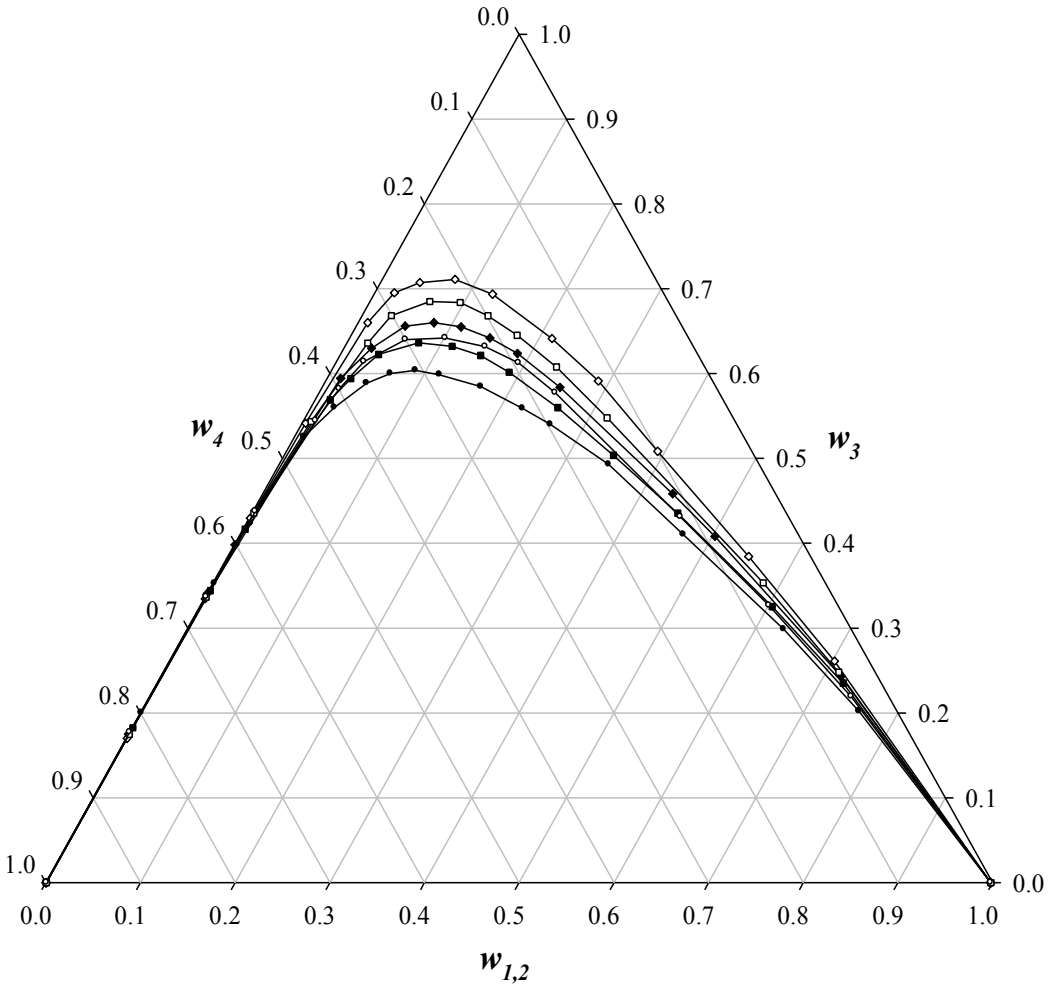

Figure 6. 1. Binodal curves of ethyl laurate (*1*) + ethanol (*3*) + water (*4*): (♦), 298.15; (■), 313.15; (●), 333.15 K, and ethyl myristate (*2*) + ethanol (*3*) + water (*4*): (◊), 298.15; (□), 313.15; (○), 333.15 K.

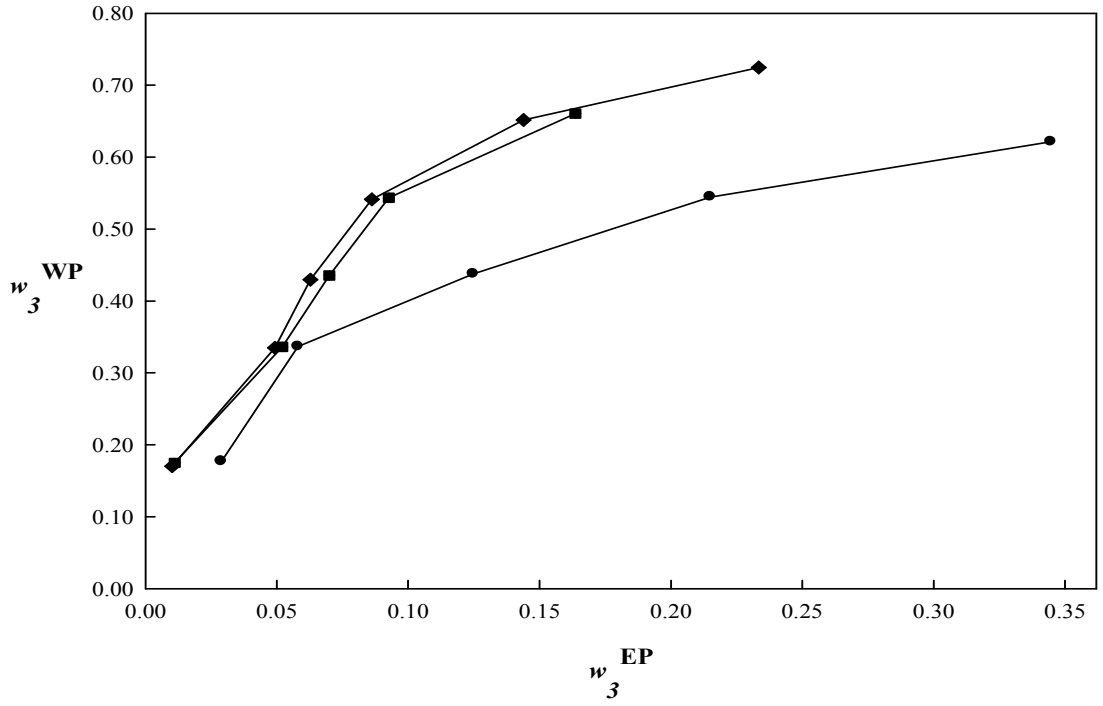

Figure 6. 2. Distribution diagram for ethyl myristate (*2*) + ethanol (*3*) + water (*4*): (♦), 298.15; (■), 313.15; (●), 333.15 K.

The ethanol mass fraction in the aqueous phase was much larger than in the ester phase, so that its distribution coefficient was, in most cases, above 1.8 for both systems (see Table 6.1). Considering that the ester mass fraction in the aqueous phase was usually low, the solvent selectivity was very high, in most cases above 100 (see Table 6.1). These results indicate that washing with water is a very effective way of extracting ethanol from the ester phase generated at the end of the ethanolysis reaction, without losing any significant amount of biodiesel to the extract phase.

The CPA EoS was previously used with success for the description of LLE in systems such as methyl oleate + methanol + glycerol, fatty acid ester + ethanol + glycerol and methyl ricinoleate + methanol + glycerol, using the same temperature independent binary

interaction and cross–association parameters.[35] Given the accuracy, predictivity and simplicity provided by the CPA EoS in modeling complex multicomponent associating systems, this equation was selected to describe the LLE of the ternary mixtures studied here.

To apply the CPA EoS to model the phase equilibrium of multicomponent systems, the CPA pure compound parameters must be estimated using a simultaneous regression of the vapor pressure and liquid density data. Non associating compounds such as fatty acid esters and self–associating compounds such as ethanol and water are present in these systems. The five CPA pure compound parameters for water were previously established[36] considering the 4C scheme for water, and were used in modeling the phase equilibrium of several water containing systems.[26,27,29,30] The three CPA parameters for esters were proposed in a previous work,[30] and it was shown that the a_0, c_1 and b CPA parameters followed the same trend with the ester carbon number. Correlations for the estimation of these parameters with new compounds were proposed, enabling the estimation of the CPA pure compound parameters in the absence of liquid density and vapor pressure data. In a previous work[37], the CPA parameters for ethyl laurate and ethyl myristate were estimated from these correlations and applied for the prediction of the VLE of the ethyl laurate/ethyl myristate + alcohol systems at near or supercritical conditions.

Recently, new density data appeared for these ethyl esters[38] and it is now possible to evaluate the predictive capability of the estimated CPA pure compound parameters. As seen in Table 6.3, where average absolute deviations are presented for the ethyl esters densities, the CPA EoS is able to correctly predict that property.

Table 6. 4. CPA Pure Compound Parameters and Critical Temperatures

compound	T_c (K)	a_0 (J·m^3·mol^{-2})	c_1	$b\times10^5$ (m^3·mol^{-1})	ε (J·mol^{-1})	β	100AAD [a]	
							P	ρ
ethyl laurate[37,38]	719.1	8.23	1.44	30.18				4.29
ethyl myristate[37,38]	744.3	9.52	1.54	34.54				6.99
ethanol[39]	514.7	0.68	0.94	4.75	21336	0.0190	0.35	0.51
water[36]	647.3	0.12	0.67	1.45	16655	0.0692	1.72	0.82

[a] AAD is the Average Absolute Deviation calculated by $\mathbf{AAD} = \frac{1}{N}\sum_{i=1}^{Np}\left|(exptl_i - calcd_i)/exptl_i\right|$

The five CPA parameters for ethanol were established previously, while performing a systematic study on the pure compound parameters for the n–alcohol family from methanol to n–eicosanol, using the 2B association scheme.[39] These parameters were used for the description of the LLE of ternary systems constituted of fatty esters, ethanol and glycerol[35], of the VLE of the glycerol + ethanol system[27] and of the VLE of fatty acid ester + ethanol systems at atmospheric pressure[40] and at near or supercritical conditions.[37] The pure compound CPA parameters used in this work can be seen in Table 6.4 along with the deviations obtained for liquid densities and vapor pressures.

The description of multicomponent systems requires the estimation of binary parameters from experimental data. Cross–association parameters, β_{ij}'s, between ethyl laurate/ethyl myristate and water, and between ethyl laurate/ethyl myristate and ethanol, were previously established by Oliveira et al.[30,40] while modeling the LLE of water + fatty acid ester systems and the VLE of ethanol + fatty acid ester systems. Taking advantage of the transferability of the CPA parameters, these β_{ij}'s were applied to the description of the phase diagrams measured. The missing binary interaction parameter for the ethanol + water system was estimated using the available experimental data for the isobaric VLE of the ethanol + water system at atmospheric pressure.[41] The k_{ij} value obtained (Table 6.5)

provides a description of the experimental data with an average deviation of 0.1 % for the bubble temperature.

Table 6. 5. Binary Interaction and Cross–Association Parameters Used to Model Ternary Systems LLE

k_{ij} (ethyl laurate + ethanol)	– 0.083
k_{ij} (ethyl laurate + water)	– 0.172
k_{ij} (ethyl myristate + ethanol)	– 0.094
k_{ij} (ethyl myristate + water)	– 0.155
β_{ij} (ethyl laurate/ethyl myristate + ethanol)[40]	0.100
β_{ij} (ethyl laurate/ethyl myristate + water)[30]	0.201
k_{ij} (ethanol + water)	– 0.100

Only the ethyl laurate/ethyl myristate + water and the ethyl laurate/ethyl myristate + ethanol interaction parameters, k_{ij}*'s*, were unavailable, and were regressed from the ternary data. The values for the binary parameters are presented in Table 6.5, and the same set of interaction and cross–association binary parameters were use to model the LLE data at (298.15, 313.15 and 333.15) K.

The CPA descriptions of the experimental phase diagrams measured in this work at the various temperatures studied are reported in Figures 6.3 and 6.4. A good description of both the saturation curves and tie lines was obtained for both systems at all the temperatures studied.

Near to the plait point, higher deviations between the experimental and calculated values were observed, with the CPA EoS predicting a somewhat larger region of two–liquid–phase coexistence. According to Zhou and Boocook,[42] the ester–rich phase obtained at the end of the ethanolysis reaction contains approximately 13 % by mass of ethanol. Even considering that this value can oscillate as a function of the ethanol/oil ratio used during the reaction step, the ethanol composition in the ester–rich phase should not be much larger than the

previously reported value. This means that the lower part of the phase splitting region in the equilibrium diagrams is the most important one for designing the water washing step of ethylic biodiesel, which is the part particularly well described by the CPA equation of state.

The results reported here represent a very stringent test of the predictive capability of the CPA EoS and the transferability of its binary parameters. The quality of the results obtained show that when reliable data are available, the parameters obtained from binary systems can be used with confidence for the estimation of ternary or high order systems. The capacity of a single set of parameters to describe the phase diagrams across a temperature range is also remarkable. The reliability of the CPA in the description of the phase equilibrium of complex polar mixtures relevant to biodiesel production makes it the model of choice for the design, optimization and operation of biodiesel production plants.

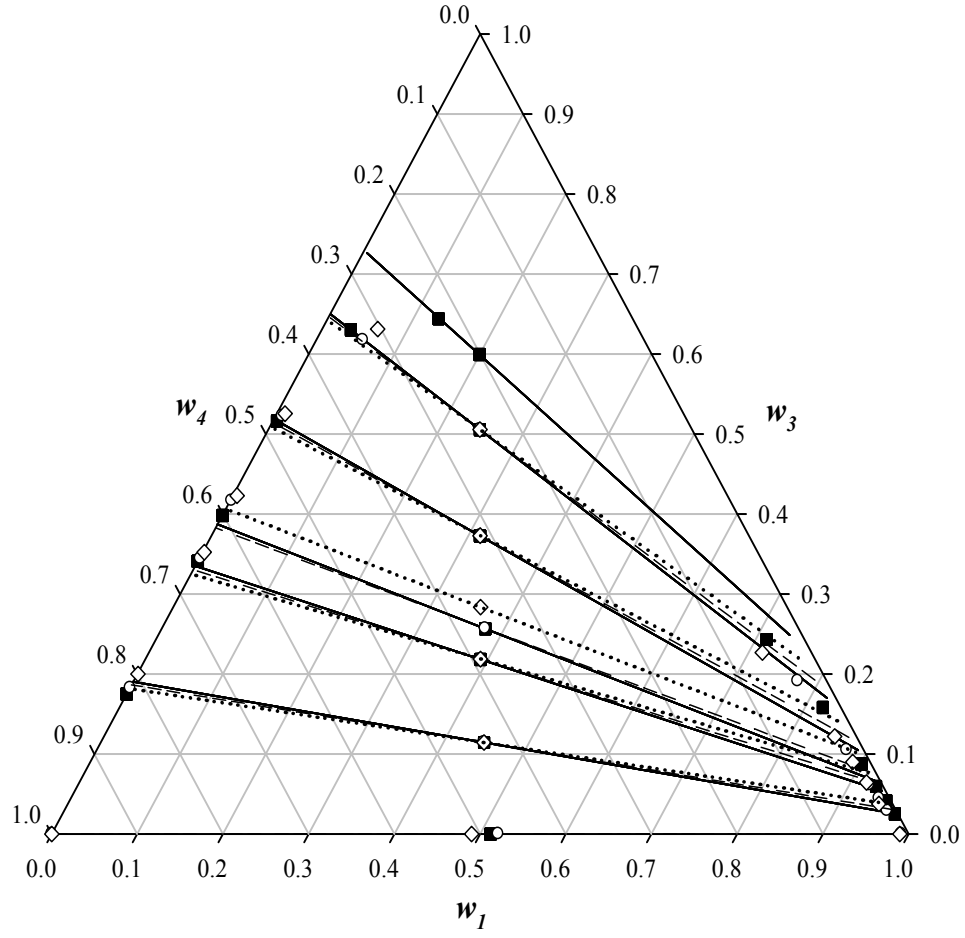

Figure 6. 3. Liquid–liquid equilibrium for the system containing ethyl laurate (*1*) + ethanol (*3*) + water (*4*): experimental (■) and CPA results (—) at 298.15 K, experimental (○) and CPA results (——) at 313.15 K and experimental (◊) and CPA results (···) at 333.15 K

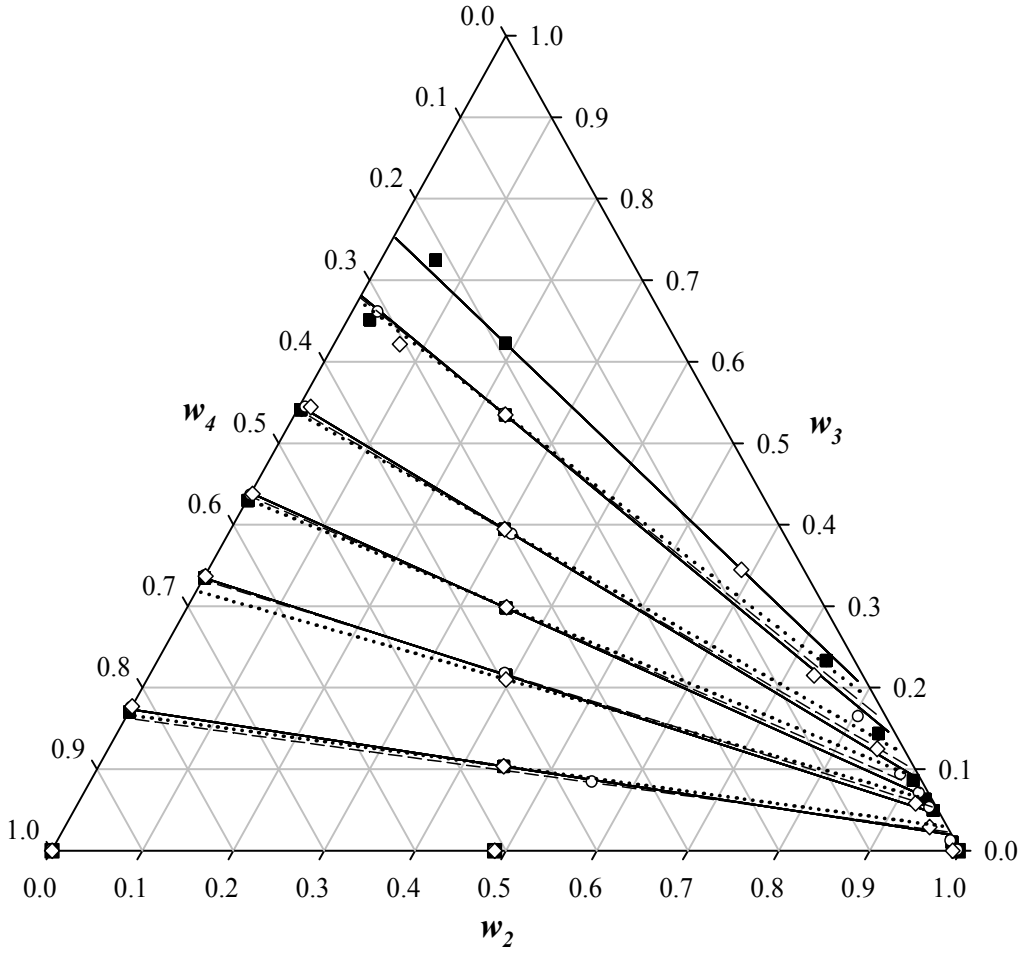

Figure 6. 4. Liquid–liquid equilibrium for the system containing ethyl myristate (*2*) + ethanol (*3*) + water (*4*): experimental (■) and CPA results (—) at 298.15 K, experimental (○) and CPA results (——) at 313.15 K and experimental (◊) and CPA results (···) at 333.15

The average deviations between the experimental and calculated compositions in both phases are shown in Table 6.6. As can be seen in Table 6.6, most deviations are within the range from 0.9 to 2.6 % and the average global deviation was 2.8 %. If the tie lines closest to the plait point were not considered in estimating these deviations, the average global deviation decreased to a value of 1.64 % and the deviations for most systems, with the

single exception of ethyl myristate at 333.15 K, would be within the range from 0.9 to 1.2 %. These results confirm that the larger deviations between the experimental and calculated values were concentrated in the phase splitting region close to the plait point.

Table 6. 6. Average Deviations (AD) between the Experimental and Calculated Phase Compositions

system	CPA EoS		
	100 AD ester in water rich phase	100 AD water in ester rich phase	100 AD[a]
ethyl laurate (*1*) + ethanol (*3*) + water (*4*) at 298.15 K	2.51	0.78	2.63
ethyl laurate (*1*) + ethanol (*3*) + water (*4*) at 313.15 K	1.45	0.81	1.66
ethyl laurate (*1*) + ethanol (*3*) + water (*4*) at 333.15 K	1.75	1.17	2.10
ethyl myristate (*2*) + ethanol (*3*) + water (*4*) at 298.15 K	1.26	0.95	1.58
ethyl myristate (*2*) + ethanol (*3*) + water (*4*) at 313.15 K	0.71	0.62	0.94
ethyl myristate (*2*) + ethanol (*3*) + water (*4*) at 333.15 K	1.66	5.27	5.53
average global deviation			2.80

[a] Average deviations calculated according to eq 13.

Liquid–liquid equilibrium data for fatty systems containing ethanol and water were recently reported by Priamo et al.[43] and by Dalmolin et al.[44] These data were measured at 298.15 and 313.15 K and correlated with the NRTL equation. The average deviations (AD) reported for these systems were within the range from 0.5 to 1.6 %. Although these deviations were slightly lower than those obtained in the present work, it should be considered that the NRTL equation requires 9 binary interaction parameters at each temperature for a ternary system, and that these parameters are specific for describing liquid–liquid equilibrium data.

In contrast, the correlation results obtained in the present work only required the adjustment of two new binary interaction parameters for each ternary system. The same set of parameters was used for the whole range of temperatures and for calculating the vapor–liquid as well as the liquid–liquid equilibrium data. Such an approach is particularly useful

for designing biodiesel production, since the purification steps involve a series of vapor–liquid and liquid–liquid mass transfer operations.

Conclusions

Equilibrium data were measured for the ethyl laurate/ethyl myristate + ethanol + water systems at (298.15, 313.15 and 333.15) K. The high ethanol distribution coefficients and very high solvent selectivities make water washing a very effective way of recovering ethanol from the ester rich phase generated at the end of the ethanolysis reaction. The experimental data were correlated successfully with the cubic–plus–association equation of state (CPA EoS), and the average global deviation between the experimental data and the calculated compositions showed a value of 2.8 %.

Nomenclature

K_d = distribution coefficient
S = solvent selectivity
a = energy parameter in the physical term
a_0, c_1 = parameters for calculating a
A_i = site A in molecule i
b = co–volume
g = simplified hard–sphere radial distribution function
k_{ij} = binary interaction parameter
P = vapor pressure
R = gas constant
T = temperature
x = mole fraction

w = mass fraction

X_{Ai} = fraction of molecule i not bonded at site A

Z = compressibility factor

Greek Symbols

β = association volume

ε = association energy

η = reduced fluid density

ρ = mole density

Δ = association strength

Subscripts

c = critical

i,j = pure component indexes

r = reduced

1= ethyl laurate

2 = ethyl myristate

3 = ethanol

4 = water

Superscripts

assoc. = association

phys. = physical

calcd = calculated

exptl = experimental

Literature Cited

(1) Jones, J. C. On the Use of ethanol in the Processing of Biodiesel Fuels (Letter to the editor). *Fuel* **2010**, *89*, 1183.

(2) Marjanovic, A. V.; Stamenkovic, O. S.; Todorovic, Z. B.; Lazic, M. L.; Veljkovic, V. B. Kinetics of the Base–Catalyzed Sunflower Oil Ethanolysis. *Fuel* **2010**, *89*, 665.

(3) Alamu, O. J.; Waheed, M. A.; Jekayinfa, S. O. Effect of Ethanol–Palm Kernel Oil Ratio on Alkali–Catalyzed Biodiesel Yield. *Fuel* **2008**, *87*, 1529.

(4) Marchetti, J. M.; Miguel, V. U.; Errazu, A. F. Possible Methods for Biodiesel Production. *Renew. Sustain. Energy Rev.* **2007**, *11*, 1300.
(5) Teixeira, M. A. Babassu–A New Approach for an Ancient Brazilian Biomass. *Biomass & Bioenergy* **2008**, *32*, 857.
(6) Firestone, D., *Physical and Chemical Characteristics of Oils, Fats and Waxes*. 2nd Edition ed. 2006: AOCS Press.
(7) Berrios, M.; Skelton, R. L. Comparison of Purification Methods for Biodiesel. *Chemical Engineering Journal* **2008**, *144*, 459.
(8) Van Gerpen, J. Biodiesel Processing and Production. *Fuel Processing Technology* **2005**, *86,* 1097.
(9) Karaosmanoğlu, F.; Cigizoglu, K. B.; Tuter, M.; Ertekin, S. Investigation of the Refining Step of Biodiesel Production. *Energy Fuels* **1996**, *10*, 890.
(10) Tizvar, R.; McLean, D. D.; Kates, M.; Dubé, M. A. Liquid–Liquid Equilibria of the Methyl Oleate–Glycerol–Hexane–Methanol system. *Ind. Eng. Chem. Res.* **2008**, *47*, 443.
(11) Liu, X.; Piao, X.; Wang, Y.; Zhu, S. Liquid–Liquid Equilibrium for Systems of (Fatty Acid Ethyl Esters + Ethanol + Soybean Oil and Fatty Acid Ethyl Esters + Ethanol + Glycerol). *J. Chem. Eng. Data* **2008**, *53*, 359.
(12) Follegatti–Romero, L. A.; Lanza, M.; da Silva, C. A. S.; Batista, E. A. C and Meirelles, A. J. A. Mutual Solubility of Pseudobinary Systems Containing Vegetable Oils and Anhydrous Ethanol at (298.15 to 333.15) K. DOI: 10.1021/je900983x.
(13) Lanza, M.; Sanaiotti, G.; Batista, E.; Poppi, R. J.; Meirelles, A. J. A. Liquid–Liquid Equilibrium Data for Systems Containing Vegetable Oils, Anhydrous Ethanol, and Hexane at (313.15, 318.15, and 328.15) K. J. Chem. Eng. Data 2009, 54, 1850.
(14) Kontogeorgis, G. M.; Yakoumis, I. V.; Meijer, H.; Hendriks, E.; Moorwood, T. Multicomponent Phase Equilibrium Calculations for Water–Methanol–Alkane Mixtures. *Fluid Phase Equilib.* **1999**, *160*, 201.
(15) Andreatta, A. E.; Casás, L. M.; Hegel. P.; Bottini, S. B.; Brignole, E. A. Phase Equilibria in Ternary Mixtures of Methyl Oleate, Glycerol, and Methanol. *Ind. Eng. Chem. Res.* **2008**, *47*, 5157.
(16) Lanza, M.; Borges Neto, W.; Batista, E.; Poppi, R. J.; Meirelles, A. J. A. Liquid–Liquid Equilibrium Data for Reactional Systems of Ethanolysis at 298.3 K. *J. Chem. Eng. Data* **2008**, *53*, 5.
(17) Kontogeorgis, G. M.; Michelsen, M. L.; Folas, G. K.; Derawi, S.; von Solms, N.; Stenby, E. H. Ten Years With the CPA (Cubic–Plus–Association) Equation of State. Part 1. Pure Compounds and Self–Associating Systems. *Ind. Eng. Chem. Res.* **2006**, *45*, 4855.
(18) Kontogeorgis, G. M.; Michelsen, M. L.; Folas, G. K.; Derawi, S.; von Solms, N.; Stenby, E. H. Ten Years With the CPA (Cubic–Plus–Association) Equation of State. Part 2. Cross–Associating and Multicomponent Systems. *Ind. Eng. Chem. Res.***2006**, *45*, 4869.
(19) Kontogeorgis, G. M.; Voutsas, E. C.; Yakoumis, I. V.; Tassios, D. P. An Equation of State for Associating Fluids. *Ind. Eng. Chem. Res.***1996**, *35*, 4310.
(20) Michelsen, M. L.; Hendriks, E. M. Physical Properties from Association Models, *Fluid Phase Equilib.* **2001**, *180*, 165.

(21) Voutsas, E. C.; Boulougouris, G. C.; Economou, I. G.; Tassios, D. P. Water/Hydrocarbon Phase Equilibria Using the Thermodynamic Perturbation Theory. *Ind. Eng. Chem. Res.* **2000**, 39, 797.
(22) Wu, J. Z.; Prausnitz, J. M. Phase Equilibria for Systems Containing Hydrocarbons, Water, and Salt: An Extended Peng–Robinson Equation of State. *Ind. Eng. Chem. Res.* **1998**, *37*, 1634.
(23) Muller, E. A.; Gubbins, K. E. Molecular–Based Equations of State for Associating Fluids: A Review of Saft and Related Approaches. *Ind. Eng. Chem. Res.* **2001**, *40*, 2193.
(24) Folas, G. K.; Gabrielsen, J.; Michelsen, M. L.; Stenby, E. H.; Kontogeorgis, G. M. Application of the Cubic–Plus–Association (CPA) Equation of State to Cross–Associating Systems. *Ind. Eng. Chem. Res.* **2005**, *44*, 3823.
(25) Voutsas, E. C.; Yakoumis, I. V.; Tassios, D. P. Prediction of Phase Equilibria in Water/Alcohol/Alkane Systems. *Fluid Phase Equilibria* **1999**, *160*, 151.
(26) Oliveira, M. B.; Pratas, M. J.; Marrucho, I. M.; Queimada, A. J.; Coutinho, J. A. P. Description of the Mutual Solubilities of Fatty Acids and Water With the CPA EoS. *Aiche Journal* **2009**, *55*, 1604.
(27) Oliveira, M. B.; Teles, A. R. R.; Queimada, A. J.; Coutinho, J. A. P. Phase equilibria of Glycerol Containing Systems and Their Description with the Cubic–Plus–Association (CPA) Equation of State. *Fluid Phase Equilib.* **2009**, *280*, 22.
(28) Folas, G. K.; Kontogeorgis, G. M.; Michelsen, M. L.; Stenby, E. H. Application of the Cubic–Plus–Association (CPA) Equation of State to Complex Mixtures with Aromatic Hydrocarbons. *Ind. Eng. Chem. Res.* **2006**, *45*, 1527.
(29) Oliveira, M. B.; Coutinho, J. A. P.; Queimada, A. J. Mutual Solubilities of Hydrocarbons and Water with the CPA EoS. *Fluid Phase Equilib.* **2007**, *258,* 58.
(30) Oliveira, M. B.; Varanda, F. R.; Marrucho, I. M.; Queimada, A. J.; Coutinho, J. A. P. Prediction of Water Solubility in Biodiesel with the CPA Equation of State. *Ind. Eng. Chem. Res.* **2008**, *47*, 4278.
(31) Huang, S. H.; Radosz, M. Equation of State for Small, Large, Polydisperse, and Associating Molecules. *Ind. Eng. Chem. Res.* **1990**, *29*, 2284.
(32) Taylor, B. N.; Kuyatt, C. E., *Guidelines for the Evaluation and Expression of Uncertainty in NIST Measurement Results* Technical Note 1297 for NIST. 1994, Gaithersburg: MD.
(33) Marcilla, A.; Ruiz, F.; Garcia, A. N. Liquid–Liquid–Solid Equilibria of the Quaternary System Water–Ethanol–Acetone–Sodium Chloride at 25–Degrees–C. *Fluid Phase Equilib.* **1995**, *112*, 273.
(34) da Silva, C. A. S.; Sanaiotti, G.; Lanza, M.; Follegatti–Romero, L. A.; Meirelles, A. J. A.; Batista, E. A. C. Mutual Solubility for Systems Composed of Vegetable Oil + Ethanol + Water at Different Temperatures. *J. Chem. Eng. Data* **2010**, *55*, 440.
(35) Oliveira, M. B.; Queimada, A. J.; Coutinho, J. A. P. Modeling of Biodiesel Multicomponent Systems with the Cubic–Plus–Association (CPA) Equation of State. *Ind. Eng. Chem. Res.* **2010**, *49*, 1419.
(36) Oliveira, M. B.; Freire, M. G.; Marrucho, I. M.; Kontogeorgis, G. M.; Queimada, A. J.; Coutinho, J. A. P. Modeling the Liquid–Liquid Equilibria of Water +

Fluorocarbons with the Cubic–Plus–Association Equation of State. *Ind. Eng. Chem. Res.* **2007**, *46*, 1415.
(37) Oliveira, M. B.; Queimada, A. J.; Coutinho, J. A. P. Prediction of Near and Supercritical Fatty Acid Ester + Alcohol Systems with the CPA EoS. *The Journal of Supercritical Fluids* **2010**, *52*, 241.
(38) Pratas, M. J.; Freitas, S.; Oliveira, M. B.; Monteiro, S. C.; Lima, A. S.; Coutinho, J. A. P. Densities and Viscosities of Fatty Acid Methyl and Ethyl Esters. *J. Chem. Eng. Data* **2010**, *55*, 3983.
(39) Oliveira, M. B.; Marrucho, I. M.; Coutinho, J. A. P.; Queimada, A. J. Surface Tension of Chain Molecules Through a Combination of the Gradient Theory with the CPA EoS. *Fluid Phase Equilib.* **2008**, *267*, 83.
(40) Oliveira, M. B.; Miguel, S. I.; Queimada, A. J.; Coutinho, J. A. P. Phase Equilibria of Ester + Alcohol Systems and Their Description with the Cubic–Plus–Association Equation of State. *Ind. Eng. Chem. Res.* **2010**, *49,* 3452.
(41) Iwakabe, K.; Kosuge, H. Isobaric vapor–liquid–liquid equilibria with a newly developed still. *Fluid Phase Equilib.* **2001**, *192*, 171.
(42) Zhou, W.; Boocock, D. G. B. Phase Distributions of Alcohol, Glycerol, and Catalyst in the Transesterification of Soybean Oil. *J. Am. Oil Chem. Soc.* **2006**, *83*, 1047.
(43) Priamo, W. L.; Lanza, M.; Meirelles, A. J. A.; Batista, E. A. C. Liquid–Liquid Equilibrium Data for Fatty Systems Containing Refined Rice Bran Oil, Oleic Acid, Anhydrous Ethanol, and Hexane. *J. Chem. Eng. Data* **2009**, *54*, 2174.
(44) Dalmolin, I.; Lanza, M.; Meirelles, A. J. A.;. Batista, E. A. C. Liquid–Liquid Equilibrium Data for Systems Containing Refined Rice Bran Oil, Anhydrous ethanol, Water, and Hexane. *J. Chem. Eng. Data* **2009**, *54*, 2182.

Acknowledgments

The authors wish to acknowledge FAPESP (08/56258–8), CNPq (306250/2007–1 and 480992/2009–6), CAPES/PEC–PG, CAPES and CAPES/PNPD for their financial support and scholarship. Mariana B. Oliveira acknowledges the *Fundação para a Ciência e a Tecnologia* for her PhD (SFRH/BD/29062/2006) scholarship.

CAPÍTULO 7

Liquid–Liquid Equilibria for Ethyl Esters + Ethanol + Water Systems: Experimental Measurements and CPA EoS Modeling

Luis A. Follegatti–Romero[a], Mariana B. Oliveira[b], Eduardo A. C. Batista[a], João A. P. Coutinho[b] and Antonio J. A. Meirelles[a,]*

[a]ExTrAE, Laboratory of Extraction, Applied Thermodynamics and Equilibria, Department of Food Engineering, Faculty of Food Engineering, University of Campinas – UNICAMP, 13083–862, Campinas, SP, Brazil

[b]CICECO, Chemistry Department, University of Aveiro, 3810–193, Aveiro, Portugal

* Corresponding author. Fax: +55 19 3521 4027, E–mail: tomze@fea.unicamp.br

Artigo submetido no Fuel, 2011 (JFUE–D–11–01025).

Abstract

The knowledge and the capacity to describe the liquid–liquid equilbria of systems composed of fatty acid ethyl esters and water are very important for an adequate design of the biodiesel purification process, which is typically carried out with water. The objective of this work was to investigate the liquid–liquid equilibria related to main esters of interest for the washing of ethylic biodiesel, in particular were measured equilibrium data for systems containing: ethyl linoleate + ethanol + water at 313.15 K, technical grade ethyl oleate + ethanol + water at 298.15 K and ethyl palmitate + ethanol + water at 298.15, 308.15 and 333.15 K. The data obtained were correlated with the Cubic–Plus–Association equation of state (CPA EoS). It was shown that this equation of state was able to provide a very good description of the phase diagrams of the systems studied.

Keywords: Liquid–liquid equilibrium, washing biodiesel, ethyl esters, ternary systems, CPA EoS.

Introduction

Ethylic biodiesel fuel production has received considerable attentions in recent years, especially in countries with higher production of ethanol because it is a completely renewable, biodegradable and non–toxic fuel. It can contribute small amounts of carbon dioxide or sulfur to the atmosphere, decreasing the pollution from the car gases, so it is environmentally beneficial.[1]

Ethylic biodiesel is produced by transesterification (ethanolysis) from vegetable oils and ethanol in presence of a catalyst to produce fatty acid ethyl esters (FAEEs).[2] Depending on the raw material, this biofuel can contain more or less unsaturated fatty acids ethyl esters in its composition. Ethyl oleate and ethyl linoleate are produced mainly in the case of soybean oil and ethyl palmitate for palm oil. Among reactants, the oleaginous of high oil content (soybean, sunflower and rapeseed seeds) and palm oils have gained much attention lately as renewable raw material for biodiesel production due to their relatively high yield.[3, 4] Methanol has been the most commonly used alcohol to perform transesterification reaction (methanolysis) in the production of biodiesel. However, the ethanol has received some attention in the last decades, once it is derived from sugar cane and so provides an alternative totally renewable biodiesel production.[5]

After the transesterification reaction is necessary the separation of ethylic biodiesel from the glycerine, a byproduct from the reaction, and must be purified in order to fulfill cleaning conditions established by international standards. For achieving high level of purity, the biodiesel can be washed with water to remove the excess catalyst, ethanol, glycerol and unreacted glycerides that may reduce drastically its quality.[6, 7]

Water washing is generally carried out to remove all these contaminants from biodiesel.[8] The process of washing biodiesel involves mixing it with water at 333.15 to 353.15 K and two phases are formed: water–rich and ester–rich phases.[9] However, one of the most serious obstacles to use of water for the ethylic biodiesel purification process is the azeotropic behavior between water and excess ethanol, wich increases the solubility of both in the biodiesel transforming it into a complicated and expensive process.

Understanding and predicting the products distribution between the immiscible phases during the water washing process of biodiesel in a range of temperatures lower than the boiling point of ethanol is required to properly evaluate operating conditions of ethylic biodiesel purification in this new process. Liquid–liquid equilibria of ternary systems composed of saturated fatty acid ethyl esters, alcohol and water have recently been the focus of several research works to design the water washing process. Di Felice et al.[10] measured the LLE of the biodiesel + water + methanol system and compared the experimental data with predictions correlated with the Wilson activity coefficient model. Kuramochi et al. [11] measured the LLE of the rapeseed oil methyl ester biodiesel + water binary system and rapeseed oil methyl ester biodiesel + water + methanol ternary systems at 298.15 and 318.15 K and compared the experimental data with predictions from the several UNIFAC models.

An alternative to the usually applied activity coefficient models to predict systems with polar compounds as the water with strong associative interactions with ethanol during the biodiesel wash processes is the use of the Cubic–Plus–Association equation of state (CPA EoS) recently proposed by Oliveira and co−workers [12] that takes advantage of the transferability of its temperature independent binary interaction parameters obtained from

binary phase equilibria data to describe the LLE of the above mentioned multicomponent systems showing a similar, if not even better, performance than the group contribution models referred above.

Recently, water solubility in biodiesel was investigated by Oliveira et al.[13] and their experimental data were satisfactory correlated using the Cubic–Plus–Association equation of state (CPA EoS). Follegatti−Romero et al. [14] experimentally determined the LLE data for ethyl laurate/ethyl myristate + ethanol + water systems at 298.15, 313.15, and 333.15 K and compared their experimental results with predictions from the CPA EoS.

The objective of this work was to increase the available liquid−liquid equilibria data for systems containing fatty acid ethyl esters, water and ethanol of interest for the purification of ethylic biodiesel, in particular the equilibria data for systems containing ethyl linoleate + ethanol + water at 313.15, technical grade ethyl oleate + ethanol + water at 298.15 K and ethyl pamitate + ethanol + water at 298.15, 308.15 and 333.15 K,. The CPA EoS was used to correlate the measured experimental data.

Experimental Section

Materials.

Ethyl palmitate used in this work were purchased from Tecnosyn (Cajamar/SP, Brazil), and its mass purity was 99.2 %. Ethyl linoleate (97 % purity) and technical grade ethyl oleate (ethyl ester mixture) used were purchased from Sigma Aldrich. The technical grade ethyl oleate composition is showed in **Table 7.1**. The purities of all fatty acid ethyl esters were determined by Gas Chromatography. The solvents used were anhydrous ethanol from

Merck (Germany), with a mass purity of 99.9 %, and acetonitrile from Vetec (Brazil), with a mass purity of 99.8 %.

Table 7. 1. Technical Grade Ethyl Oleate Composition

ethyl ester	% mass
ethyl caprylate	0.02
ethyl caprate	0.03
ethyl laurate	2.30
ethyl myristate	0.17
ethyl pentadecanoate	0.02
ethyl palmitate	8.80
ethyl palmitoleate	0.03
ethyl heptadecanoate	0.09
ethyl cis–heptadec–9–enoate	0.04
ethyl stearate	1.89
ethyl elaidate	0.73
ethyl oleate	74.10
ethyl trans,trans–9,12–octadecadienoate	0.56
ethyl linoleate	10.60
ethyl all–trans–octadeca–9,12,15–trienoate	0.14
ethyl arachidate	0.18
ethyl eicosanoate	0.30

Quantification of the ethyl palmitate/ethyl linoleate and ethanol was carried out in a Shimadzu (GC–17A) capillary gas chromatograph system with programmable pneumatics and a flame ionization detector (FID). A DB–WAX capillary column (0.25 μm, 30 m × 0.25 mm i.d) from J&W Scientific (Rancho Cordoba, CA, USA) was used, and the carrier gas was helium from White Martins (Brazil), with a mass purity of 99.9 %.

In the case of technical grade ethyl oleate, the quantification was carried out in a Shimadzu VP series HPLC equipped with two LC–10ADVP solvent delivery units for binary gradient elution, a model RID10A differential refractometer, an automatic injector

with an injection volume of 20 μL, a model CTO−10ASVP column oven for precision temperature control even at sub−ambient temperatures, a single HPSEC Phenogel column (100 Å, 300 mm × 7.8 mm ID, 5 mm), a Phenogel column guard (30 mm × 4.6 mm), a model SCL–10AVP system controller and LC–Solution 2.1 software for remote management.

The water content of both phases for all systems was determined by Karl Fischer titration using a model 701 Metrohm apparatus (Switzerland) equipped with a 5 mL burette. The Karl Fischer reagent used in the titration was from Merck (Germany).

Apparatus and Procedures

The liquid–liquid equilibrium data for the systems containing ethyl esters (pamitate/linoleate) + ethanol + water at temperatures between 298 and 333.15 K and ethyl ester mixture (oleate/linoleate/palmitate/laurate) + ethanol + water at 298.15 K were determined. The binodal curve for ethyl palmitate + ethanol + water system at 298.15 K was determined by the cloud–point method following the same procedures described by Lanza et al.[15] The tie lines were determined using glass test tubes with screw caps (32 mL). Known quantities of each component were weighed on an analytical balance with a precision of 0.0001 g (Precisa, model XT220A, Sweden), and added directly to the glass test tubes. The ethyl ester, ethanol, and water were maintained under intensive agitation for 10 min at constant temperature and pressure using a test tube shaker (Phoenix, model AP 56). The ternary mixture was then left at rest for 24 h in a thermostatic water bath at the desired temperature, until two separate, transparent liquid phases were clearly observed. At the end of the experiment, samples were taken separately from the upper and bottom phases

using syringes containing previously weighed masses of acetonitrile, so as to guarantee an immediate dilution of the samples and avoid further separation into two liquid phases at ambient temperature. [16]

Samples from ethyl esters (linoleate/pamitate) + ethanol + water systems were analyzed by gas chromatography (GC). The detector and injector temperatures were 553 K and 523 K, respectively. The column oven was maintained at 313.15 K for 8 min and subsequently submitted to the following heating program: from 313.15 to 473.15 K at a rate of 20 $K \cdot min^{-1}$, maintained at 473.15 K for 8 min; from 473.15 to 483.15 K at a rate of 10 $K \cdot min^{-1}$, and finally maintained at 483.15 K for 2 min. The absolute pressure of the column was approximately 114 kPa; the carrier gas flowed at a rate of 1.6 $mL \cdot min^{-1}$; the linear velocity was 34 $cm \cdot s^{-1}$ and the sample injection volume was 1.0 μL. In the case of technical grade ethyl oleate + ethanol + water system, the samples from the two phases were analized by gel permeation chromatography (HPSEC).

The quantitative determination for all systems was carried out using calibration curves (external calibration) obtained using standard solutions for each system component: ethyl linoleate, technical grade ethyl oleate, ethyl palmitate and ethanol. These compounds were diluted with acetonitrile in the concentration range from 0.05–150 mg/mL. The experimental data for each tie–line were replicated at least three times and the values reported in the present work are the average ones.

The water mass fractions for all systems were determined at least three times using the Karl Fisher titration and the values reported are the average ones.

The distribution coefficients and the solvent selectivity were calculated according to eq 1 and 2, respectively, using the experimental compositions of both phases.

$$k_{d4} = \frac{w_4^{WP}}{w_4^{EP}} \quad (1) \qquad S_{4/i} = \frac{K_{d4}}{K_{di}} \quad (2)$$

where k_{d4} is the distribution coefficient for ethanol, w_4 is its mass fraction in the water (WP) or ester (EP) phases, respectively, and $S_{4/i}$ stands for the solvent selectivity. The solvent selectivity reflects its effectiveness in separating ethanol from the ester phase (i=1 for ethyl linoleate for first instance).

Thermodynamic Modeling. The modeling of polar and highly non ideal systems in wide ranges of temperature and pressure requires the use of association equations of state that explicitly take into account specific interactions between like (self–association) and unlike (cross–association) molecules. One of these equations is the Cubic–Plus–Association (CPA) equation of state, proposed by Kontogeorgis and co–workers,[17–19] that combines a physical contribution from a cubic equation of state, in this work the Soave–Redlich–Kwong (SRK) one, with an association term accounting for intermolecular hydrogen bonding and solvation effects,[20–22] originally proposed by Wertheim and used in other association equations of state such as SAFT.[23]

It can be expressed in terms of the compressibility factor as:

$$Z = Z^{phys.} + Z^{assoc.} = \frac{1}{1-b\rho} - \frac{a\rho}{RT(1+b\rho)} - \frac{1}{2}\left(1 + \rho\frac{\partial \ln g}{\partial \rho}\right)\sum_i x_i \sum_{A_i}\left(1 - X_{Ai}\right) \quad (3)$$

where a is the energy parameter, b the co–volume parameter, ρ is the molar density, g a simplified hard–sphere radial distribution function, X_{Ai} the mole fraction of pure component i not bonded at site A, and x_i is the mole fraction of component i.

The pure component energy parameter, *a*, is obtained from a Soave–type temperature dependency:

$$a(T) = a_0 \left[1 + c_1\left(1 - \sqrt{T_r}\right)\right]^2 \tag{4}$$

where a_0 and c_1 are regressed (simultaneously with *b*) from pure component vapor pressure and liquid density data.

When CPA is extended to mixtures, the energy and co–volume parameters of the physical term are calculated employing the conventional van der Waals one–fluid mixing rules:

$$a = \sum_i \sum_j x_i x_j a_{ij} \qquad\qquad a_{ij} = \sqrt{a_i a_j}\left(1 - k_{ij}\right) \tag{5}$$

and

$$b = \sum_i x_i b_i \tag{6}$$

X_{Ai} is related to the association strength Δ^{AiBj} between sites belonging to two different molecules and is calculated by solving the following set of equations:

$$X_{Ai} = \frac{1}{1 + \rho \sum_j x_j \sum_{B_j} X_{Bj} \Delta^{A_i B_j}} \tag{7}$$

where

$$\Delta^{A_i B_j} = g(\rho)\left[\exp\left(\frac{\varepsilon^{A_i B_j}}{RT}\right) - 1\right] b_{ij} \beta^{A_i B_j} \tag{8}$$

where ε^{AiBj} and β^{AiBj} are the association energy and the association volume, respectively.

The simplified radial distribution function, $g(\rho)$ is given by[24]:

$$g(\rho) = \frac{1}{1 - 1.9\eta} \qquad \text{where} \qquad \eta = \frac{1}{4} b\rho \tag{9}$$

For non–associating components, such as esters, CPA has three pure component parameters in the cubic term (a_0, c_1 and b) while for associating components, such as water and alcohols, it has two additional parameters in the association term (ε and β). In both cases, the parameters are regressed simultaneously from the vapor pressure and liquid density data. The objective function to be minimized is the following:

$$OF = \sum_{i}^{NP} \left(\frac{P_i^{\text{exptl}} - P_i^{\text{calcd}}}{P_i^{\text{exptl}}} \right)^2 + \sum_{i}^{NP} \left(\frac{\rho_i^{\text{exptl}} - \rho_i^{\text{calcd}}}{\rho_i^{\text{exptl}}} \right)^2 \tag{10}$$

For a binary mixture composed solely of non–associating compounds, the binary interaction parameter, k_{ij} (Eq. 5), is the only adjustable parameter.

When CPA is used for mixtures containing two self–associating compounds, combining rules for the association term are required,[24, 25] and in this work, the Elliott Combining Rule (ECR)[25] was used:

$$\Delta^{A_i B_j} = \sqrt{\Delta^{A_i B_i} \Delta^{A_j B_j}} \tag{11}$$

The Elliot combining rule provided very good results in modeling the phase equilibrium of several systems of interest for the production of biodiesel, such as, for example, the LLE of water + fatty acid systems[26] and the VLE of glycerol + alcohol systems.[27]

Solvation can occur in some systems containing self–associating and non self–associating compounds, as in the case of the ethyl ester + water or ethanol mixtures investigated in this work. For this type of system, the solvation phenomena is considered as a cross–association by the CPA EoS, where the cross–association energy (ε^{AiBj}) is considered to be half the value of the association energy for the self–associating component, and the cross association volume (β^{AiBj}) is left as an adjustable parameter, fitted to the equilibrium data. This approach, proposed by Folas et al.,[28] was successfully applied to model the phase equilibrium of several water + aromatic[12] and water + fatty acid ester[13] systems and to correlate the water solubility in biodiesels.[13] In these cases, the following objective function was minimized to estimate the parameters k_{ij} and β^{AiBj}:

$$OF = \sum_{i}^{NP} \left(\frac{x_i^{\text{calcd}} - x_i^{\text{exptl}}}{x_i^{\text{exptl}}} \right)^2 \tag{12}$$

where single phase or all phase data can be selected during optimization of the parameter. The association term depends on the number and type of association sites. According to the nomenclature of Huang and Radosz,[29] for alcohols, the two–site (2B) association scheme is applied, which proposes that hydrogen bonding occurs between the hydroxyl hydrogen and one of the lone pairs of electrons from the oxygen atom of another alcohol molecule. For the ester family, a single association site is considered that can cross–associate with self–associating molecules. For water, a four–site (4C) association scheme is adopted, considering that hydrogen bonding occurs between the two hydrogen atoms and the two lone pairs of electrons of the oxygen of the water molecule.

The average deviations (AD) between the experimental compositions and those estimated by the CPA EoS were calculated according to equation 13.

$$\mathrm{AD} = \sqrt{\frac{\sum_{n}^{N}\sum_{i}^{R}\left[\left(w_{i,n}^{\mathrm{WP},exptl} - w_{i,n}^{\mathrm{WP},calcd}\right)^2 + \left(w_{i,n}^{\mathrm{EP},exptl} - w_{i,n}^{\mathrm{EP},calcd}\right)^2\right]}{2NR}} \tag{13}$$

where AD is the average deviation for each system, N is the total number of tie lines of the corresponding system, R is the total number of components (R=3), w is the mass fraction, i is the component, the subscript n stands for the tie line number and the superscripts exptl and calcd refer to the experimental and calculated compositions.

Results and Discussion

Table 7.2 shows the experimental liquid–liquid equilibrium data for pure ethyl esters (ethyl linoleate and ethyl palmitate) + ethanol + water and mixture of ethyl esters (technical grade ethyl oleate) + ethanol + water systems at several temperatures are given in percentage by mass. The type A standard uncertainties [30] of the equilibrium compositions ranged from (0.058 to 0.082) % by mass for ethyl esters, (0.059 to 0.637) % for ethanol and (0.0888 to 0.933) % for water, with the lowest figures associated with the lowest mass fractions within the composition range investigated.

Table 7. 2. Experimental Liquid–Liquid Equilibrium Data for the Ternary Systems Containing Ethyl Ester (*i*) + Ethanol (*4*) + Water (*5*) at temperatures between 298.15 and 333.15) K

ethyl ester (*i*)	T/*K*	overall comp.			water–rich phase			ester–rich phase			K_{d4} [a]	$S_{4/i}$ [b]
		100 w_i	100 w_4	100 w_5	100 w_i	100 w_4	100 w_5	100 w_i	100 w_4	100 w_5		
linoleate (*1*)	313.15	18.860	61.630	19.510	4.391	71.860	23.749	83.091	12.571	4.338	5.716	108.170
		23.440	53.190	23.370	2.113	67.291	30.596	89.252	8.192	2.560	8.214	346.965
		27.830	43.200	28.980	0.672	57.810	41.518	92.163	5.481	2.360	10.547	1446.540
		36.810	26.260	36.930	0.312	39.514	60.174	94.530	3.181	2.320	12.422	3763.591
		45.380	10.050	44.570	0.121	18.690	81.189	96.811	1.482	1.710	12.611	10090.215
		51.360	0.000	48.640	0.081	0.000	99.919	99.220	0.000	0.800		
oleate (*2*)	298.15	18.427	63.221	18.352	4.730	74.040	21.230	87.391	11.470	1.139	6.455	119.264
		22.728	54.618	22.654	1.780	68.030	30.190	91.130	8.441	0.429	8.059	412.618
		26.719	44.413	28.868	0.380	59.370	40.250	92.662	6.971	0.367	8.517	2076.778
		36.223	29.109	34.668	0.200	44.520	55.280	95.801	4.030	0.169	11.047	5291.376
		42.524	15.290	42.185	0.100	23.890	76.010	98.640	1.250	0.110	19.112	18852.077
		51.412	0.000	48.588	0.050	0.000	99.950	99.280	0.000	0.720		
palmitate (*3*)	298.15	15.290	68.960	15.750	7.100	74.140	18.760	81.680	16.600	1.720	4.466	51.381
		20.020	59.960	20.020	2.568	71.252	26.180	87.227	11.743	1.030	6.068	206.098
		25.130	49.800	25.070	0.770	63.560	35.670	90.665	8.631	0.704	7.364	867.105
		30.053	39.964	29.983	0.172	55.538	44.290	93.524	6.012	0.464	9.238	5023.031
		34.890	29.680	35.430	0.080	45.090	54.830	95.176	4.521	0.303	9.973	11865.422
		40.520	19.840	39.640	0.045	31.535	68.420	96.598	3.122	0.280	10.101	21682.810
		44.496	10.459	45.045	0.028	16.412	83.560	97.429	2.361	0.210	6.951	24187.765
		49.530	0.000	50.470	0.009	0.000	99.991	99.856	0.000	0.144		
	308.15	20.100	59.900	20.000	3.109	72.317	24.574	85.628	12.161	2.211	5.947	163.768
		25.201	49.702	25.097	0.902	65.230	33.868	91.768	7.419	0.813	8.793	894.753
		25.302	42.701	31.997	0.303	56.105	43.592	94.118	5.375	0.507	10.438	3245.082
		34.901	29.703	35.396	0.201	44.020	55.779	95.736	3.858	0.406	11.410	5434.658
		40.503	19.820	39.677	0.093	31.385	68.522	96.913	2.720	0.367	11.537	12042.643
		44.501	10.510	44.989	0.072	16.756	83.173	98.500	1.180	0.319	14.195	19510.167
		55.101	0.000	44.899	0.013	0.000	99.987	99.500	0.000	0.500		
	333.15	25.140	49.770	25.090	1.705	63.070	35.225	75.221	19.000	5.779	3.319	146.448
		30.040	39.950	30.010	0.472	54.187	45.341	81.944	14.021	4.035	3.865	670.952
		34.900	29.680	35.420	0.112	43.025	56.862	85.644	11.090	3.266	3.880	2966.663
		40.540	19.820	39.640	0.058	30.124	69.818	89.346	7.463	3.191	4.036	6217.937
		44.460	10.540	45.000	0.037	17.187	82.776	92.749	4.461	2.790	3.853	9657.737
		49.610	0.000	50.390	0.016	0.000	99.984	98.109	0.000	1.891		

[a] K_{d4} is the ethanol distribution coefficient according to eq 1.
[b] $S_{4/i}$ is the solvent selectivity according to eq 2.

On the basis of the total system mass and of the phase and overall compositions, the mass balances were checked according to the procedure suggested by Marcilla et al.[31] and recently applied to fatty systems by Follegatti–Romero et al.[14] According to this procedure, the masses of both liquid phases were calculated and checked against the total initial mass used in the experimental runs.

The distribution diagram for ethanol in a pure ethyl ester (ethyl palmitate) and for mixture of ethyl esters (technical grade ethyl oleate) systems at 298.15 K is shown in **Figure 7.1**. The ethanol mass fraction in the aqueous phase was much larger than in the ester phase, so that its distribution coefficient was, in most cases, above 4.46 for both systems and above 3.3 for all systems. Considering that the ester mass fraction in the aqueous phase was usually low, the solvent selectivity was very high; in most cases above 50 (see **Table 7.1**). These results indicate that water washing of biodiesel is a very effective process for extracting residual ethanol from the ester phase generated at the end of the ethanolysis reaction, without losing any significant amount of FAEEs to the extract phase.

The average results obtained for the mass balance deviations of each set of experimental data are shown in **Table 7.3**. In all cases, the values were lower than 0.40 %, which indicates the good quality of the experimental data.

Table 7. 3. Deviations for the Global Mass Balance of the Phase Compositions

system	100 δ [a]
ethyl linoleate + ethanol + water at 313.15 K	0.32
technical grade ethyl oleate + ethanol + water at 298.15 K	0.29
ethyl palmitate + ethanol + water at 298.15 K	0.39
ethyl palmitate + ethanol + water at 308.15 K	0.25
ethyl palmitate + ethanol + water at 333.15 K	0.18

[a] relative deviation of the overall mass balance, calculated by $\delta = \frac{1}{N}\sum_{n}^{N}\left|\left(m^{\mathrm{EP}} + m^{\mathrm{WP}} - m^{\mathrm{OS}}\right)/ m^{\mathrm{OS}}\right|$, where m^{EP} is the calculated mass of the ester–rich phase, m^{WP} is the corresponding value of the water–rich phase, m^{OS} is the total mass of the system, and n is the tie line number.

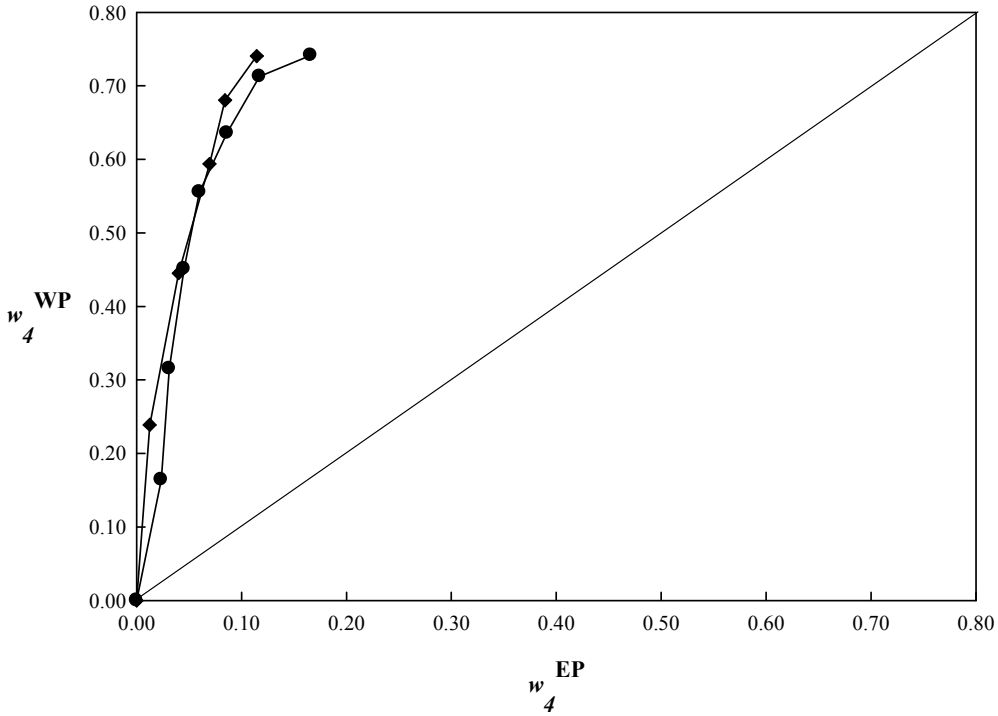

Figure 7. 1. Distribution diagram for: (–■–), technical grade ethyl oleate (*2*) + ethanol (*4*) + water (*5*) and (–●–), ethyl palmitate (*3*) + ethanol (*4*) + water (*5*) at 298.15 K.

In this work, the CPA EoS was used to predict the experimental liquid–liquid equilibria data of pure ethyl esters and mixture of ethyl esters with ethanol and water systems. The

CPA EoS was previously used with success for the description of the LLE of saturated ethyl esters systems such as ethyl laurate/myristate + ethanol + water[14] and canola oil ethylic biodiesel + ethanol + glycerol [32], using the same temperature independent binary interaction and cross–association parameters for pure ethyl esters and for mixtures.

To apply the CPA EoS to model the phase equilibria of multicomponent systems, the CPA pure compound parameters (a_0, c_1 and b) for several ethyl esters (linoleate, oleate, estearate, palmitate and laurate) were first estimated trough a simultaneous regression of vapor pressure and liquid density data. With the recent appearance of experimental data for ethyl esters vapor pressures [33] and liquid densities [34] it was also possible, in this work, to estimate esters CPA pure compound parameters. The critical temperatures for the fatty acid ethyl esters were calculated from the group contribution method of Nikitin et al. [35], that was previously assessed to be the best one to compute this property for ethyl esters [36]. The parameters obtained are presented at **Table 7.4** as well as liquid densities and vapor pressures deviations. The five CPA pure parameters for ethanol were previously established while performing a systematic study on the pure compound parameters for the n–alcohol family from methanol to n–eicosanol, using the 2B association scheme [37]. These parameters were recently used for the description of the LLE of ternary systems constituted ethyl esters + ethanol + water [14], of canola oil biodiesel, ethanol and glycerol[32] and of the VLE of the glycerol + ethanol system [27] and of the VLE of fatty acid ester + ethanol systems at atmospheric pressure [38] and at near or supercritical conditions [39].

Table 7. 4. CPA Pure Compound Parameters, Modeling Results and Critical Temperatures

compound	T_c (*K*)	a_0 (J·m^3·mol^{-2})	c_1	$b\times10^5$ (m^3·mol^{-1})	ε (J·mol^{-1})	β	100 AAD[a]	
							P	ρ
ethyl linoleate	785.19	11.99	1.82	36.13	–	–	0.27	0.26
ethyl oleate	771.07	14.36	1.34	37.64	–	–	6.00	0.61
ethyl palmitate	766.41	9.82	2.12	33.80	–	–	0.37	0.17
ethyl laurate	719.13	7.00	1.92	26.12	–	–	–	4.29
ethanol	514.70	0.68	0.94	4.75	21336	0.0190	0.35	0.51
water	647.30	0.12	0.67	1.45	16655	0.0692	1.72	0.82

[a]AAD is calculated by: $\mathbf{AAD} = \frac{1}{N}\sum_{i=1}^{Np}\left|\left(\text{exptl}_i - \text{calcd}_i\right)/\text{exptl}_i\right|$

The five CPA pure compound parameters for water were previously established considering the 4C scheme for water [40], and were used in modeling the liquid–liquid equilibria data of ethyl laurate/ethyl myristate + ethanol + water systems and the phase equilibrium of others water containing systems [12, 13, 26, 27].

The remaining parameters to be obtained are the binary interaction parameters, k_{ij}, and the cross– association volumes, β_{ij}. In the same way as performed when predicting the LLE of ternary systems composed of canola oil biodiesel + ethanol + glycerol, [32] and taking advantage of the transferability of the CPA parameters, binary interaction parameters for the binary subsystems were obtained from binary equilibria data.

The possible subsystems comprise fatty acid ethyl ester + ethanol, fatty acid ethyl ester + water and ethanol + water mixtures. The binary interaction parameter, k_{ij}, between ethyl esters and ethanol/water were obtained from a linear correlation with the ethyl ester carbon number. These correlations and the constant value were previously established by Oliveira et al.[13, 38] when correlating isothermal vapor–liquid equilibria of esters + ethanol systems, with esters from 5 up to 19 carbons and for the other binary (ethyl ester + water) were established through of the studies involving the phase equilibria of biodiesel + water

systems. The cross–association volume (β_{ij}) for ethyl esters + ethanol and esters + water binaries were fixed to 0.1 and 0.201, respectively, were used for a similar system [14] and utilized for predicting all systems studied.

In the case of the ethanol + water binary, the k_{ij} parameter was taken from the work by Follegatti–Romero et al. [14] who used a 4C scheme for correlating the corresponding liquid–liquid equilibria data. All parameters mentioned above are given in **Table 7.5**.

Table 7. 5. Binary Interaction and Cross–Association Parameters Used to Model Ternary Systems LLE

k_{ij} (unsaturated fatty acid ester + ethanol)	– 0.0260
k_{ij} (ethyl palmitate + ethanol)	– 0.0200
k_{ij} (ethyl laurate + ethanol)	– 0.0830
k_{ij} (unsaturated fatty acid ester + water)	– 0.0602
k_{ij} (ethyl palmitate + water)	– 0.0874
k_{ij} (ethyl laurate + water)	– 0.1720
β_{ij} (fatty acid ester + ethanol)	0.1000
β_{ij} (fatty acid ester + water)	0.2010
k_{ij} (ethanol + water)	– 0.1000

Having the CPA pure compounds, the binary interaction parameters and the cross−association volumes, it was then possible to predict the measured liquid−liquid equilibria systems containing pure ethyl esters and mixture of ethyl esters. Technical grade ethyl oleate + ethanol +water system was treated as a system of seven compounds, the ethyl oleate was considered as a mixture of five compounds: ethyl oleate, ethyl linoleate, ethyl palmitate ethyl laurate, and ethyl stearate.

The CPA EoS prediction results of the phase diagrams measured in this work are reported in **Figures 7.2 to 7.4**. Tie lines was properly predicted by the CPA EoS for all ternary and for multicomponent systems and in the selected temperature range, using the same temperature independent binary interaction and cross−association parameters correlated from binary phase equilibria data. **Figure 7.1** shows the binodal curve for the

ethyl palmitate system (The experimental data used are presented in the Supporting Information, **Table 7.6**).

Table 7. 6. Experimental Data for Binodal Curve of Palmitate (*3*) + Ethanol (*4*) + Water (*5*) at 298.15 K

100 w_i	**100 w_4**	**100 w_5**
0.9986	0.000	0.0014
0.9102	0.0832	0.0066
0.8084	0.1751	0.0165
0.6415	0.3233	0.0352
0.4869	0.4571	0.056
0.3296	0.5875	0.0829
0.2356	0.6629	0.1015
0.1731	0.7085	0.1184
0.1346	0.732	0.1334
0.1005	0.7505	0.1489
0.0722	0.7587	0.1691
0.0503	0.7569	0.1927
0.0269	0.7351	0.2379
0.0155	0.7089	0.2756
0.0071	0.6561	0.3368
0.0048	0.6206	0.3794
0.0043	0.0000	0.9957

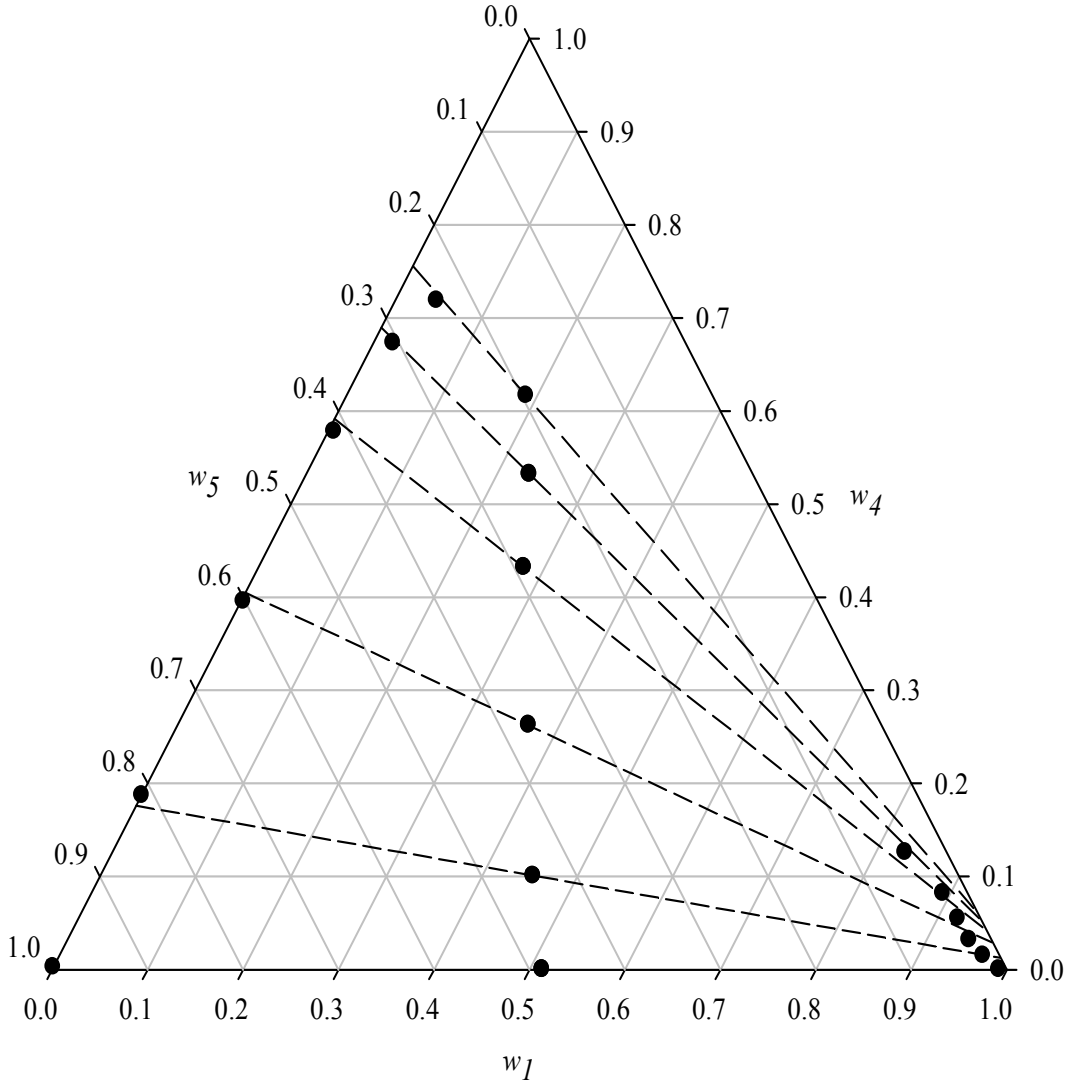

Figure 7. 2. Liquid–liquid equilibrium for the system containing ethyl linoleate (*1*) + ethanol (*4*) + water (*5*): experimental (●) and CPA results (——) at 313.15 K.

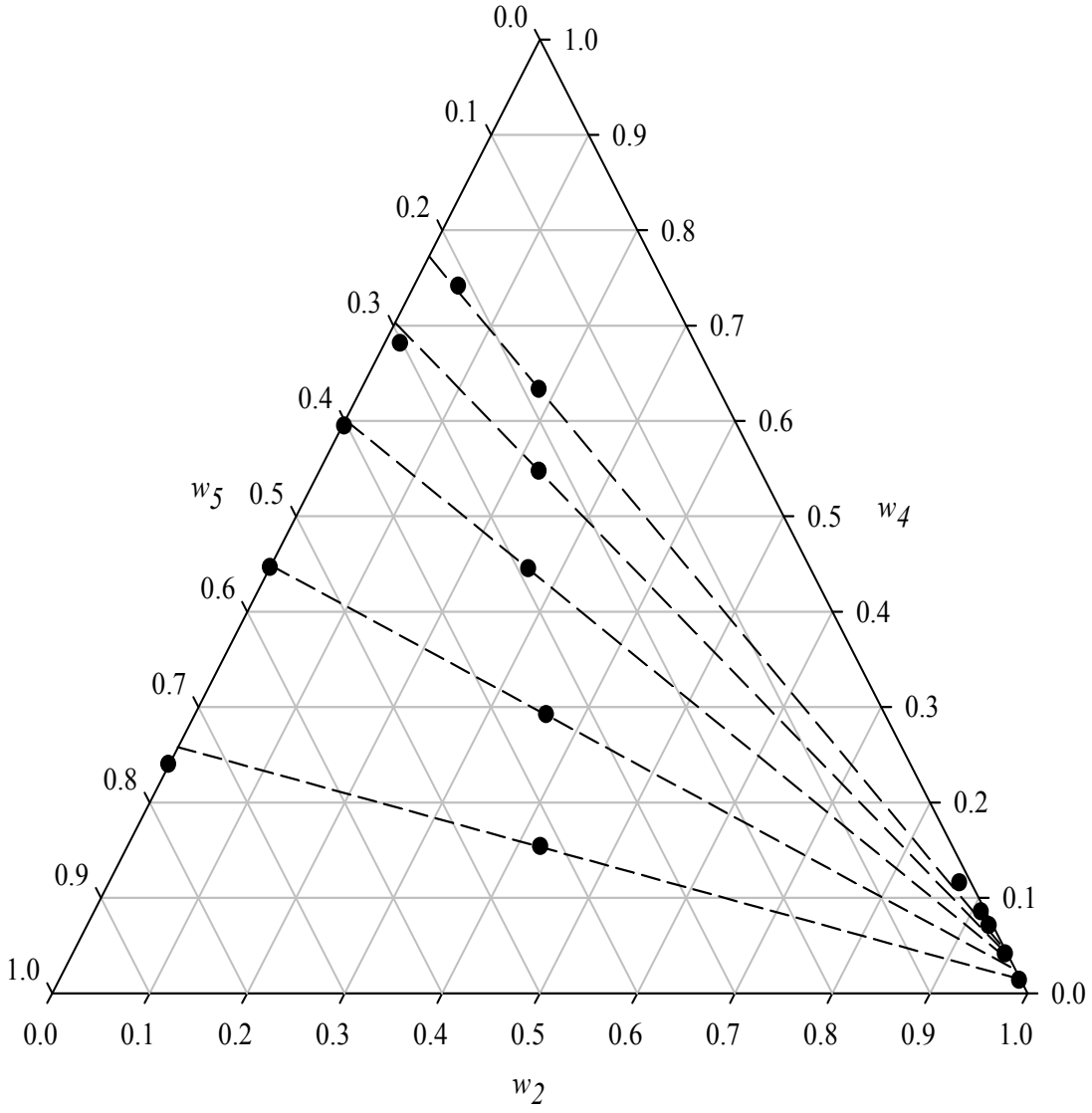

Figure 7. 3. Liquid–liquid equilibrium for the system containing ethyl oleate (*2*) + ethanol (*4*) + water (*5*): experimental (●) and CPA results (——) at 298.15 K.

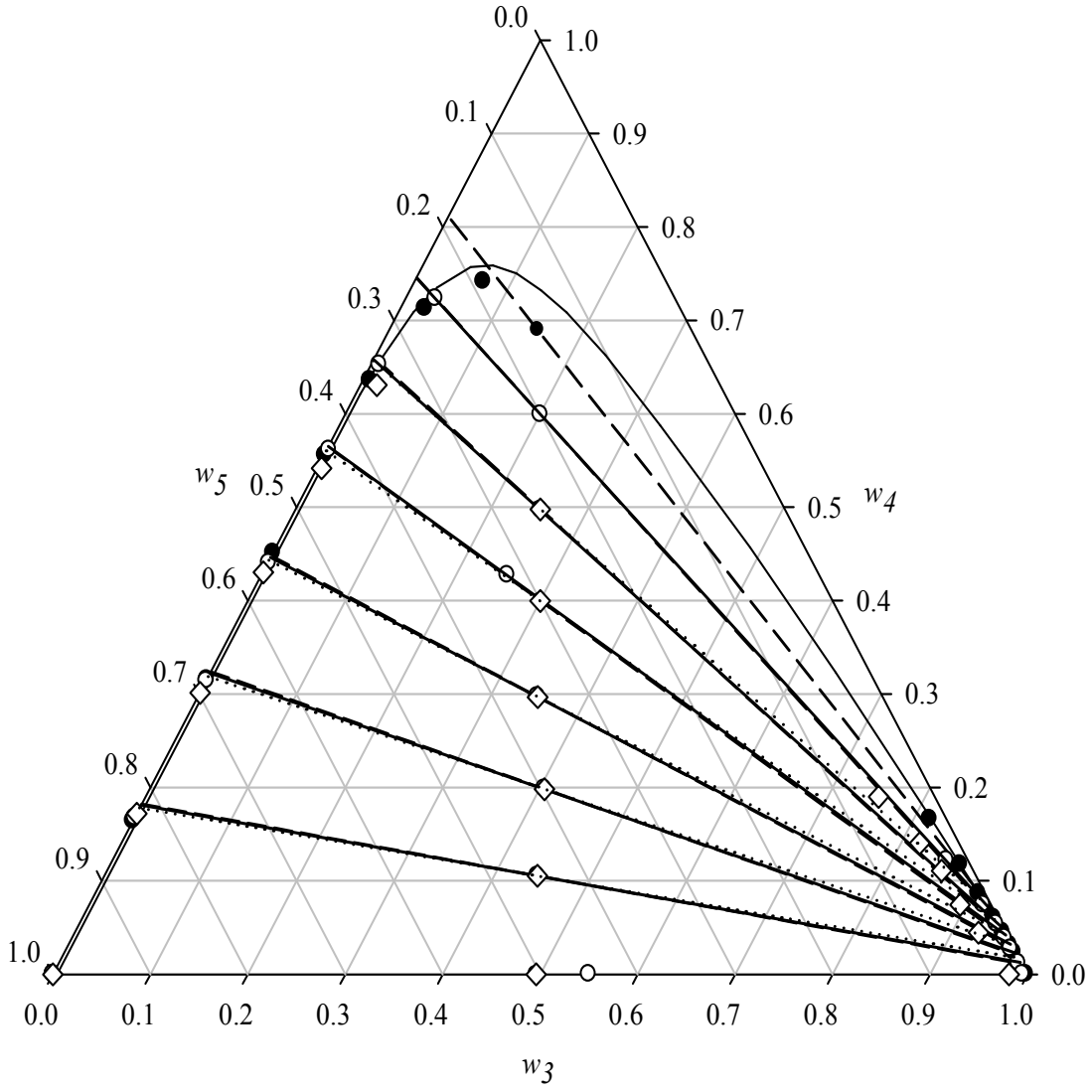

Figure 7. 4. Liquid–liquid equilibrium for the system containing ethyl palmitate (*3*) + ethanol (*4*) + water (*5*): experimental (●) and CPA results (——) at 298.15 K, experimental (○) and CPA results (—) at 308.15 K and experimental (◊) and CPA results (···) at 333 K.

Average deviations between the experimental and calculated compositions in both phases are shown in **Table 7.7**. Most deviations are within the range 2.41 – 5.28 % and a global average deviation of 3.09 % were obtained. Similar results were recently reported by

Follegatti–Romero et al. [14] for liquid–liquid equilibrium data of fatty systems containing ethanol and water.

Table 7. 7. Average Deviations (AD) between the Experimental and CPA Phase Compositions

system	100AD[a]
technical grade ethyl oleate + ethanol + water at 298.15 K	2.41
ethyl linoleate + ethanol + water at 313.15 K	2.77
ethyl palmitate + ethanol + water at 298.15 K	3.20
ethyl palmitate + ethanol + water at 308.15 K	1.79
ethyl palmitate + ethanol + water at 333.15 K	5.28
average global deviation	3.09

[a]Eq. (13).

Conclusions

New experimental equilibrium data were measured for ethyl linoleate/technical grade ethyl oleate/palmitate + ethanol + water systems at temperatures between 298.15 and 333.15 K. The high ethanol distribution coefficients and very high solvent selectivities make water washing a very effective alternative to recovering ethanol from ester phase. The experimental data were correlated successfully with the Cubic–Plus–Association equation of state (CPA EoS), and the average global deviation between the experimental data and the calculated compositions showed a value of 3.09 %.

Nomenclature

K_d = distribution coefficient

S = solvent selectivity

a = energy parameter in the physical term

a_0, c_1 = parameters for calculating a

A_i = site A in molecule i

b = co–volume

g = simplified hard–sphere radial distribution function

k_{ij} = binary interaction parameter

P = vapor pressure

R = gas constant

T = temperature

x = mole fraction

w = mass fraction

X_{Ai} = fraction of molecule i not bonded at site A

Z = compressibility factor

Greek Symbols

β = association volume

ε = association energy

η = reduced fluid density

ρ = mole density

Δ = association strength

Subscripts

c = critical

i,j = pure component indexes

r = reduced

Superscripts

assoc. = association

phys. = physical

calcd = calculated

exptl = experimental

Literature Cited

1. Moser, B.R., *Biodiesel Production, Properties, and Feedstocks*, in *Biofuels*, D. Tomes, P. Lakshmanan, and D. Songstad, Editors. 2011, Springer New York. p. 285–347.
2. Meher, L.C., D. Vidya Sagar, and S.N. Naik, *Technical aspects of biodiesel production by transesterification—a review.* Renewable and Sustainable Energy Reviews, 2006. **10**(3): p. 248–268.
3. Knothe, G., *"Designer" Biodiesel: Optimizing Fatty Ester Composition to Improve Fuel Properties†.* Energy & Fuels, 1997. **22**(2): p. 1358–1364.
4. Qiu, F., et al., *Biodiesel production from mixed soybean oil and rapeseed oil.* Applied Energy, 2011. **88**(6): p. 2050–2055.
5. Meneghetti, S.M.P., et al., *Biodiesel from Castor Oil: A Comparison of Ethanolysis versus Methanolysis.* Energy & Fuels, 2006. **20**(5): p. 2262–2265.
6. Atadashi, I.M., M.K. Aroua, and A.A. Aziz, *Biodiesel separation and purification: A review.* Renewable Energy, 2011. **36**(2): p. 437–443.
7. Berrios, M. and R.L. Skelton, *Comparison of purification methods for biodiesel.* Chemical Engineering Journal, 2008. **144**(3): p. 459–465.
8. Karaosmanoğlu, F., et al., *Investigation of the Refining Step of Biodiesel Production.* Energy & Fuels, 1996. **10**(4): p. 890–895.
9. Gonzalo, A., et al., *Water Cleaning of Biodiesel. Effect of Catalyst Concentration, Water Amount, and Washing Temperature on Biodiesel Obtained from Rapeseed Oil and Used Oil.* Industrial & Engineering Chemistry Research, 2010. **49**(9): p. 4436–4443.
10. Di Felice, R., et al., *Component Distribution between Light and Heavy Phases in Biodiesel Processes.* Industrial & Engineering Chemistry Research, 2008. **47**(20): p. 7862–7867.
11. Kuramochi, H., et al., *Application of UNIFAC models for prediction of vapor–liquid and liquid–liquid equilibria relevant to separation and purification processes of crude biodiesel fuel.* Fuel, 2009. **88**(8): p. 1472–1477.
12. Oliveira, M.B., J.A.P. Coutinho, and A.J. Queimada, *Mutual solubilities of hydrocarbons and water with the CPA EoS.* Fluid Phase Equilibria, 2007. **258**(1): p. 58–66.
13. Oliveira, M.B., et al., *Prediction of Water Solubility in Biodiesel with the CPA Equation of State.* Industrial & Engineering Chemistry Research, 2008. **47**(12): p. 4278–4285.
14. Follegatti–Romero, L.A., et al., *Liquid−Liquid Equilibrium for Ternary Systems Containing Ethyl Esters, Anhydrous Ethanol and Water at 298.15, 313.15, and 333.15 K.* Industrial & Engineering Chemistry Research, 2010. **49**(24): p. 12613–12619.
15. Lanza, M., et al., *Liquid–Liquid Equilibrium Data for Reactional Systems of Ethanolysis at 298.3 K.* Journal of Chemical & Engineering Data, 2007. **53**(1): p. 5–15.
16. Follegatti–Romero, L.A., et al., *Mutual Solubility of Pseudobinary Systems Containing Vegetable Oils and Anhydrous Ethanol from (298.15 to 333.15) K.* Journal of Chemical & Engineering Data, 2010. **55**(8): p. 2750–2756.

17. Kontogeorgis, G.M., et al., *Ten Years with the CPA (Cubic–Plus–Association) Equation of State. Part 1. Pure Compounds and Self–Associating Systems.* Industrial & Engineering Chemistry Research, 2006. **45**(14): p. 4855–4868.
18. Kontogeorgis, G.M., et al., *Ten Years with the CPA (Cubic–Plus–Association) Equation of State. Part 2. Cross–Associating and Multicomponent Systems.* Industrial & Engineering Chemistry Research, 2006. **45**(14): p. 4869–4878.
19. Kontogeorgis, G.M., et al., *An Equation of State for Associating Fluids.* Industrial & Engineering Chemistry Research, 1996. **35**(11): p. 4310–4318.
20. Michelsen, M.L. and E.M. Hendriks, *Physical properties from association models.* Fluid Phase Equilibria, 2001. **180**(1–2): p. 165–174.
21. Voutsas, E.C., et al., *Water/Hydrocarbon Phase Equilibria Using the Thermodynamic Perturbation Theory.* Industrial & Engineering Chemistry Research, 2000. **39**(3): p. 797–804.
22. Wu, J. and J.M. Prausnitz, *Phase Equilibria for Systems Containing Hydrocarbons, Water, and Salt: An Extended Peng−Robinson Equation of State.* Industrial & Engineering Chemistry Research, 1998. **37**(5): p. 1634–1643.
23. Müller, E.A. and K.E. Gubbins, *Molecular–Based Equations of State for Associating Fluids: A Review of SAFT and Related Approaches.* Industrial & Engineering Chemistry Research, 2001. **40**(10): p. 2193–2211.
24. Folas, G.K., et al., *Application of the Cubic–Plus–Association (CPA) Equation of State to Cross–Associating Systems.* Industrial & Engineering Chemistry Research, 2005. **44**(10): p. 3823–3833.
25. Voutsas, E.C., I.V. Yakoumis, and D.P. Tassios, *Prediction of phase equilibria in water/alcohol/alkane systems.* Fluid Phase Equilibria, 1999. **158–160**: p. 151–163.
26. Oliveira, M.B., et al., *Description of the mutual solubilities of fatty acids and water with the CPA EoS.* AIChE Journal, 2009. **55**(6): p. 1604–1613.
27. Oliveira, M.B., et al., *Phase equilibria of glycerol containing systems and their description with the Cubic–Plus–Association (CPA) Equation of State.* Fluid Phase Equilibria, 2009. **280**(1–2): p. 22–29.
28. Folas, G.K., et al., *Application of the Cubic–Plus–Association (CPA) Equation of State to Complex Mixtures with Aromatic Hydrocarbons.* Industrial & Engineering Chemistry Research, 2005. **45**(4): p. 1527–1538.
29. Huang, S.H. and M. Radosz, *Equation of state for small, large, polydisperse, and associating molecules.* Industrial & Engineering Chemistry Research, 1990. **29**(11): p. 2284–2294.
30. Taylor, B.N.K., C. E., *Guidelines for the Evaluation and Expression of Uncertainty in NIST Measurement Results Technical Note 1297 for NIST.* 1994: p. Gaithersburg: MD.
31. Marcilla, A., F. Ruiz, and A.N. García, *Liquid–liquid–solid equilibria of the quaternary system water–ethanol–acetone–sodium chloride at 25 °C.* Fluid Phase Equilibria, 1995. **112**(2): p. 273–289.
32. Oliveira, M.B., et al., *Liquid–liquid equilibria for the canola oil biodiesel + ethanol + glycerol system.* Fuel, 2011. **90**(8): p. 2738–2745.

33. Silva, L.Y.A., et al., *Determination of the vapor pressure of ethyl esters by Differential Scanning Calorimetry*. The Journal of Chemical Thermodynamics, 2011. **43**(6): p. 943–947.
34. Pratas, M.J., et al., *Densities and Viscosities of Fatty Acid Methyl and Ethyl Esters*. Journal of Chemical & Engineering Data, 2010. **55**(9): p. 3983–3990.
35. Poling B, P.J., O'Connel J, *The Properties of gases and liquids*. 2001. **(5th edition). Mc−Graw Hill**.
36. Lopes, J.C.A., et al., *Prediction of Cloud Points of Biodiesel†*. Energy & Fuels, 2007. **22**(2): p. 747–752.
37. Oliveira, M.B., et al., *Surface tension of chain molecules through a combination of the gradient theory with the CPA EoS*. Fluid Phase Equilibria, 2008. **267**(1): p. 83–91.
38. Oliveira, M.B., et al., *Phase Equilibria of Ester + Alcohol Systems and Their Description with the Cubic–Plus–Association Equation of State*. Industrial & Engineering Chemistry Research, 2010. **49**(7): p. 3452–3458.
39. Oliveira, M.B., A.J. Queimada, and J.A.P. Coutinho, *Prediction of near and supercritical fatty acid ester + alcohol systems with the CPA EoS*. The Journal of Supercritical Fluids, 2010. **52**(3): p. 241–248.
40. Oliveira, M.B., et al., *Modeling the Liquid−Liquid Equilibria of Water + Fluorocarbons with the Cubic–Plus–Association Equation of State*. Industrial & Engineering Chemistry Research, 2007. **46**(4): p. 1415–1420.

Acknowledgments

The authors wish to acknowledge FAPESP (08/56258–8), CNPq (306250/2007–1 and 480992/2009–6), CAPES/PEC–PG, CAPES and CAPES/PNPD for their financial support and scholarship

.

CAPÍTULO 8

8.1 CONCLUSÕES GERAIS

- O objetivo desta tese de doutorado foi plenamente atingido obtendo–se dados experimentais de equilíbrio líquido–líquido das misturas envolvidas nas diferentes etapas do processo de produção do biodiesel com boa qualidade e desvios nos balanços de massa globais muito baixos. Os dados obtidos possuem informações relevantes, principalmente em relação às composições determinadas das fases em equilíbrio, para serem utilizadas na projeção e desenho dos principais equipamentos de reação e separação para produção de biodiesel etílico.
- Resultados para o ELL de sistemas compostos de óleos vegetais + etanol, o ELL de sistemas compostos de FAEEs + etanol + glicerol, a solubilidade de FAEEs em água e a recuperação do etanol do biodiesel na faixa de temperatura de operação das unidades de reação e separação em usinas de biodiesel, foram investigados.
- A CPA EoS (*Cubic–Plus–Association equation of state*) foi aplicada para descrever o ELL de vários sistemas multicomponentes de relevância para a reação de alcoólise e para o processo de purificação. Tornou–se claro que o modelo termodinâmico escolhido demonstrou ser capaz de correlacionar corretamente sistemas altamente polares e não ideais. Além de combinar previsibilidade, precisão e simplicidade.
- A CPA EoS mostrou ter muita flexibilidade em representar o ELL e ELV (a altas

pressões e altas temperaturas) usando o mesmo conjunto de parâmetros. É interessante concluir que esta equação de estado pode ser aplicada para simular todo o processo de produção do biodiesel etílico.

8.2 SUGESTÕES PARA TRABALHOS FUTUROS

Trabalhos adicionais no campo do equilíbrio de fases e modelagem com a equação de estado CPA para a produção de biodiesel ainda podem ser realizados:

- Determinar experimentalmente dados de ELL de sistemas ternários contendo óleos vegetais + FAEEs + álcool ou sistemas contendo óleos vegetais + FAEEs + glicerol numa ampla gama de temperatura.
- Determinar experimentalmente dados de ELL de sistemas quaternários contendo óleos vegetais + FAEEs + álcool + glicerol a altas temperaturas.
- Aplicar a CPA EoS para simular todos os tipos de equilíbrios de fase formados no processo de produção de biodiesel etílico.